



<https://theses.gla.ac.uk/>

Theses Digitisation:

<https://www.gla.ac.uk/myglasgow/research/enlighten/theses/digitisation/>

This is a digitised version of the original print thesis.

Copyright and moral rights for this work are retained by the author

A copy can be downloaded for personal non-commercial research or study, without prior permission or charge

This work cannot be reproduced or quoted extensively from without first obtaining permission in writing from the author

The content must not be changed in any way or sold commercially in any format or medium without the formal permission of the author

When referring to this work, full bibliographic details including the author, title, awarding institution and date of the thesis must be given

Enlighten: Theses

<https://theses.gla.ac.uk/>
research-enlighten@glasgow.ac.uk

INVESTIGATION OF THE VERTICAL VESTIBULO-OCULAR REFLEXES IN THE
DOGFISH Scyliorhinus canicula(L.)

Rukhsana Chouhdary

A thesis presented for the Degree of
Doctor of Philosophy in the University
of Glasgow, Faculty of Science,
Department of Zoology.

July, 1988

ProQuest Number: 10998189

All rights reserved

INFORMATION TO ALL USERS

The quality of this reproduction is dependent upon the quality of the copy submitted.

In the unlikely event that the author did not send a complete manuscript and there are missing pages, these will be noted. Also, if material had to be removed, a note will indicate the deletion.



ProQuest 10998189

Published by ProQuest LLC (2018). Copyright of the Dissertation is held by the Author.

All rights reserved.

This work is protected against unauthorized copying under Title 17, United States Code
Microform Edition © ProQuest LLC.

ProQuest LLC.
789 East Eisenhower Parkway
P.O. Box 1346
Ann Arbor, MI 48106 – 1346

... ..
... ..
... ..

TO ARSHAD

Declaration:

I declare that this thesis represents, except where a note is made to the contrary, work carried out by myself and that the text was composed by myself.

Rukhsana Chouhdary

7th. July 1988

ACKNOWLEDGEMENTS

I would like to express my gratitude to many people who helped me during the period of research and in writing up my thesis.

First of all I would really like to thank my supervisor Dr D.M. Neil for his continuous assistance, advice and unlimited patience during this time, and also for his valuable time which he spent in writing computer programmes for the data analysis.

I am grateful for the efficient help from the technical staff of the Zoology Department especially Margaret Mullin for her assistance during the histological work, and Mr P. Rickus for his help with photography. I wish to thank Professor R.S. Phillips for making available departmental facilities and equipment.

Thanks are also due to Dr N.C. Spurway of the Institute of Physiology for making a cryostat available for my histochemical work. Technical advice and help from Dr A. Rowlerson, and especially the provision of material for immunohistochemistry, is greatly acknowledged.

I owe it to my husband and family for their endless emotional and financial support during my period of study and I would really like to thank them just for being there for me.

SUMMARY

In the dogfish Scyliorhinus canicula (L.) an investigation of the vertical vestibulo-ocular reflexes (VOR) has been made by recording the vertical eye reflexes and the myographic activity of the extra-ocular muscles (EOM) which induce these reflexes. Control of this reflex has been determined by selective ablation of the different components of the vestibular apparatus.

The physiological profile of the EOM has been determined by investigating their histochemical, immunohistochemical, mechanical properties, their innervation, and the size of their motor units. In the dogfish all six EOM contain TYPE I and TYPE II fibres. Type I fibres are small, lie mostly in the orbital region, stain negatively with the Mg^{2+} activated $\dagger m$ -ATPase, give a positive reaction for the succinate dehydrogenase and stain positive with antisera specific for slow fibre myosin (α ALD and α SHC). TYPE II fibres are large, lie mostly in the global region, stain positively with Mg^{2+} activated myosin-ATPase, give a negative reaction for SDH and do not stain with α ALD and α SHC. Both Type I and TYPE II fibres are innervated by the en plaque and engrappe endplates. Mechanically two levels of response are shown by the EOM fibres and individual twitches and tetanic contraction is elicited in all the EOM. The size of motor units in the $\dagger SO$, IO and SR is 9 muscle fibres per one motor axon, and in the EXT-R is 13 muscle fibres per one motor axon. In their physiological and mechanical properties, and in their innervation the TYPE I and TYPE II fibres resemble the **slow** and **fast** fibres of other vertebrates.

-V-

$\dagger m$ ATPase = myofibrillar ATPase

\dagger Abbreviations of muscles by initial letters: Superior oblique, Inferior oblique, Superior rectus, External rectus.

Vertical eye reflexes have been studied by fixing the animal in a frame and recording eye movements by video and movement transducer techniques. Vertical eye reflexes are compensatory and vestibular effects are strongly shown. Vision is generally weaker and is only seen when the animal is provided with a strong visual stimulus. The gain of the eye movements is generally smaller during tilts in the pitch plane. There is no nystagmus during the vertical eye reflexes, but it occurs in the horizontal VOR. The gain of the eye reflexes is significantly reduced after ablation of the vertical semicircular canals and the utricle.

Myographic recordings in all six EOM have been made during tilts in the roll and pitch planes and at intermediate angles. Co-activation of the SO and SR combined with inactivity of IO and [†]IR induces counter-rolling of the downward eye in the roll plane. Reciprocal activation occurs in the muscles of the upward eye. In the pitch plane SO and SR of the two eyes remain co-activated, and it is the difference in the relative strength of firing of the two EOM which induces the observed torsional movement in the two eyes. The action of the horizontal EOM stabilizes the activity of vertical EOM in all planes of the tilt. Tilts in vertical intermediate planes have demonstrated that transitions occur in the relationship between the cycle of tilt and the phase of EOM myogram burst. For right leading rotations between tilt planes, beginning with roll, the phase shifts occur in the left EOM around 45° and 225° , and in the right eye around 135° and 315° . Nystagmus is totally absent during tilts in the vertical plane, although when tilted in yaws, not only the horizontal EOM, but also the vertical EOM show a nystagmus response. A strong tonic firing is shown by the EOM during static tilts.

The control of the vertical VOR by the vertical semicircular canals and the utricle have been determined by selective ablation of these two components at a range of frequencies. The effects of utricle ablation are best seen at 0.2Hz, while the semicircular canals ablation affects the reflexes at 0.8Hz. The sequence of ablation experiments has ranged from the ablation of a single vertical canal to the ablation of all four vertical canals and the utricle, and in each has produced a particular pattern of EOM firing for tilts between 0° - 360° , which is different from the algebraic model of the input strength of the vertical semicircular canals. The ablation of a single vertical canal reduces the strength of both the ipsilateral and contralateral EOM significantly. The ablation of posterior vertical canal suggests an inhibitory interaction between the vertical canal outputs. In experiments where only single vertical canal is left intact the myographic response of the EOM in two eyes is controlled by contralateral effects. These patterns of EOM firing under various ablated conditions differ from those predicted by a simple algebraic model of the input strengths of the 4 vertical semicircular canals, and suggests that a complex central wiring exists between different components of the vestibular system.

CONTENTS

SUMMARY

CHAPTER 1. GENERAL INTRODUCTION	1
CHAPTER 2. PHYSIOLOGICAL PROFILE OF THE EOM.	20
2.1 Introduction	21
2.2 Materials and methods	26
2.3 Results	34
2.3.A Myosin-ATPase activity of EOM	34
2.3.A.a Alkaline pre-incubation	34
2.3.A.b Acid pre-incubation	35
2.3.A.c Mg^{2+} dependent m_2 -ATPase	36
2.3.B SDH staining of EOM	37
2.3.C Type specific myosin in EOM determined by immunohistochemical staining	37
2.3.D Quantitative analysis of histochemical oxidative and immunohistochemical properties of EOM	38
2.3.E Mechanical recordings	41
2.3.F Motor endplates in EOM	42
2.3.G EOM motor units	43
2.4 Discussion	46

CHAPTER 3. VERTICAL EYE REFLEXES.	61
3.1 Introduction	52
3.2 Materials and methods.	54
3.3 Results	57
3.3.A Recordings in the intact fish, in light	57
3.3.A.a Compensation in roll	57
3.3.A.b Compensation in pitch	57
3.3.B Recordings in the intact fish, in dim red light	57
3.3.B.a Compensation in roll	57
3.3.B.b Compensation in pitch	58
3.3.C Tests for optokinetic nystagmus	58
3.3.C.a Visual stimulus opposing eye movements	58
3.3.C.b Visual stimulus reinforcing eye movements	58
3.3.C.c Visual stimulus reinforcing eye movements in dim red light	58
3.3.D Recordings after the ablation experiments	59
3.3.D.a Left anterior and posterior canals ablated	59
3.3.D.b All four vertical canals ablated, utriculi intact	60
3.3.D.c All four vertical canals and right utriculus ablated	60
3.4 Discussion	61
CHAPTER 4. COORDINATED ACTIVATION OF THE EOM.	66
4.1 Introduction	67

4.2 Materials and methods	70
4.3 Results	72
4.3.A EOM activation in roll	73
4.3.B EOM activation in pitch	74
4.3.C Transition of EOM between roll and pitch	74
4.3.C.a Response of SO	75
4.3.C.b Transition in IO between 0^0 & 180^0 , 0.2Hz, 0.8Hz	78
4.3.C.c Transition in SR response between 0^0 and 180^0 , 0.2Hz, 0.8Hz	79
4.3.C.d Transition in IR response between 0^0 and 180^0 , 0.2Hz, 0.8Hz	80
4.3.C.e Transition in the response of INT-R between 0^0 and 180^0 , 0.2Hz, 0.8Hz	81
4.3.C.f Transition in the response of EXT-R between 0^0 and 180^0 , 0.2Hz, 0.8Hz.	82
4.3.D Analysis of integrated phase plots	83
4.3.E Tonic activity of the EOM	84
4.3.F Nystagmus response	84
4.4 Discussion	86
CHAPTER 5. THE CONTROL OF EOM RESPONSE	90
5.1 Introduction	91
5.2 Materials and methods	95
5.3 Results	96
5.3.A SO response in intact fish, canals exposed	96
5.3.B Single canal ablation	97

5.3.B.a	Anterior canal ablated	97
5.3.B.b	Posterior canal ablation	98
5.3.C	Two vertical semicircular canals ablated	99
5.3.C.a	Two anterior canals ablated, S0	99
5.3.C.b	Two anterior canals ablated, I0	100
5.3.C.c	Two posterior canals ablated, S0	100
5.3.C.d	Diagonal pair ablated, S0	101
5.3.C.e	Ipsilateral pair ablated, S0	101
5.3.D	Single vertical canal intact	102
5.3.D.a	Single anterior canal intact, S0	102
5.3.D.b	Single anterior canal intact, I0	102
5.3.D.c	Single anterior canal intact, SR	103
5.3.D.d	Posterior canal intact, S0	103
5.3.D.e	Posterior canal intact, SR	103
5.3.D.f	Single posterior canal intact, I0	104
5.3.E	Four vertical canals ablated, utriculi intact, S0, I0, SR.	104
5.3.F	Single utricle intact, S0	104
5.3.G	Unilateral ablation of the utricle and vertical canals.	105
5.3.H	Two utriculi ablated.	105
5.3.I	Modelling of the semicircular canal system	105
5.3.J	Myographic activity to static tilts after ablating four vertical canals and the right utricle	107
5.4	Discussion	108

REFERENCES

Chapter 1. GENERAL INTRODUCTION.

GENERAL INTRODUCTION.

The compensatory eye and head movements assist stability of gaze and of posture. In animals capable of moving both their head and eyes by a reciprocal coordination of the two, the retinal image slip is stabilized. It was suggested by Walls (1962) that the requirement for image stabilization has initiated the evolution of eye movements. A relatively stable image would be more susceptible for neural analysis than a moving one, and visual performance therefore would be improved.

The experiments performed on vertebrate species have established that sensory information which originates in the vestibular system is significantly involved in establishing the relationship of the head in space (Camis and Creed, 1930). The semicircular canals and labyrinth code head position and the angular and linear acceleration of the head. Angular head accelerations are primarily perceived by the semicircular canals (Lowenstein & Sand 1940; Egmond, Groen & Jongkeets, 1949; Money & Scott, 1962). The utricle and saccule sense changes in linear velocity of the head movements or the static position of head in space (Lowenstein & Roberts, 1950; Jongkeets, 1950).

The anatomy and physiology of the vestibulo-ocular reflex (VOR) and its components have been extensively studied. Central vestibular mechanisms responsible for the processing of vestibular input and the generation of VOR have been thoroughly analysed in mammals (Buttner, Henn & Young, 1981) in amphibians (Blanks & Precht, 1976) and in fish (Allum, Graf, Dichgans & Schmidt, 1976, Allum & Graf, 1977).

Elasmobranchs such as the lesser-spotted dogfish (*Scyliorhinus canicula* (L.)) provide an interesting subject for comparative physiological and neurobiological studies, as these animals possess a body form and organization that reflects the early developmental

stages of other higher vertebrate. Also the eye reflexes in three dimensions ^{are} controlled by a small number of discrete muscles and a detailed analysis of the VOR by the extra-ocular muscles (EOM) can be made. Due to an easily accessible labyrinth the eye movements in these animals can be induced through several reflex pathways.

Harris (1965) has recorded and classified the eye reflexes in a freely swimming dogfish. He demonstrated five categories of the eye movements in a freely swimming fish that included compensatory eye movements, swimming eye movements, turning eye movements, fine eye movements, and the protective eye reflexes.

The sense organs of the vestibular apparatus, especially the semicircular canals, show marked similarities throughout vertebrate species. Because of these similarities and due to the easy accessibility of the elasmobranch vestibular apparatus the studies of primary afferent fibre responses to physiological stimulation of the vestibular system in ray and dogfish have been regarded as fundamental to understanding of sensory transduction process of semicircular canals (reviewed by Lowenstein, 1974; O' Leary et al., 1974; O' Leary, Dunn, Honrubia, 1976).

The horizontal VOR in vertebrate species have been studied in detail and various aspects of the system in general and at the neuronal level have been worked out.

Horizontal VOR.

Extensive studies of the horizontal VOR have been made. This reflex is induced by the angular displacement of the cupulo-endolymph system of the horizontal semicircular canals evoked by angular acceleration of the head in the horizontal plane (reviewed by Mayne, 1974).

Harris (1965) has investigated the horizontal VOR in the elasmobranchs and it was concluded that eyes of a freely swimming dogfish were undercompensated by 15° (during the $\pm 25^{\circ}$ head rotations eyes were counter-rotated by only 10°). His results have suggested a control of these eye reflexes by central programming and by the vestibular input.

A more complete and detailed assessment of the horizontal VOR were made by Easter & Johns (1974). In their experiments on the goldfish they have compared the eye movements of a visually deprived fish with the normal animal and have also compared the eye reflexes of an intact fish after ablating its functional horizontal semicircular canal. Since the nystagmic response persisted in the absence of the horizontal canal but in the presence of vision, these results have suggested a possible control of nystagmic eye movements primarily by a visual stimulus and to some extent by inputs from the semicircular canals. The control of saccadic eye reflexes in the brain stem was also determined by Easter (1972). These studies have concluded that the ability to stabilize the retinal image of the environment by means of the compensatory eye reflexes develop very early in a fish's life. These movements depend critically on non visual signals and to a lesser degree on visual signals and it has been suggested that the neuronal control of these eye movements is exerted by the brain stem posterior to the telencephalon.

In monkeys Bizzi, Kalil, Tagliasco (1971) and Bizzi et al. (1972) have revealed the nature of the horizontal eye reflexes and have concluded that these movements were controlled by proprioceptive signals from the neck and the labyrinth without the help of visual information.

Investigation of the horizontal vestibulo-ocular reflexes at the neuronal level.

A control of the vestibular input and the generation of vestibular reflexes has been studied extensively in the mammals (eg Buettner, Buttner & Henn, 1978), in frogs (Blanks, Pracht & Giretti, 1977) and in goldfish (Allum, Graf, Dichgans & Schmidt, 1976).

The existence of efferent discharges in the vestibular nerve of frog during the horizontal and vertical rotations was first neurophysiologically investigated by Gleisner & Henriksson (1963), and Schmidt (1963). They demonstrated the generation of the contralateral efferent impulses as a result of semicircular canals and utricular stimulation. Llinas & Precht (1969) have experimentally proved in mammals that not only vestibular nystagmus but also the optokinetic nystagmus and spontaneous fixation movements are correlated with discharge frequency modulation in the peripheral vestibular nerve and have suggested the identification of eye movement related neurons among efferent neurons on the basis of their bidirectional activation in response to vestibular stimuli or by recording from the proximal stump of the vestibular nerve. Schmidt, Wist & Dichgans (1971) have recorded the saccadic eye movements in goldfish that resulted from the efferent frequency modulation in the vestibular nerve. Their experimental work, in which they have demonstrated the non-activation of any neuron with ampullo-petal and its inhibition with ampullo-fugal vestibular stimuli, has provided the basis for consideration that phase modulation of these neurons was always linked with the saccadic eye movements and they have not found it in the pursuit eye movements and in the slow phases of a nystagmus.

Compensatory eye movements in the monkeys (Skavenki, Robinson, 1973) has been known to be extremely effective over a certain range of

the frequencies (0.01Hz-0.5Hz and up to the rate of 6.5Hz). They have suggested a possible input to the reflex by the semicircular canals. Fuchs & Kimm (1975) have recorded the unit activity in vestibular nuclei of the alert monkeys during horizontal head and eye movements. They have discovered the groups of neurons within the vestibular nuclei on the basis of their functional characteristics. The units sensitive to the vestibular stimulus alone and to the eye movements were identified. In alert animals an equal number of ^{each} units of ^{the} two types were identified, the first of these responded to the ipsilateral accelerations and the units of second type responded to the contralateral acceleration. Based on the behaviour of these two types of units it was suggested that discharge patterns of both unit types were appropriate to participate in the compensatory eye movements of vestibular origin.

The spontaneous activity of semicircular canal afferent neurons enables them to respond in a bidirectional manner, increasing their firing rate during the head rotations in one direction and decreasing it during the rotations in the opposite direction (Lowenstein & Sand, 1936). In mammals it was recorded by Markham, Yagi & Curthoys (1977) that the ablation of one labyrinth reduced the sensitivity of vestibular neurons to the head rotation. Blanks & Precht (1976) have suggested that in cats bilateral interactions are more strongly developed and the reciprocal innervation might have been significantly involved in determining the rotation responses of central neurons, to supply the animal with accurate bidirectional information.

Montgomery (1983) has established that at lower frequencies there was a larger phase delay in the response of the central vestibular neurons than that of primary afferents and as a result the phase of the vestibular neuron response was insensitive to the stimulus

frequency. While in mammals (Shimazu & Precht, 1965; Johns & Milsum, 1971; Schinoda & Yoshida, 1974) it has been established that the rotation responses in the vestibular nuclei are essentially similar to that of the vestibular afferents.

In goldfish the single unit activity in the abducens nucleus has been recorded simultaneously along with the eye movements by Gestrin & Sterling (1977). In these studies two cell types were identified as possibly to be the motoneurons and it was suggested that the mechanism regulating the amplitude and velocity of the slow and fast eye movements appear to be different. Fast eye movements are initiated by simultaneous firing of all the phasic-tonic cells, and therefore the amplitude and the velocity of saccades could only be regulated by the various parameters of the phasic burst of spikes. Slow movements are controlled both by the recruitment and by tonic firing frequency.

In their experiments on goldfish, Allum, Graf, Dichgans, and Schmidt (1976) has established that responses to horizontal body rotation in the dark were similar to those observed in the vestibular nerve afferents. The optokinetic nystagmus response in this experiment was proved to be direction specific, but on the contrary the vestibular responses exhibited a tonic response to the constant velocity. In the light, responses to the body rotations were found to combine linearly the vestibular and optokinetic effects to obtain the accurate velocity information for the sensory and motor functions.

Montgomery (1983) has reported that the operating frequencies of oculo-motor neurons in the carpet shark are considerably lower than those reported in other animals. In mammals the oculomotor firing rates are highest (Fuchs & Luschei, 1970). In goldfish the firing rates are also comparatively high (Hermann, 1971. Gestrin & Sterling, 1977). The lower firing rates in the carpet shark have been thought to

be correlated with the poorly developed saccadic system in these fish.

Baarsma & Collewijn (1974) have studied the gain and phase of the eye reflexes as a function of change in the stimulus frequency and they concluded that the phase was very obviously a function of the stimulus frequency.

Vertical VOR.

Compared to the horizontal VOR, the VOR in the vertical plane has been less extensively studied, and only a few reports are available in mammals.

Darlot, Barneo, Tracey (1981) have measured asymmetries in the vertical VOR and have reported that gains measured in the absence of the visual stimuli for vertical VOR are generally larger for the downward response than the upward response. In this respect they are different from horizontal VOR, which are reported to be symmetrical in the absence of visual stimuli (Robinson, 1976. Davis, 1978).

Snyder & King (1988) investigated the vertical vestibulo-ocular reflexes in the cat. Their experiments have described a velocity of eye movements immediately after the onset of head rotation (during the first 2 seconds) and by characterizing the early time course of VOR they have suggested that only the first few seconds of VOR are necessary for visual stabilization. The reflexes employing visual rather than vestibular input accurately stabilize the persistent image movement across the retina after this time (also reported in monkeys by Miles, Kawano & Optican, 1986).

Snyder et al. (1988) have also reported that vertical VOR gain adaptation in relation to the head rotation was symmetrical during upward and downward rotations.

The existing literature lacks information about the operation of

vertical VOR in fish. Since fish swimming behaviours are comprised of movements about three primary axes the pattern of VOR in the vertical plane is equally significant and needs to be explained in the roll and pitch planes.

Vestibular input to the EOM response.

The compensatory vertical as well as horizontal eye movements induced by the vestibular apparatus involve activity carried by VOR to the EOM.

Semicircular canal input.

It was demonstrated by Cohen, Suzuki, Shanzer, Bender (1964) that in mammals the reflex contraction of an EOM induced by an electrical stimulation of a semicircular canal was effectively depressed by preceding stimulation of another canal, which has indicated an inhibitory interaction between the VOR arising from different canals.

Ito, Nisimaru & Yamamoto (1976) have experimentally concluded that in rabbits inhibitory interaction in the VOR occurs in three particular combinations of the testing canals: anterior and posterior canals of the same side, anterior and posterior canals of the opposite side, and horizontal canals of the opposite side.

Highstein (1972, 1973) has recorded intracellularly and extracellularly from the motoneurons in the IIIrd and IVth cranial nuclei of anaesthetised rabbits and has identified five subgroups of the neurons innervating the SR, IO, IR and MR and the SO (IV) by their antidromic activation from the branches of the III and IVth cranial nerves. In the SR, IO, IR and IV subgroups the effects of the ipsilateral VIII nerve stimulation were inhibitory producing disynaptic IPSPS, while the effects of the contra-lateral VIII nerve

stimulation were excitatory producing di-synaptic EPSPS. In the MR subgroup a mixture of the EPSPS and IPSPS was produced by VIII nerve stimulation.

It was demonstrated by several authors that the discharge frequency in the vestibular nerve fibres from the horizontal canal of fish or frog is increased by the ipsilateral horizontal acceleration and decreased by opposite rotation (Lowenstein & Sand, 1940; Ross, 1936).

The classic studies of the system have demonstrated that the cupula-endolymph system responds to the changes in angular velocities (Steinhausen, 1931. Lowenstein & Sand, 1940; Precht, Linas & Clarke, 1971) This system however lacks the information about constant velocities for motion control, and therefore the vestibular system is deficient and supplementary sensory information is required. In goldfish it was experimentally demonstrated that this supplementary information about the constant velocity movement of the body is provided by the visual sense.

The response characteristics of the afferent nerve fibres from the semicircular canals have been determined in a variety of vertebrates with regard to both spontaneous and evoked activity (Goldberg & Fernandez, 1971; O'Leary et al., 1974; Blanks, Estes & Markhem, 1975).

Lowenstein & Sand (1940) first reported a class of higher threshold units which are silent at rest and which discharge only in response to rotation in one direction. Oman, Frishkop & Goldstein (1979) have also reported the recruitment of these units with progressively larger spike amplitudes during excitatory caloric stimulation of semicircular canals. Taglitti, Valli & Casella (1973) have reported that in frog the efferent nerve spike size was related to the threshold.

The semicircular canal reflexes in terms of their input to myographic activation of EOM was predicted by Lowenstein & Sand (1940). Based on these suggestions the reflex activation of different EOM by different combinations of semicircular canals have still to be experimentally tested. The myographic activation of EOM in the roll and pitch planes needs to be determined. Also these responses have to be checked at intermediate planes to determine the integration of vertical canal outputs during the operation of vertical VOR. Also the control of vertical VOR by the semicircular canals and the utricle needs to be determined.

Possible contribution of the otolith organ.

The low frequency response of the otolith to the sinusoidal roll tilt was derived by Barmack (1981). From his experiments he has suggested that the utricle would be suitably involved in detecting low frequency changes in the head position in the vertical VOR.

It has been considered that static tilt responses originate from the otolith organs. It was established by Lowenstein & Roberts (1950), Fernandez, Goldberg & Abend (1973) and Loe, Tomko & Werner (1973) in recordings from the primary afferents in many vertebrate species that firing of the utricle afferents are roughly proportional to the sine of the angle of the tilt. Also the static tilt responses have been recorded by Fernandez (1963) and Shimazu & Smith (1971) from single brain stem vestibular neurons, and their utricular origin was confirmed by the fact that the response persisted at the lowest tested frequency of the tilt (0.01Hz). Within the utricular receptors an origin for the dynamic response has also been recorded in the ray (Lowenstein & Roberts, 1950) and in cat (Vidal, Jeannerod, Lifschitz, Levitan, Rosenberg & Segundo, 1971). This effect consisted of a

directional component to the tilt response approaching a given position from the opposite directions. It was suggested that this effect could be due to neural adaptation (Goldberg & Fernandez, 1971).

Schor (1974) has made extracellular recordings in the lateral and the inferior vestibular nuclei of cats and has studied the firing patterns of single units using small amplitude sinusoidal roll tilts at a low frequency range (0.01Hz-1.0Hz). He concluded that in the majority of the tilt-sensitive units firing rates were increased by increasing the frequency of the sinusoidal roll tilt. He also checked these responses after plugging the semicircular canals and suggested a probable origin of these units in the utricle, since they remained unchanged in the absence of semicircular canal input. These results have been confirmed by Peterson, 1970; Schimazu & Smith, 1971).

Little is known about the utricle input to EOM in fish, the nature of these reflexes and how they affect the myographic activity of EOM in the absence of semicircular canal input.

Physiological profile of EOM.

The EOM are highly organized striated muscles. They are required to make extremely rapid movements, as when the gaze is suddenly shifted, or during scanning eye movements. They must also produce sustained contractions for long periods, in maintaining the position of the eyes during imposed head and body tilts.

Six EOM are consistently present in craniates and among fishes they are similar in innervation and in their position within the orbit. There are two oblique muscles, the superior oblique (SO) and the inferior oblique (IO), and four rectus muscles, the superior rectus (SR), the inferior rectus (IR), the external rectus (EXT-R) and the internal rectus (INT-R). The motor innervation of EOM is carried

by three cranial nerves: branches of the oculomotor nerve (CNIII) innervate IO, SR, IR, and INT-R muscles, SO receives a branch of the trochlear nerve (CN IV) and EXT-R is innervated by the abducens nerve (CN VI).

Since the eye movements in three dimensions are controlled by EOM their physiological properties, ultrastructural features and innervation are significant in determining their role in different types of eye reflexes. The EOM structure and physiology is a well studied subject and reflects the differences related to different modes of life and relative use of the eyes according to the animal's special needs.

The structure of vertebrate skeletal muscle provides a basis for the identification of different fibre types within the EOM. Based on differences in the histochemical and immunohistochemical staining, ultrastructural features and innervation of the fibre types, two main fibre types have been identified and named as **slow** and **fast**.

The ultra-structural features most commonly used to distinguish fibre types include size and shape of the myofibrils, amount of sarcoplasm (Hess, 1970), and in case of slow fibres the absence of M-line in the middle of A-band and a wavy Z-line.

The work of Peachy^e & Huxley (1962) has identified single slow fibres by measuring their contraction speed in response to direct electrical stimulation. In a review by Hess (1970) the muscle fibres that can respond to a nerve stimulation with a prolonged contraction and that usually do not exhibit an action potential have been named as **slow** fibres.

Certain differences have also been reported in the innervation of the two fibre types. According to these reports the slow muscle fibres are innervated by multiple nerve terminals of the engrappe type, while

the twitch fibres have been innervated by a single end plate of en plaque type. It has also been demonstrated that small motor nerve fibres innervate slow fibres, whereas large nerve fibres innervate twitch fibres (review by Morgan & Proske, 1984).

As far as the physiological profile of the vertebrate slow fibres is concerned it always reflects an overall high ratio of oxidative metabolism to ATP consumption rate. In the amphibia the consumption rate (reflected by m-ATPase activity) is extremely low. Consequently metabolic supply capacity is itself low compared with that of most twitch fibres. Thus mitochondria, oxidative enzymes such as SDH, lipid droplets and glycogen stores are all sparse (Morgan & Proske, 1984). However in other vertebrate classes including both teleosts and elasmobranchs m-ATPase activity, while less than in fast fibres, is still appreciable. Consequently they have moderate or high levels of oxidative metabolism as indicated by all the above markers (Morgan & Proske, 1984; Bone, 1966).

Based on the ultrastructural characteristics, innervation and physiological profile of the fibre types within the vertebrate groups, it proves nearly impossible to segregate the muscle fibre types as true slow or true fast fibres and various subgroups of the two fibre types have been known to exist. Morgan & Proske (1984) have reviewed the slow fibre types among vertebrates and proposed different categories. 1. Fibres that do not propagate action potentials and do not relax in the depolarizing solution, are called slow fibres; they are apparently multiply innervated. 2. Fibres that maintain a contracture but are also able to twitch are called intermediate or tonic-twitch fibre types. They are also multiply innervated. 3. Fibres which have ^{only} some features of the slow fibres, like multiple

innervation and which do not respond to a single nerve stimulation (non-twitch); these fibres appear structurally more like twitch (fast) muscle. 4. Normal **twitch** fibres which include those with very slow contraction speed but which always produce a measurable contraction in response to a single nerve impulse.

The fish myotomes are comprised of ^{both} **slow** and **twitch** fibres. The **slow** superficial fibres are referred to by various authors as red fibres, and the mass of the myotome is comprised of more deeply located **twitch** fibres which have been termed white. In many fish, fibres located between the **slow** (red) and **twitch** (white) fibres are commonly recognised as intermediate fibres and are intermediate in color (pink) as well as location (Bone, 1978).

In the existing literature reports are available on the innervation pattern of the red and white muscle fibres. Stanfield (1972) has reported that red fibres in fish have engrappe endplates and are slow-contracting non-twitch fibres that do not propagate action potentials. The earliest data in this context was provided by Hess (1961) in his work on fast extrafusar fibres and their nerve endings in mammalian EOM. He established that engrappe endings occur on the **slow** fibres and the fibres with enplaque type endings were suggested to be fast fibres. Based on the physiological studies in the cat (Hess & Pilar, 1963. Matyushkin, 1961. Bach-Y-Rita & Ito, 1966 and in rabbits (Kern, 1965) the fibres with engrappe nerve endings were called **slow tonic** or **slow** multi-innervated **twitch** fibres. The fibres with enplaque endings were named **fast twitch** fibres.

Peters & Mackay (1961) have named the ^{body wall} muscle fibres of the lamprey as parietal and central. Electron microscopic studies have revealed that myofibrils of the parietal muscles are more widely separated by the sarcoplasm than those of the central fibres. From

their micrographs it appears that both kinds of fibres have an M-line. The parietal muscle fibres of the lamprey have multiple terminals. The central fibres are innervated at both ends. The parietal muscle fibres does not exhibit folds under the multiple nerve terminals.

In elasmobranchs the red superficial fibres of the myotome are innervated by several small engrappe type terminations and they do not have propagated action potentials, while the intermediate pink and deep white fibres are innervated by an individual ending located at one end of the fibre and have propagated action potentials (Bone, 1966).

Nishihara (1967) has correlated the innervation with the ultrastructural features of the red and white muscle in carp and reported that both red and white fibres have well developed sarcoplasmic reticulum, M-lines, and triads at the level of Z-line. Both fibre types appear to have multiple terminals with smooth membranes between nerve terminals and muscle fibres. The fibres do differ in the distribution of their multiple terminals; the red fibres have densely grouped nerve terminals in some areas. The distance between the multiple nerve terminals is not given. The red fibres are similar physiologically to **slow** fibres, the white fibres to **twitch** fibres. However Bergmann (1964) has concluded that it is not necessary for red fibres to be of **slow tonic** type. In his studies of the muscle fibres in the dorsal fin of the sea horse, apparently red in color, it was demonstrated that the mechanical properties of these muscles showed that they are are fast enough to be considered as twitch fibres. Bergman considered the red fibres in the sea horse to be twitch fibres that have multiple nerve terminals without sarcolemmal infoldings under them and established that slow fibres could sometimes be innervated multiply.

Teravainen (1971) has analysed the lamprey body wall muscle and concluded the parietal fibres stain intensively for oxidative enzymes, whereas central fibres stain weakly (Meyer, 1979). Pre-incubation of the tissue at different pH values has revealed the acid-resistant myosin-ATPase activity only in the fibres of the parietal layer, which are presumably **slow** fibres. The synaptic junctions on parietal fibres were also typically of a **slow muscle**.

In general red muscle ^{in Fish} is considered to be **slow**. However as various studies have suggested in some fish, red fibres do not constitute a uniform population but several functionally distinct fibre types. It is likely that red fibres are able to twitch and the suggestion has been made, based on the protein composition of red and white teleost muscles, that they should be compared with the **slow-twitch** and **fast twitch** mammalian muscles (Hess, 1970).

Fibres intermediate between the twitch and true slow fibres according to most structural criteria were named as Type 4 by Smith and Ovale (1973). They were identified as intermediate on mechanical grounds. These fibres were characterised by staining weakly for myosin-ATPase and succinate dehydrogenase and by a low fat content, low mitochondrial volume, a thick Z-line, an irregular M-line and a poorly developed sarcoplasmic reticulum.

In all EOM, near the insertion of these muscles with the eye ball, the fibres are arranged in two distinct regions; there is an outer region of small fibres generally recognized as the orbital region and an inner region of comparatively large fibres known as the

global region.

On the basis of their histological profile, contractile activity (myosin-ATPase), oxidative potential (succinate dehydrogenase), glycolytic tendencies, ultrastructure and their response to an electrical or mechanical stimulus, several functionally different fibre types have been identified and classified in vertebrate species (Hess, 1963; Zenker and Azenbacher, 1964; Dietert, 1965; Pilar & Hess, 1966; Cheng & Brenin, 1966; Mukuno, 1967; Miller, 1967; Mayer, 1971; Kordylewski, 1974; Davey, Mark, Marotte & Proske, 1975).

Ultrastructural studies of lamprey EOM have distinguished three (Witalinski & Labuda, 1982) fibre types. In teleost EOM two fibre types have been reported (Kilarski & Bigaj, 1969; Kordylewski, 1974; Davey, Mark, Marotte & Proske, 1977). Based on their histochemical profile two fibre types have been known to exist in amphibians (Nowogrodzka-zagorska, 1974) and in grass snake (Witalinski & Loesch, 1975). Three fibre types have been identified in the lizards (Kaczmarewski, 1969) and in birds (Kaczmarewski, 1970). In mammals the number varies and ranges up to six (Pachter, Davidowitz & Brenin, 1976). Among these fibre systems, the first classification in fish, amphibian and mammalian EOM (revised by Buchthal & Schmalbruch, 1980) recognised small, orbital, slow Type I fibres and mostly large, global, fast twitch Type II fibres (Close & Luff, 1974). Several subpopulations of these two fibre types have been identified in different vertebrate groups.

The physiological studies in vertebrate EOM and in dogfish myotomal muscles provide a basis to investigate the number of fibre types present within the dogfish EOM. How do these types compare with the other vertebrate EOM in terms of their enzyme content, contractile properties and innervation? Do both, or only one fibre type,

contribute to the VOR at vertical plane? Since eye reflexes at the horizontal and vertical planes are reported to be different it is interesting to know if these differences can also be found in the structure and physiology of the horizontal and the vertical EOM.

Chapter 2. PHYSIOLOGICAL PROFILE OF EOM

2.1 INTRODUCTION

2.1.A Contractile and physiological profile of EOM.

In the EOM as in other striated muscles, the ATP molecule is attached to the globular head region of the myosin molecule and it is the energy-releasing hydrolysis of ATP that drives the reaction, which in turn produces the muscle contraction. Barany (1967) has demonstrated that the speed of muscle contraction is directly proportional to its myosin-ATPase activity.

Histochemical procedures have demonstrated the differences in the myosin-ATPase content of small orbital (Type I) fibres and large global (Type II) fibres. The results obtained from lamprey (Witalinski & Labuda, 1982) have demonstrated a high myosin-ATPase activity in the thin (orbital) fibres and comparatively low activity in thick (global) fibres. On the other hand histochemical data of dogfish myotomal muscles (Bone & Chubb, 1978) have indicated a progressive increase in myosin-ATPase activity from the superficial red (Type I) fibre layer towards the white (Type II) fibre region. Similar results have been reported by Johnston, Davison & Goldspink (1977) for carp muscles.

The classification of muscle fibre types on the basis of myosin-ATPase activity is sometimes complicated by the presence of two qualitatively different kinds of myosin-ATPase (Guth & Samaha, 1969). The myosin-ATPase isolated from the mammalian slow-contracting soleus muscle (known to contain 98% slow fibres) shows relative acid stability and alkali lability of the Ca^{2+} activated myosin-ATPase. Conversely the myosin-ATPase of flexor hallucis longus muscle (known to have 90% fast fibres) shows alkali stability and acid lability.

Mammalian EOM are composed of both fast-and slow-contracting components. The Type I fibres show an alkali labile and acid stable

myosin-ATPase reaction like slow skeletal muscle fibres. The Type II fibres demonstrate alkali stable and acid labile myosin-ATPase, similar to that of fast skeletal muscle fibres (review by Morgøn & Proske, 1984)

ratio of $\frac{\text{m-ATPase consumption}}{\text{oxidative potential}}$

Since the $\frac{\text{m-ATPase consumption}}{\text{oxidative potential}}$ determines the resistance of muscle fibres to fatigue, the muscle fibre types in vertebrate skeletal muscles are widely classified by combining the reaction of myosin-ATPase with physiological and metabolic properties (Brook & Kaiser, 1970; Peter, Barnard, Edgerton, Gillespie & Stempel, 1972; Burke, Levine, Tsairis & Zajac III, 1973). Based on this scheme a wide heterogeneity of fibre types has been described in skeletal muscles and EOM of mammalian species (Peachey, Takeichi & Nag, 1974; Alvarado & Vonhorn, 1975; Vita, Mastaglia & Johnston, 1980; Gueritaud, Horcholle-bossavit, Thiesson & Tyc-Dumont, 1984). The three most generally recognized types are: Type I slow-oxidative belonging to slow-contracting fatigue-resistant motor units; Type IIA fast-twitch glycolytic/oxidative, belonging to fast-contracting fatigue-resistant motor units and Type IIB fast-twitch glycolytic, belonging to fast-contracting, fast-fatiguing motor units. In the case of fish, studies have been made only for the lamprey EOM, in which small fibres of the orbital region (Type I) demonstrate high SDH activity compared to the large fibres of global region (Type II).

In mammalian skeletal muscles and EOM, several detailed accounts of immunohistochemical staining of fibre types have been made and the results of these experiments have revealed the nature of the unique contractile properties of fast and slow fibre types (Pierobon-Bormioli, Sartore, Dalla-Libera, Vitadello & Schiaffino, 1981; Rowlerson, Pope, Murray, Whalen & Weeds, 1981; Sartore, Mascarello, Rowlerson, Gorza, Ausoni, Vianello & Schiaffino, 1987).

No immunohistochemical staining has been performed on fish EOM. There is also lack of data in the fish EOM for the identification and description of different fibre types histochemically and the confirmation of the nature of these types by immunohistochemical methods.

2.1.B Ultrastructure distinction of fibre types.

The experiments based on ultrastructural studies have revealed differences in mitochondrial densities, position of triads and development of sarcoplasmic reticulum (SR) between the two fibre types. In vertebrates, Type I fibres have a relatively poorly-developed capacity for aerobic and anaerobic metabolism their mitochondrial densities are generally less, the mitochondrial cristae are poorly developed (Ovale, 1982) and the position of the triads is at the level of the A/I junction (Kilarski & Bigaj, 1969).

The ultrastructure of fish EOM has been extensively studied in Carassius (Davey et al, 1975) and carpet shark (Hously & Montgomery, 1984). Type I fibres in these studies appear to be rich in mitochondria, with little SR and infrequent, dispersed triads. Type II fibres have regular myofibrils, with extensive SR, triads located at the Z-disc and a pronounced H-band and M-line. However these ultrastructural features of the carpet shark muscle were not correlated with its contractile and metabolic properties, so the functional significance of the differences found in the two fibre types has not been interpreted.

2.1.C Response to a mechanical stimulus.

The mechanical responses of isolated red and white fibre bundles have been investigated in teleost fishes (Fliteny & Johnston, 1979).

The results obtained for mechanical responses of isolated red and white fibre bundles in teleosts have demonstrated differences in the pattern of the activation of the two fibre types. Only white fibres (similar to Type II in case of EOM) responded to a single stimulus. The red fibres (Type I) responded only at frequencies above 5Hz and 10Hz. Both fibre types were able to produce graded fused tetani. Type I fibres have been identified in EOM of mammalian species and it has been suggested that these slow fibres have mechanical properties similar to those of amphibian slow muscles. Cat EOM gave a fused tetanic contraction only when stimulated at 30Hz (Hess & Pilar, 1963; Bach-y-Rita & Ito, 1966, Pilar, 1967). In some other experiments on cat and monkey EOM, no evidence was found for a contractile component which could produce contraction at lower frequencies (Barmack, Bell & Rence, 1971; Fuchs & Luschei, 1971) and it was suggested that slow fibres were unlikely to contribute any significant tension during eye movements. The slow fibres studied in the EOM of cat and rabbit gave a smooth contraction at all frequencies (Matyushkin, 1964). Maximum tension was developed at 100Hz and contributed about 10% of the whole muscle tetanic tension. However there are no data available to explain the mechanical responses of fish EOM.

2.1.D Innervation.

There is experimental evidence that EOM are provided with more than one type of innervation (Bach-Y-Rita, 1971, 1975); polyneuronal as well as focal innervation has been found in several vertebrate species (Peachy, 1971; Lennerstrand, 1972). In mammalian EOM it has been reported by Kackzmarski (1974) that Type I fibres are innervated by motor endplates of the engrappe type, while the Type II fibres are innervated by single endplates of the enplaque type.

In a review by Hudson (1969) it was suggested that the majority of teleost myotomal muscle fibres of the slow (Type I) and fast (Type II) were both innervated by multiple nerve endings. Only in a few teleost species and in elasmobranchs (Bone, 1964, 1966) and hagfish (Jansen, Anderson & Janson, 1963), have fast (Type II) muscle fibres been found with focal innervation.

2.1.E Aims of the project.

Slow and fast motor units in mammalian EOM have been known to have distinct histochemical profiles (Gueritaud et al, 1984). In fish there is very little known about functionally segregated and histochemically or mechanically identifiable motor units.

Although properties of EOM fibre types have been studied and described in terms of their functional significance, no direct correlation of the physiological, contractile and mechanical properties has been made with the innervation of these fibre types to explain the heterogeneity in the responses of EOM. Since eye nystagmus is comprised of slow (compensatory) and fast (nystagmus) responses, it could be that two functionally identifiable components are also present in EOM. In the present study an attempt has been made to identify and segregate these two components.

The size of muscle fibres and their location in the EOM play a significant role in determining their histochemical and immunohistochemical properties. A quantitative analysis has been made to obtain a more detailed picture of the relationship between fibre sizes and their physiological profiles.

2.2 MATERIAL AND METHODS.

2.2.A Histochemical procedures.

Dogfish (Scyliorhinus canicula (L)) were anaesthetised with a high dose of MS222 (20mg/litre) and dissected immediately to remove the EOM from the orbit. The location of EOM within the orbit is shown in Fig 2.1. The tissue sample was then cut into smaller pieces, which were mounted in a drop of Tissue-tek II O.C.T compound on a piece of cork. In some cases, as a control, a piece of lateral ^{body wall} muscle was mounted together with the EOM. The cork piece was immersed in isopentane (which itself was chilled with liquid nitrogen) to rapidly freeze the tissue (<2 seconds). Direct immersion in liquid nitrogen actually cools tissues less rapidly because they become insulated by an envelop of nitrogen gas. For short-term storage frozen blocks were placed in either the cryostat or in an ordinary deep freeze at -20°C . For long-term storage the frozen blocks were kept in a deep freeze at -70°C to maintain the enzymatic activities of the muscle fibres.

The composite blocks of EOM with lateral muscle were cut serially in a cryostat, taking sections from near the insertion of EOM with eye ball. These were taken up on coverslips and incubated for myosin-ATPase, succinate dehydrogenase (SDH) and immunohistochemical staining procedures.

2.2.A.a Myosin-ATPase staining techniques of Bone & Chubb (1978).

Initially the method of Bone and Chubb (1978) used for staining of fish body wall muscles was tested for myosin-ATPase staining of EOM. The following steps were followed:

1. Preincubate the sections in 0.2M di-ethanolamine at pH 10.4 for 1-5 minutes. add 3g of urea for 100ml.

2. Blot around the sections and back of the coverslip. Put the sections in incubating solution (4ml of 0.18 CaCl_2 + 36ml 0.2M di-ethanolamine solution at pH 9.4 and 60.8mg ATP [2.5mM in final solution] + 148mg KCL).
3. Rinse in three changes (30s each) in 0.18M CaCl_2 .
4. Transfer to 0.01M CoCl_2 solution for two minutes.
5. Four rinses (30s) each in 0.2M Di-ethanolamine adjusted to pH 9.0.
6. Develop in 2% Ammonium sulphide solution for two minutes.
7. Tap water rinse.
8. Fix in 5ml of 4% formaline solution + 42.5ml sea water + 42.5ml distilled water.
9. Mount in glycerol.

In order to avoid the floating of sections off the slides, gelatine coated slides were used.

The second technique tested was that of Snow (1982) which was originally used for mammalian (dog skeletal) muscle. Urea (3g for 100ml) was added to the incubating solution. The method finally approached was:

2.2.A.b Myosin-ATPase staining with alkaline pre-incubation.

1. Pre-incubate sections for 20 minutes in alkaline buffer (0.075M Na Barbital + 0.01M Na acetate + 0.1M CaCl_2 adjusted to pH 9.4-10.4 with NaOH + 3g urea for each 100ml of solution).
2. Incubate sections in alkaline buffer for 30 minutes at room temperature. ATP added to incubating solution ie 5mg/ml.
3. Three rinses in 0.2M CaCl_2 .
4. Put sections in CoCl_2 for two minutes.
5. Distilled water rinse.
6. Develop in 1% Ammonium sulphide solution for one minute.

7. Tap water rinse.
8. Dehydrate and mount.

2.2.A.c Myosin-ATPase staining with acid Pre-incubation.

1. Pre-incubate sections for 5 minutes in acid buffer (0.2M acetate + 3g urea for 100ml adjusted to pH 4.6-6.0) at room temperature.
2. Incubate sections for 60 minutes in solution of 0.075M Na Barbital + 0.01M CaCl_2 adjusted to pH 9.4-10.4 + 1.5mg ATP at room temperature.
3. Rinse in three changes with 0.2M CaCl_2 for two minutes.
4. Put the sections in CoCl_2 for two minutes.
5. Distilled water rinse.
6. Develop in 1% Ammonium sulphide solution for one minute.
7. Tap water rinse.
8. Dehydrate sections and mount in histomount.

2.2.A.d Mg^{2+} activated myofibrillar (m) ATPase

The staining technique of Mabuchi & Sreter (1980) was used for Mg^{2+} activated m-ATPase which gave the total m-ATPase content of EOM fibres. It involved the following steps:

1. Stock buffer solution.

40mM Na Barbital.

20mM CaCl_2 .

20mM MgCl_2 .

Make up total volume to 50ml + 1.2g urea + add 9mg ATP for each 10ml of the solution.

2. Incubate sections in stock solution from 15-30 minutes.
3. Remaining steps same as in above procedure (Sec. 2.2.A.c).

2.2.A.e SDH staining procedure by Pearse (1972).

The stock solution for the reaction was succinate buffer, that was made up of :

1 Vol 0.2M phosphate buffer + 0.2 Na succinate, final pH adjusted to 7.6.

Reaction:

1 Vol Succinate buffer.

1 Vol H₂O.

1mg/1ml Nitroblue tetrazolium.

2.2.B Immunohistochemical staining procedure.

The technique used for immunoperoxidase staining was a simplified version of the method described by Rowleson et al., (1981).

1. Incubate the sections overnight in antiserum (α ALD, α SHC raised against mammalian tonic fibres) diluted 1:2000 in 1% albumin containing phosphate buffered saline (PBS).
2. Rinse in PBS + 0.025% Tween 20.
3. Incubate sections in peroxidase labelled antirabbit IgG antibody (diluted 1:200 in PBS + 1% albumin).
4. Rinse in PBS + 0.025% tween 20.
5. Incubate sections finally in 0.03% H₂O₂ + PBS + 1mg/1ml Di-aminobenzidine.
6. Dehydrate through ethyl alcohol and HistoClear.
7. Mount sections in HistoMount.

2.2.C Acetyl cholinesterase staining.

Technique by James Toop (1976).

The six EOM were dissected from the orbit, and were frozen in

isopentane chilled with liquid nitrogen. The frozen blocks could be stored in cryostat, or deep freeze at (-20⁰C) for few weeks without affecting the acetylcholinesterase activity along the neuromuscular junctions. The reaction involved the following steps:

1. In cryostat cut sections, 20-100um thick (most often 20um).
2. Pick up sections on slides and dry at room temperature.
3. Incubate in acetyl choline medium for 9-12 minutes at 37⁰C.

Stock solution.

CuSO ₄	0.3gm
Maleic acid	1.75gm
Glyceine	0.375g
MgCl ₂ 6H ₂ O	1.0gm
1N NaoH	30.0ml
20-25% Na ₂ So ₄	170.0ml

For use dissolve about 20mg acetylcholine iodide in 0.1ml distilled water and add 10ml stock solution. Adjust to pH 5.5 with 1N HCl before use.

4. Three rinses in distilled water.
5. If necessary to prevent section loss, take slides to 100% alcohol, place in 0.5-1.0% celloidin (W/V) in 1:1 ether alcohol for 30s.
6. Rinse three times in distilled water.
7. Place in fresh 0.5% K₃ Fe (CN)₆ for 5-10 min at room temperature.
8. Rinse three times in distilled water.
9. Fix sections for 30 minutes at room temperature in either (a) buffered formol saline at pH 7.0 or (b) buffered formol calcium with cadmium and magnesium, adjusted to pH 7.0.
10. Wash in repeated changes of distilled water for 15-20 minutes.
11. Incubate in fresh 20% aqueous AgNO₃ containing 0.1% CuSO₄ 5H₂O from

20-30 minutes at 37⁰C, a small amount of CaCO₃ should be placed in the bottom of staining jar.

12. Rinse in distilled water for 30-60 seconds for optimal results.
13. Develop in 1gm Quinol or Hydro-Quinol and 5gm Na₂SO₃ in 100ml distilled water at room temperature for as long as necessary to demonstrate the innervation. Sections should be evenly golden brown all over. Use 2 baths of developer and allow sections to remain only 10 seconds in first bath.
14. Rinse 3 times in distilled water.
15. Fix in 5% Sodium Thiosulphate for 1-12 minutes.
16. Rinse 3 times in distilled water.
17. Dehydrate in graded alcohol, leave for 15 minutes in a mixture of equal parts of ether and alcohol to remove celloidin, clear in HistoClear and mount in HistoMount.

2.2.D Glutaraldehyde-Cocadylate fixation for TEM.

The processing of fish and dissection were the same as described in section 2.2.A.

Stock.

1M Sodium cacodylate	10-15gm in 50ml distilled H ₂ O.
1M Sodium chloride	5.844gm in 100ml distilled H ₂ O.
1M Calcium chloride	5.549gm in 50ml distilled H ₂ O.

Fixation.

1M Na. CaCod	10ml.
25% Gluteraldehyde	8ml.
1M NaCl	5ml.
1M CaCl ₂	0.05ml.

Filtered sea water 50ml.

Distilled water to make up to 100ml.

Buffer.

1M Na CaCod 10ml.

1M NaCl 20ml.

1M CaCl₂ 50ml.

pH adjusted to 7.6.

Filtered sea water 50ml.

Distilled water is added to make up to 100ml.

Osmium fixation.

1M Na CaCod 5ml.

4% OsO₄ 12.5ml.

1M NaCl 7.5ml.

1M CaCl₂ 0.025ml.

Filtered sea water 25.0ml.

pH of the stock solution is maintained at 7.6 before adding 4% OsO₄.

Two rinses.

EOM fixed in above stock for 100 minutes.

Rinse in distilled water for 70 minutes.

2 distilled water top rinses.

Dehydration.

30% 10min.

50% 10min.

70% 10min.

90% 10min.

100% 10min (2).

Dried absolute alcohol 10min.

3 rinses in the Epoxy-propane 5min each rinse.

1:1 mix of araldite + Epoxy-propane (overnight mixing on the rota mixer).

EOM were embedded in the fresh Araldite at 60⁰ for about 48 hours.

2.2.E Mechanical recordings

Recordings were made in an isolated nerve and muscle preparation that was dissected immediately before the experiment and was left in dogfish saline for the recordings. The motor nerve was stimulated by a suction electrode. The trigger input to the suction electrode received pulses from a pulse generator device. The mechanical response of the EOM was recorded by a force transducer. The signal from the force transducer was amplified, and was recorded on an FM tape recorder, or a pen recorder.

2.3 RESULTS.

2.3.A Myosin-ATPase activity of EOM.

Since differences have been found in the lability of myosin-ATPase, depending on the pH of pre-incubation, i.e alkaline/acid, sections from the same EOM were stained for three different reactions

- (1) Ca^{2+} -activated myosin-ATPase staining with alkaline pre-incubation.

- (2) Ca^{2+} -activated myosin-ATPase staining with acid pre-incubation.

- (3) Mg^{2+} -activated myosin-ATPase staining which gives the total myosin-ATPase content of fibres.

In order to identify the fibre types correctly, a piece of lateral muscle was stained along with the EOM as a control for all three reactions described above.

2.3.A.a Alkaline pre-incubation.

It was established in several experiments using all the EOM pre-incubated at room temperature (20°C) and for a range of pH between 9.0-10.4, that the best enzymatic activity and preservation of fibre structure occurred at pH 9.4. At this pH most of the small fibres in the orbital region were stained dark and most of the large fibres in the global region showed light staining for myosin-ATPase (Fig 2.2.A). However a few fibres situated in both orbital and global regions did not follow this pattern: some small orbital fibres were lightly stained and large global fibres were darkly stained (Fig 2.2.A). The reaction did not demonstrate a temperature sensitivity: when repeated at a temperature of 4°C , the intensity of the reaction in the small orbital and large global fibres remained the same as before. It was established in several different experiments that if the reaction continued after the standard incubation time (20 minutes) the pattern

and intensity of staining among small fibres of the orbital region and large fibres of the global region remained unaffected.

In the lateral body wall muscle at pH 9.4 and at room temperature the small fibres of the outermost layer were stained dark and the large fibres of the innermost layer were stained light with the myosin-ATPase, but in contrast to the EOM there was an intermediate layer of fibres that was intermediate in size between small and large fibres and stained relatively more darkly than the small fibres of the outermost layer (Fig 2.2.B).

2.3.A.b Acid pre-incubation.

Sections from the same EOM were pre-incubated at room temperature at a range of pH between 4.6-6.0. The preservation of muscle fibres varied with pH and a well defined pattern of enzymatic activity was only seen at pH 5.0-5.6. The small fibres of the orbital region which stained darkly at alkaline pre-incubation (Fig 2.3.A), and the few small fibres scattered in the global region also stained darkly at pH 5.6. The majority of poorly defined large fibres of the global region were stained light for myosin-ATPase, although again a small number stained darkly (Fig 2.3.A). With pre-incubation of sections in cold media (4⁰C) a better preservation of fibre structure was observed, but in contrast to alkaline pre-incubation the reaction was not significantly reduced (Fig 2.3.B).

For lateral body wall muscle unlike EOM at pH 5.6 and at room temperature, a better preservation of the fibre structure was demonstrated. As with the alkaline pH, two levels of staining

intensity were seen: the small fibres of outermost layer and the fibres intermediate in size were stained dark, while the large fibres were stained lightly with myosin-ATPase (Fig 2.4.A).

When incubated at 4⁰C, reaction has demonstrated temperature sensitivity and three levels of staining were observed. The fibres in the outermost layer were stained dark, while the fibres intermediate in size had the darkest reaction. Large fibres in the innermost layer were stained light (Fig 2.4.B)

2.3.A.c Mg²⁺-activated M-ATPase.

The incubation of sections in Mg²⁺-containing media demonstrated the total ATPase content of muscle fibres. The majority of small fibres of the orbital region showed light or no staining, while the majority of large fibres in the global region were either stained very dark or comparatively darker than M-ATPase negative small orbital fibres (Fig 2.5.A). The staining properties of muscle fibres were little affected by temperature. Different incubation times were tested and it was established in several experiments that staining of fibres continued after the standard incubation period of 20 minutes. Some fibres in the global region which appeared light after 30 minutes incubation attained maximum staining only after 60 minutes. However this did not change the overall staining pattern (Fig 2.5.B).

With Mg²⁺-activated M-ATPase in lateral body wall muscle, an identical pattern of the staining was seen as for the EOM. The small fibres of outer layer and fibres intermediate in size were both stained light, while the large fibres of the intermediate layer were stained comparatively dark with the M-ATPase (Fig 2.5.C).

2.3. SDH staining of EOM.

An orbital layer of SDH positive, heavily stained small orbital fibres was seen in all EOM, and a few small fibres lying in the global region were also stained dark. In the global region the large fibres were stained lightly, but a few large fibres lying in the orbital region were also stained lightly with SDH (Fig 2.6.A, B).

In lateral body wall muscle three fibre types were identified on the basis of their staining with SDH. The comparatively small fibres in the outermost layer were stained lightly, the fibres intermediate in size were heavily stained (most commonly recognised as pink fibres in the literature) and the large fibres of the innermost layer were lightly stained with SDH (Fig 2.6.C).

2.3.C Type specific myosin in EOM determined by immunohistochemical staining.

The histochemical studies have identified different fibre types in the EOM. The molecular basis of their contractile properties has been investigated by staining the EOM with their type-specific antimyosin sera. The EOM sections were pre-incubated with antibodies raised against several antifast and antislowl myosins, but a reasonably defined staining pattern was only obtained for two antislowl myosin antibodies. 1. α ALD, antislowl tonic myosin specific antisera that was raised against mammalian slow tonic muscle; 2. α SHC antislowl myosin that was raised against the heavy chain portion of slow myosin in fish.

As a control the lateral muscle was also stained for the two antibodies.

2.3.C.a α ALD.

A positive reaction to ALD was obtained in most of the small fibres of orbital region. In the global region, only small scattered fibres gave a positive α ALD reaction, while the large fibres were α ALD negative. Hence a small number of fibres lying adjacent to α ALD positive fibres were not stained. The possibility that these and other unstained fibres contained a slow myosin that was other than tonic was tested by using the other antibody (Fig 2.7.A).

In the lateral body wall muscle, as in EOM, the outer layer of small fibres was stained dark with α ALD and large fibres of global region were stained light (Fig 2.8.A).

2.3.C.b α SHC.

Generally the small fibres of the orbital region were positively stained with α SHC and a few small fibres in global region were also identified as α SHC positive fibres. Most of the fibres in the global region and a few fibres in the orbital region were unstained (Fig 2.7.B).

With α SHC a similar pattern of staining was seen in lateral body wall muscle fibres as in EOM. The small fibres of the outermost layer were stained comparatively dark and the large fibres of the inner layer were stained light (Fig 2.8.B).

2.3.D. Quantitative analysis of histochemical, oxidative and immunohistochemical properties of EOM.

In order to examine the relationship between fibre size and staining properties the muscle sections were analysed using a quantitative morphometric method. For each staining reaction an area comprised of both orbital and global regions and with a bimodal

distribution of staining and size types was selected in the EOM. Within this area each fibre was traced on the digitizing tablet and was assigned a code either as lightly or darkly stained fibre. The computer programme calculated the area and location of each fibre.

The Mg^{2+} -activated M -ATPase activity of the EXT-R was analysed for quantitative studies and to establish a ratio between small orbital and large global fibres (Fig 2.9.A). Among 465 analysed fibres lying mostly in the orbital region and a few scattered fibres in the global region, 255 fibres were stained lightly (Fig 2.10). In terms of area the estimated size range of these fibres was between $8.32\mu m^2$ - $80\mu m^2$. 210 fibres mostly lying in the global region were stained dark with M -ATPase (Fig 2.11) and the estimated area of these fibres ranged between $9\mu m^2$ - $495\mu m^2$ (Fig 2.11).

From a histogram of the size distribution of fibres of both staining types (Fig 2.12) a boundary between fibres designated as small and large fibres was chosen at $30\mu m^2$. Segregating fibres on the basis of this criterion of size (rather than staining properties) generated a distribution histogram, expressed as stacked histogram bars, which demonstrates the strength of the relationship between fibre size and staining pattern. Among 465 fibres analysed, the 281 fibres designated as small (size range 8.32 - $30\mu m^2$) lay mostly in the orbital region (Fig 2.12). 255 of these fibres showed only weak staining for M -ATPase, while 26 small fibres lying both in the orbital and global region were strongly stained (Fig 2.12). The remaining 184 fibres were designated large (size range $30\mu m^2$ - $495\mu m^2$) and lay mostly in the global region (Fig 2.12). 160 of these fibres stained strongly for M -ATPase, but 24 large fibres lying both in the orbital and global regions were weakly stained (Fig 2.12).

A similar area with two staining and fibre size types was

selected and analysed in the EXT-R for SDH staining (2.9.B). In this muscle 476 fibres were analysed. In terms of their staining pattern 362 small, mostly orbital fibres were stained darkly with SDH (Fig 2.13) and they ranged in size between $2.85\mu\text{m}^2$ - 80.5^2 (Fig 2.14). 114 large mostly global fibres were stained lightly (Fig 2.14) and their estimated size range was between $9.21\mu\text{m}^2$ - $350\mu\text{m}^2$ (Fig 2.14)

Based on the criterion of size only and from the histogram of staining types (Fig 2.15) the boundary between small and large fibres was taken at $30\mu\text{m}^2$. In this analysis, among 476 fibres, the 370 fibres designated as small (size range 2.85 - $30\mu\text{m}^2$) lay mostly in the orbital region (2.15). 350 of these fibres stained strongly for SDH, but 20 small fibres lying both in the orbital and global layers showed no SDH reactivity (Fig 2.15). The remaining 106 fibres designated large (size range 30 - $350\mu\text{m}^2$) lay mainly in the global region (Fig 2.15). 95 of these fibres showed no SDH reactivity, but 11 large fibres lying both in the orbital and global regions stained strongly for SDH (Fig 2.15).

The IO stained with α : ALD was used for the quantitative analysis of immunohistochemical staining of the EOM. The area selected in this muscle contained both small and large fibres with a differential staining pattern (2.9.C). Within this area 762 fibres were analysed for the quantitative estimation of α ALD stain, of which 545 small fibres mostly lying in the orbital region were stained dark (Fig 2.16) and in terms of area they ranged in size between $2.17\mu\text{m}^2$ - $75.5\mu\text{m}^2$ (Fig 2.17). 217 fibres lying mostly in the global region were stained light with α ALD (Fig 2.17) and they ranged in size between $21.7\mu\text{m}^2$ - $220\mu\text{m}^2$ (Fig 2.17).

Based on the composite histogram of staining types (Fig 2.18) and the criterion of size a boundary between small and large fibres was taken at $25\mu\text{m}^2$ and 762 fibres were analysed. 584 fibres were

designated as small (size range $2.17-25\mu\text{m}^2$) and lay mainly in the orbital region (Fig 2.18). 530 of these fibres stained positively for α ALD, while 54 fibres lying both in the orbital and global regions gave a negative reaction. The remaining 178 fibres were designated large (size range $25-220\mu\text{m}^2$), and of these 132 gave a negative reaction, and only 46 gave a positive reaction (2.18).

A piece of lateral muscle stained for Ca^{2+} activated myosin-ATPase at alkaline pH and which contained both small and large fibres was analysed to estimate the ratio of fibre sizes between EOM and body wall muscle and to determine the size related staining properties this muscle. The fibre area of lateral muscle is eight times greater than that of the EOM. As found by others, three distinct staining types were distinguishable. Among 76 analysed fibres 14 fibres which stained dark with the myosin-ATPase were identified as TYPE I and their size ranged from $2000\mu\text{m}^2-6000\mu\text{m}^2$ (2.19). 20 fibres with the largest area and comparable with the global fibres in terms of their staining pattern were stained light and they ranged in size between $14000\mu\text{m}^2-50000\mu\text{m}^2$ (Fig 2.19). 40 fibres which have shown an intermediate staining for myosin-ATPase and ranged in size from $6000\mu\text{m}^2-12000\mu\text{m}^2$ (Fig 2.19).

2.3.E Mechanical recordings.

Isolated nerve-muscle preparations of the EOM were used for mechanical recordings. The stimulation of the motor nerve at various frequencies and voltages produced mechanical activation of the muscle fibres. These responses were tested over a range of stimulus voltages and frequencies.

In a recording from IO during a frequency series at 2V, individual twitches were elicited at 1Hz (Fig 2.20), an unfused

tetanic contraction of muscle fibres was seen at 10Hz (Fig 2.20), and fused tetani occurred at greater frequencies. At 20Hz the fibres were activated slowly and gradually to produce a contraction with a force plateau of 1.4g. With increasing frequency to 50Hz, and 100Hz, (Fig 2.20) the rate of contraction was greater, and a stronger force was developed. The twitch tetanus ratio between 1Hz and 100Hz was 1:3.

A voltage threshold between two levels of fibre responses was established in a voltage series at 50Hz (Fig 2.21). At this frequency a force plateau of an approximately constant value was seen between 0.3 and 20V. It was only when the inferior oblique was stimulated at 0.2V that the force declined (Fig 2.21). In a frequency series below the voltage threshold (0.2V) very little response was seen either at 20Hz (Fig 2.22) or at frequencies above 20Hz (Fig 2.22).

Experiments on other EOM gave similar results, especially in terms of voltage threshold. However in some cases it was found that the maximum tetanic force was generated at 20Hz and was slightly reduced at higher frequencies.

2.3.F Motor endplates in EOM.

Two different types of nerve ending were commonly seen in all EOM: enplaque type or single endplates, and engrappe type or multiple endplates in which numerous small nerve terminations are distributed along the fibres. Both of these types were best defined in longitudinal sections. The multiple terminals of the engrappe type were seen either as distributed in the form of several tree-like branches (Fig 2.23.A) or as one axon with several unbranched terminals (Fig 2.23.B). One engrappe type ending could be innervating two adjacent fibres or some fibres were seen receiving multiple multiterminal endplates. In transverse sections the multiterminal endings were seen innervating two or three different fibres (Fig

2.25.A.B).

Enplaque endings were equally abundantly distributed in fibres. In longitudinal sections these endplates appeared as single terminals at one end of an axon (Fig 2.24.A). Some times fibres with more than one enplaque endings were also seen adjacent to each other (Fig 2.24.B). Also in some transverse sections enplaque type endings were seen innervating a single fibre only (Fig 2.25.C).

The motor endplates of both single and multiple types were seen distributed among populations of small and large fibres and it was observed that one type of endplate was not confined to one region only.

2.3.F EOM motor units.

Dogfish EOM are innervated by three cranial nerves. The motor nerve of SO is a branch of CN IV and EXT-R receives a branch of CN VI. The IO, SR, IR and INT-R are innervated by branches of the CN III.

In order to estimate the size of motor units in the EOM, studies were made to obtain the muscle fibre count within the EOM and the motor axon count in the nerves innervating these EOM. In histological thin sections of the nerve and the EOM, motor axons and muscle fibres were counted either by hand or in one case by the computer assisted reconstruction technique. For this purpose motor axons were traced on the digitizing tablet to determine precisely the cross-sectional area of axons and the pattern of their size distribution within the nerve.

Serial sections of the CN III were taken within the cranium to obtain a fibre count before the nerve entered in to the orbit and branched. In a section like this, small and large fibres were seen to be randomly distributed. At this level 1832 nerve axons were counted

(Fig 2.26.A). Another fibre count was made in the CN III after it has been branched to SR. The CN III at this level was comprised of 279 axons which ranged in area between $61.56\mu\text{m}^2$ - $1860\mu\text{m}^2$ (Fig 2.26.B). It appeared to have two distinct halves in which small and large fibres were randomly distributed. The number of muscle fibres present within the SR was obtained by extrapolation from the counts made on a limited region. The number of fibres present within the SR was 2500. Based on these counts the average motor unit size is 9 muscle fibres per motor axon.

The nerve axons in the main branch of the CN III which leads towards the IO were also counted. The number of axons present at this level was 300. The approximate number of muscle fibres present in the IO was 2680 fibres (Fig 2.26.C). Therefore the estimated motor unit size for this muscle is also 9 muscle fibres per motor axon.

Fibre counts were also made in the trochlear nerve (IV) and the abducens nerve (VI), and these counts were in turn compared with the muscle fibre counts.

In sections of the IVth nerve taken just after its entry into the orbit 476 fibres were present (2.27.A). In the SO muscle the number of fibres present was approximately 3200, yielding an estimate for the motor unit size of 8 muscle fibres for one motor axon.

In a section of VIth nerve taken near the entry of this nerve in to the orbit 158 fibres were counted (Fig 2.27.B). In a cross-section of this nerve a small part was comprised of only small nerve axons (25 in number), a feature which was not seen in case of IIIrd and IVth nerves. It was found that in a section of VIth nerve taken near the EXT-R there were large number of axons (200). Therefore the possibility that these fibres may be sensory seems unlikely. Approximately 1800 fibres were present in the EXT-R muscle. The

estimated motor unit size of this muscle is therefore 13 muscle fibres to one motor axon.

In the case of all three nerves, sections taken close to the EOM demonstrated branching of the nerve into separate bundles. In total these bundles contained a greater number of fibres than were present near the entry of this nerve into the orbit. This suggests that axons are branching at this point to supply the individual muscle fibres which make up their motor units. The nerve fibres in two EOM were seen in forms of several branches innervating the periphery of the EOM (2.28.B). In two EOM, the IO and SR, these bundles form characteristic flattened bands over the periphery of the muscle (Fig 2.28.B).

2.3.4 DISCUSSION

The number of fibre types that can be identified in the EOM is based on criteria of ultrastructural features of the fibres, their physiological properties, electrical or mechanical response, innervation and on the basis of their size and location in the EOM.

In this investigation of the histochemical profile of the dogfish EOM, based on m -ATPase and SDH reactions, two fibre types were identified: small orbital fibres that stained negatively with Mg^{2+} -activated m -ATPase and stained positive with the SDH, and large global fibres that were stained positive with Mg^{2+} -activated m -ATPase and negative for SDH. However some variations to this staining pattern were observed among fibres lying both in the orbital and global regions.

Positive staining of small orbital fibres with SDH reflects the presence of high levels of oxidative enzymes and thus suggests the presence of a greater number of mitochondria in these fibres as compared to the large global fibres. Number of mitochondria present in a muscle fibre is associated with its mode of function as slow or fast fibres. Reports available on the ultrastructural profile of the small orbital and large global (also known as red & white fibres) have demonstrated the mitochondria in greater number within the orbital fibres (Goldspink, 1972, Davey et al., 1975, Montgomery, 1984). The lateral body wall muscle stained along with EOM has shown different staining properties and unlike EOM an intermediate layer of fibres with intermediate staining and size was present between small and large fibres (also known as pink fibres, Bone, 1966, Walker, 1970). These fibres were not seen in the EOM.

The total m -ATPase content is higher in the large global

fibres than in small orbital fibres. Small orbital fibres have also demonstrated an alkaline and acid stability of their Ca^{2+} -activated myosin ATPase. Not only the pH of pre-incubation media but temperature and the duration of reaction has also affected the preservation and the intensity of staining. Differences between the myosin-ATPase content of the orbital and global region has also been reported in other fish. In the lateral body wall muscle of fish the myosin ATPase content of the small fibres has been demonstrated to be three to four times higher than that of large fibres (Johnston et al., 1972, Nag, 1972). The myosin-ATPase reaction and SDH activity of small fibres leads to the suggestion that these fibres are possibly of the slow type, while the large global fibres are of fast type. Further evidence was provided by immunohistochemical staining. In these studies small orbital fibres were stained positively with two antibodies specific for slow fibres. However with ALD and SHC some of the fibres present in the global region were also stained positively suggesting a possible occurrence of slow type fibres also in the global region.

Differences in the innervation of the slow and fast fibre types have been reported in the vertebrate species. Hess (1962), Stanfield, (1972), Eddington & Johnston (1982) have demonstrated that in mammalian EOM and fish lateral muscle, fast fibres were innervated focally by en plaque endplates, while small fibres were innervated by engrapple endplates. However some variation has also been reported as in some teleost^s, both red and white fibres have been reported to receive multiple endplates (Bone, 1978). In dogfish EOM both engrapple and en plaque endplates were distributed among small orbital and large global fibres.

Mechanical recordings in the dogfish EOM has revealed two levels

of response. A threshold level was established in the EOM fibre activity and two levels of fibre responses were observed at the voltages above and below threshold. Also individual twitches, unfused tetani and fused tetanic contractions were observed. Although on the basis of these studies the nature of the mechanical response elicited by orbital and global fibres can not be concluded, however a suggestion could be made that this response may be elicited by two different fibre types. The clear segregation is consistent with the recruitment of the fibres with twitch like properties above a voltage threshold.

Two levels of mechanical response were indicated and based on these results it can be suggested that tonic response maintained over few seconds could have been elicited by the tonic fibre activation, while the individual twitches were elicited by the activation of the TYPE II fibres. Such a suggestion would only be based on an assumption, because it is not necessary for TYPE I fibres to always contract tonically. Red fibres in the teleost fish have been found to react with a twitch in response to a single stimulus (Granzier, et al., 1982; Johnston et al., 1982, Akster et al., 1985). The two main fibre types (TYPE I & TYPE II) can in turn be divided into subtypes that differ in histochemical, immunohistochemical and mechanical profile as well as in the type of their innervation. One subgroup would be the small fibres lying in the global region which remained unstained with SDH but stained positively with M-ATPase. Based on the physiological, ultrastructural and functional variations different subgroups of the two fibre types has also been proposed by Johnston et al. (1977), Kyrvi (1977), Akster & Osse, (1978), Ramsdonk et al., (1980) and Akster (1981).

In dogfish EOM correlation can be made between the fibre size and

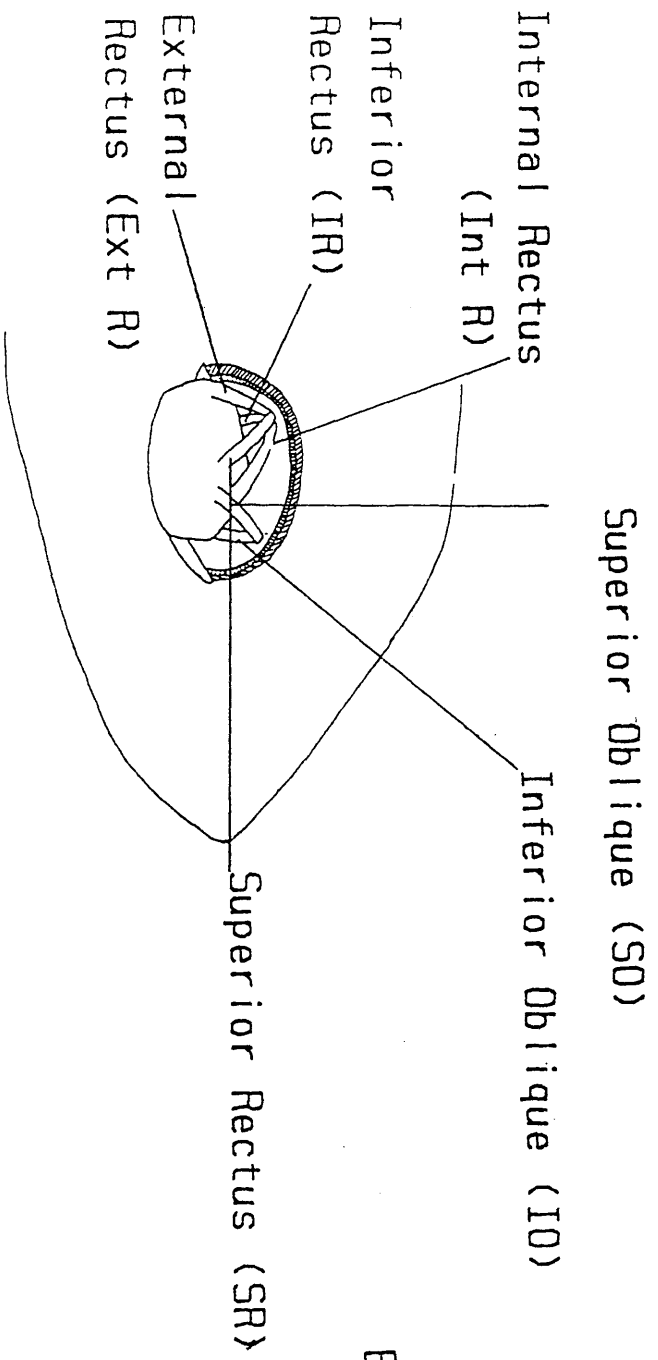
their physiological profile. The majority of small fibres in the orbital region stained negative with m -ATPase, had high SDH activity stained positive with two slow antibodies and were innervated by single and multiple endplates; they resemble Type I fibres in the EOM and skeletal muscle of vertebrate species. Large global fibres were stained positive with Mg^{2+} -activated m -ATPase, had little SDH activity, were not stained with slow antibodies and receive single and multiple endplates; they resemble Type II fibres in the EOM and skeletal muscle of other vertebrate species. Location of the two fibre types is significant in determining their physiological profile. The majority of small fibres lying in the orbital region behave differently to the large fibres lying mostly in the global region. It was suggested by Maier et al., 1972 that the arrangement of fibres in the orbital and global regions is a basic feature of all vertebrate EOM. Similar results have been reported by Kaczmarek, 1970a, Kordylewski, 1974, Zagorska, 1974, Housley et al, 1984).

Based on the quantitative data in the present studies a strong relationship has been demonstrated between the fibre size and their physiological properties. In the quantitative analysis obtained for three different reactions it was clearly demonstrated that size and location of the fibre types were the factors that influenced their oxidative and contractile properties and only a small number of fibres did not follow this scheme.

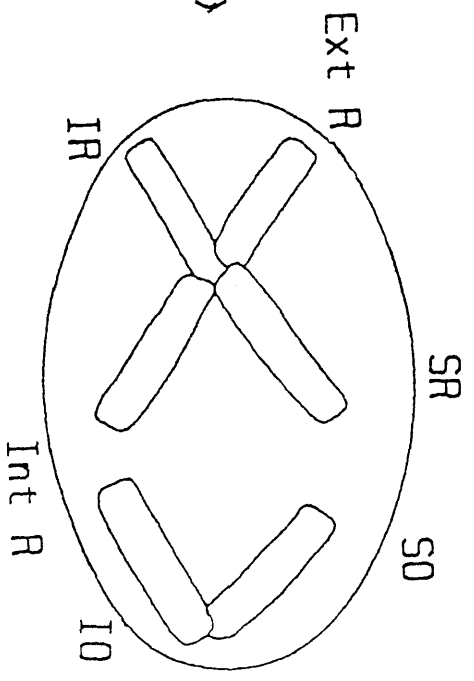
It was suggested by Zagorska (1974) that in amphibians fast fibres are responsible for fast movements of the eye ball, while slow tonic fibres are responsible for the continuous slow contractions of EOM required to maintain the eye ball in a constant position, also very precise slow movements could have been achieved by their alternate activation and inhibition.

In dogfish EOM the Size of motor units is an average of 8 muscle fibres for 1 motor axon in the SR , IO and SO, while in the EXT-R motor unit size is 13 muscle fibres for 1 motor axon. The size of EOM motor units in vertebrates is smaller compared with the motor units size in the skeletal muscles (Buchthal & Schmalbr uch, 1980). Eye movements are achieved and controlled by the six EOM. It is inevitable that their morphology and physiological profile would reflect the type of eye movements present in that species. The physiological profile and morphology of the six EOM has not shown any differences between horizontal and vertical muscles. In all six muscles the TYPE I & TYPE II fibres were present consistently in the orbital and global regions.

In other vertebrates there is nystagmus in vertical plane (Darlot, Barneo & Tracey, 1981; Synder & King, 1988) but this is not known for dogfish, so it is important to determine before any conclusion can be drawn. An alternate possibility is that the horizontal nystagmus, which is known to occur in all vertebrates including dogfish involves not only the EXT-R and INT-R but the vertical EOM as well, perhaps as stabilizing elements. In order to discriminate between these two possibilities a study has been made of VOR in the vertical plane (Chapter 3) and of EOM myographic activity (Chapter 4).



A



B

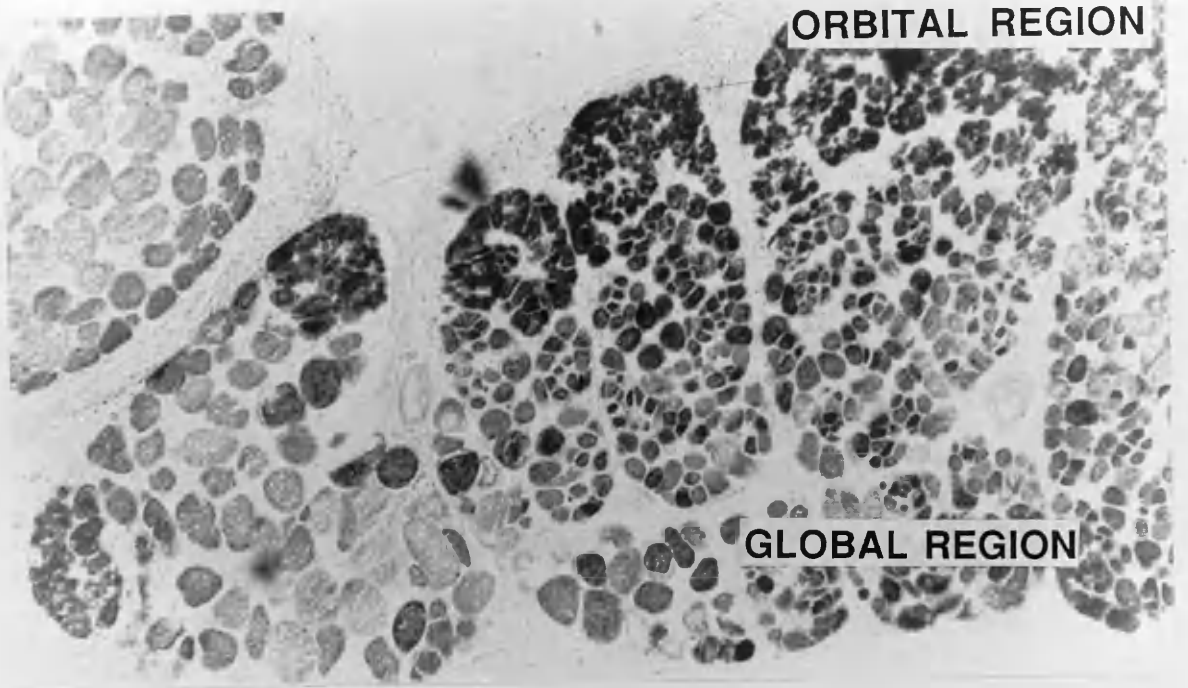
Fig 2.1 The dogfish EOM as seen (A) behind the eye ball
(modified from Rowett (1965) and (B) in the orbit.



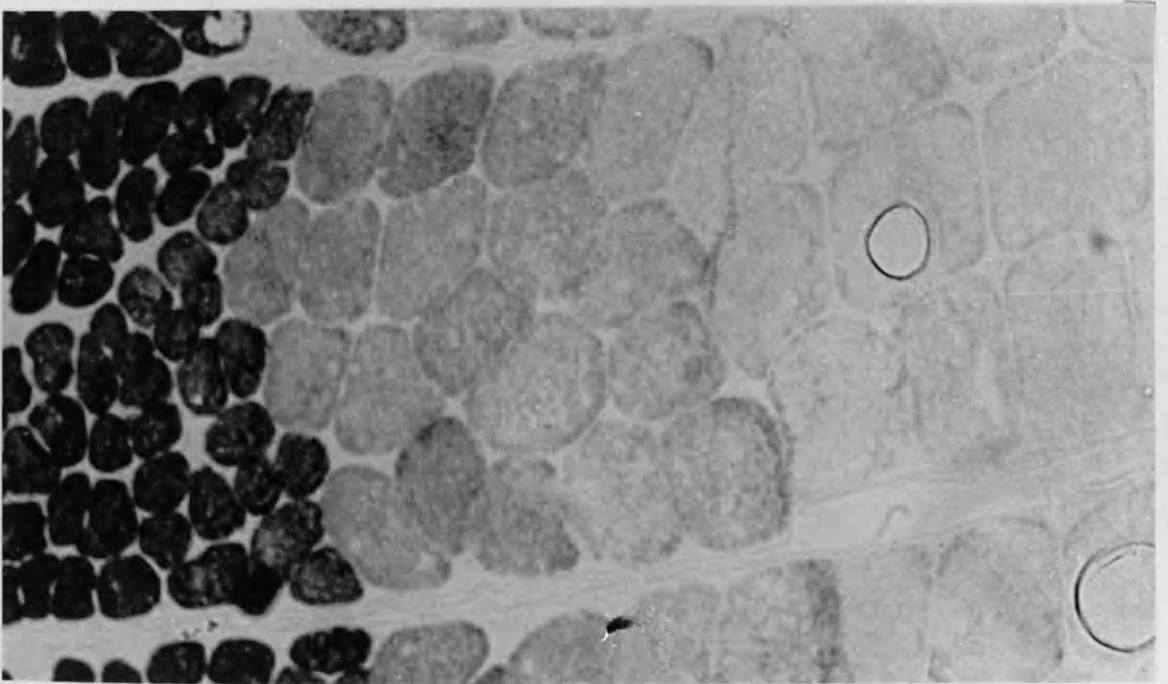
Fig 2.2.A The Ca^{2+} activated myosin-ATPase staining of the SR at pH 9.4 at room temperature.
Sale bar = 750um

Fig 2.2.B The lateral body wall muscle is stained with Ca^{2+} activated myosin-ATPase for pH 9.4 at room temperature.
Scale bar = 900um

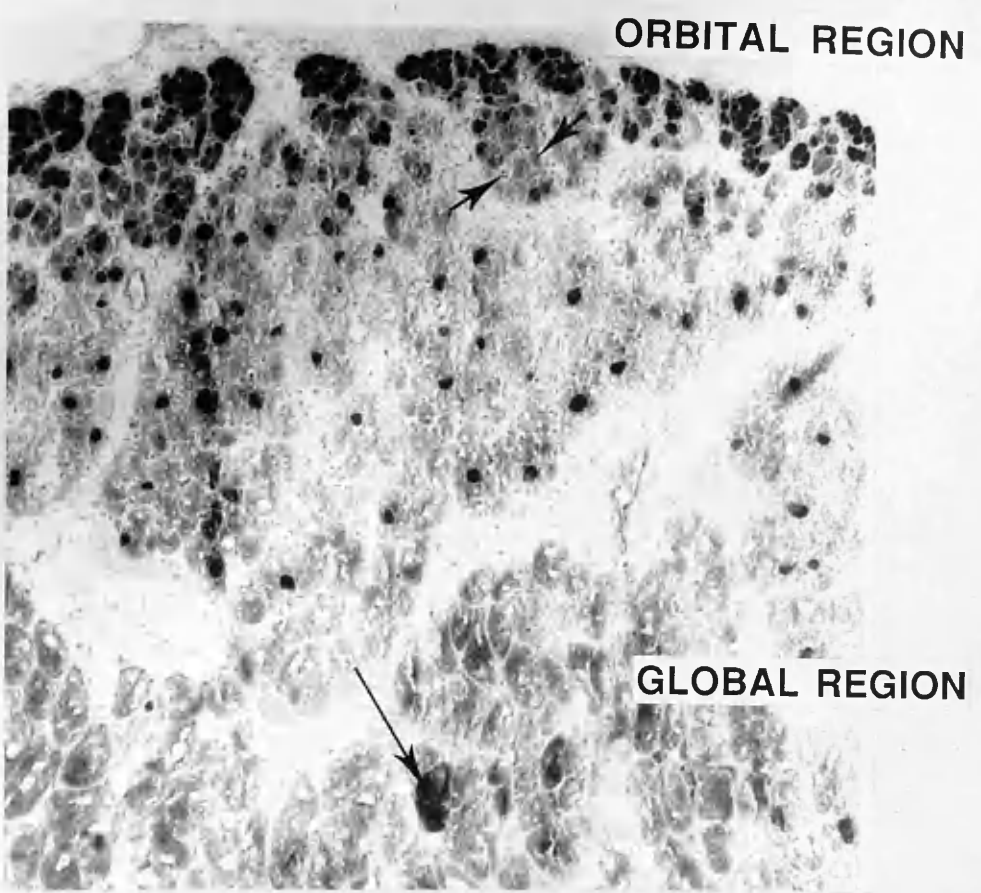
A



B



A



B

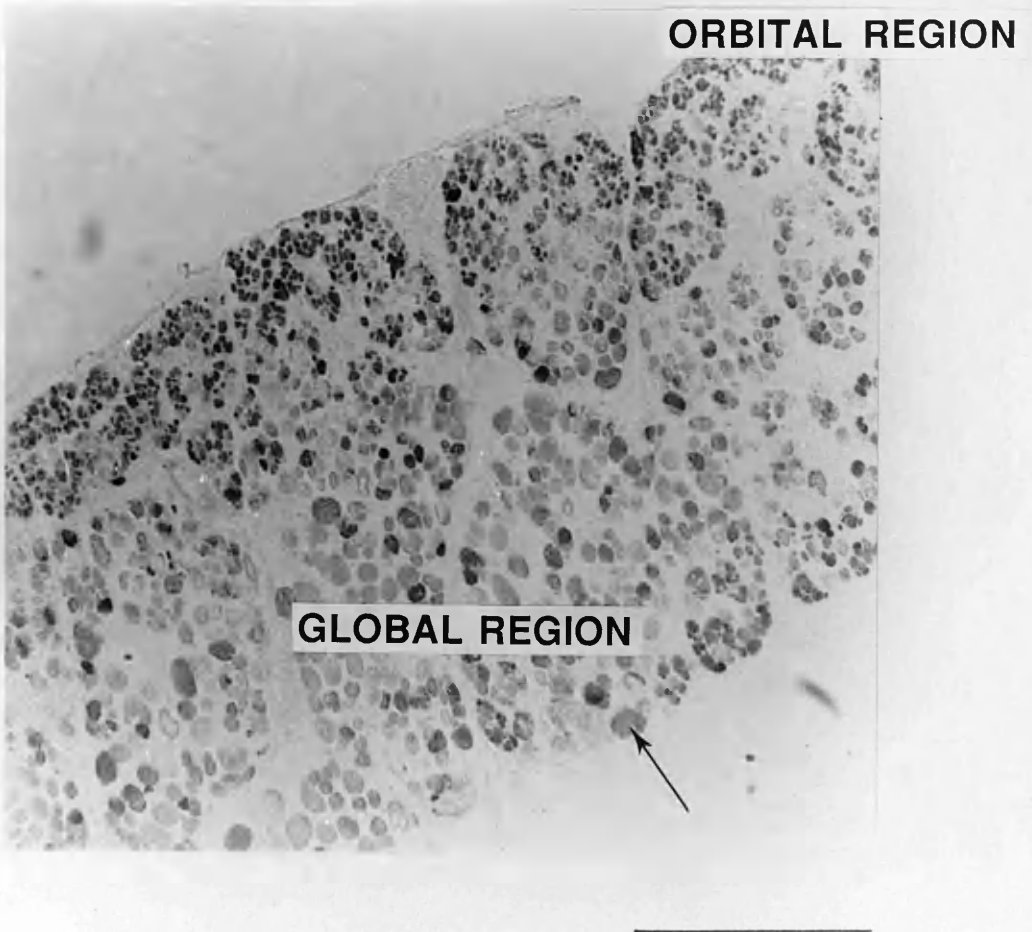


Fig 2.3.A

The SR is stained with Ca^{2+} activated myosin ATPase at room temperature for pH 5.6.

Scale bar = 350um

Fig 2.3.B

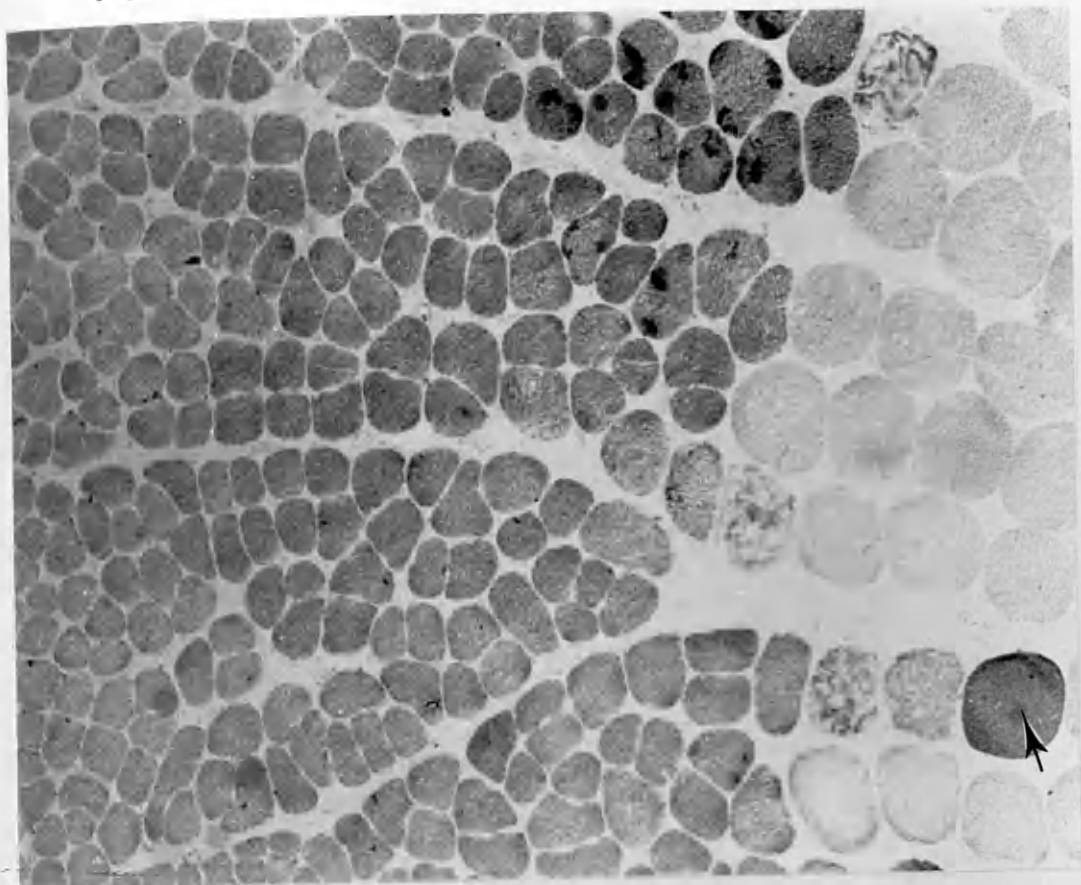
The SR is stained with Ca^{2+} activated myosin-ATPase at pH 5.6 at temperature of 4°C .

Scale bar = 600um

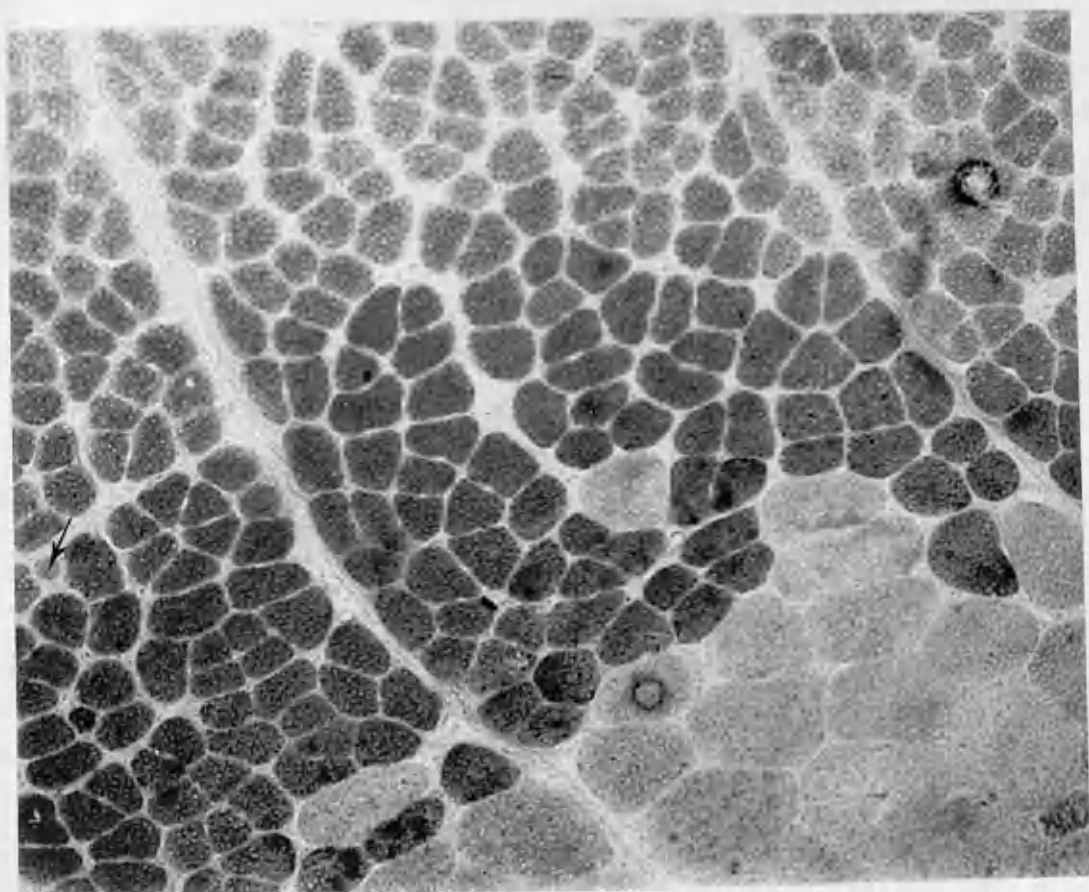
Fig 2.4.A The lateral body wall muscle is stained with Ca^{2+} activated myosin-ATPase at room temperature at pH 5.6.
Scale bar = 900um

Fig 2.4.B The lateral body wall muscle is stained with Ca^{2+} activated myosin-ATPase at 4°C for pH 5.6.
Scale bar = 900um

A

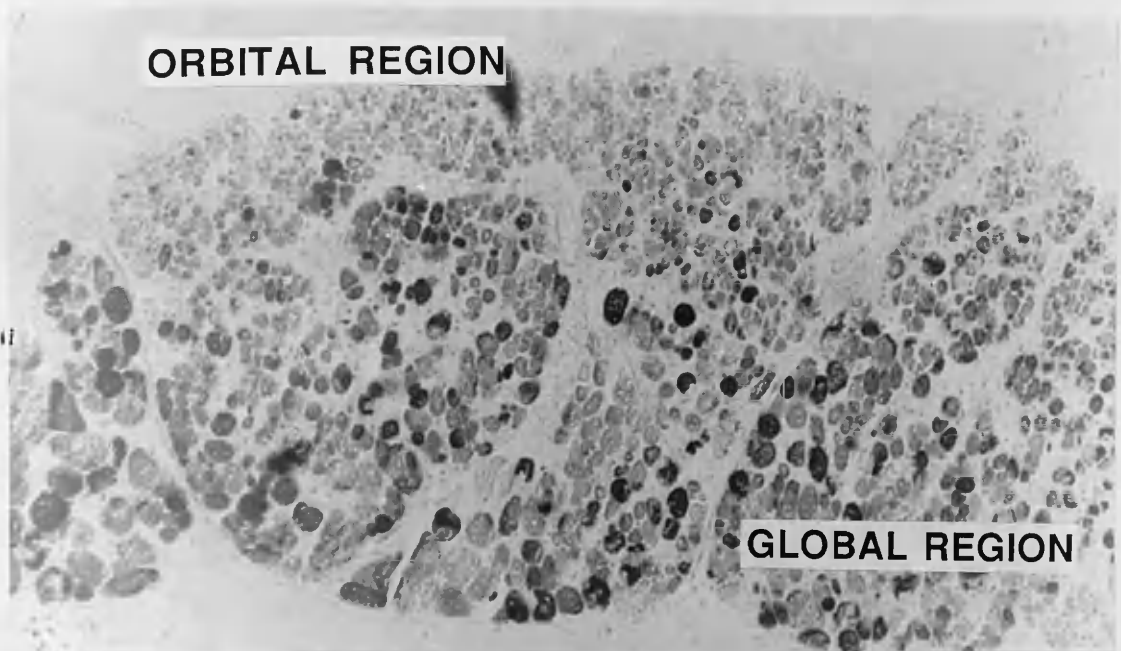


B



A

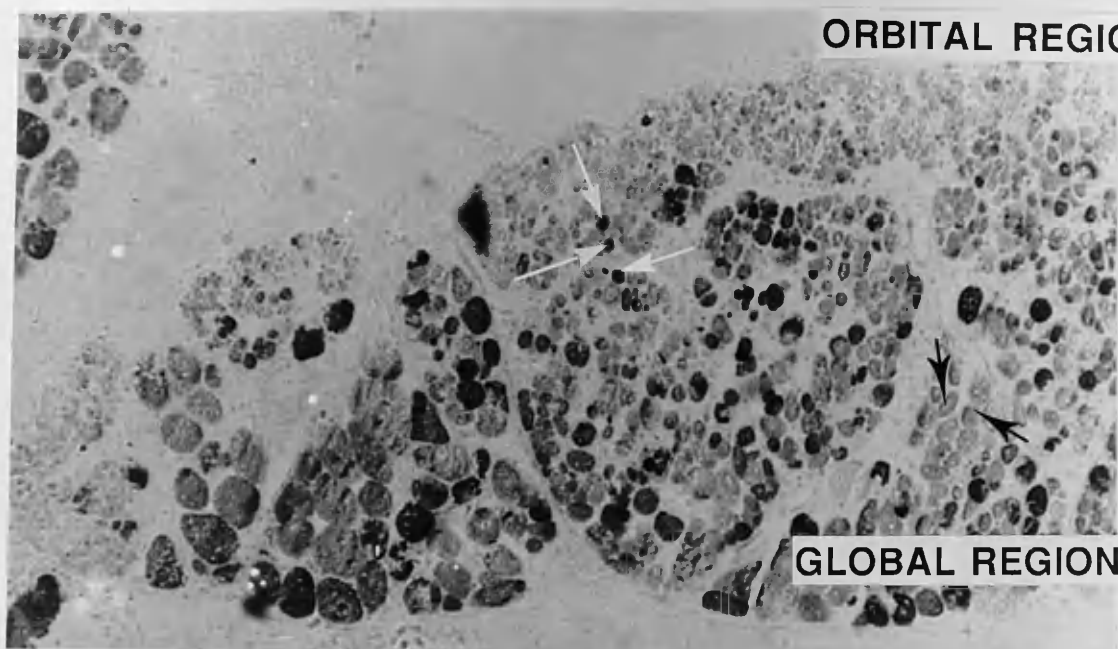
ORBITAL REGION



GLOBAL REGION

B

ORBITAL REGION



GLOBAL REGION

C

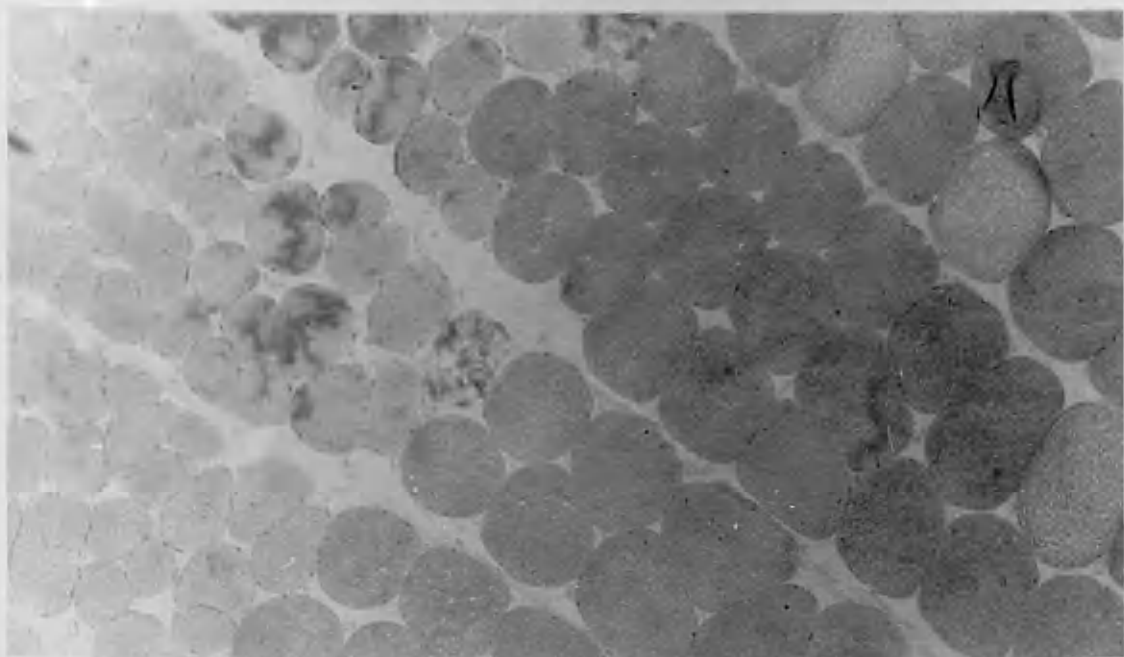


Fig 2.5.A The SR is stained with Mg^{2+} activated Ca^{2+} -ATPase at room temperature for 20 minute incubation.
Scale bar = 400um

Fig 2.5.B The SR is stained with Mg^{2+} activated Ca^{2+} -ATPase at room temperature after 30 minutes incubation.
Scale bar = 350um

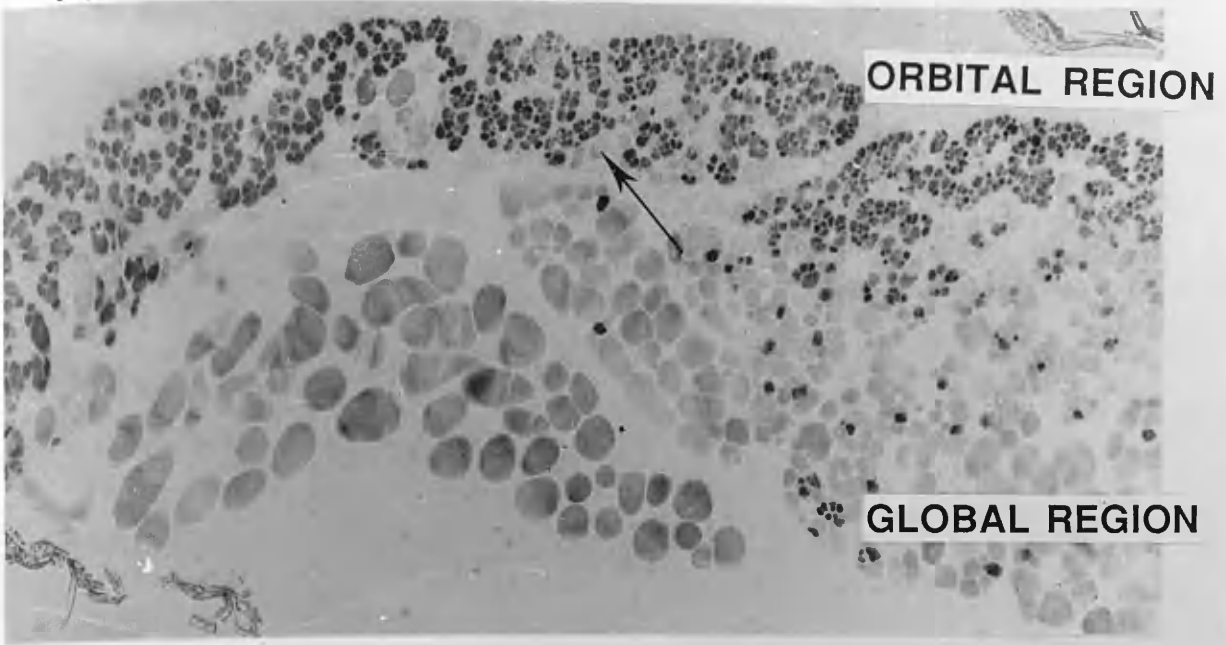
Fig 2.5.C The lateral body wall muscle is stained with Mg^{2+} activated Ca^{2+} -ATPase at room temperature.
Scale bar = 900um

Fig 2.6.A The EXT-R is stained with SDH at room temperature.
Scale bar = 450um

Fig 2.6.B The SDH staining of SR and IR at room temperature.
Scale bar = 800um

Fig 2.6.C The SDH staining of lateral muscle at room
temperature.
Scale bar = 900um

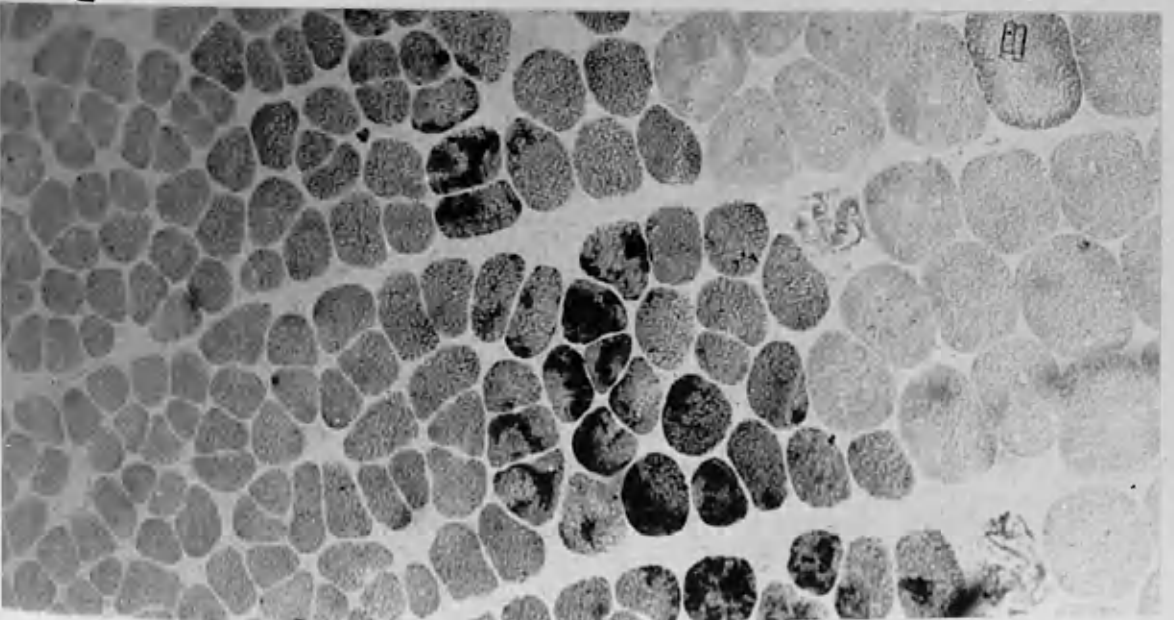
A



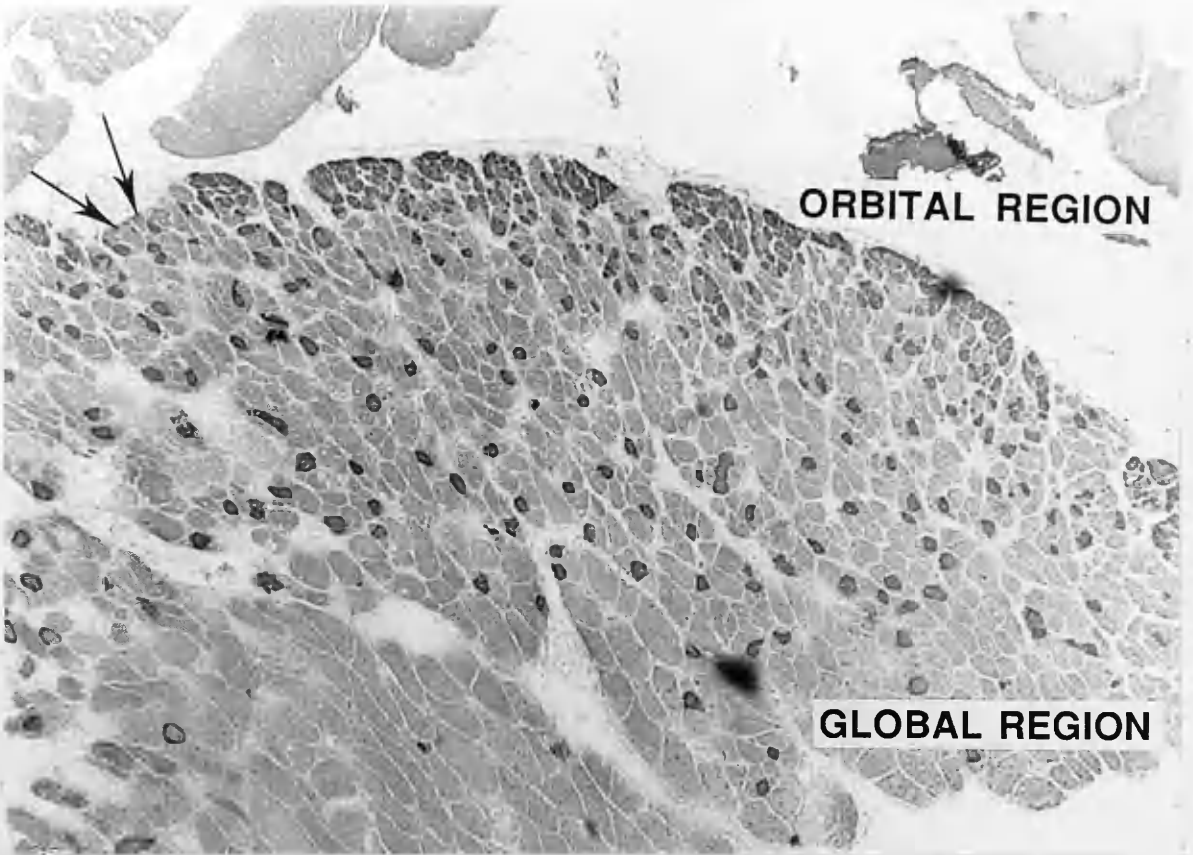
B



C



A



B

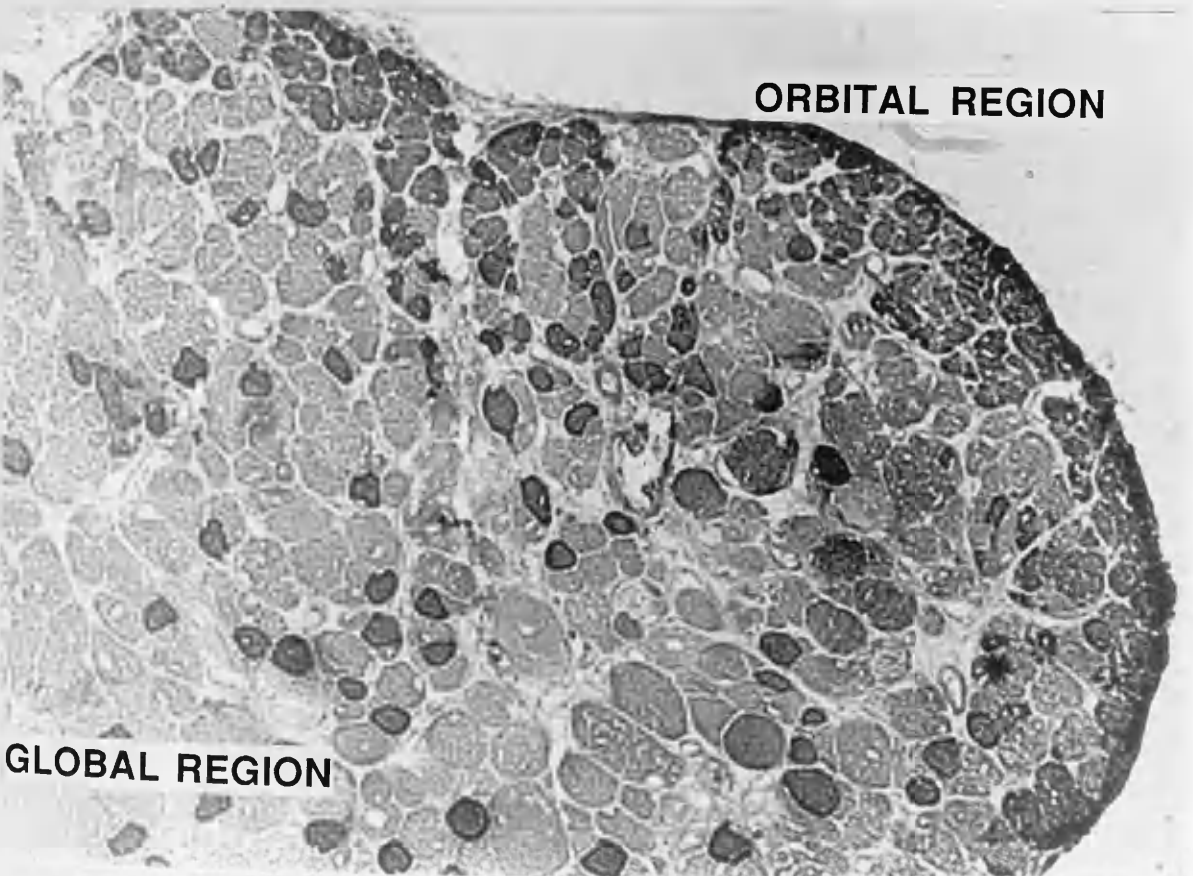


Fig 2.7.A The IO is stained for α . ALD at room temperature.
Scale bar = 300um

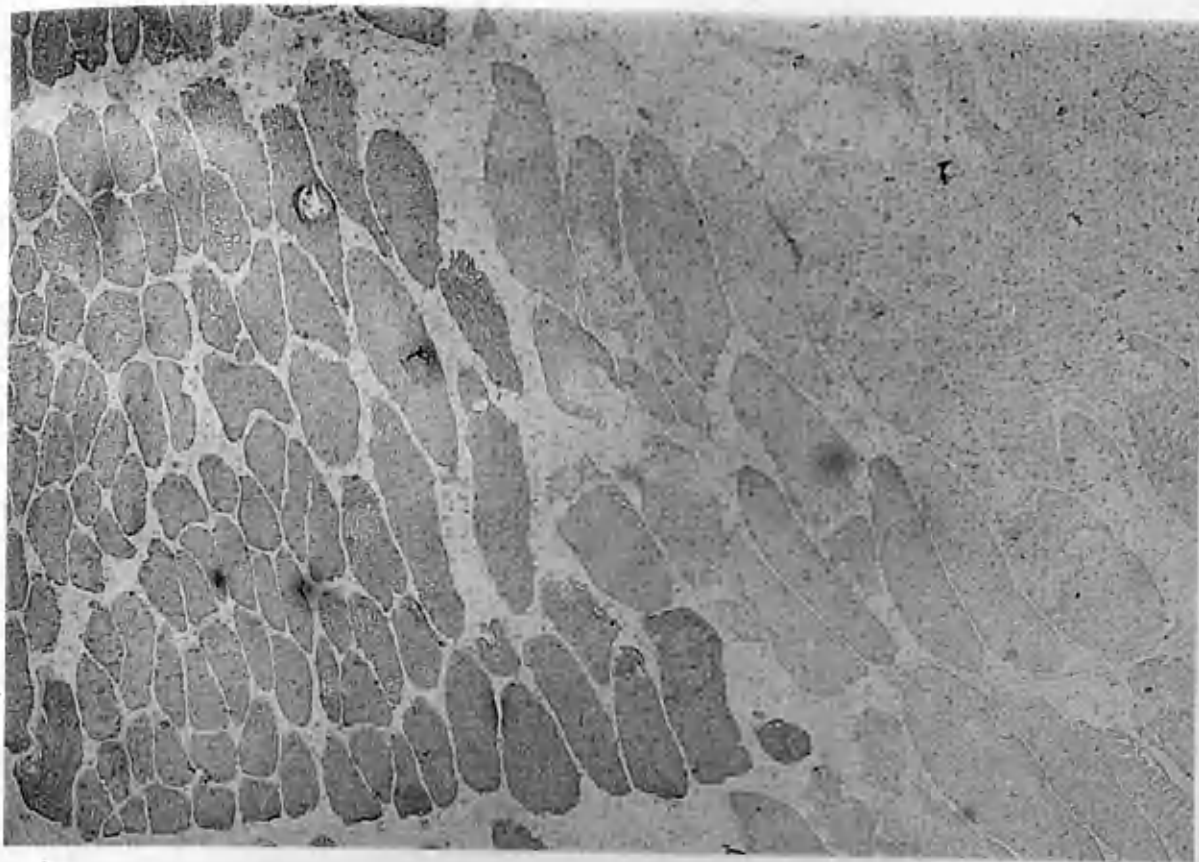
Fig 2.7.B The SR is stained with SHC at room temperature.
Scale bar = 150um

Fig 2.8.A The lateral body wall muscle is stained with α ALD at room temperature.

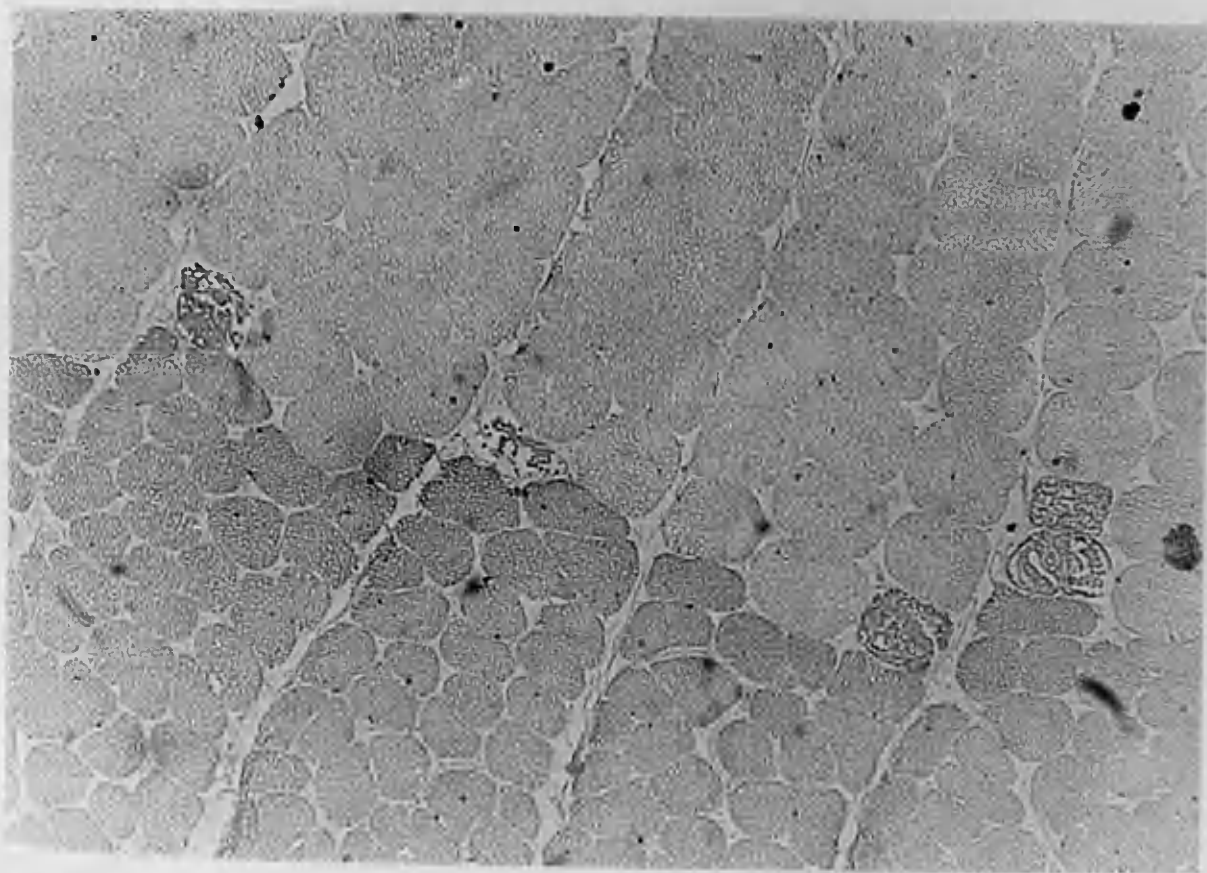
Scale bar = 900um

Fig 2.8.B The lateral muscle is stained with α SHC at room temperature.

Scale bar = 900um

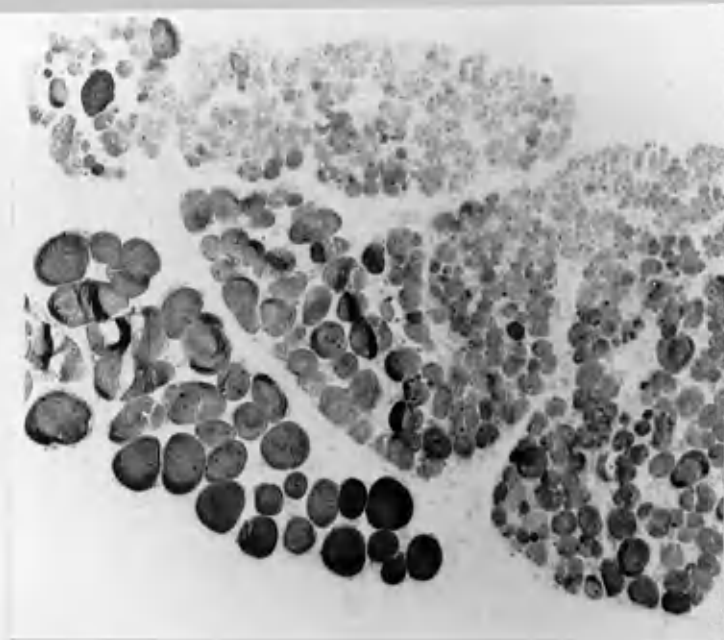


A

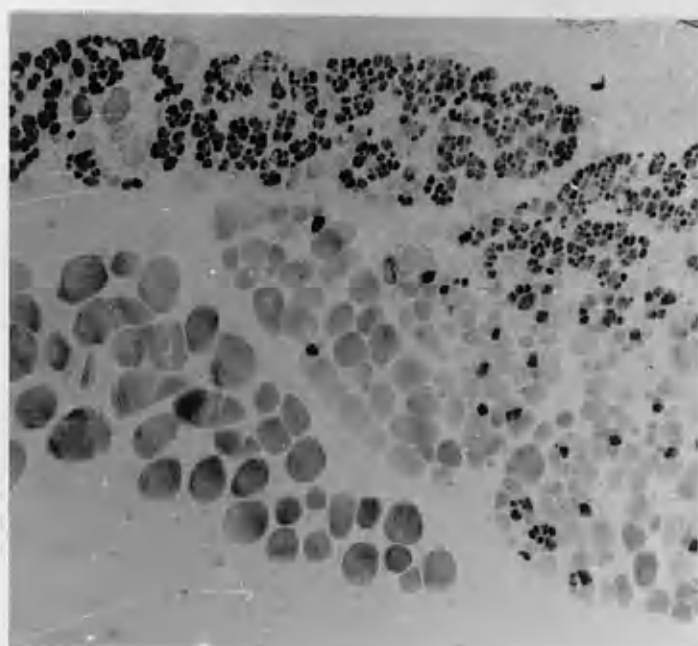


B

A



B



C

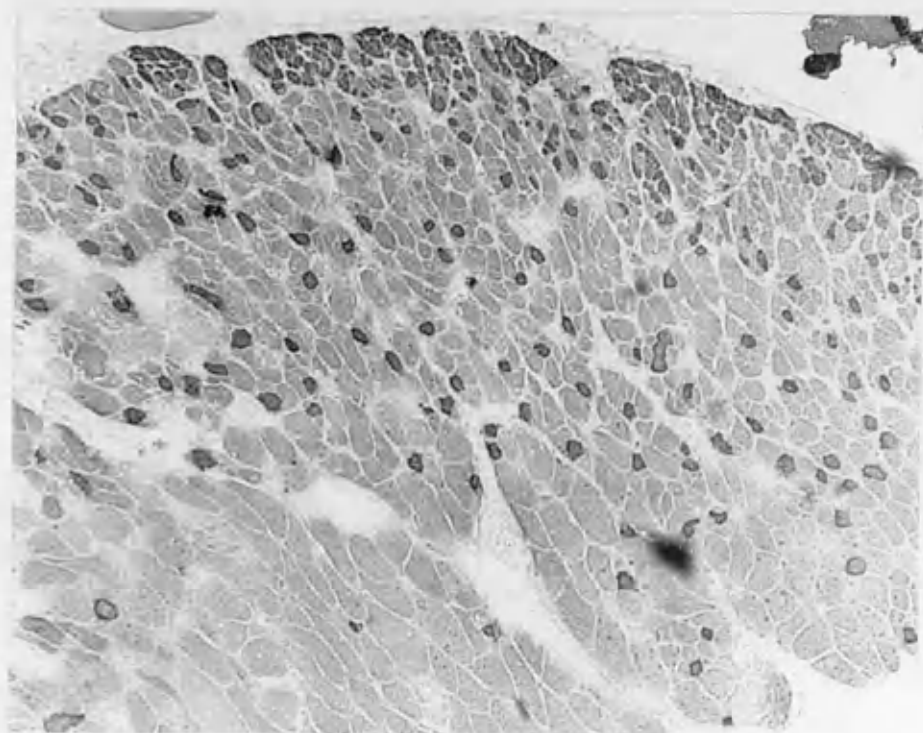


Fig 2.9.A The EXT-R is stained for Mg^{2+} activated m-ATPase.

Scale bar = 250um

Fig 2.9.B The EXT-R is stained for SDH.

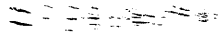
Scale bar = 250um

Fig 2.9.C The IO is stained for ALD.

Scale bar = 315um

Fig 2.10

The digitised image of Mg^{2+} activated $(M)-ATPase$ staining.



Histochemical stain for myosin ATP'ase activity, EXT-R

Red = negative reaction

Blue = positive reaction

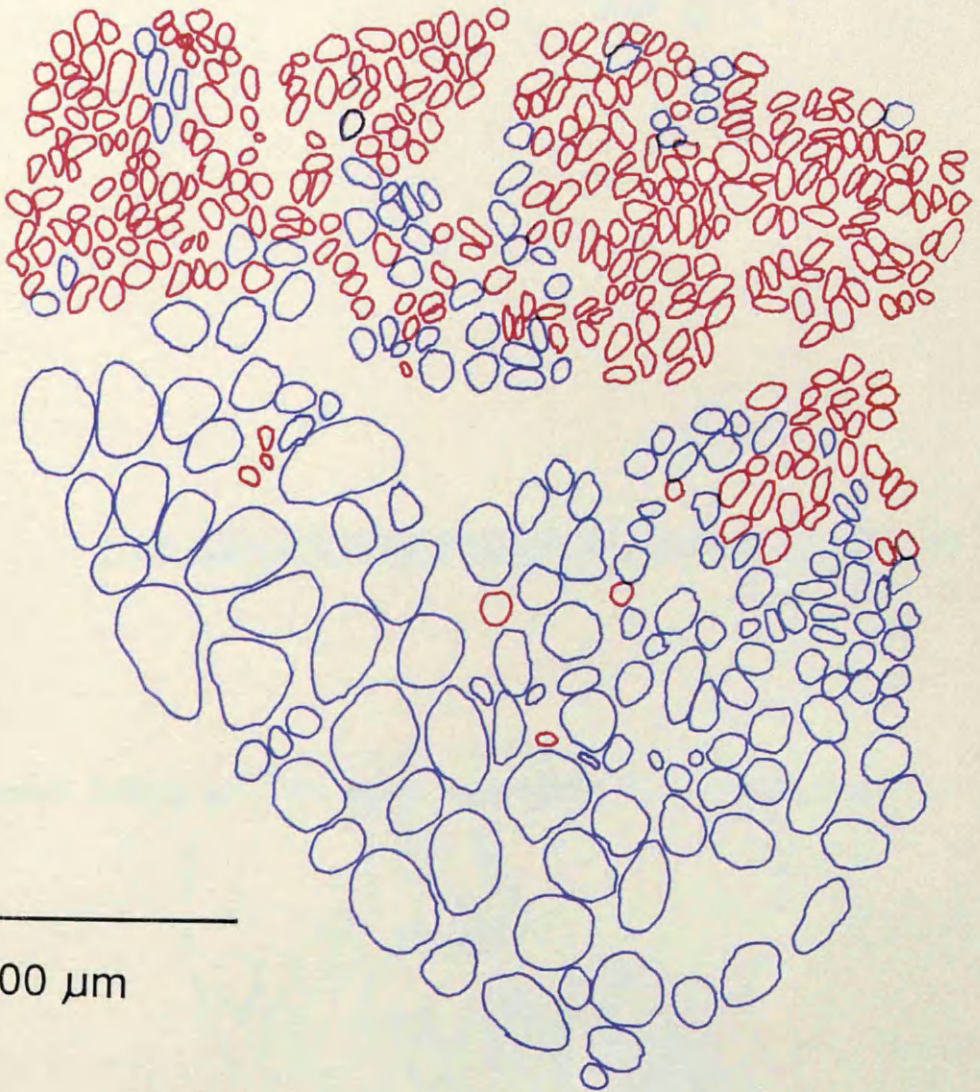


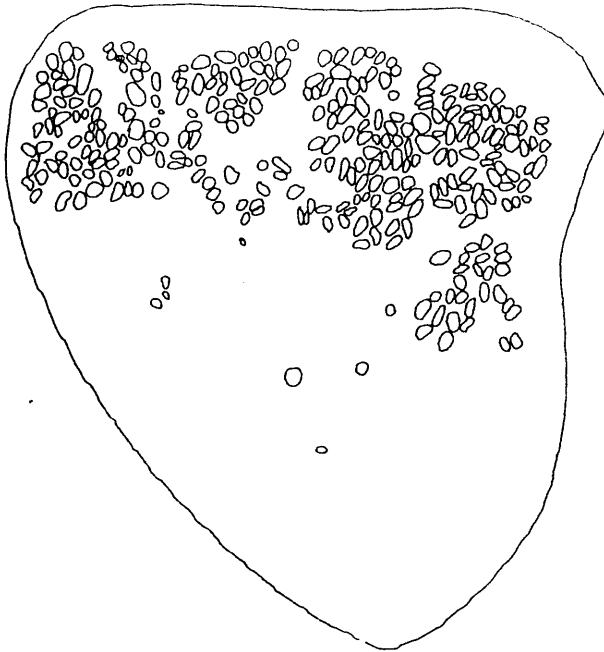
Fig 2.11.A The digitised image of small orbital fibres.



Fig 2.11.B The digitised image of large global fibres.

SMALL ATPase NEGATIVE FIBRES, EXT-R

A



B

LARGE ATPase POSITIVE FIBRES, EXT-R

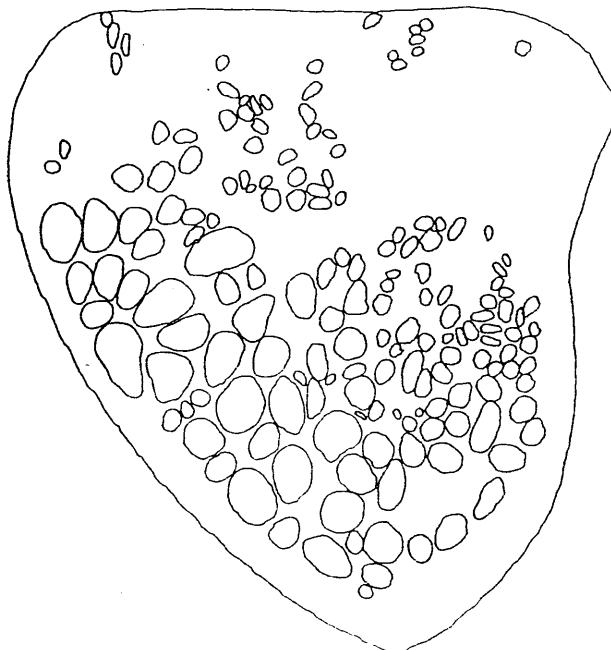
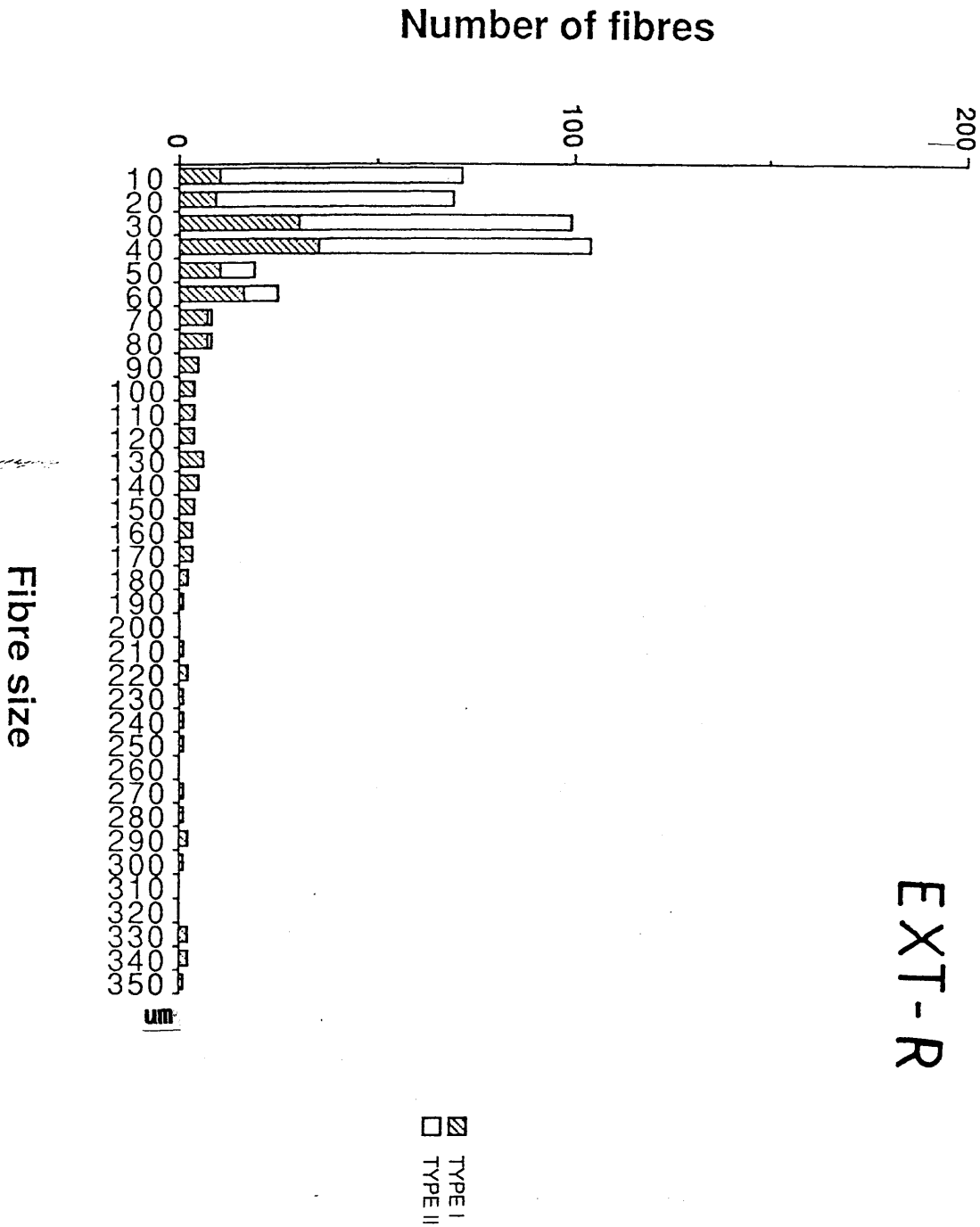


Fig 2.12

The histogram of small orbital and large global fibres showing distribution of these fibres according to their staining properties.

EXT-R



Number of fibres

Fibre size

TYPE I
TYPE II

Fig 2.13

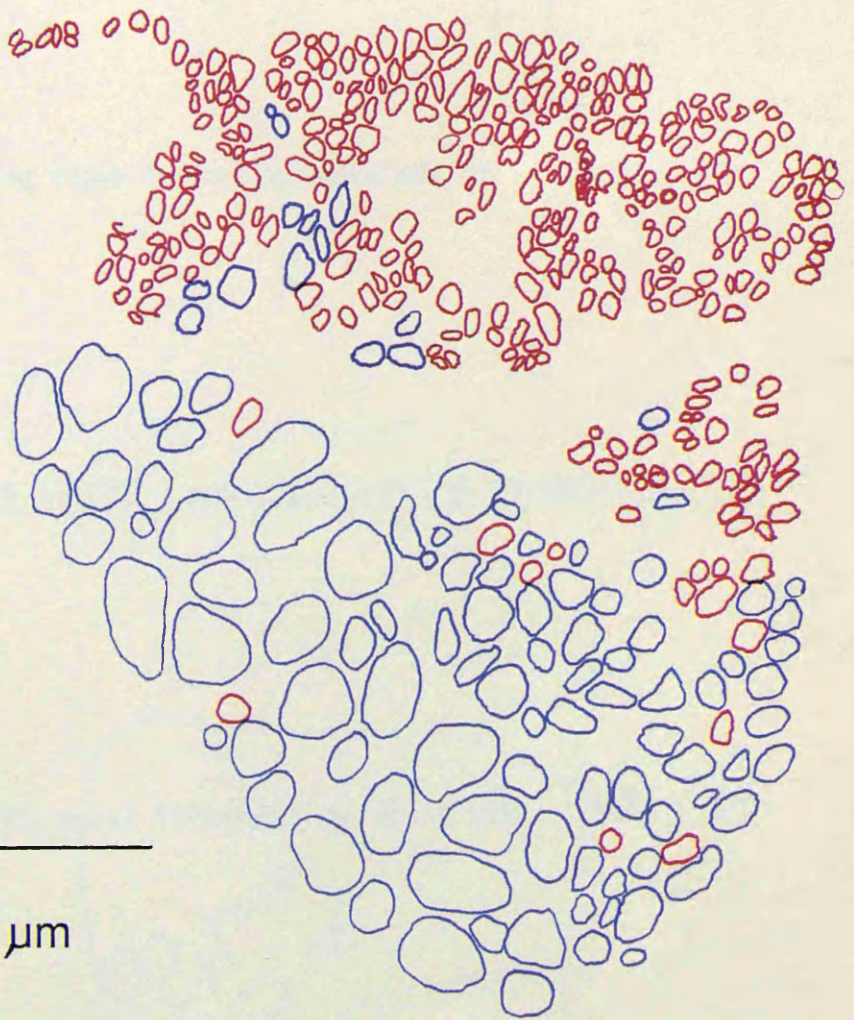
The digitised image of SDH staining in the EXT-R.



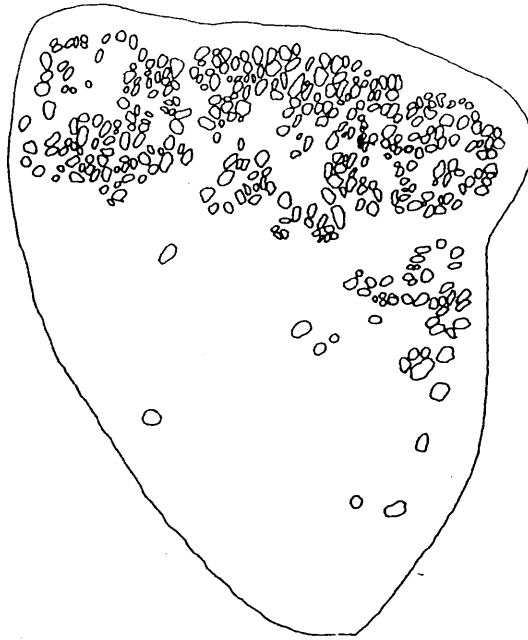
Histochemical stain for SDH activity

Red = positive reaction

Blue = negative reaction



SMALL SDH-POSITIVE FIBRES, EXT-R



LARGE SDH-NEGATIVE FIBRES, EXT-R

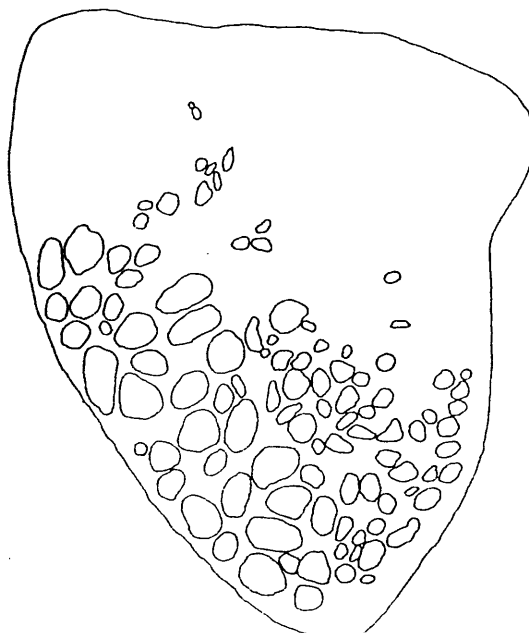


Fig 2.14.A The staining pattern of small orbital fibres.



Fig 2.14.B The staining pattern of large global fibres.

Fig 2.15

The histogram of two fibre types for SDH staining showing the distribution of orbital and global fibres according to their staining properties.

EXT-R

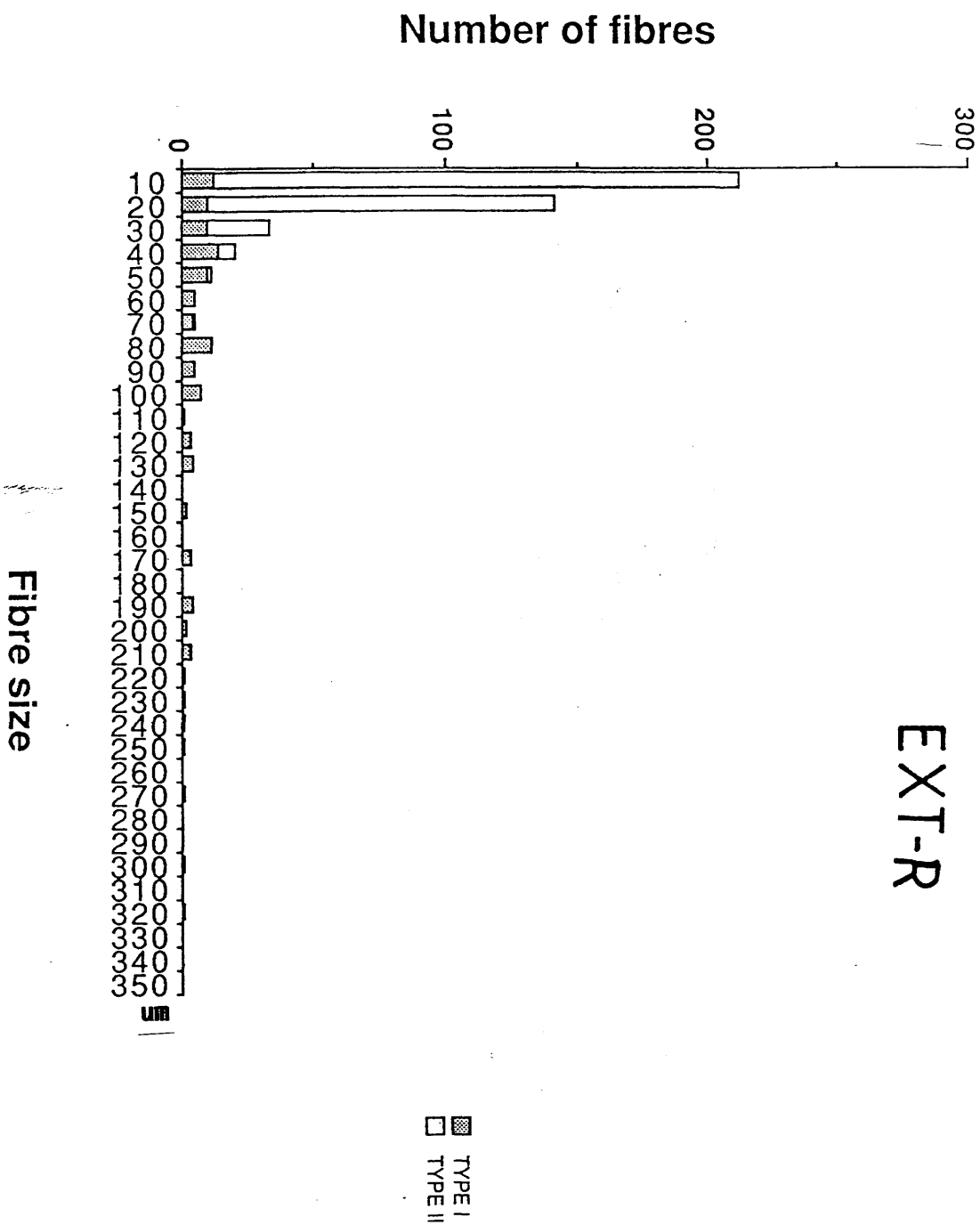


Fig 2.16 The digitised image of α ALD staining in the IO.

Immunohistochemical stain with
antiserum specific for tonic fibre myosin

Red = positive reaction

Blue = negative reaction

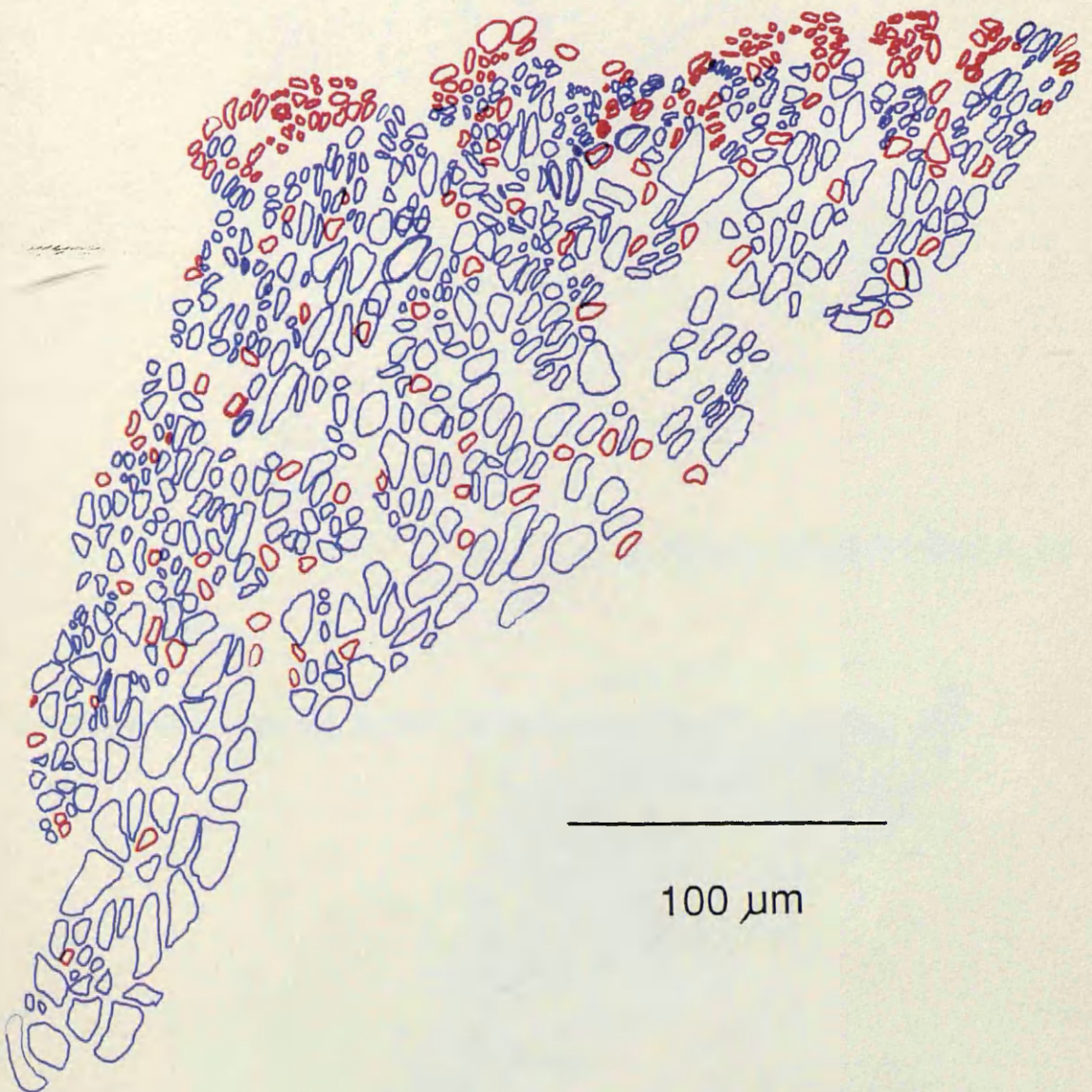


Fig 2.17.A The distribution of fibres for positive α ALD staining.



Fig 2.17.B The distribution of fibres for negative α ALD staining.

ALD-POSITIVE FIBRES, 10

A



ALD-NEGATIVE FIBRES, 10

B

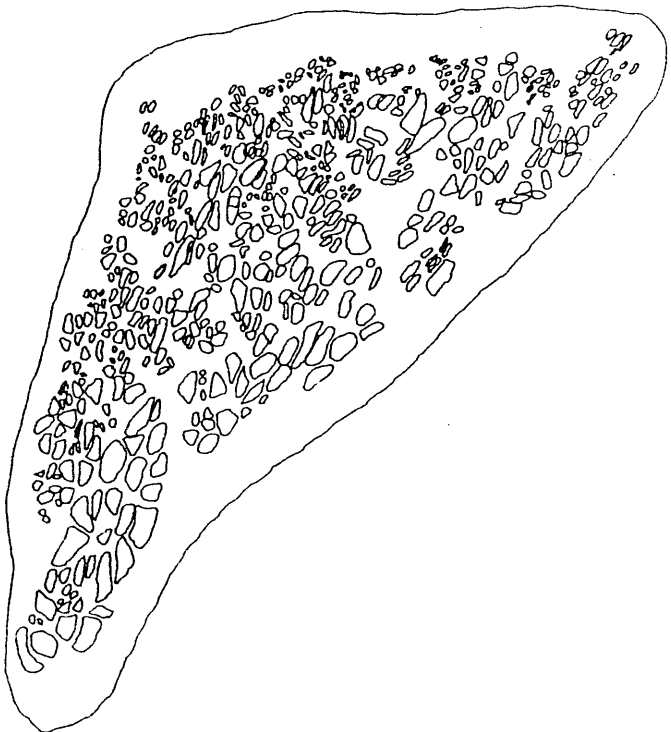


Fig 2.18

The histogram of two fibre types in the IO showing their distribution for α ALD staining.

Number of fibres

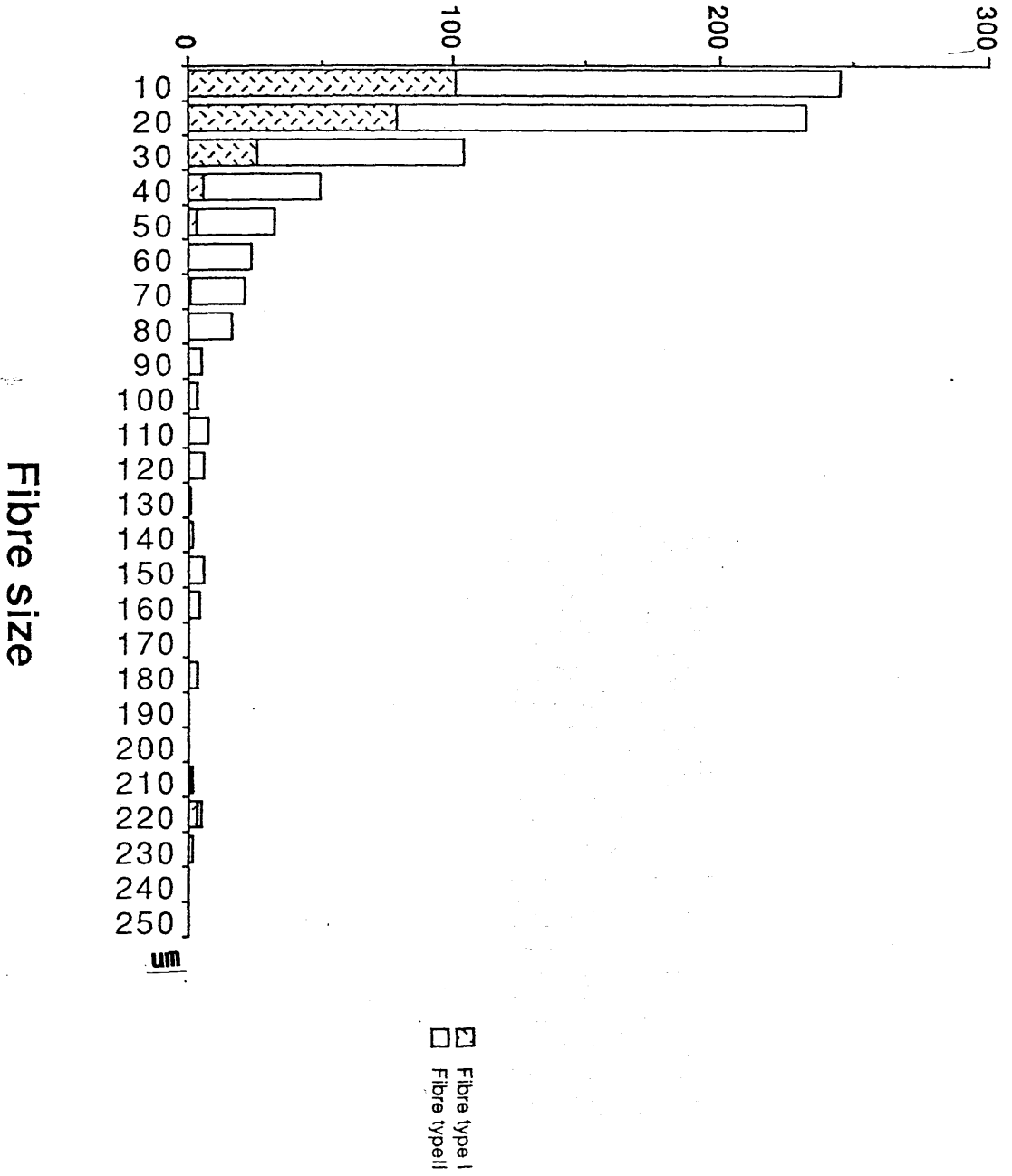


Fig 2.19

The histogram of three fibre types showing their distribution for SDH staining in the lateral muscle.

Number of fibres

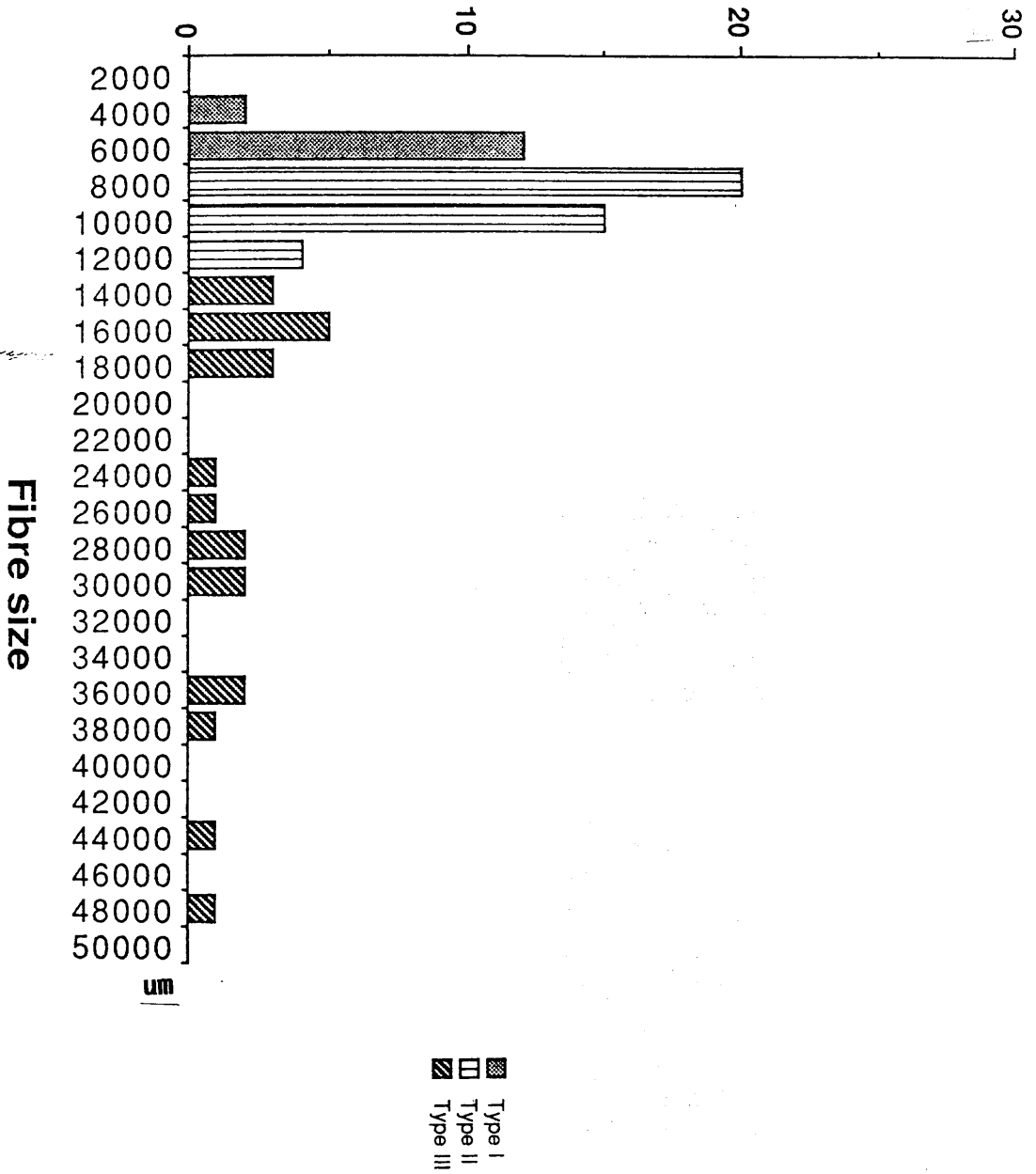
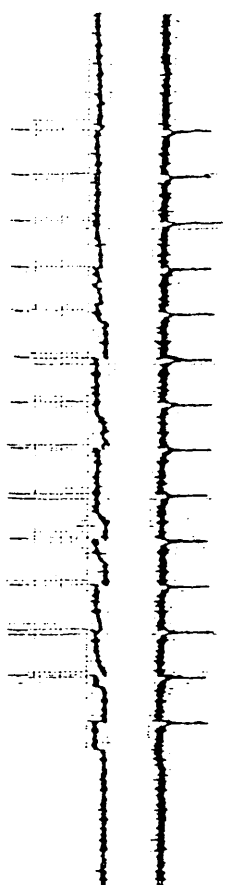
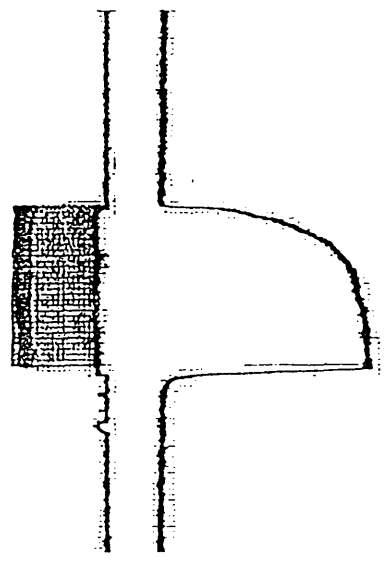


Fig 2.20

The frequency series performed at 2V in the mechanical recordings from IO.



1 Hz

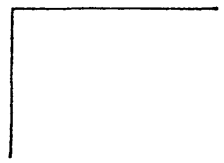


50 Hz



10 Hz

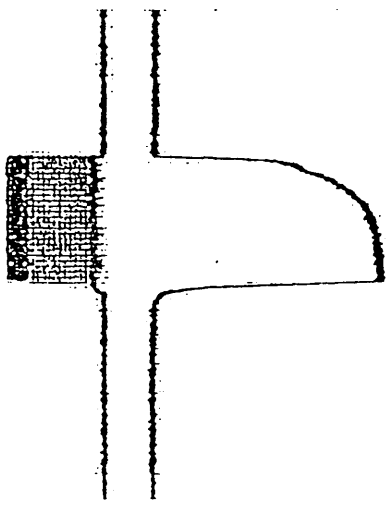
4g



4S



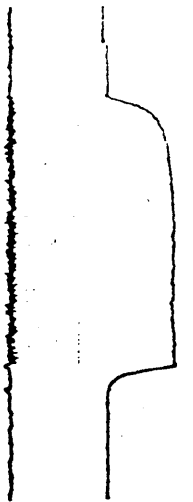
20 Hz



100 Hz

Fig 2.21

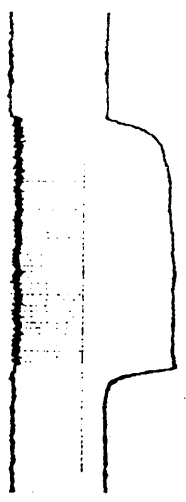
The voltage series performed at 50Hz to establish the threshold value in mechanical recordings from IO.



20V



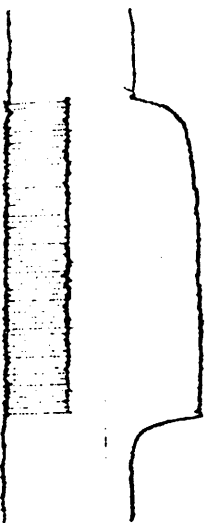
0.31



4V



0.21



1V



0.1

29

55

Fig 2.15

The histogram of two fibre types for SDH staining showing the distribution of orbital and global fibres according to their staining properties.

EXT-R

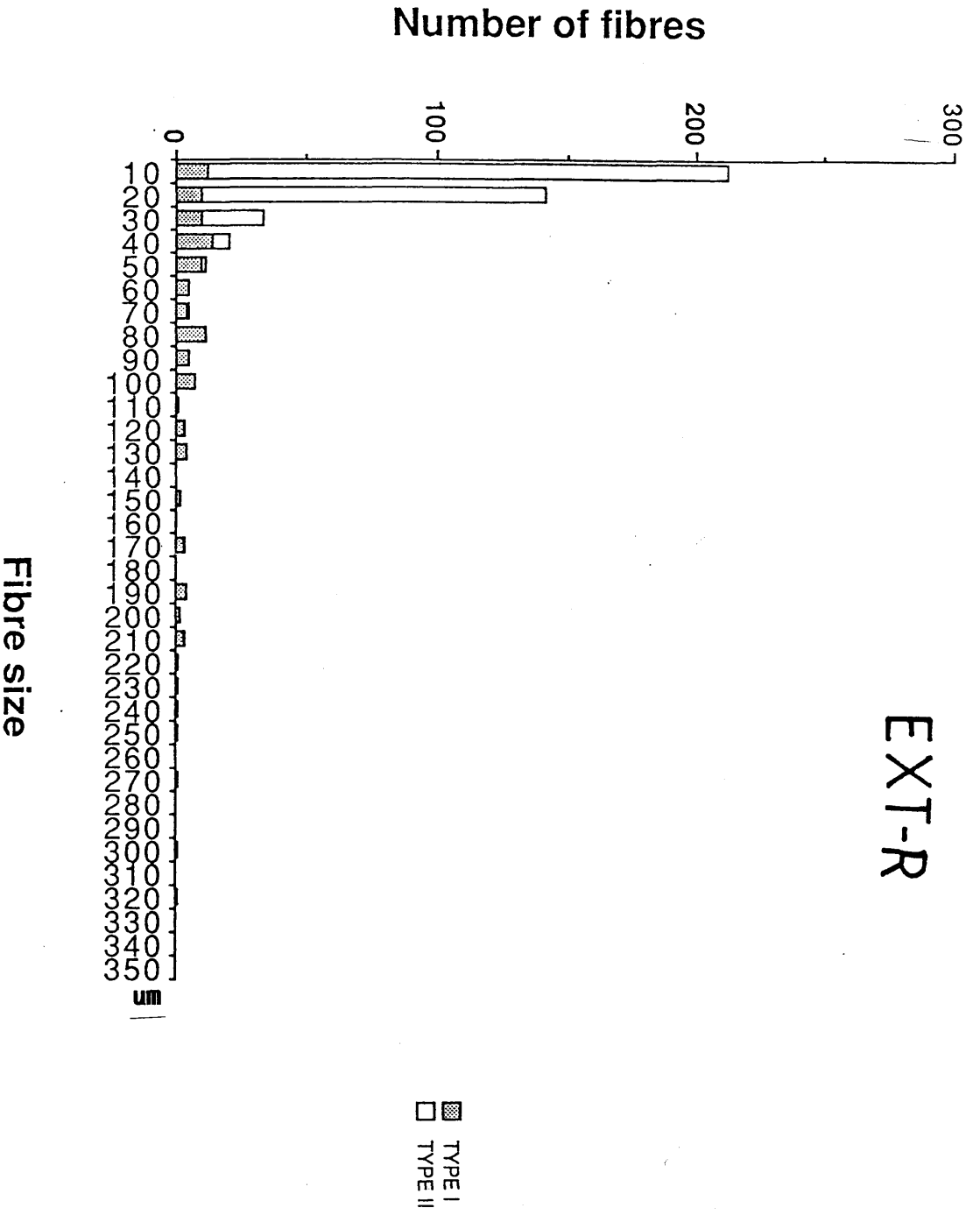


Fig 2.16 The digitised image of α ALD staining in the IO.

Immunohistochemical stain with antiserum specific for tonic fibre myosin

Red = positive reaction

Blue = negative reaction

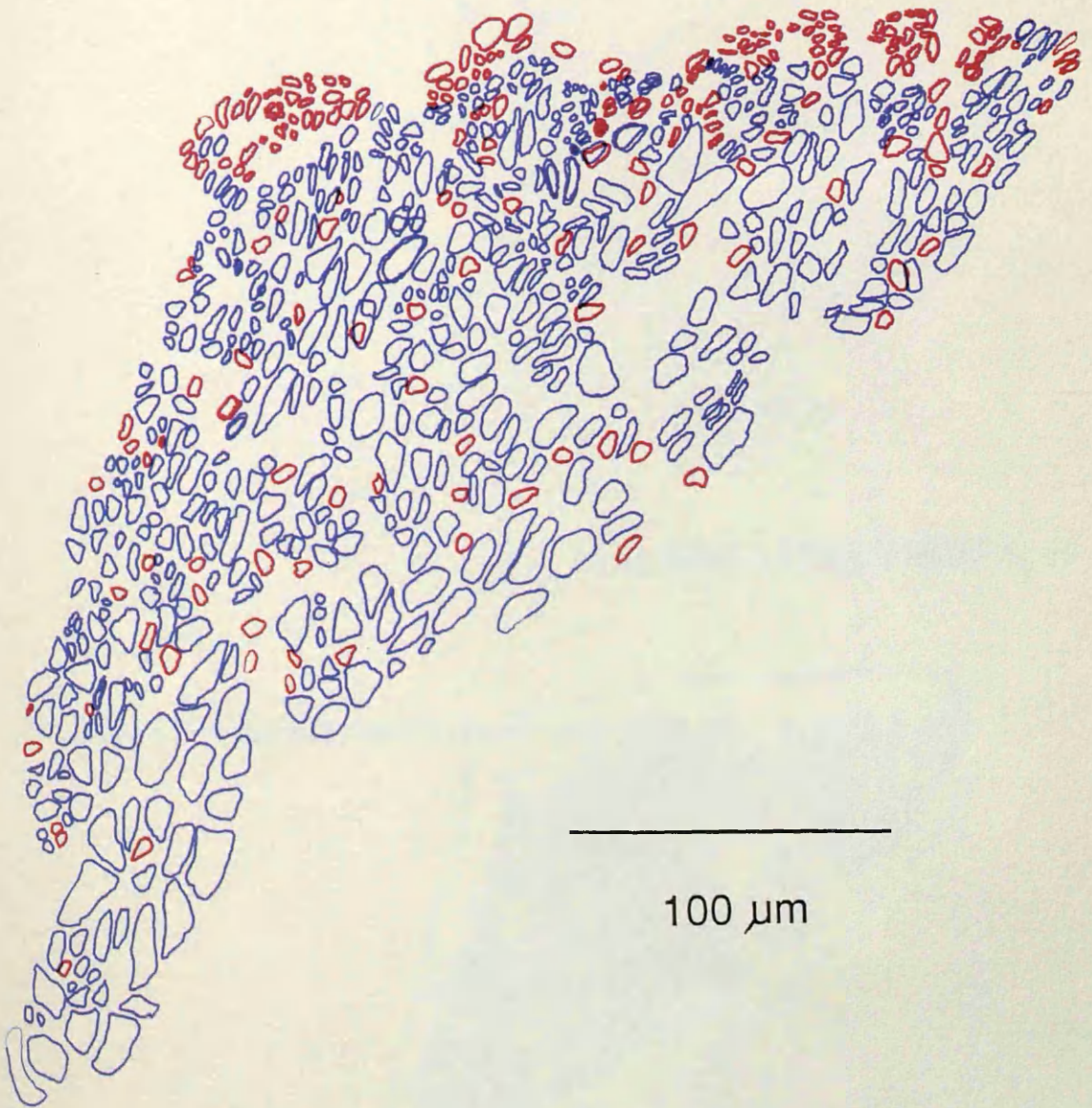


Fig 2.17.A The distribution of fibres for positive α ALD staining.

Fig 2.17.B The distribution of fibres for negative α ALD staining.

A

ALD-POSITIVE FIBRES, 10



B

ALD-NEGATIVE FIBRES, 10

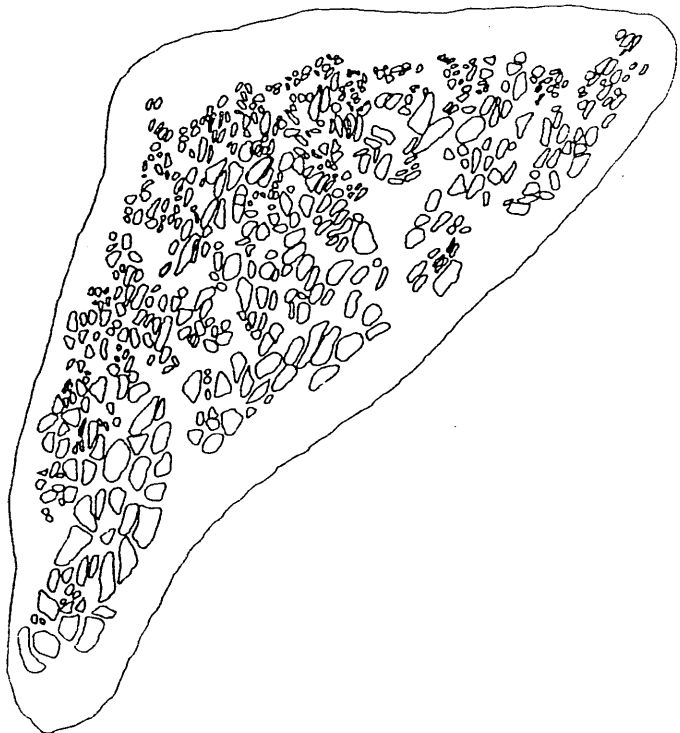


Fig 2.18

The histogram of two fibre types in the IO showing their distribution for α ALD staining.

Number of fibres

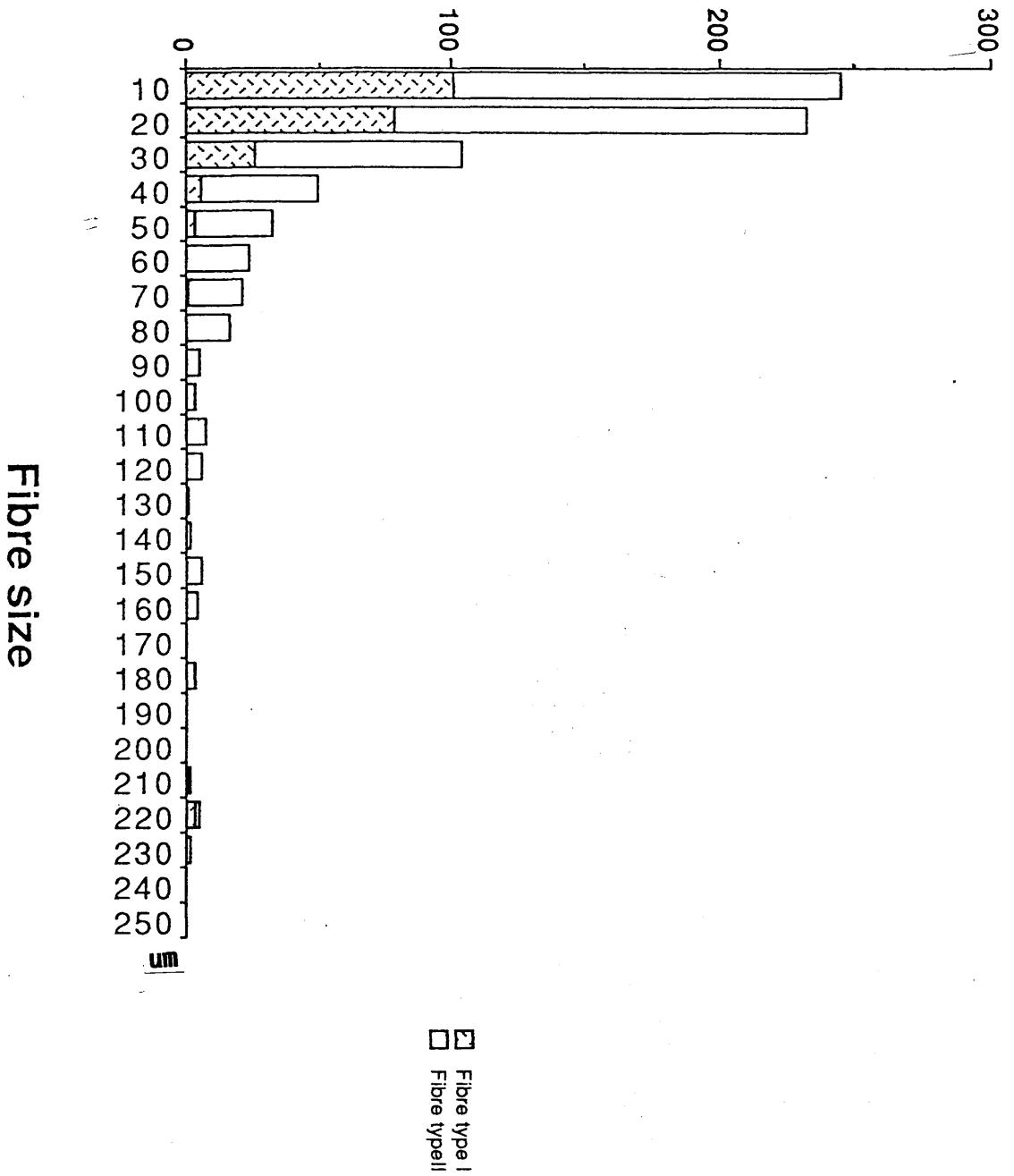


Fig 2.19 The histogram of three fibre types showing their distribution for SDH staining in the lateral muscle.

Number of fibres

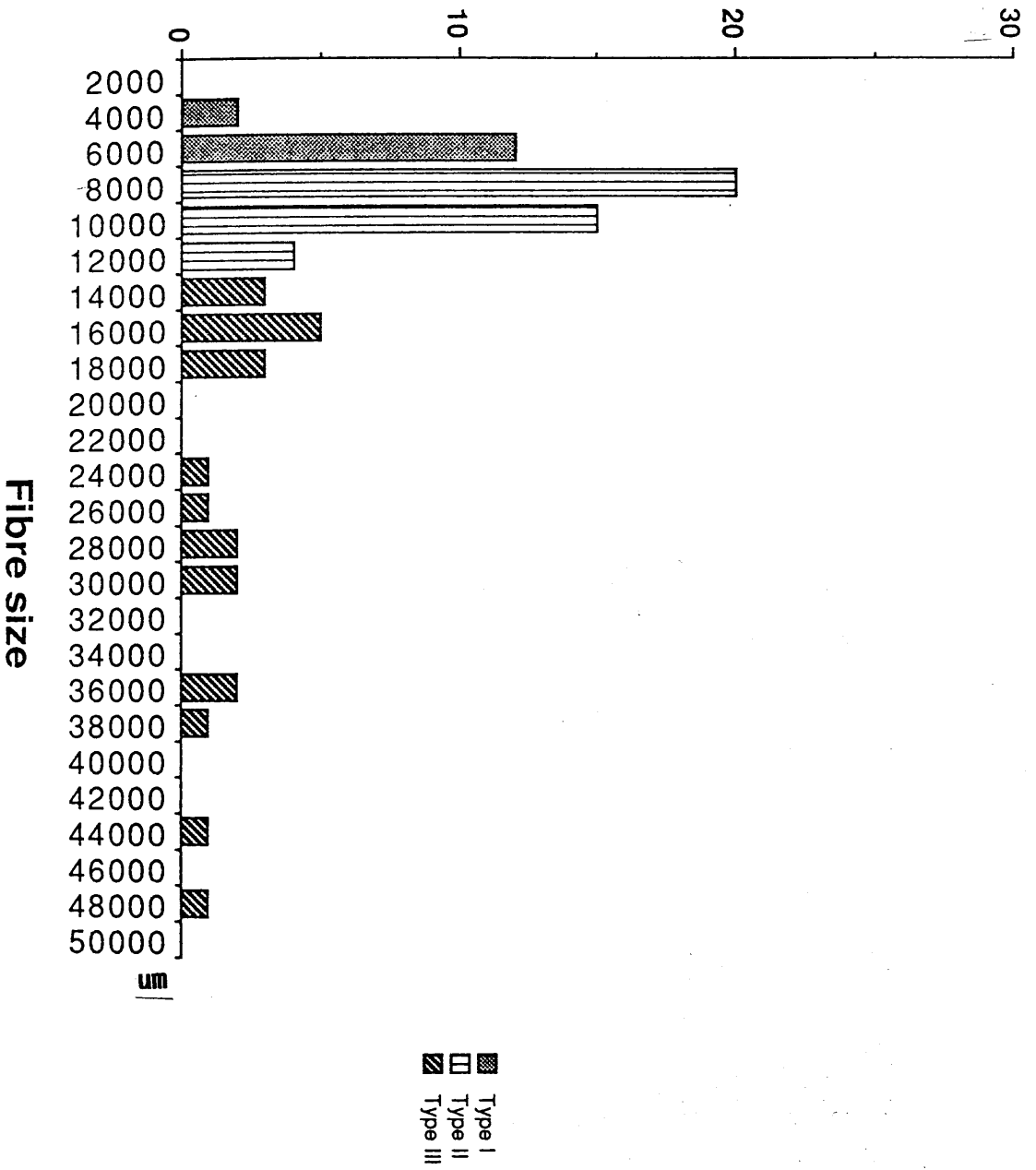
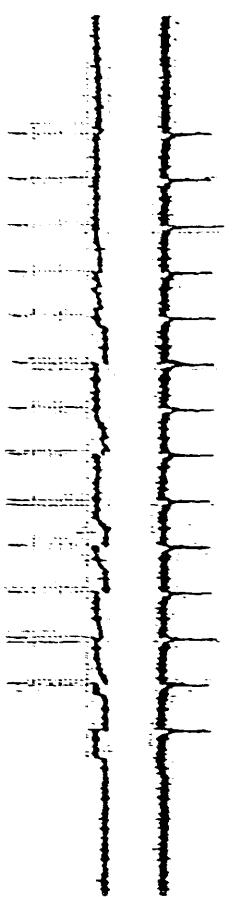


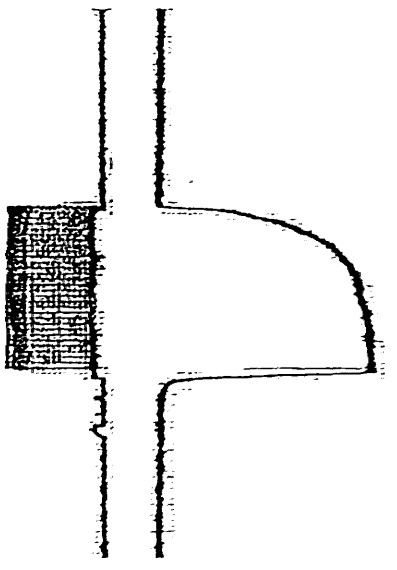
Fig 2.20 The frequency series performed at 2V in the mechanical recordings from IO.



1 Hz



10 Hz

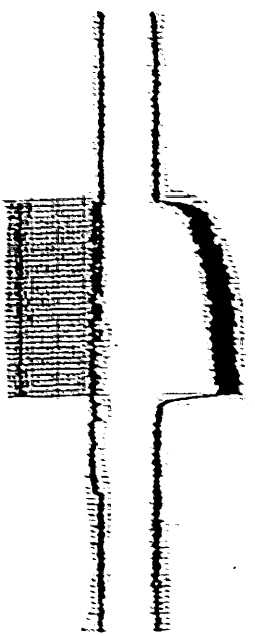


50 Hz

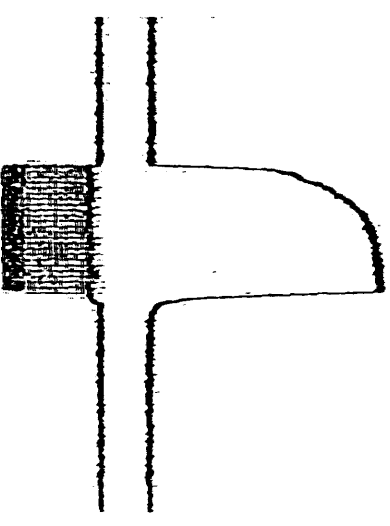
4g



4S



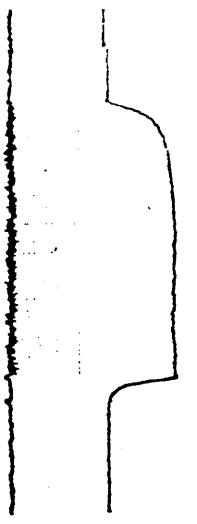
20 Hz



100 Hz

Fig 2.21

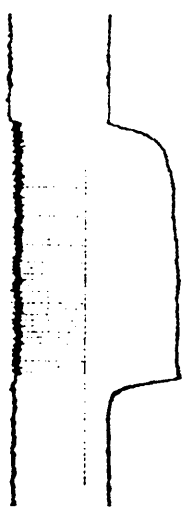
The voltage series performed at 50Hz to establish the threshold value in mechanical recordings from IO.



20V



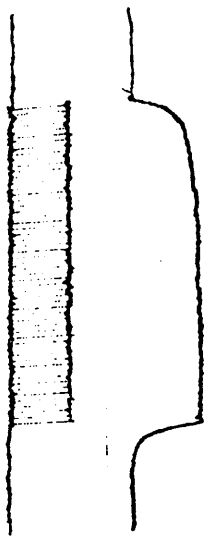
0.3V



4V



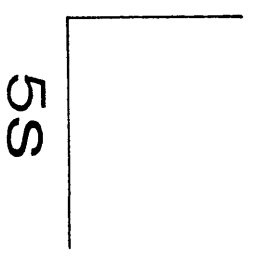
0.2V



1V
2g



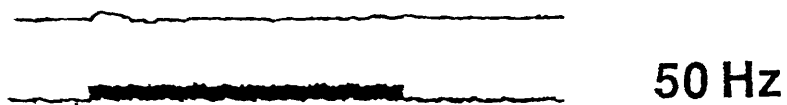
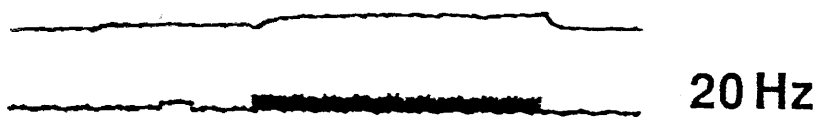
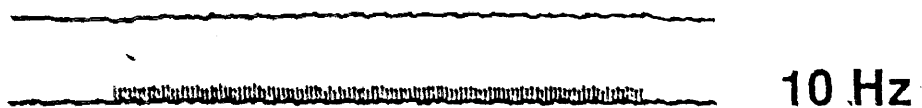
0.1V



5S

Fig 2.22 The frequency series performed at 0.2V in mechanical recordings from I0.

FREQUENCY SERIES AT 0.2V



2g

A vertical scale bar consisting of a vertical line segment on the left and a horizontal line segment at the bottom, forming an L-shape.

5s

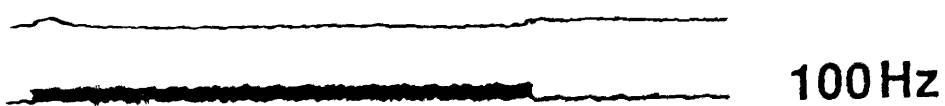


Fig 2.23

The engrappe endplates in longitudinal sections of S0.

Scale bar = 75um

ENGRAPPE ENDPLATE

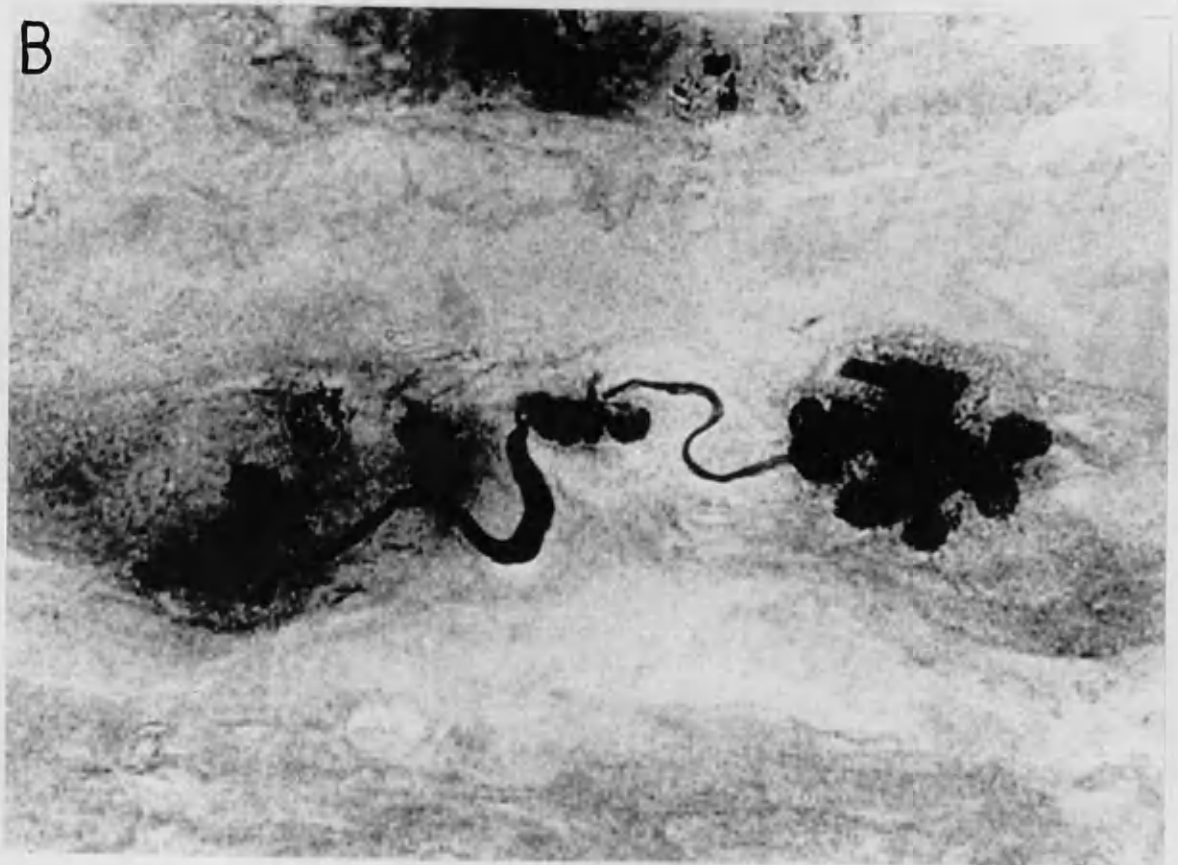
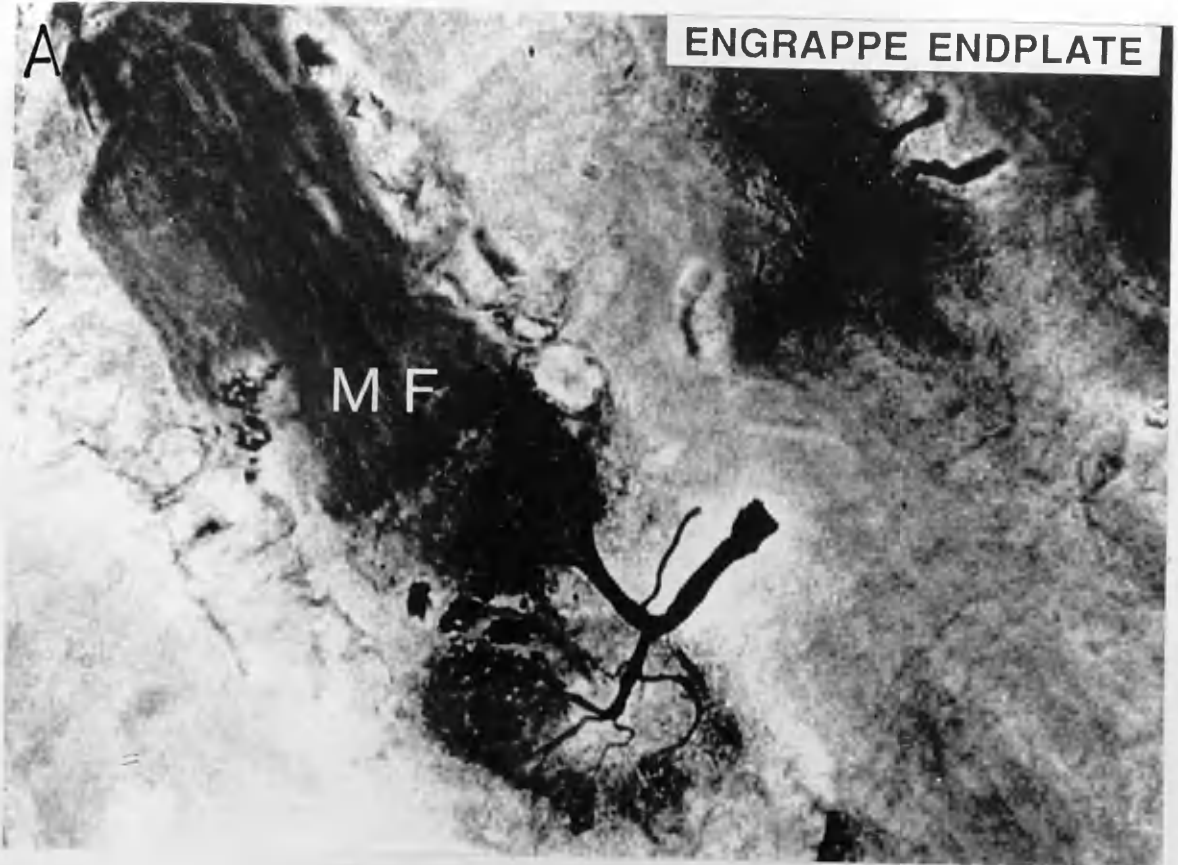


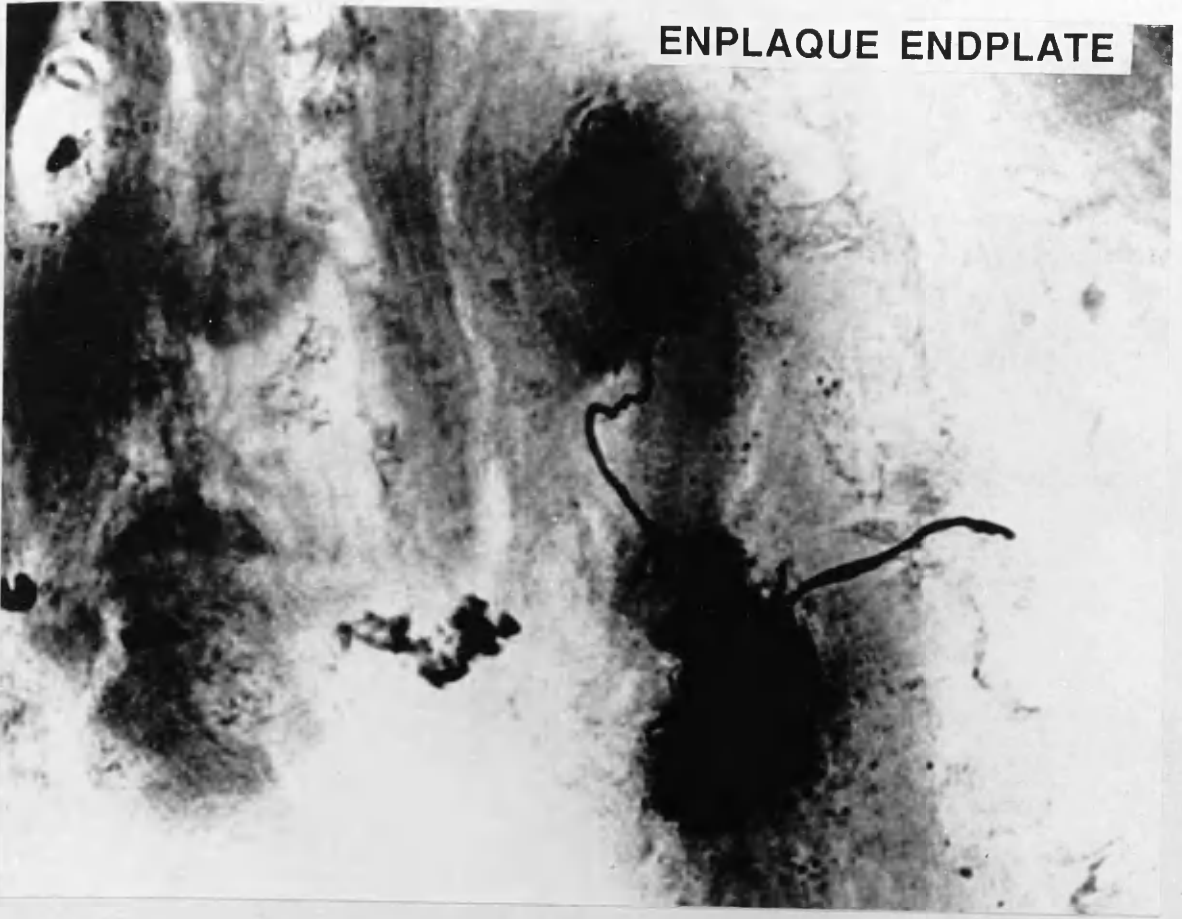
Fig 2.24

The enplaque endplates in the longitudinal sections of S0.

Scale bar = 80um

A

ENPLAQUE ENDPLATE



B

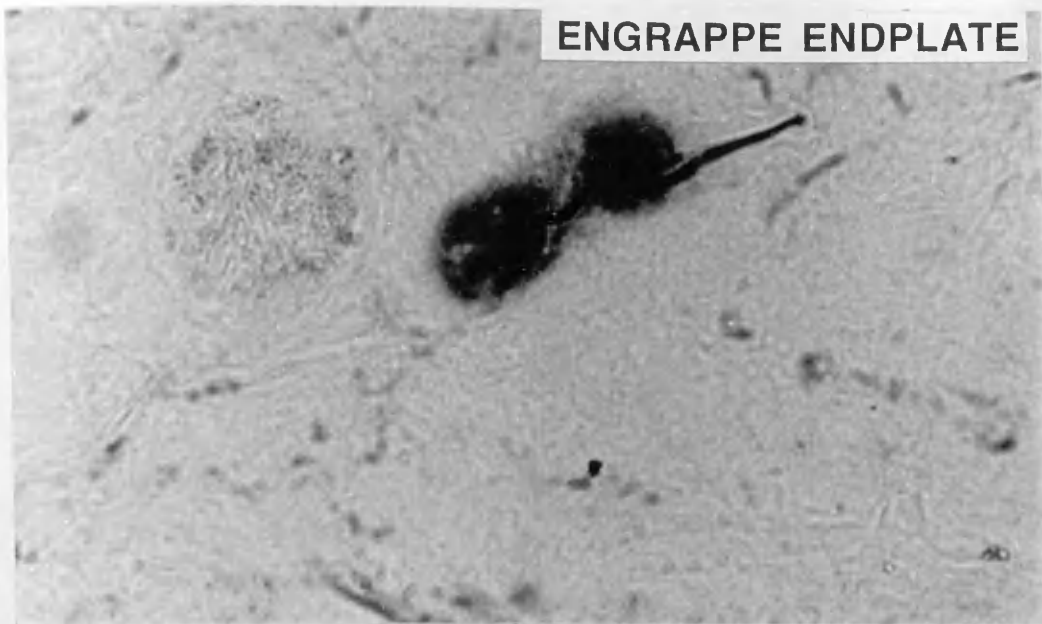


Fig 2.25

The engrappe and enlaque endplates in the transverse sections of S0.

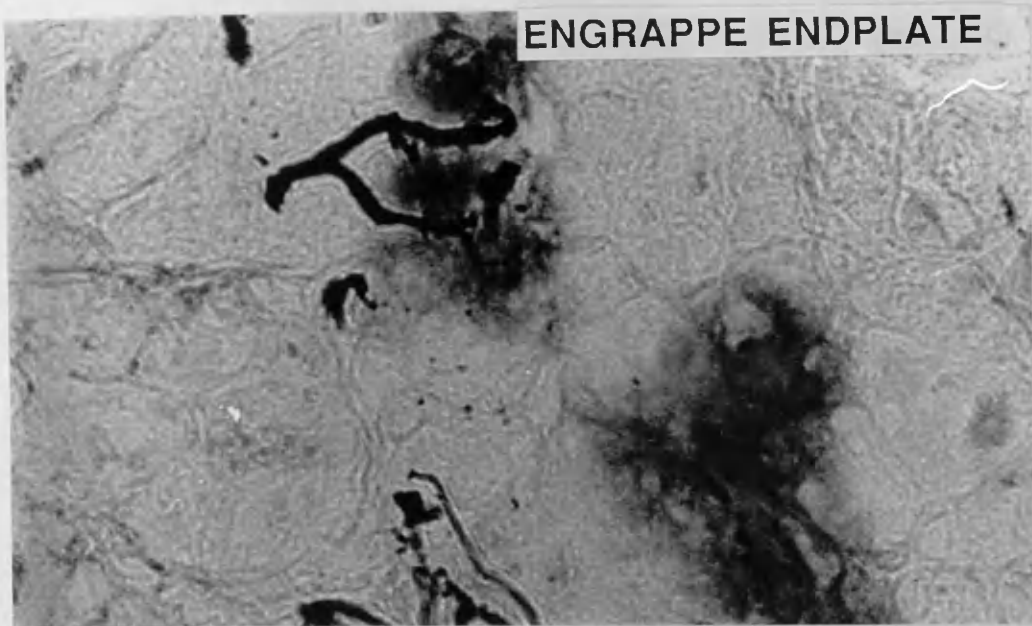
Scale bar = 70um

A



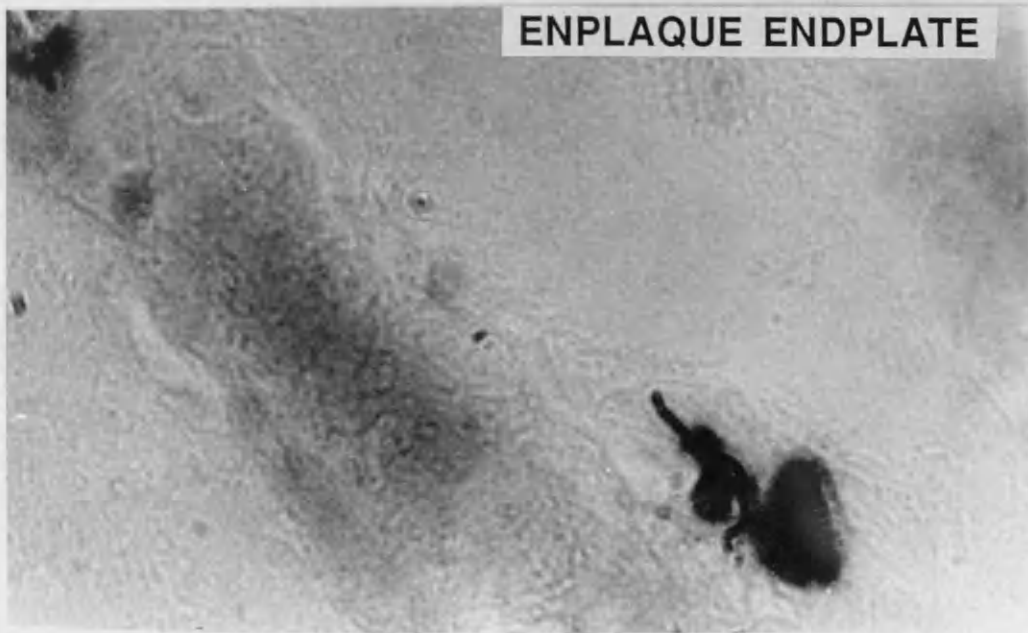
ENGRAPPE ENDPLATE

B



ENGRAPPE ENDPLATE

C



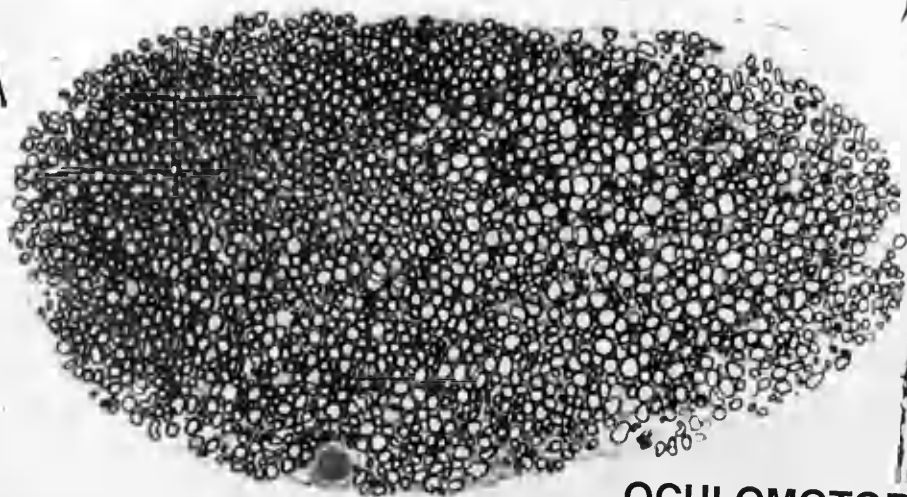
ENPLAQUE ENDPLATE

Fig 2.26.A The section of CN III in the cranium.
Scale bar = 60um

Fig 2.26.B The section of CN III after branching to SR.
Scale bar = 40um

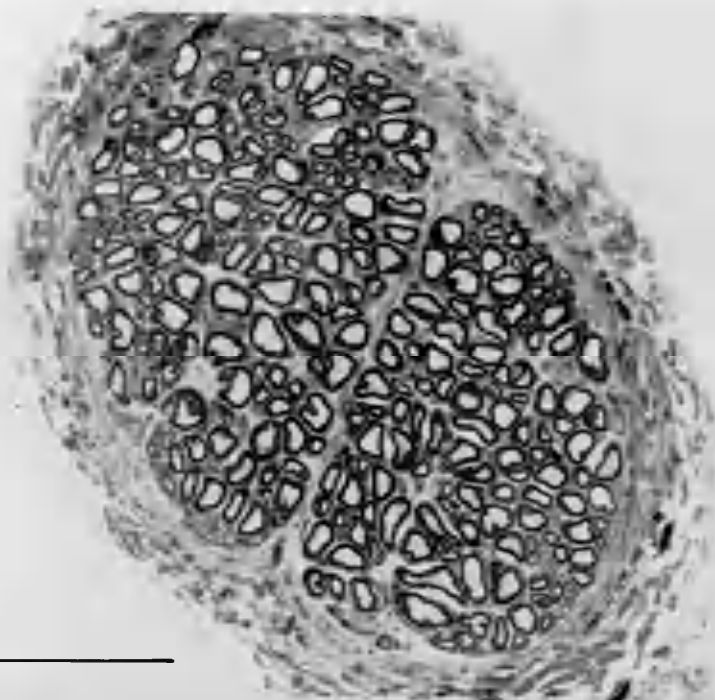
Fig 2.26.C The section of CN III branch to IO.
Scale bar = 32um

A



OCULOMOTOR NERVE

B



C

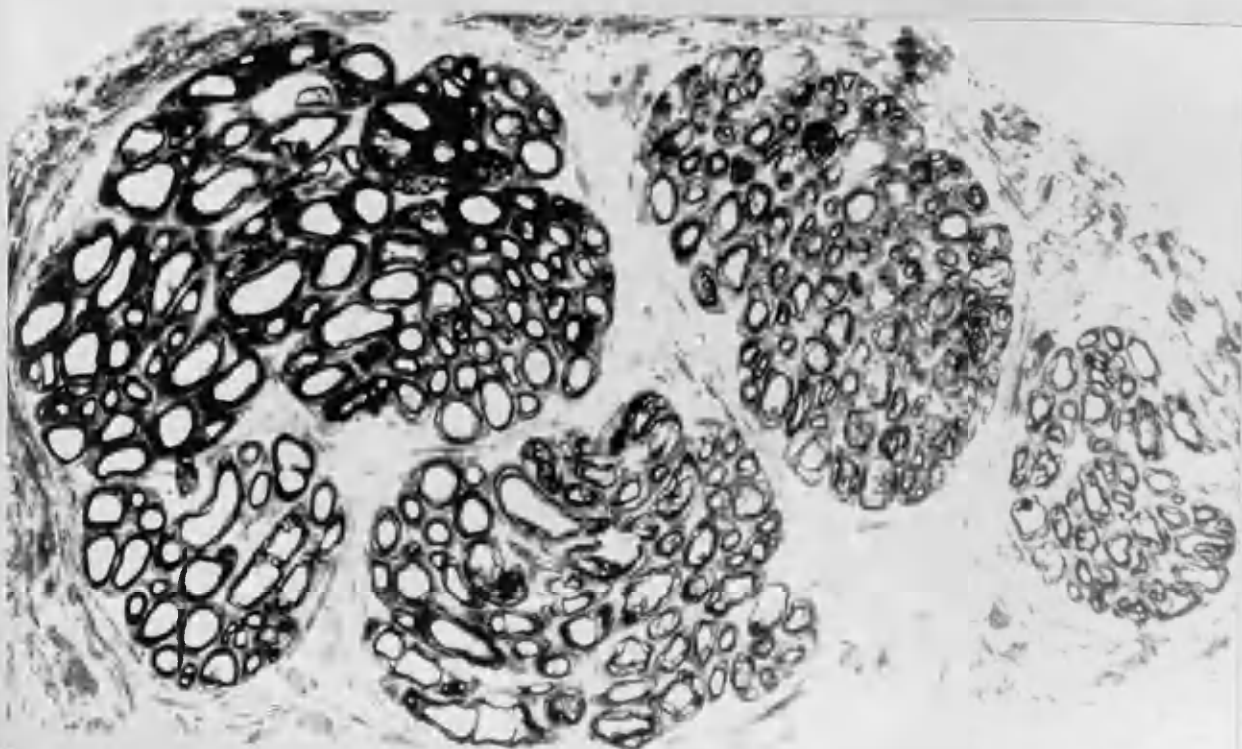
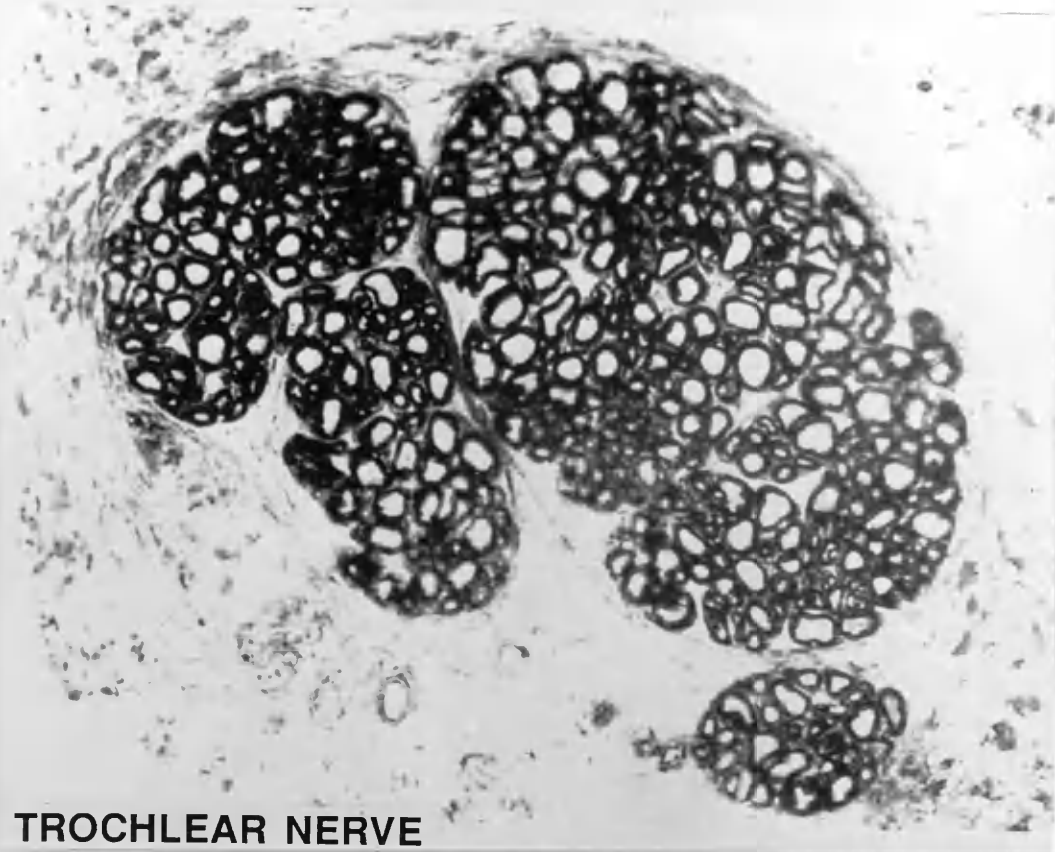


Fig 2.27.A The section of CN IV after its entry into the orbit.
Scale bar = 25 μ m

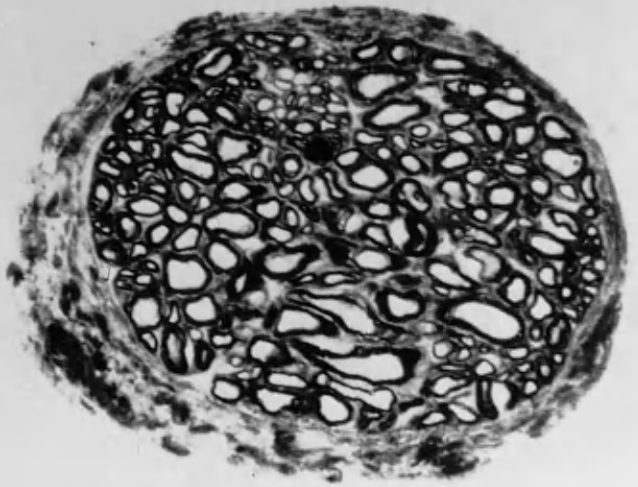
Fig 2.27.B The section of CN VI after its entry in to the orbit.
Scale bar = 19 μ m

A



TROCHLEAR NERVE

B

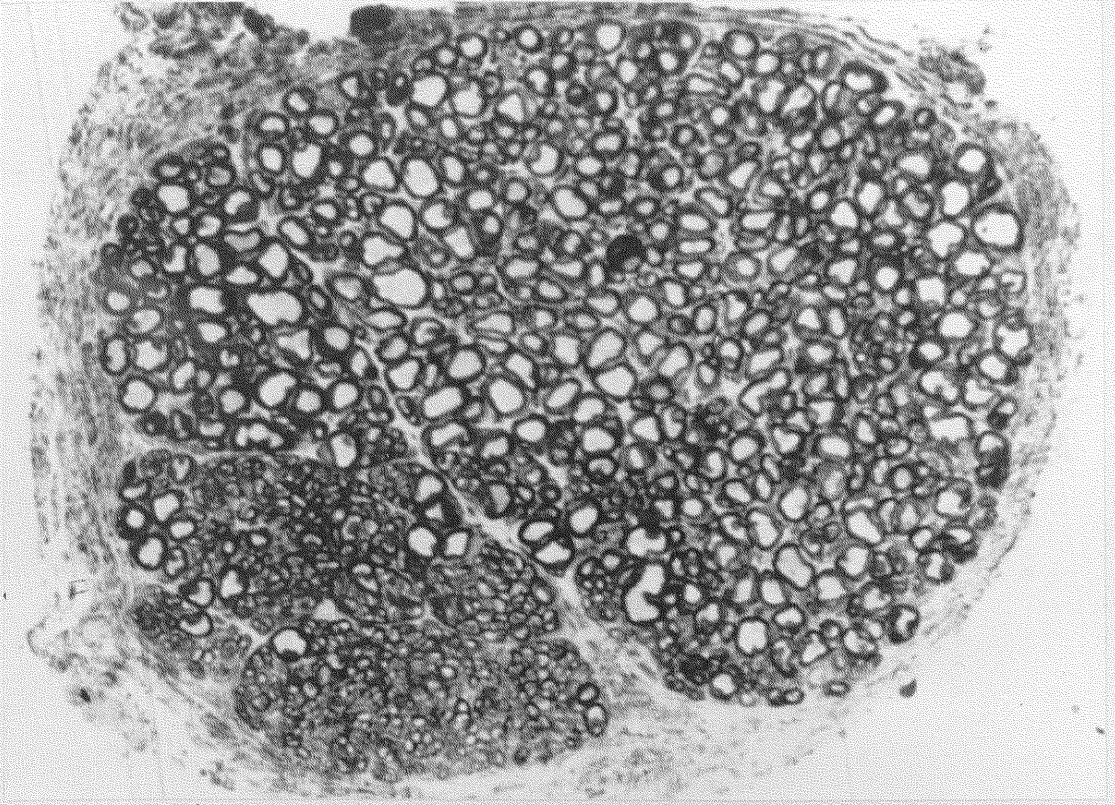


ABDUCENS NERVE

Fig 2.28.A The section of CN VI near EXT-R.
Scale bar = 35um

Fig 2.28.B The branches of CN IV are shown to be innervating the periphery of S0.
Scale bar = 450um

A



B



CHAPTER 3. VERTICAL EYE REFLEXES.

3.1 INTRODUCTION.

The control of eye movements among vertebrates is well studied and most of the significant aspects of this system have been analysed and worked out in detail in humans and in mammalian species and to some extent in the birds, amphibians and fishes (Fuchs & Kim, 1975. Collewijn, 1977. Barmack, 1981. Montgomery, 1983. Dieringer & Precht, 1986. Easter, 1975. Harris, 1965).

Compensatory eye and head movements assist stability of gaze and of posture. These reflexes are initiated by the head accelerations and by retinal image slip, resulting from the drifts of the eye and from the passive displacements of the head positions at rest.

The eye movements exhibited by various animals in the horizontal and vertical planes include slow pursuit eye movements. Fast flicks of eye called saccades are voluntary eye movements made to bring a new part of the visual field in to the foveal region. Nystagmus is a fast flick of eyes made to bring the eye back to its original position. Optokinetic nystagmus is observed when the animal is provided with some kind of visual stimulus. Another kind of the eye movement, commonly known as compensatory eye movements, is induced by vestibular stimuli.

The responses of the vestibular reflexes in relation to the horizontal head position has been determined by Montgomery (1983). His work has described the relationship between the electrical stimulation of the abducens nerve and the horizontal vestibulo-ocular reflexes.

In fish the slow pursuit compensatory eye movements have been most extensively studied in the goldfish (Easter, 1972; Hermann & Constantine, 1971). The horizontal compensatory eye movements in the gold fish have been studied by Easter, Pamela, Johns & Heckenlively,

(1974). They have also compared the horizontal eye reflexes of intact fish with the same reflexes in the gold fish after ablating its horizontal semicircular canals. This comparison has provided an insight into the control of eye reflexes in the horizontal plane by the horizontal canals. The vertical canal input to these horizontal reflexes and to the vertical compensatory eye movements still needs to be determined.

Harris (1965) has also studied the operation of the vestibulo-ocular reflexes in the dogfish in the horizontal plane. In his work on the dogfish (Squalus acanthias) the eye movements of freely swimming fish were recorded and classified to determine the interaction of labyrinthine reflexes and the body movements as they affected the eye movements during swimming. His work has provided a good base to extend these studies to the eye reflexes of these fish in other planes and to determine the control of these eye movements more directly by ablating different combinations of the vertical semicircular canals.

3.1.b Aims of the present project.

The aim of this part of the project were to determine the vertical eye reflexes of the dogfish for low (0.2Hz) and high (0.8Hz) frequencies by tilting the animal in the roll and pitch planes, and to determine the visual contribution to these eye movements. This was determined by recording in controlled light conditions and by providing the animal with visual stimuli (tests for optokinetic nystagmus).

The control of eye movements by vertical semicircular canals was further investigated by recording eye movements after the ablation of different combinations of the vertical semicircular canals.

3.2 MATERIALS AND METHODS.

For recording the eye movements, an anaesthetised (0.02% MS222 20mg/l) dogfish was pithed and decerebrated. To hold the body of the animal still the fish was restrained in an specially designed frame assembly and the eye lids were carefully removed. This operation proved essential to observe the eye movements. The fish was then brought back to the sea water tank and left until it recovered completely (typically 1/2hr-1hr).

3.2.A Recordings in the intact fish.

The eye movements were either filmed by a video camera or recorded by the automatic movement monitor.

By using a video camera the animal was filmed either from the front (in roll) or from the side (in pitch) during imposed vertical body tilts. Tilts of $\pm 25^{\circ}$ were generated by a DC motor device for a range of frequencies (0.2Hz, 0.3Hz, 0.5Hz, 0.8Hz). Two sticks with a bright marking point at their ends were fixed on the cornea of each eye using cyanoacrylate glue for recording from both eyes simultaneously. A bright marker on the corneal surface was used for recording from the side of the animal. A reference point on the bar holding the animal's body was used as a marker to define the body tilts. To discriminate between the compensatory eye movements and visually-evoked eye reflexes the filming was performed both in white light and in dim red light. Precautions were taken to block the other sources of light. Under these conditions the animal's eye showed no visually-evoked responses.

Tests for optokinetic nystagmus.

In the intact animal the visually-evoked eye reflexes were

further checked by performing tests for optokinetic nystagmus. In these experiments a striped drum mounted on horizontal bearings was rotated around the head of the animal in the following tests:

- A. Striped drum rotated around the stationary animal in the frame.
- B. Striped drum and the frame (ie animal) rotated together.
- C. Striped drum rotated around stationary animal.

3.2.B Recordings in the operated fish.

A series of operations was performed on the anaesthetised decerebrated dogfish in which the vestibular apparatus was exposed by slicing through the cartilaginous roof of the auditory capsule. After this operation the fish was left in the sea water tank to recover for a few hours. Recordings were then made firstly with the semicircular canals intact but exposed. In a series of subsequent experiments different combinations of the vertical semicircular canals were ablated and the eye movements were recorded using the video technique.

3.2.C Analysis.

The data from the video tape were analysed by an image analyser (HV110). Crosswires superimposed on the video image were moved by a joystick to lie in turn over the tip of the eye stick and the reference mark for the body. The XY coordinates of these points obtained from a series of frames were then sent to an especially designed computer programme on the BBC micro which was programmed to reconstruct the curves for the movements of the body and the eyes in space. The eye movements were also calculated relative to the body movements to give a direct measure of the their compensatory responses by subtracting the eye movement curves from the body curve. The stored values for these curves were plotted on a XY plotter (Epson HI-80)

Data from the movement monitor were analysed to provide the measure of both the amplitude of the eye movements and its phase relationships to the body movements, in the white light. They also provided the only method to compare responses of the eyes in white light, and in dim red light.

3.3 RESULTS.

3.3.A Recordings in the intact fish, in light.

In the intact fish recordings were made in the light to measure the compensation and phase position of the left and right eyes in the roll and pitch planes for tilts at 0.2Hz and 0.8Hz. Data represented in this section were obtained from 8 fish.

3.3.A.a Compensation in roll.

In the roll plane for tilts of an amplitude of $\pm 22^\circ$ at a frequency of 0.2Hz the two eyes undercompensated, the average gain being 0.65. At this frequency the two eyes were in phase with the body. (Fig 3.1.a)

For tilts at 0.8Hz the average gain for the two eyes was 0.6 and in contrast to the tilts at 0.2Hz at this frequency the right and left eyes were phase advanced relative to the body movement by 7.2° (Fig 3.1.b).

3.3.A.b Compensation in pitch.

In the pitch plane recordings were made individually for the left and right eyes. For the tilts at 0.2Hz and 0.8Hz the average gain for the two eyes was 0.5, and they were in phase with the body movement (Although measures of 0.2Hz sometimes showed a phase lag of up to 14°) Fig 3.1.c, d, e, f.

3.3.B Recordings in the intact fish, in dim red light.

3.3.B.a Compensation in roll.

For tilts in the roll plane, in dim red light the compensation in the two eyes was better than observed in the white light. For tilts at 0.2Hz the average gain for the two eyes was 0.68. The eyes phase

lagged the body tilt by an average of 11° (Fig 3.2.a). For tilts at 0.8Hz the gain of the response was an average 0.5. The two eyes were advanced in phase relative to the body by an average of 18° (Fig 3.2.b).

3.3.B.b Compensation in pitch.

For tilts in the pitch plane left and right eyes had an average gain of 0.6 for tilts at 0.2Hz, for tilts at 0.8Hz an average gain of 0.5 was recorded in two eyes (Fig 3.2.c, d, e, f).

3.3.C Tests for optokinetic nystagmus.

3.3.C.a Visual stimulus opposing eye movement.

Recordings were made during the simultaneous roll of striped drum and the frame (ie animal), through an amplitude of ± 22 . At 0.2Hz the average gain of the two eyes was 0.62 and the two eyes were in phase with the body (Fig 3.3.a).

For tilts at 0.8Hz the average gain for the two eyes was 0.6 and they were phase advanced by 22° .

3.3.C.b Visual stimulus reinforcing eye movement.

When the animal was rolled inside the stationary drum, for the tilts at 0.2Hz the average gain of the two eyes was 0.73 and at this frequency the two eyes were in phase with the body (Fig 3.3.c). For tilts at 0.8Hz the gain of the response was reduced (to an average of 0.49) and as for low frequency tilts the two eyes were in phase with the body (Fig 3.3.d).

3.3.C.c Visual stimulus reinforcing eye movements (test in dim red light)

In this test for checking the visually evoked responses in which the animal was rolled inside the stationary drum, the average gain of the right and left eyes was 0.79, and at this frequency the two eyes were in phase with body (Fig 3.3.e).

For tilts at 0.8Hz the average gain of the two eyes was 0.67 and as for low frequency tilts the two eyes were in phase with body (3.3.f)

3.3.C.d Test for optokinetic nystagmus (visual stimulus only).

Recordings were made by rotating a striped drum around the head of stationary animal. The pattern of eye movements during this test was not very clear, although there was an indication of a deviation in the two eyes as a result of following the striped drum.

3.3.D Recordings after the ablation experiments.

3.3.D.A Left anterior and posterior vertical canals ablated.

In the experiments in which recordings were made after the ablation of left anterior and posterior vertical canals, for tilts at 0.2Hz the left eye (ablated side) gain was reduced to 0.57 while in the right eye the gain, at 0.71, measured close to its value in the intact animal. The right eye was in phase with body, while left eye lagged in phase by 25.2° (Fig 3.4.a).

For tilts at 0.8Hz left eye gain was severely reduced (0.17) and it was in phase with body, while in the right eye the gain was 0.60 and it lagged in phase by 10.8° (Fig 3.4.b).

Similar deficits occurred for the left eye during tilts in the

pitch plane. For tilts at 0.2Hz left eye gain was 0.55 and it lagged in phase by 10.8° , and in right eye at this frequency a gain of 0.59 was obtained and it was in phase with body (Fig 3.4.c). For tilts at 0.8Hz gain of the right eye was 0.57 and as for low frequency tilts it was in phase with the body, while left eye gain was 0.33 and it was in phase with body (Fig 3.4.d).

3.3.D.b All four vertical canals ablated, utriculi intact.

After the ablation of the four vertical canals, recordings were made in the right and the left eyes at the roll and pitch planes. Gain remained relatively high for tilts at 0.2Hz (0.46 for right eye, 0.61 for left eye), but was significantly reduced at 0.8Hz (0.21 and 0.18 in the left and right eyes respectively) (Fig 3.5.b).

Similar differences were obtained for tilts in the pitch plane at low and high frequencies. For tilts at 0.2Hz right eye gain was 0.63, while for tilts at 0.8Hz a gain of 0.13 was recorded (Fig 3.5.d). In the left eye for tilts at 0.2Hz a gain of 0.5 was recorded (Fig 3.5.e).

3.3.D.c All four vertical canals and right utricle ablated.

The eye movements were recorded in fish after the ablation of all four vertical canals and the right utricle with the left horizontal canal and the left utricle intact. For tilts at 0.2Hz and 0.8Hz there was an almost total absence of the response in the right eye (ablated side). However in the left eye (intact side) for tilts at 0.2Hz gain of 0.53 was obtained and it lagged in phase by 21.6° . For tilts at 0.8Hz gain in the left and right eyes was reduced to 0.15 (Fig 3.5.a,b).

In the pitch plane for tilts at 0.2Hz a gain of 0.23, and for

tilts at 0.8Hz a gain of 0.18 was recorded (Fig 3.6.c,d). In the left eye for tilts at 0.2Hz left eye gain was 0.42 and it lagged in phase by 7.2° (Fig 3.6.e). In the left eye for tilts at 0.8Hz gain of 0.22 was obtained (Fig 3.6.f).

3.4 DISCUSSION.

In the present study of the vertical VOR of restrained fish in the intact condition were recorded at two stimulus frequencies 0.2Hz & 0.8Hz. The eye movement studies of a freely swimming dogfish (Harris, 1965) and studies made by electrical stimulation of the abducens nerve to elicit horizontal eye movements (Montgomery, 1983) have demonstrated that the oculomotor system of these fish operate at considerably lower frequencies than those reported in mammals and in goldfish (goldfish: Hermann, 1971, Gestrin & Sterling, 1977).

For tilts in the roll and pitch planes at 0.2Hz and 0.8Hz, in white light and in dim red light, gain of the dogfish eyes is nearly similar and compensation in the dark was ^{the} same as seen in the white light which suggests that vision (if present) is not dominantly shown in the vertical eye reflexes.

Tests were also made to obtain the optokinetic nystagmus response during vertical VOR. The visual input given in combination with the vestibular input failed to suppress the vestibular influence and in this test at low and high frequency tilts in the two eyes reflexes of nearly equal gain value was elicited as observed during other recordings in the intact fish.

Another test involving frame roll (ie animal) inside the stationary drum was made to observe if dogfish eyes followed the striped drum pattern. In this test for low frequency tilts high^{er} gain values were observed than seen in other experiments, which suggests that there may be visually evoked responses involved in these reflexes, which are shown only when the animal is provided with a strong visual stimulus.

Also in these two tests the movement of the two eyes was in phase with that of the body , which reflects another property of the VOR

system in which visual and vestibular reflexes if operating simultaneously tend to induce phase locking of the eyes to the body.

Another test made to obtain optokinetic nystagmus involved ^{revolving} a striped drum roll around the head of a stationary animal. The eye reflexes of animal during this recording suggested a little following of the striped drum pattern, but no flick at the end of this movement. Results of these experiments show a strong, dominant vestibular influence during the vertical eye reflexes, although a weak visual response may be present under the influence of a strong visual stimulus even in the dim red light.

In all these recordings there was a general tendency towards a phase lag in the two eye^s at low frequency tilts, while for most of the recordings in white light and in dim red light for tilts at 0.8Hz, the two eyes phase advanced the body phase position. These differences are may be due to differences in the semicircular canal and utricle input on to the eye reflexes.

In these experiments smaller gains of the eye reflexes were recorded in the pitch plane than observed in roll, which suggests that the eye movements during the pitch tilts may be very small and of less significance to the animal.

In all these experiments eye movements were recorded over a time period of 3-5 minutes, and during this time there was no indication of gain adaptation after the first few seconds of the response and an approximately similar gain value was obtained even after first few minutes of the recording.

In all these recordings unequal gain values have been observed in the right and left eyes. The slightly unequal gain values for the right and left eyes have also been recorded in other fish (Easter et al., 1974.I).

Compensation in the two eyes was never absolute and a gain value less than 1.0 was obtained for recordings in the roll and pitch plane, at two tilt frequencies and in white light and dim red light. The gain value less than 1.0 is difficult to interpret in this case. Harris (1965) and Easter et al., (1974 I) have explained the partial compensation consistently observed in freely swimming dogfish and goldfish during horizontal VOR. Partial compensation was favoured in freely swimming animals because an absolute compensation during swimming would only stabilize objects at infinity. In case of dogfish in the present project a possible answer could be that in all these case fish was subjected to an angular tilt of ($\pm 25^0$) which exceeded the capacity of the oculomotor system to follow.

The dogfish eyes did not show nystagmic response during vertical VOR and eye movements observed in the present study were strictly compensatory. Poorly developed saccadic systems have been reported in Cephalloscyllium and Squalus (Harris, 1965; Montgomery, 1983) during horizontal VOR. Harris (1965) has concluded that in dogfish the eye movements during swimming are primarily compensatory and saccades were only observed to occur just before fish turns. In mammals and birds nystagmus is common during horizontal and vertical VOR (Snyder & King, 1988; Anastasio & Correia, 1988).

A series of operations was performed on dogfish to establish the variations in gain and phase position of the two eyes after ablating different components of the vestibular system. In these experiments after ablation of the left (ipsilateral) pair of canals the left eye gain for 0.8Hz tilts declined from 0.7 to 0.17 in the roll plane. For tilts in the pitch plane after ablation a gain of 0.33 was recorded in the eye of the ablated side at 0.8Hz. The intact side eye was little affected by the ablation and it showed similar value of gain for tilts

at 0.2Hz and 0.8Hz in the roll and pitch planes. The results of this experiment suggest a predominant but not total ipsilateral control of the left eye response by the semicircular canals. In experiments where all four vertical canals were ablated, gain declined to 0.21 & 0.18 in the left and right eyes respectively for tilts at 0.8Hz. However for tilts at 0.2Hz little variations were observed in the gain of the two eyes compared to the intact condition.

In another recording in which vertical semicircular canals were ablated along with the utricle of right side a reduction in the gain value was observed in the ablated side eye at low and high frequency tilts, while in the intact side eye the gain value remained unchanged for low frequency tilts.

The significantly reduced gain in the two eyes after ablation of semicircular canals mainly for tilts at 0.8Hz suggests a possible activation of this system at fairly high frequencies. Also the results of utricle ablation suggest activation of the utricle component mainly at lower frequencies (0.2Hz and below).

This study represents preliminary investigations of the vertical VOR studied by recording eye movements. The detailed analysis of the operation and control of these reflexes has in turn been made by recording myographically from the EOM, which provides more direct information about vertical vestibulo-ocular reflexes in the intact and ablated animals (Chapter 4 & 5).

Fig 3.1 The vertical eye movements of intact fish are recorded in light. Data from 8 animals is represented as mean and standard deviation values *

(a) 0.2Hz in the roll plane (b) 0.8Hz in the roll plane.

(c) 0.2Hz in the pitch plane (d) 0.8Hz in the pitch plane.

(e) 0.2Hz in the pitch plane (d) 0.8Hz in the pitch plane.

Every 50th frame analysed for tilts at 0.2Hz. Every 8th frame analysed for tilts at 0.8Hz.

Curve offset for curve one = 25° .

Curve offset for curve two = 25° .

Curve offset for curve three = 50° .

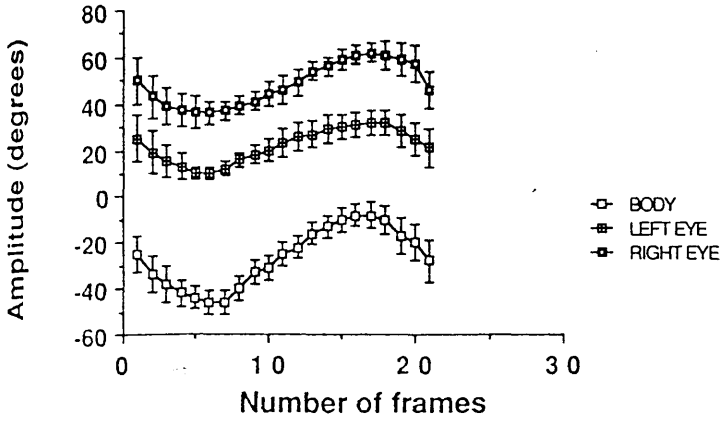
GAIN	ROLL	0.2Hz	0.8Hz	PITCH	0.2Hz	0.8Hz
RIGHT EYE		0.60	0.60		0.51	0.49
LEFT EYE		0.70	0.60		0.50	0.50

* Curve one = relative to space

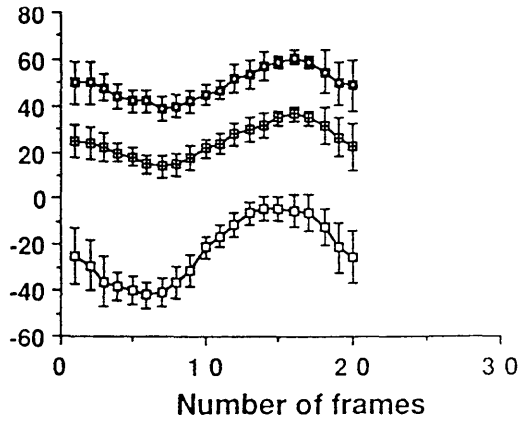
Curve two = relative to body

ROLL

a

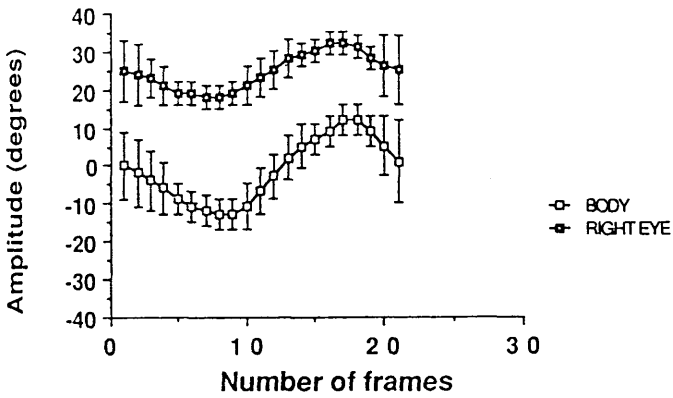


b

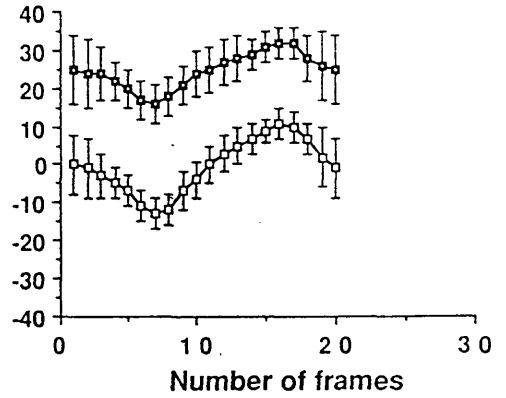


PITCH

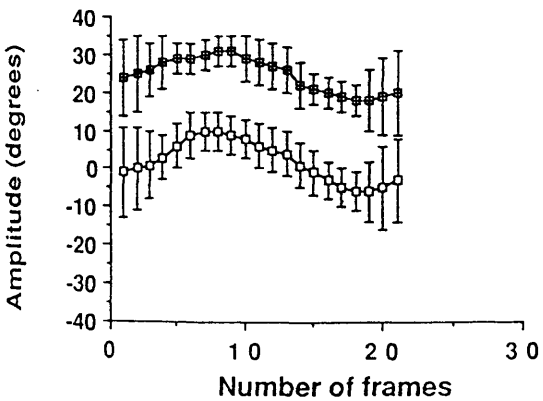
c



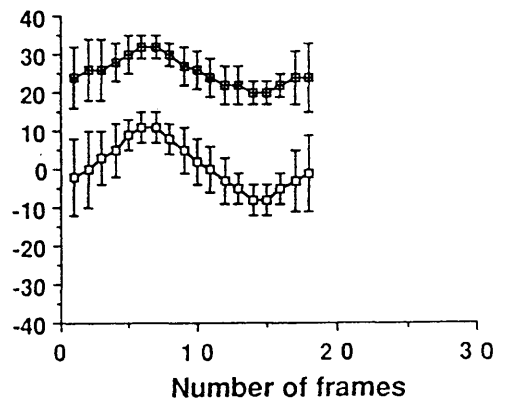
d



e



f



0.2Hz

0.8Hz

Fig 3.2 The eye movements of intact fish are recorded in dim red light. Data from 4 animals presented as mean and standard deviations values.

(a) For tilts at 0.2Hz in roll (b) For tilts at 0.8Hz in roll plane.

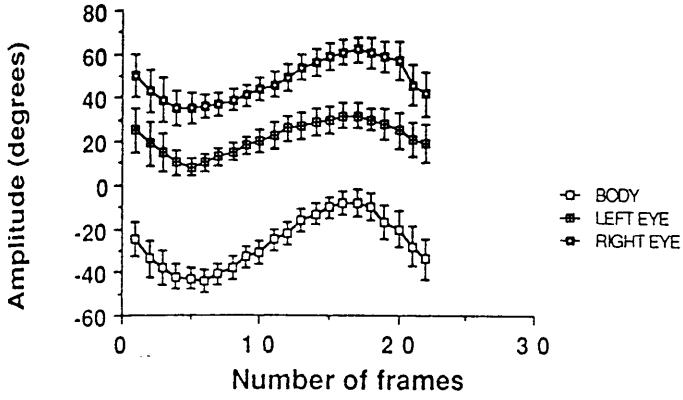
(c) For tilts at 0.2Hz in pitch plane (d) For tilts at 0.8Hz in pitch plane.

(e) For tilts at 0.2Hz in the pitch plane (f) For tilts at 0.8Hz in the pitch plane.

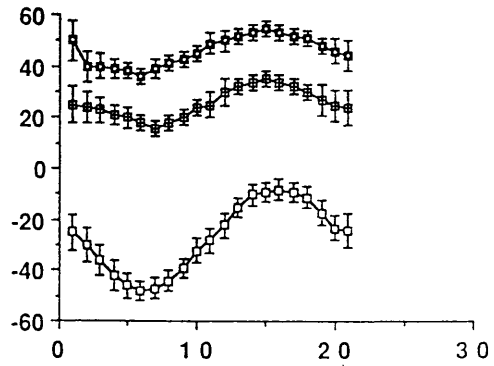
GAIN	ROLL	0.2Hz	0.8Hz	PITCH	0.2Hz	0.8Hz
RIGHT EYE		0.66	0.61		0.50	0.52
LEFT EYE		0.71	0.59		0.46	0.52

ROLL

a

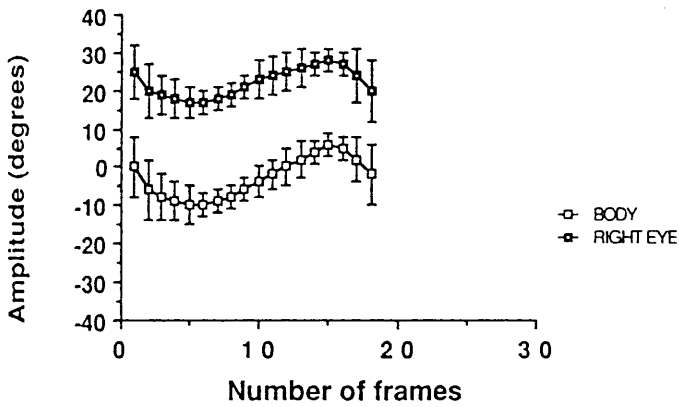


b

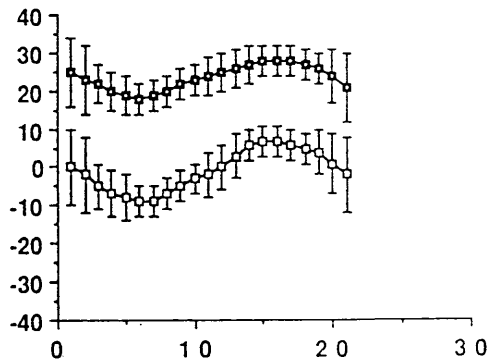


PITCH

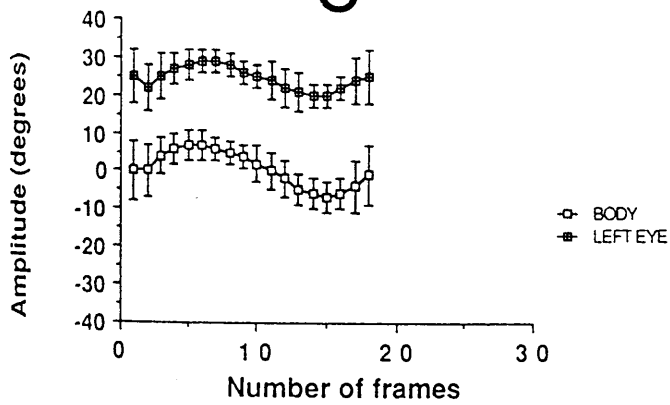
c



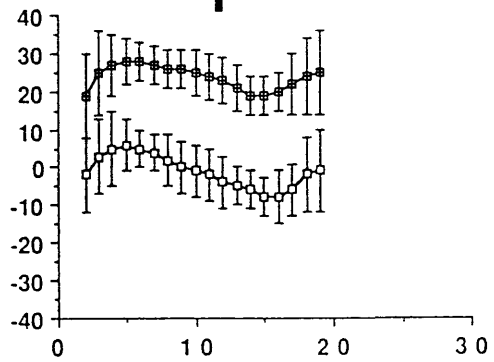
d



e



f



0.2Hz

0.8Hz

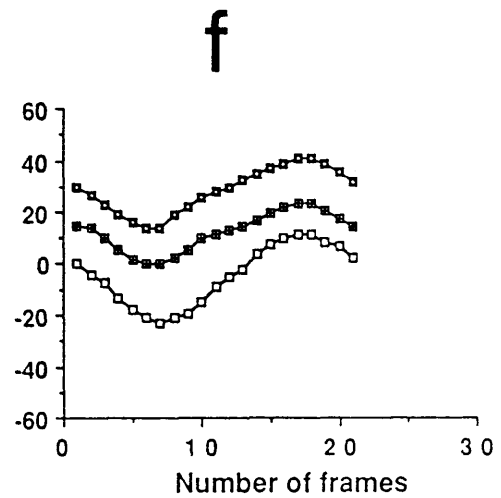
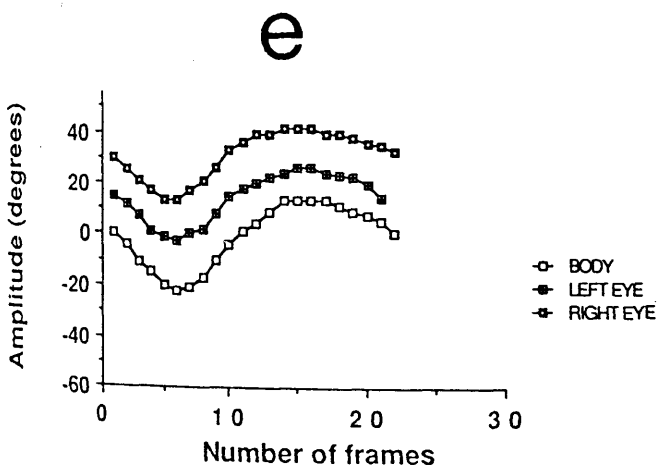
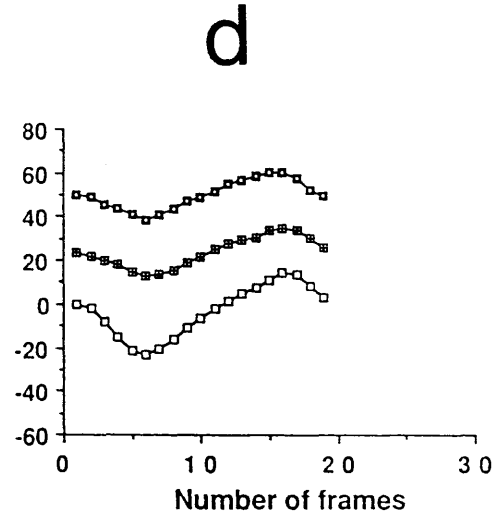
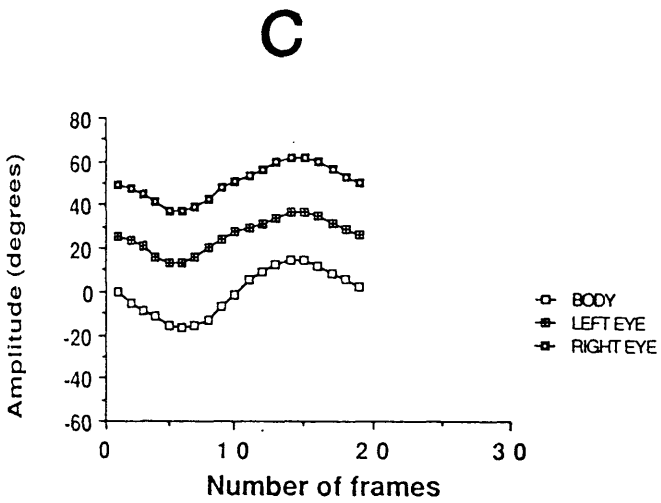
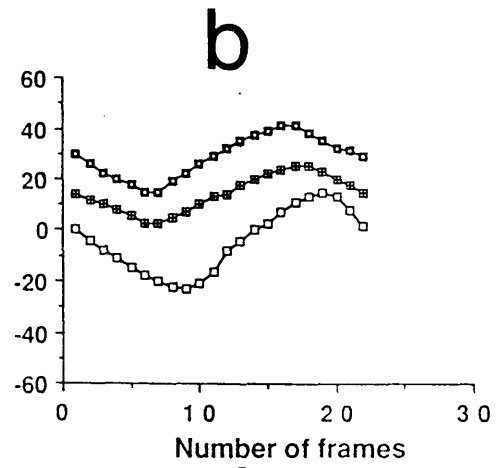
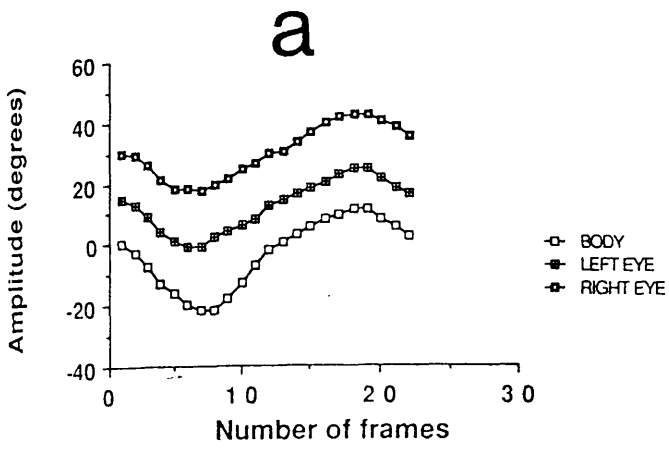
Fig 3.3 Tests for optokinetic nystagmus in the intact fish.

(a) Simultaneous roll of the striped drum and animal for tilts at 0.2Hz and (b) 0.8Hz.

(c) Animal roll inside the stationary drum in white light for tilts at 0.2Hz and (d) 0.8Hz.

(e) Animal roll inside stationary drum for tilts at 0.2Hz in dim red light and (f) 0.8Hz

GAIN	SIMULTANEOUS ROLL OF DRUM AND ANIMAL.	0.2Hz	0.8Hz
RIGHT EYE		0.59	0.68
LEFT EYE		0.69	0.52
GAIN	ANIMAL ROLL INSIDE THE STATIONARY DRUM, IN WHITE LIGHT.		
RIGHT EYE		0.76	0.47
LEFT EYE		0.70	0.52
GAIN	ANIMAL ROLL INSIDE THE STATIONARY DRUM, IN DIM RED LIGHT.		
RIGHT EYE		0.77	0.69
LEFT EYE		0.81	0.65



0.2Hz

0.8Hz

Fig 3.4 The eye movement recordings in fish after ablating left ipsilateral pair of canals.

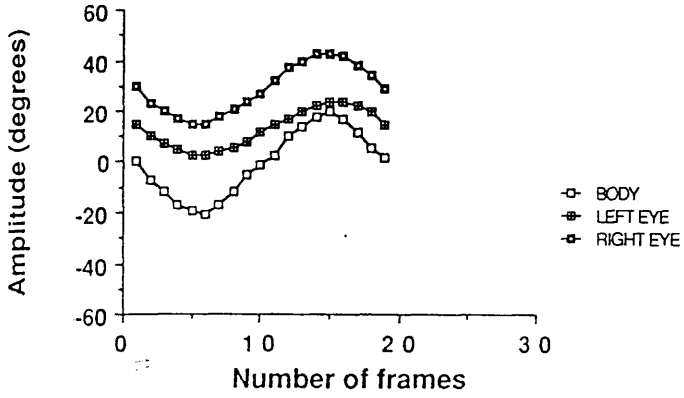
(a) For tilts at 0.2Hz in the roll plane (b) For tilts at 0.8 Hz in the roll plane.

(c & e) For tilts at 0.2Hz in the pitch plane. (d & f) For tilts at 0.8Hz in the pitch plane.

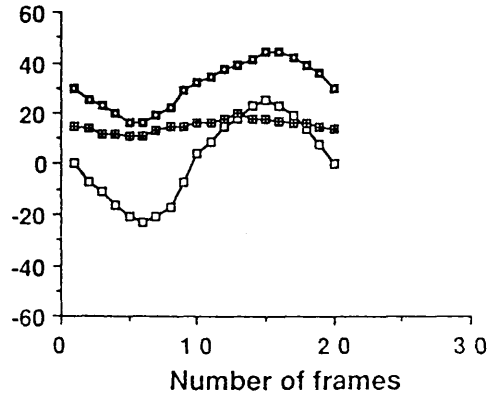
GAIN	ROLL 0.2Hz	0.8Hz	PITCH 0.2Hz	0.8Hz
RIGHT EYE	0.71	0.60	0.59	0.57
LEFT EYE	0.57	0.17	0.55	0.33

ROLL

a

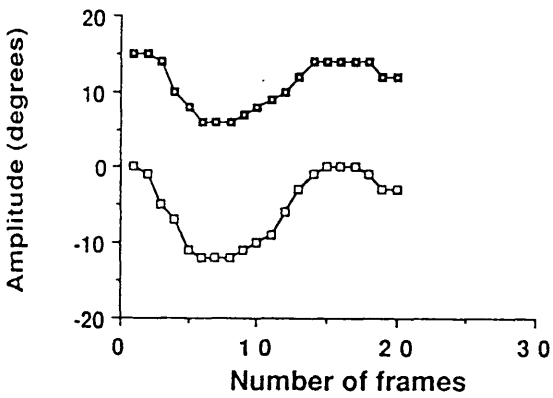


b

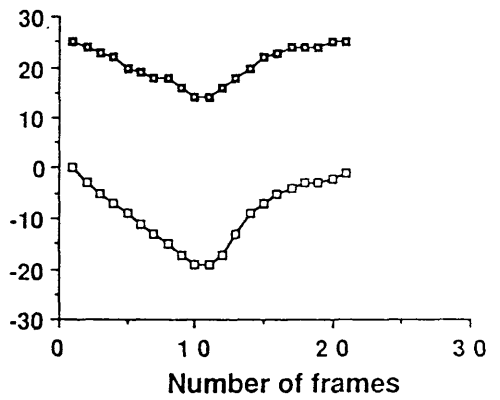


PITCH

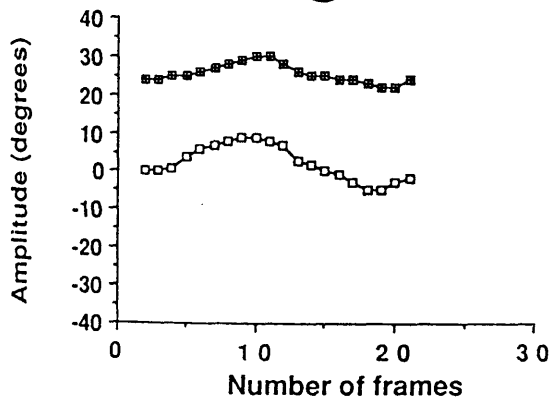
c



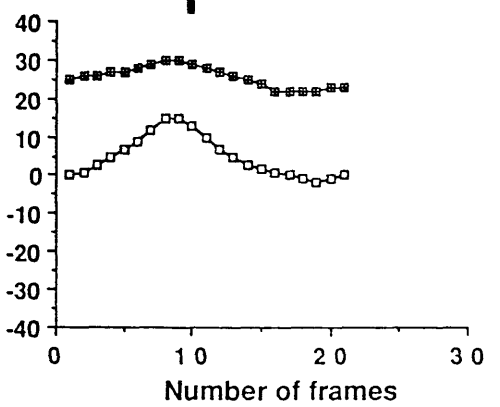
d



e



f



0.2Hz

0.8Hz

Fig 3.5 The eye movement recordings after ablating vertical semicircular canals.

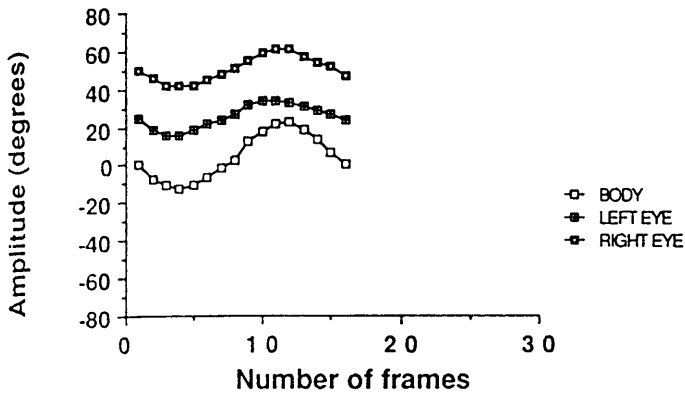
(a) For tilts at 0.2Hz in the roll plane (b) For tilts at 0.8Hz in the roll plane.

(c & e) For tilts at 0.2Hz in the pitch plane (d & f) For tilts at 0.8Hz in the pitch plane.

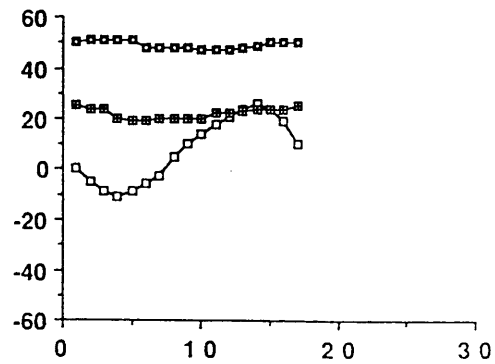
GAIN	ROLL	0.2Hz	0.8Hz.	PITCH	0.2Hz	0.8Hz.
RIGHT EYE		0.46	0.18		0.63	0.13
LEFT EYE		0.61	0.21		0.5	

ROLL

a

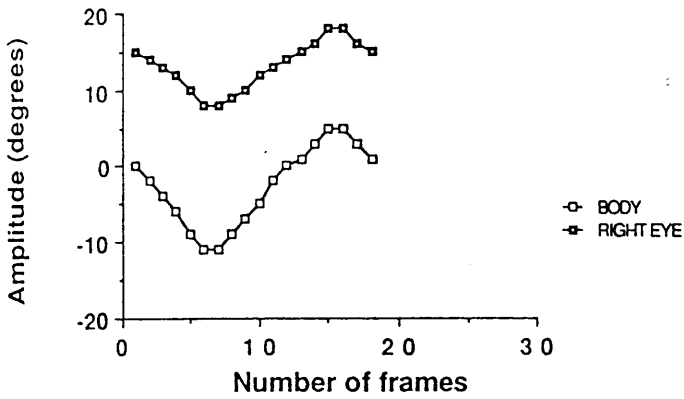


b

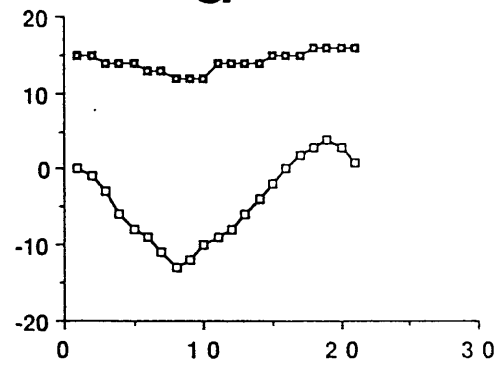


PITCH

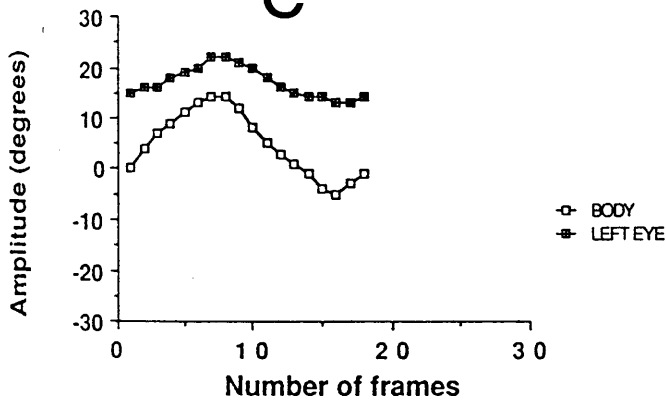
c



d



e



0.2Hz

0.8Hz

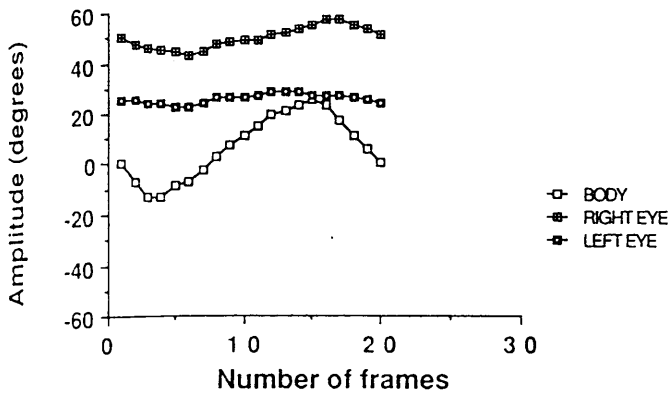
Fig 3.6 The eye movement recordings after ablating four vertical canals and the utricle of right side.

(a) For tilts at 0.2Hz in the roll plane (b) For tilts at 0.8Hz in the roll plane.

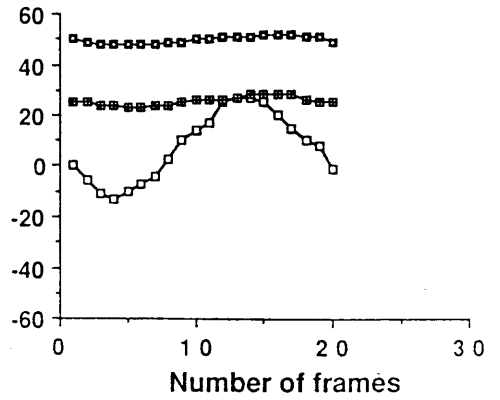
(c & e) For tilts at 0.2Hz in the pitch plane (d & f) For tilts at 0.8Hz in the pitch plane.

GAIN	ROLL	0.2Hz	0.8Hz	PITCH	0.2Hz	0.8Hz
RIGHT EYE		---	---		0.23	0.18
LEFT EYE		0.53	0.15		0.42	0.22

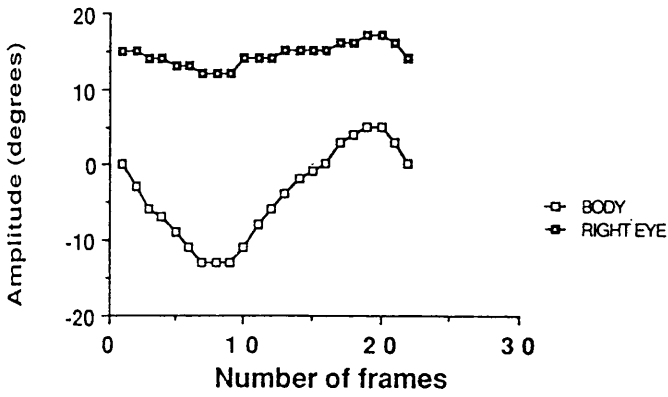
ROLL a



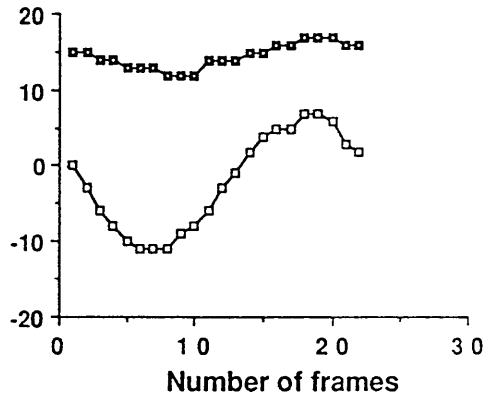
b



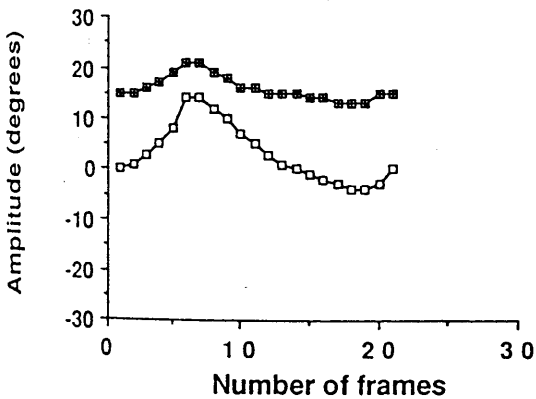
PITCH c



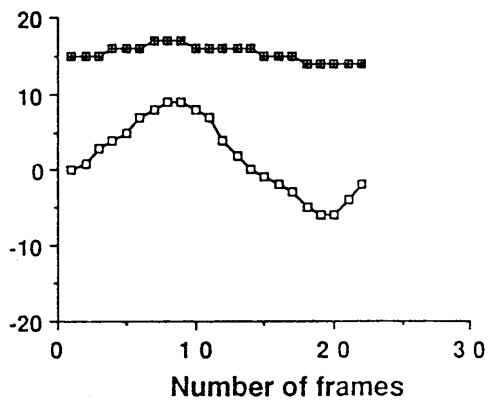
d



e



f



0.2Hz

0.8Hz

CHAPTER 4. COORDINATED ACTIVATION OF THE EOM.

4.1 INTRODUCTION.

It is the coordinated action of EOM which induces eye movements. During eye movements the activity of EOM can be measured by EMG electrodes inserted into the muscle. Depending on the intensity of contraction, the discharge frequency of individual units and overall unit activity of EOM varies, and this can be used in assessing the contributions of individual EOM to given eye movements. The location, innervation, physiological profile and mechanical responses of the six EOM have been discussed in Chapter 2.

The pattern of coordinated activation of the six EOM has been widely studied in vertebrates. In man (Boeder, 1962) for horizontal eye reflexes, they can be divided into three distinct muscle groups. The line of action of the two horizontal EOM (EXT-R & INT-R) is coincident with the horizontal plane of eye: each of these EOM induces the horizontal rotation of eye ball when the eye is in a straight forward position. The INT-R rotates the eye medially or rostrally and EXT-R rotates the eye laterally or caudally. The SR and IR have a complex movement divided into horizontal, vertical and torsional components. In terms of horizontal eye movements the SR and IR induce a rotation of the eye about the line of sight in the horizontal plane. The plane of action of SO and IO makes an angle of about 51° with the line of sight when the eye is in a straight forward position, and the resulting horizontal component is an abduction. This decreases to zero when the line of action of the muscles becomes parallel to the line of sight and the horizontal components of SO & IO are same.

In vertical eye reflexes the SR, IR, SO & IO play major roles. When the eye is in a straight forward position the contraction of SR elevates it, while contraction of IR depresses it. The SO and IO primarily induce counter rotation of the eye ball. The SO makes the

eye rotate inward (intorsion) and IO rotates the eye outward (extorsion). The contraction of either of the horizontal muscles (EXT-R & INT-R) in the vertical plane acts to increase the elevation if the eye ball is elevated. When the eye ball is depressed the contraction of these two muscles acts to depress it further.

Horizontal eye reflexes of freely moving and restrained animals have been described in all vertebrates (Harris, 1965; Easter, et al., 1974a,b; Hermann & Constantine, 1971; Collins, 1977, Carpenter, 1977, Robinson, 1981; Montgomery, 1983).

In his experiments on dogfish Montgomery (1980) sampled the activities of horizontal canal primary afferents, vestibular neurons and neurons in the auricular lobe of cerebellum, during horizontal head rotation. He also recorded the eye reflexes to abducens nerve stimulation and determined the transfer characteristic of the oculomotor system in the direct horizontal VOR (Montgomery, 1983).

Our only knowledge of vertical VOR in fish is indirect, being based upon the sensory recordings from the isolated labyrinth made by Lowenstein & Sands (1940). From these results, and from general observations, they have predicted the activation pattern of all the EOM in relation to the stimulation of individual canals. Despite the fact that the labyrinth and EOM of elasmobranchs are easily accessible and provide an ideal system in which to work out the connections between vestibular input and responses of EOM, no further work has been done to check these predictions experimentally.

4.2 Aims of the project.

Since very little is known about the function of fish horizontal and vertical VOR and much of this relies upon predictions rather than actual recordings. I have recorded the myographic activity of all six

EOM of the dogfish while providing physiological stimuli to the vestibular system for roll and pitch. In some experiments the response of EOM was also checked for yaws in order to observe the differences in EOM responses between the vertical and horizontal planes.

A transition in the response of EOM is a functional characteristic that occurs in between roll and pitch tilts. The animal was therefore also tilted at intermediate angles in each 90° quadrant to determine exactly at which point this transition occurred. In this way a detailed analysis of the changes in coupling of VOR between roll and pitch has been made.

4.2 Materials and methods.

30 dogfish approximately 1m in length were used for these experiments. The anaesthetised (MS222, 2mg/l) pithed dogfish was decerebrated and held in a frame assembly, that was designed to hold the head and body of the animal still (Fig 4.1.A). The EOM were exposed by cutting the upper and lower eye lids and a piece of skin behind the eyes. The myographic electrodes were prepared from stainless steel insect pins by insulating them with epoxy resin except for the tip and baking them in an oven at 60⁰ for about 48 hours. The electrodes were advanced through the orbital membrane so that the tips lay near the insertions of EOM, although in a few experiments the electrodes were inserted more deeply in order to check if any difference in the myographic response occurred. To hold the electrodes firmly in position, the wires attached to these electrodes were glued on to the head of the animal. During the operation the bleeding was controlled by cauterising the blood vessels (although it was found that excessive blood flow rarely occurred) and the gills of fish were kept slightly moist. The animal was then left in sea water to recover. A deeply anaesthetised fish took about an hour to recover normal breathing movements. If water flow was maintained this preparation could then last for as long as a week, and usually the fish was left overnight before experiments were begun, since the myographic responses became larger after this time. The inner frame assembly was fixed into an outer frame that pivoted on horizontal bearings inside the tank, allowing tilts to be delivered to the animal in any vertical plane (Fig 4.1.B). The connection was made through a vertical bar that could be rotated freely through 360⁰; furthermore the vertical pivot projected through the midpoint between the vestibular organs, so that all the tilts were centred at this point. The sinusoidal oscillations

of the body were generated by a DC motor connected through a drive arm to the outer frame. The myographic activity of the EOM made during the tilts, together with the potentiometer signal indicating angular movement of the frame were stored on a FM tape recorder.

To test responses in different vertical planes, the fish was rotated in 45° increments beginning at roll (designated 0°) in a right-leading direction (Fig 4.5).

4.2.B Analysis of the data.

The data from the tape recorder were analysed for the phase position of muscle firing in the tilt cycle. The myographic signals were fed through a window discriminator which was set to pick up all the spikes above the noise level and to convert the activity to a series of TTL pulses. The stimulus waveform was fed through a zero-point crossing device, which produced a TTL pulse at a chosen point on successive cycles of the waveform. These pulses were fed to a Tuscan S100 computer which was programmed to generate post stimulus time histograms. By setting the time interval to equal the cycle period and triggering from the stimulus pulses, phase histograms of myographic activity were accumulated over ten cycles of body oscillation. For some purposes the myographic activity was passed through an EMG integrator, with the time constant set to 20ms, and the integrated signals were in turn fed to a computer interface (CED 1401) for averaging. From the phase histogram a number of statistical parameters could be calculated. For most purposes the circular mean of the distribution was used to express the phase position of EOM activity relative to the angles of body tilts, and the total number of TTL pulses counted in the bursts was used to express the strength of the response.

4.3 RESULTS.

As demonstrated in Chapter 2 the compensatory eye movements in the roll plane are achieved by an upward counter-roll of the downward eye and a downward counter-roll of upward eye. Tilts in the pitch plane induce torsional counter-rotation of both eyes, which move conjugately to compensate for the head up and head down tilts. Myographic recordings of EOM have been made to demonstrate the pattern of muscle activation in the two eyes which bring these movements about. Data are represented as EMG records of EOM, phase histograms of EOM activity accumulated over ten cycles of sinusoidal body oscillations, or averaged integrated signals. The measures of circular mean value derived from phase histograms have been used for comparing the phases of EOM firing under different experimental conditions.

The fish were tilted at a range of frequencies between 0.2Hz and 0.8Hz, many of which bring both components of the vestibular system in to action (see Chapter 5).

The myographic record of each EOM in the roll and pitch plane was comprised of separate populations of small and large units that were active during the tilt in one direction. Generally the burst was initiated by the units smallest in size, and the largest units fired near the peak of displacement.

There appeared to be no difference in the relative contributions of small and large units to the myographic bursts at low (0.2Hz) and high (0.8Hz) frequencies. Therefore no obvious correlation between the dominant component of the vestibular system acting at a given frequency and a particular population of motor units.

4.3.A EOM activation in roll.

During a right side down tilt (second half of the phase histogram) that induced an upward counter-roll of the right eye and downward counter roll of the left eye, the SO and SR of the right eye were co-activated, the SO activated around a mean phase position of 0.62 and the IR fired around a mean phase of 0.65, while the right IO and IR were silent (Fig 4.2). In the left eye the SO and SR were both silent, while the left IO and IR were co-activated. The left IO discharged around a mean phase of 0.65 and the left IR discharged around a mean phase of 0.70 (Fig 4.2).

In a left side down tilt (the first half of the phase histogram) the reciprocal pattern of the muscle activation was produced. The left SO and SR fired together, the left SO firing around a mean phase of 0.19 and the left IR firing around mean phase of 0.22, while left IO and IR were silent (Fig 4.2). In the right eye the SO and SR were silent in this half of the tilt, while the IO and IR were coactivated. The right IO fired around a mean phase of 0.31 and the right IR discharged around a mean phase of 0.21 (Fig 4.2).

The horizontal EOM EXT-R and INT-R were also recorded in the roll plane. In the right side down tilt of the body the EXT-R of the right eye fired at a mean phase of 0.60, while the INT-R of right eye in this half of the tilt was silent. In the left eye the EXT-R was inactivated while the INT-R was activated and it fired around a mean phase of 0.78 (Fig 4.3). In a left side down tilt the reciprocal pattern of muscle activation was produced: the EXT-R was activated and INT-R was inactivated in the left eye, while the EXT-R was inactivated and INT-R was activated in the right eye (Fig 4.3).

4.3.B Pitch.

Tilts in the pitch plane induce torsional counter-rotation of both eyes, which move conjugately to compensate for the head up and head down tilts. During a head down tilt (second half of the phase histogram in Fig 4.4) the SO and SR of both eyes co-contracted. The SO in the right and left eyes fired around a mean phase of 0.65, while the right SR fired around a mean phase of 0.57 and the left SR fired around mean phase of 0.78. The IO and IR of both eyes were silent (Fig 4.4). In a head up tilt the SO and SR of both eyes were silent, while the IO and IR of the two eyes co-contracted, the right IO discharging around a mean phase of 0.31 and left IO firing around mean phase of 0.19. The right and left IR discharged around mean phase of 0.22 (Fig 4.4).

Among horizontal muscles, a similar change in their discharge was observed compared with that in the roll. In pitch plane the EXT-R and INT-R of both eyes still contracted in antiphase to each other. The EXT-R of both eyes co-contracted on head down tilt, while the INT-R of both eyes were silent in this half of the tilt (Fig 4.3). In a head up tilt the INT-R of the two eyes were co-contracted and EXT-R of the left and right eyes were silent (Fig 4.3).

4.3.C Transition of EOM between roll and pitch.

A transition must occur between the patterns of activation of EOM seen in roll (Section 4.3.A) and pitch (4.3.B). In order to determine the exact angle at which transition occurred a number of experiments were performed in which fish were also tilted in intermediate vertical planes (Fig 4.5). Data were obtained for all six EOM for a series of imposed body tilts in vertical planes between 0° and 360° . Recordings were made at every 45° , and the transition angle was assessed

precisely by moving in smaller increments (5^0 - 15^0) to either side of these 45^0 angles. The myographic activity of the EOM at the angle of transition was generally composed of simultaneous firing of small and large units continuously through the cycle of tilt (rather than as a burst in one half cycle). Transitions were passed within one 15^0 increment, and where the tested position did not exactly coincide with the null point, a somewhat increased level of firing was superimposed on one half of the continuous firing. However in some cases there was an indication of somewhat increased level of firing in either the first or second half of the cycle, indicating a slight offset either towards the pre-or post-transition angles.

4.3.C.a Response of SO.

4.3.C.a.I SO response in roll (0^0), 0.2Hz, 0.8Hz.

As described above (Section, 4.3.A) in roll, the left SO fired to a left side down tilt, while the right SO was silent in this half of tilt (Fig 4.6). The right SO was activated during a right side down tilt and it compensated the right eye downwards, while the left SO was silent in this half of the tilt (Fig 4.6). There was no change in the phase of left and right SO firing as a result of changing stimulus frequencies at this plane of the tilt (4.6, 4.7).

4.3.C.a.iii SO response at 45^0 , 0.2Hz.

To an imposed body tilt at 45^0 (Fig 4.6), there was an indication of firing in the left SO, but in contrast to that at 0^0 this firing was not confined to a particular phase of tilt. Both small and large units fired continuously to tilts on both sides, suggesting that this angle was close to the transition. To determine the exact angle at which the phase of left SO firing shifted to the other half of tilt,

recordings were made 15° before (30°) and after (60°) 45° and it was established that at this frequency transition occurred between 45° and 60° . At 60° a comparatively stronger response was elicited at the phase position of 0.63 rather than at the phase position of 0.13 observed at 0° (Fig 4.6).

There was no change in the phase of right SO at this angle of the tilt and its burst had a mean phase position of 0.63 same as at 0°). However it was consistently recorded in several experiments that the right SO demonstrated its strongest myographic response at this angle (Fig 4.6).

4.3.C.a.iv SO response at 45° , 0.8Hz.

For tilts at an angle of 45° and frequency of 0.8Hz the phase of the SO burst in the left eye was already shifted from the value of 0.21 at 0° to a value of 0.61. It was determined by tilting at angles between 0° and 45° that the transition occurred at 30° , where the left SO fired continuously throughout the tilt cycle (Fig 4.7). There was no change in the phase of the right SO at this angle. However a stronger myographic response of right SO was seen than observed at other angles (Fig 4.7).

4.3.C.a.v SO response to pitch (90°), 0.2Hz.

The pattern of SO (left & right) firing has been described in section 4.3.B. There was no change in the phase of right and left SO response at this angle and both EOM fired to a head down tilt for tilts at 0.2Hz and 0.8Hz (Fig4.4).

4.3.C.a.vii SO response at 135° , 0.2Hz.

For the low frequency tilt at 135° the left SO retained its mean

phase position of 0.63 and its response at this frequency was generally stronger than observed at other angles (Fig 4.6). The myographic activity of the right SO showed that it was approaching the transition angle (Fig 4.6). To determine the angle of transition exactly the fish was tilted 15° before (120°) and after (150°) 135° . It was established in several recordings that at 120° the right SO discharge had a mean phase of 0.65 and the transition occurred at 150° . After this angle the right SO burst had a mean phase of 0.09 (ie on other side of the stimulus curve) (Fig 4.6).

4.3.C.a.viii SO response at 135° , 0.8Hz.

As found at 45° for the left SO at this frequency, the transition for the right SO had already been passed for a tilt in the 135° plane. Therefore at this angle of tilt the right and left SO were activated in antiphase to each other. It was repetitively observed in several experiments that the right SO changed its phase of firing to the other side of stimulus curve at an angle between 120° and 135° and not after 135° (Fig 4.7).

4.3.C.a.ix SO response at 180° , 0.2Hz, 0.8Hz.

At this angle of the tilt there was no change in the phase of the right and left SO and they were activated in antiphase to each other (Fig 4.6, 4.7). However their phase positions relative to the stimulus monitor were different from those calculated for 0° as an inevitable consequence of the rotation of the fish within the tilting frame (see section 3.2). Thus at 0° the extreme left side down tilt position is represented as 0.25 phase position while at 180° the left side down position is represented as 0.75.

4.3.C.a.x SO response between 180° and 360° , 0.2Hz, 0.8Hz.

Recordings were also made between the angles of 180^0 and 360^0 to determine the further transitions in phase of left and right SO responses. It was recorded in several experiments that tilts at these angles demonstrate a mirror-image pattern of transition in the phase of right and left SO at low (0.2Hz) and high (0.8Hz) frequency. Therefore the transition in the phase of left SO occurred after 225^0 (in between 225^0 and 240^0) at 0.2Hz, and for tilts at 240^0 left SO discharged in phase with the right SO (Fig 4.6). With a stimulus frequency of 0.8Hz the transition in the firing of left SO occurred before 225^0 . For tilts at 210^0 it fired continuously on both sides of the tilt cycle, although a comparatively strong response was elicited near its original phase position (Fig 4.7). For tilts at 270^0 SO in the right and left eyes were activated in phase.

The transition in the firing of right SO occurred at 330^0 for tilts at 0.2Hz (Fig 4.6). For tilts at 0.8Hz it shifted in its phase at 300^0 and at 295^0 the right SO discharged in phase with the left SO (Fig 4.7). At 360^0 (0^0) the left SO discharged around a mean phase position of 0.3 and the right SO discharged at a mean phase of 0.6 (Fig 4.6, 4.7).

The circular mean phase values derived from the analysed phase histograms of EOM myographic activity have been plotted against the angles of tilts between 0^0 and 360^0 (Fig 4.13, 4.14).

Using the same procedure to establish transitions, the activity of the other five EOM were analysed.

4.3.C.b Transition in IO response between 0^0 & 180^0 , 0.2Hz, 0.8Hz.

For tilts at 0^0 , with stimulus frequency of both 0.2Hz and 0.8Hz the IO from the right and left eyes were activated in antiphase to each other. The right IO fired around a mean phase position of 0.31

(i.e during right side up tilt) and the left IO discharged around mean phase of 0.65 (i.e during left side up tilt, Fig 4.8).

With a stimulus frequency of 0.2Hz the transition in the phase of left IO occurred just beyond 60^0 , at this angle of tilt the left IO fired to a mean phase of 0.18. At high frequency tilts the transition in the phase of the left IO occurred before 45^0 and at this plane left IO discharged to a mean phase of 0.18 (Fig 4.8). There was no change in the phase of right IO at this angle of tilt and at 45^0 it fired towards a mean phase of 0.32 (Fig 4.8).

At 90^0 the IO from right and left eyes were activated in phase with each other during head up tilt (Fig 4.8).

The transition in the phase of the right IO with both low and high stimulus frequency occurred at 120^0 . At 135^0 the right IO discharged around mean phase position of 0.65 (Fig 4.8).

At 180^0 , and for both low and high stimulus frequencies, right and left IO were activated in antiphase to each other, the right IO discharging around a mean phase of 0.68 and the left IO around a mean phase of 0.22 (Fig 4.8).

The circular mean value obtained from the phase histograms of IOR and IOL has been plotted for the tilt angles between 0^0 and 360^0 (Fig 4.13, 4.14).

4.3.C.c Transition in SR response between 0^0 and 180^0 , 0.2Hz, 0.8Hz.

For tilts at 0^0 , and with stimulus frequency of both 0.2Hz and 0.8Hz the right SR fired around a mean phase position of 0.51 (i.e during right side down tilt) and the left SR discharged around a mean phase of 0.21 (i.e during left side down tilt, Fig 4.9).

The transition in the firing of the left SR with low frequency tilts occurred at 60^0 , while with high frequency tilts it occurred at

30^0 (Fig 4.9). After the transition the left SR discharged at a mean phase of 0.65 (Fig 4.9).

For tilts in pitch at 90^0 the SR of the left and right eyes were co-activated during a head down tilt (around a mean phase of 0.54) for low and high frequency tilts (Fig 4.9).

With a stimulus frequency of 0.2Hz the transition in the phase of right SR firing occurred at 150^0 , while for tilts at a frequency of 0.8Hz the right SR shifted in its phase of firing at 135^0 (Fig 4.9). After the transition the right SR fired around a mean phase position of 0.18 (Fig 4.9).

For tilts at 180^0 , with both low and high stimulus frequencies the right SR fired at a mean phase of 0.20 (now representing a right side down tilt) and the left SR discharged around mean phase of 0.58 (now representing a left side down tilt)(Fig 4.9).

4.3.C.d Transition in the IR response between 0^0 and 180^0 , 0.2Hz, 0.8Hz.

In the roll plane at stimulus frequencies of both 0.2Hz and 0.8Hz, the IR from the two eyes were activated in antiphase to each other, The right IR discharged around a mean phase of 0.21 (i.e during a right side up body tilt) and the left IR discharged at a mean phase of 0.7 (during a left side up body tilt, Fig 4.10).

At low frequency tilts, the transition in the firing of the left IR occurred between the angles of 45^0 and 60^0 (Fig 4.10), while for high frequency tilts it occurred at 75^0 (Fig 4.10). After its transition the left IR discharged in phase with the right IR around a mean phase position of 0.25 (Fig 4.10).

For tilts in the pitch plane at 90^0 the right and left IR were co-activated during a head up tilt (Fig 4.10).

The transition in the phase of right IR firing at low stimulus frequency occurred at 120^0 , while at high frequency it occurred between 120^0 and 135^0 . After its transition the right IR discharged around a mean phase position of 0.67 (4.10).

For tilts at 180^0 the right and left IR were activated in antiphase to each other, the right IR discharging around a mean phase position of 0.65 (now representing right side up tilt) and the left IR discharged at a mean phase of 0.25 (now representing left side up tilt).

3.3.C.e Transition in the response of INT-R between 0^0 and 180^0 , 0.2Hz, 0.8Hz.

For tilts in roll plane at 0^0 the INT-R of the left and the right eyes were activated in antiphase to each other. The right INT-R fired around a mean phase of 0.17 (i.e during right side up) and the left INT-R discharged around a mean phase position of 0.65 (i.e during a left side up tilt). There was no variation in the firing pattern and mean phase values of the two EOM by varying stimulus frequency from 0.2Hz to 0.8Hz (Fig 4.11, 4.12).

At the angle of 45^0 , for tilts at 0.2Hz the right and left EOM were activated in antiphase. It was established in several recordings that the transition in the phase of left INT-R occurred at 55^0 (Fig 4.11). With a stimulus frequency of 0.8Hz the transition in the phase of left INT-R occurred at 65^0 , and at this angle the right and left INT-R were activated in phase at a mean phase position of 0.18 (Fig 4.12).

For the tilts in pitch plane at 90^0 and with stimulus frequencies of 0.2Hz and 0.8Hz the left and right INT-R were activated in phase during a head up tilt (Fig 4.12).

The transition in the phase of right INT-R firing with the stimulus frequency of 0.2Hz occurred at 150^0 (Fig 4.11). With a stimulus frequency of 0.8Hz the right INT-R shifted in the phase of its firing at 165^0 . After the transition the right INT-R discharged at a mean phase position of 0.68 (fig 4.12).

As in the roll plane (0^0) the right and left INT-R discharged in antiphase to each other at 180^0 , the mean phase value of 0.18 for the left INT-R burst now representing the activation of the left side up tilt and the mean phase of 0.68 for the right INT-R now representing activation on the right side up tilt (Fig 4.12).

4.3.C.f Transition in the response of EXT-R between 0^0 and 180^0 , 0.2Hz, 0.8Hz.

In the roll plane (0^0) the right and left EXT-R were activated in antiphase: the right EXT-R firing around a mean phase position of 0.71 (i.e during a right side down tilt) and the left EXT-R firing around a mean phase position of 0.16 (i.e during a left side down tilt) with stimulus frequencies of 0.2Hz and 0.8Hz (Fig 4.11, 4.12).

For tilts at 45^0 , and with a stimulus frequency of 0.2Hz the transition in the phase of left EXT-R occurred at 50^0 (Fig 4.11). With a stimulus frequency of 0.8Hz the left EXT-R shifted in its phase of firing at 60^0 (Fig 4.12). After the transition the right and left EXT-R discharged in phase with each other around a mean phase position of 0.70. For tilts in the pitch plane, and with stimulus frequencies of 0.2Hz and 0.8Hz right and left EXT-R were co-activated during a head down tilt (Fig 4.12).

The transition in the phase of the right EXT-R with a stimulus frequency of 0.2Hz occurred between 120^0 and 135^0 (Fig 4.11). With a stimulus frequency of 0.8Hz the transition in the phase of right EXT-R

occurred at 150° . After the transition right EXT-R discharged around a mean phase position of 0.19 (Fig 4.12).

For tilts in the roll plane at 180° the left EXT-R fired around a mean phase position of 0.7 (i.e during a left side down tilt) and right EXT-R discharged around a mean phase position of 0.19 (i.e during a right side down tilt) (Fig 4.12).

4.3.D Analysis of integrated phase plots.

In some recordings where myographic activity in two EOM was elicited in phase, small phase differences were noticed at the beginning of a burst. EMG signals fed through an integrator were used to analyse these differences in burst onset.

Recordings were made in the right and left SR for tilts in the pitch plane. A phase advance of 10.8° was observed in the activity of right eye over the left eye for tilts at 0.2Hz. For tilts at 0.8Hz the right SR phase advanced the myographic activity of left SR by 21.6° (4.15).

In recordings from right and left SO for tilts in the 90° plane the bursts of two EOM were initiated in phase for tilts at 0.2Hz, while during tilts at 0.8Hz SO in the left eye was advanced in phase over the left eye by 21.6° (Fig 4.15).

In the two EOM for tilts at 270° SO in the right eye was advanced in phase over the left eye by 28.8° . For tilts at 0.8Hz in the same plane SO in the right eye was advanced in phase by 46.8° (4.16).

Recordings were also made in the right SO and right SR for tilts at 0° plane. SO in the right eye phase advanced by 21.6° the SR in the right eye for tilts at 0.2Hz and 0.8Hz (4.16).

4.3.E. Tonic activity of the EOM.

In order to determine the tonic level of firing, recordings in the left and right SO were made during ramp tilts. In the first experiment ramp tilts of an amplitude of 0° , 15° , 30° , 45° , 60° , 75° were imposed towards right side down and myographic response in the left and right SO was recorded. No myographic response was elicited in the left SO during this half of the tilt (Fig 4.17). In the right SO there was an indication of the tonic firing at 0° , however after the fish was tilted to 30° and the frame was held in that position a continuous firing was seen that lasted during the first 60 seconds of that hold. A few small units were seen at the beginning of the burst that was followed by units of the large size mostly (Fig 4.17). The myographic response was strongest at 75° right side down.

In the myographic activity of the left SO during left side down tilts, recordings were made at 20° , and 60° . The myographic activity of the SO for tilts at 20° and 60° was comprised of mostly large individual units that were also similar in size, although few small units were also seen. For tilts at 60° left side down tonic units were bigger than those that fired at 20° left side down (Fig 4.18).

4.3.F Nystagmus response.

Since nystagmus was not seen in the horizontal EOM for tilts in the vertical plane, recordings during horizontal imposed body tilts were made to observe the nystagmus response.

The basic pattern in horizontal muscles is that there is tonic activity (representing nystagmus slow phase) during rotation in one direction (right side leading for right INT-R (Fig 4.19) but phasic bursts (representing nystagmic flicks) during rotation in the opposite

direction (right side trailing for right INT-R in Fig 4.19).

In association with these activities, the vertical muscles show relatively tonic firing for both rotations (Fig 4.19), which is interrupted at times when there is a nystagmus flick (4.20).

4.4 DISCUSSION.

The myographic recordings were made from six EOM during imposed vertical body tilts at low (0.2Hz) and high frequency (0.8Hz). The EOM activity in the roll and pitch planes has provided a pattern of the coordinated activity of vertical and horizontal EOM for counter-rolling and torsional eye movements in the roll and pitch planes.

During a side-down roll tilt the SO and SR in the downward eye were co-contracted, while IO and IR remained inactive, which brought about an upward counter-roll of the this eye. A reciprocal pattern of SO, SR, IO & IR activation in the upward eye induced a downward counterroll in that eye. Tilts in the pitch plane induced torsional counter-rolling of both eyes, which moved in the same direction as each other. For a head up pitch the IO and IR of both eyes were co-activated while SO and SR in these two eyes remained silent. The head down pitch has induced a reciprocal pattern of the EOM activation, SO and SR were co-contracted while IO and IR were remained inactive. The observed pattern was different from what was expected in the pitch plane, and co-contraction of the SR and IR was not observed to occur exactly for tilts at 90^0 plane. However in recordings in which the myographic activity of these EOM was recorded at each 15^0 increment between the roll and pitch planes it was consistently seen that phase shift in the myographic activity of these EOM occurred after 90^0 (120^0 , 135^0 , 150^0 , 165^0 , depending on the tilt frequency). To explain this unexpected pattern of vertical EOM activation in the pitch plane, eye movements, and the relative strength of EOM firing in this plane should be considered of primary significance. As the study of eye movements in dogfish (section 3.4) has demonstrated that in the pitch plane gain of eye movements is always lower than that observed during the counter-rotation of eyes, so it could be that torsional movements

are generally small and can be achieved by differences in the relative strength of SO, SR, IO and IR firing rather than their phase position.

The contraction of the horizontal EOM is known to provide fixed pivot points to stabilize the coordinated action of the vertical EOM (Boeder, 1961). In studies of the dogfish EOM, EXT-R and INT-R were recorded for tilts in the roll and pitch planes and at intermediate angles. The EXT-R and INT-R share the same transition points, so that they discharge in antiphase to each other in all planes. The contraction of EXT-R accompanies the activity of SO and SR while the INT-R firing has accompanied the activity of IO and IR. It therefore seems that their stabilizing function is partitioned and if we only think of tilt in a given plane each of the horizontal muscles is activated alternatively to stabilize the activity of vertical EOM.

The induced vertical tilts at different intermediate planes have reflected the nature of successive changes that occur in coupling of the VOR as the plane of tilt is changed. Tilts around the 45° plane induced a torsional counter-rolling in the left eye as well as in the right eye, which is a result of a transition in the phase of left EOM as compared to that observed for tilts in the roll plane. Similar shift in the phase of right EOM was observed around 135° . Certain differences in the transition angles in the myographic activity of same EOM were observed for tilts at 0.2Hz and 0.8Hz. The offset of transition at the same planes of tilt while recording within the other half circle (180° - 360°) and the transition occurring consistently at same planes of tilt in all experiments make it convincingly possible that these differences were real and not due to experimental artefacts. For tilts at 0.2Hz there was a general tendency for the transition to occur after the transition at 0.8Hz had passed.

In the myographic activity of vertical EOM (SOR & SOL, SOR & SRR)

for tilts in the planes where peaks of their bursts were in phase, small differences were observed in the phase of two EOM firing at the initiation of their burst, which suggest subtle differences in the input from vestibular components to the myographic activity of these EOM.

During the ramp-and-hold tilts, tonic discharge that was in most cases composed of units of one size was recorded in all EOM. This tonic activity was greatly enhanced in a hold during bigger angular tilts. EOM fired strongly in tilts towards their excitatory sides.

There was a total absence of the nystagmus response in the vertical as well as in the horizontal EOM during tilts in the vertical plane. However when a fish was subjected to the tilts in horizontal plane nystagmus was observed in the vertical (SO, IO, SR, IR) as well as in the horizontal (EXT-R, INT-R) EOM. In a freely swimming dogfish fast flicks of eyes are made at the end of each turn to ensure the required compensation. This compensation is primarily achieved by the action of horizontal EOM but the presence of the nystagmus response in the vertical EOM at the same time might have a stabilizing affect to the activity of the horizontal EOM.

The myographic activity of EOM as a result of tilts in the roll and pitch planes and at intermediate angles in the intact fish has given an insight to the coordinated activation of EOM during compensatory eye reflexes. The control of EOM activity by vestibular components has been studied by recording myographically from the EOM after ablating different combinations of the vertical semicircular canals in the presence or absence of utriculus. These experiments are discussed in Chapter 5.

Fig 4.1. The frame assembly designed to hold the animal body for the tilts in the roll and pitch planes and at the intermediate angles.

(A) Side view.

(B) Plane of the tilt apparatus.

(C) Apparatus during a circular tilt. Fish is shown during a rotation at 20° .

TILT BAR

OUTER FRAME

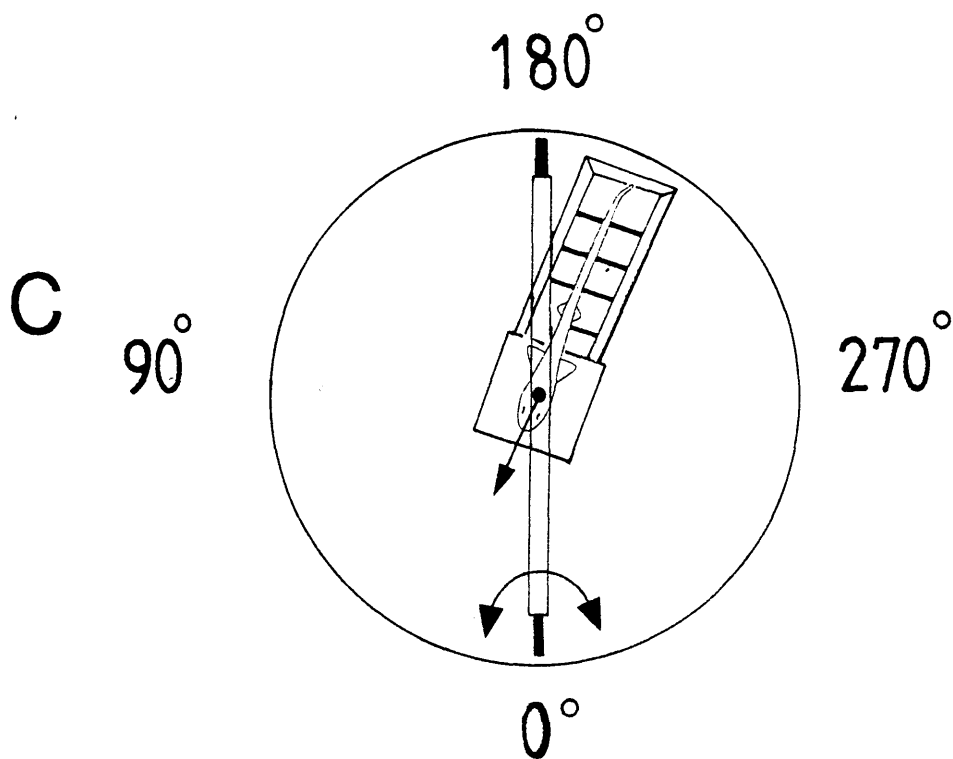
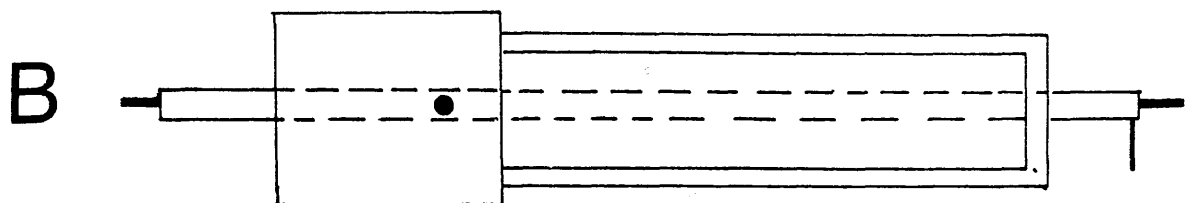
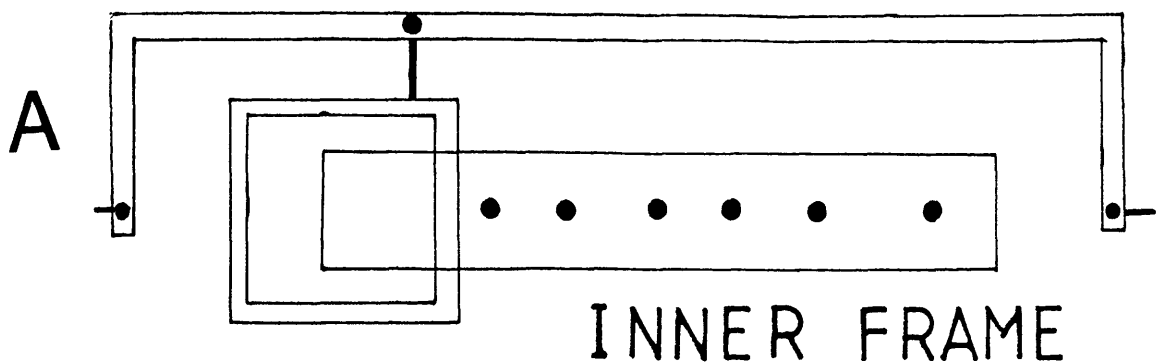
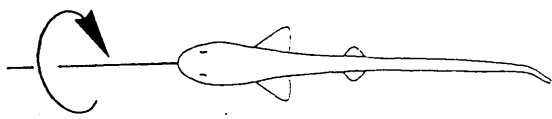


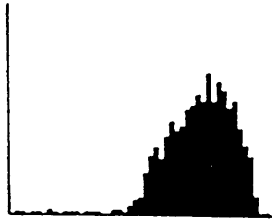
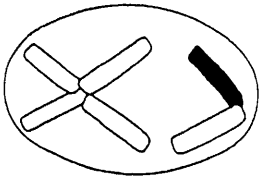
Fig 4.2 The pattern of activation of the vertical EOM (SO, SR, IO & IR) in the right and left eyes is presented as phase histograms of the EOM activity accumulated over ten cycles of sinusoidal body oscillations in the roll plane.



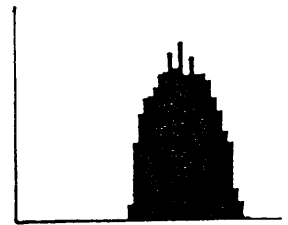
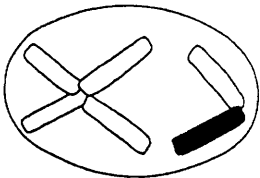
RIGHT EYE

LEFT EYE

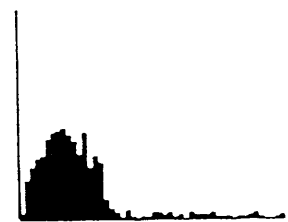
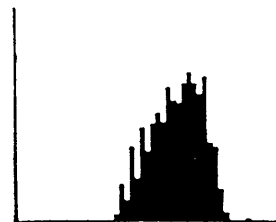
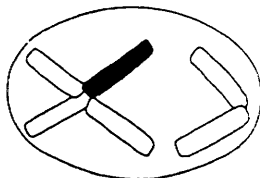
SO



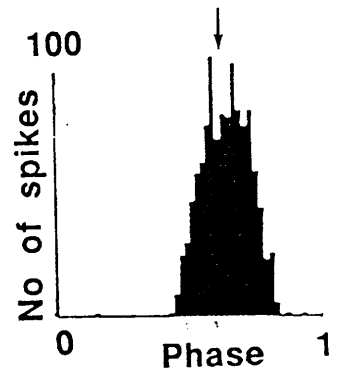
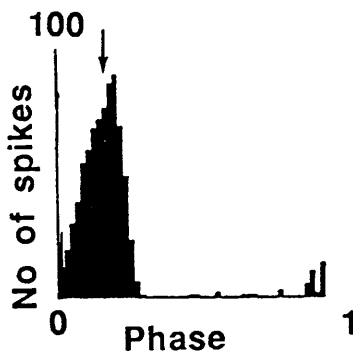
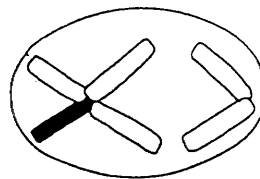
IO



SR



IR



RIGHT SIDE UP



RIGHT SIDE DOWN

Fig 4.3 The pattern of activation of the horizontal EOM (EXT-R, INT-R) in the right and left eyes is presented as phase histograms in the roll and pitch planes for tilts at 0.8Hz.

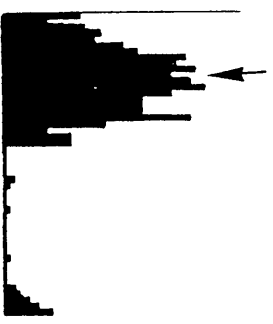
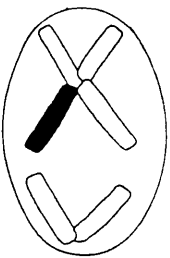


RIGHT EYE

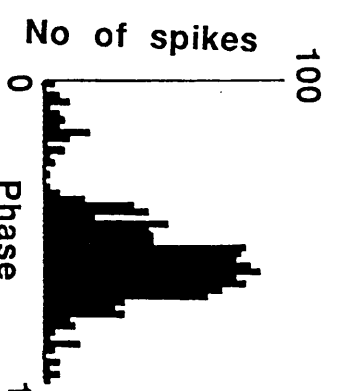
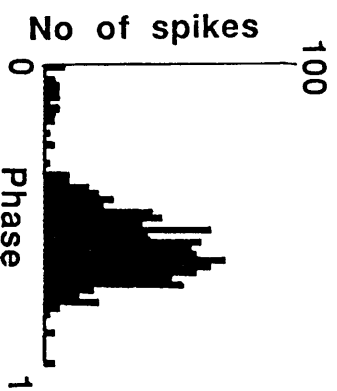
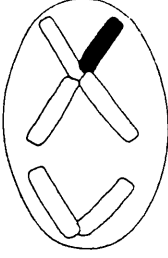
LEFT EYE

RIGHT EYE

LEFT EYE



INT-R

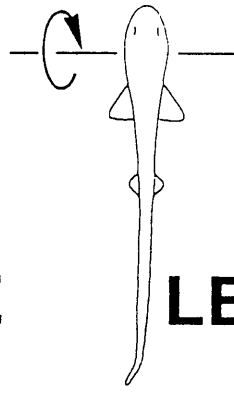


EXT-R

RIGHT SIDE DOWN

HEAD DOWN

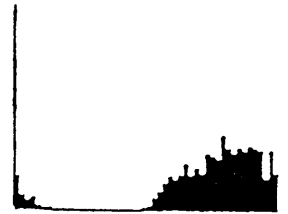
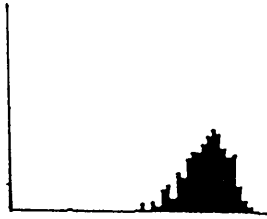
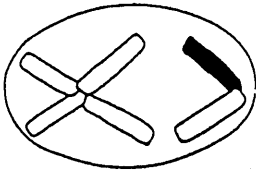
Fig 4.4 The vertical EOM activity is presented as phase histograms in the roll and pitch planes for tilts at 0.8Hz.



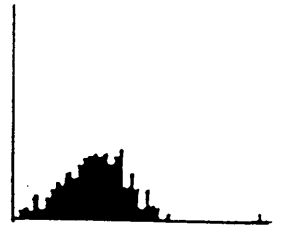
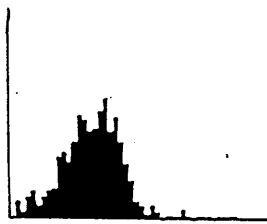
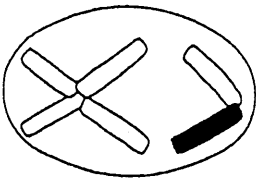
RIGHT EYE

LEFT EYE

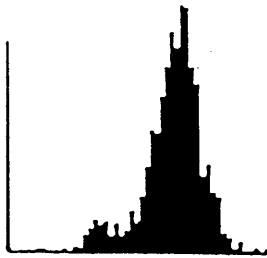
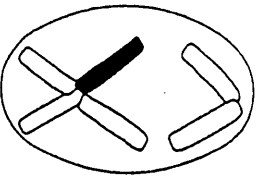
SO



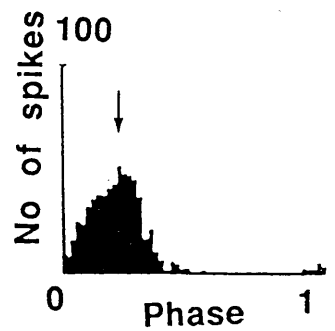
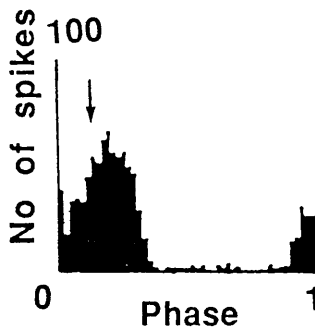
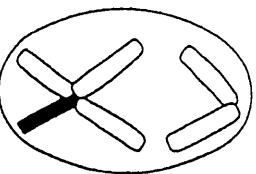
IO



SR



IR



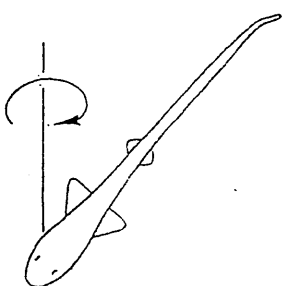
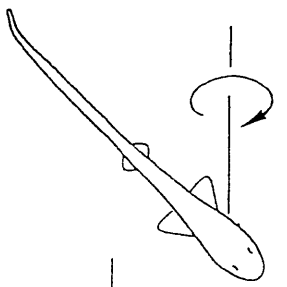
HEAD UP



HEAD DOWN



Fig 4.5 The angular tilts of the dogfish in the roll and pitch planes and at intermediate angles.



180

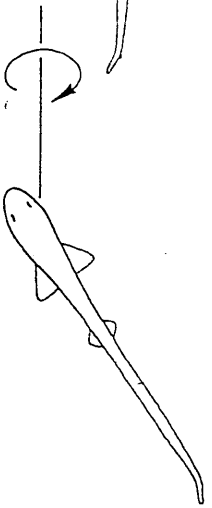
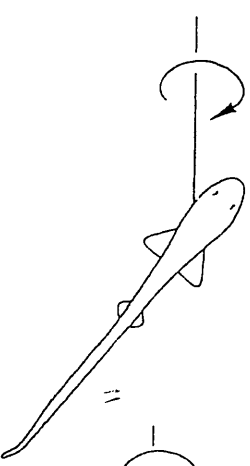
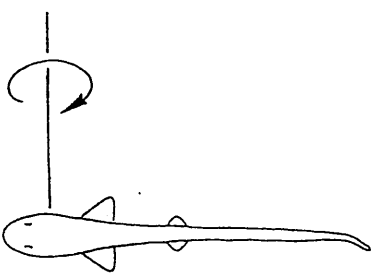
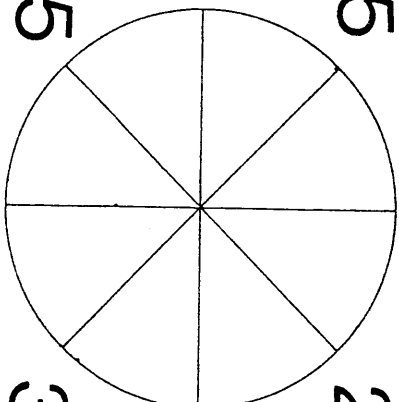
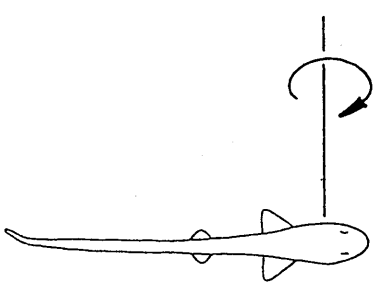
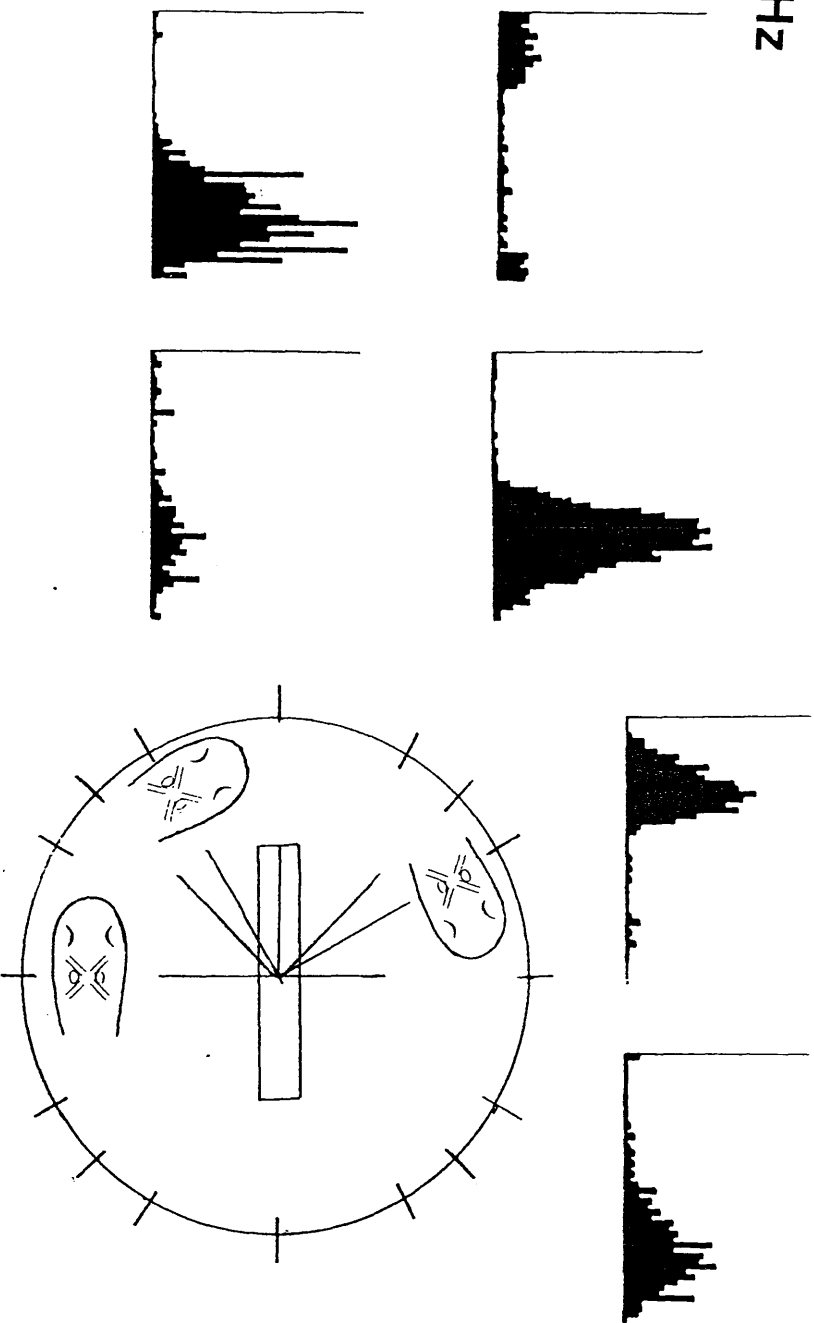
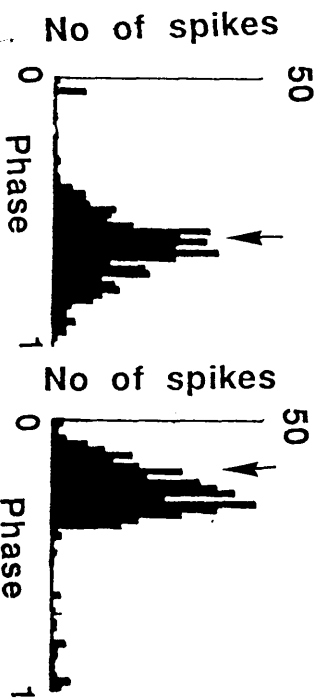


Fig 4.6 The SOR and SOL activity for tilts at 0.2Hz is illustrated by phase histograms at the planes of 0^0 , 60^0 , 150^0 , 180^0 , 240^0 , and 330^0 .

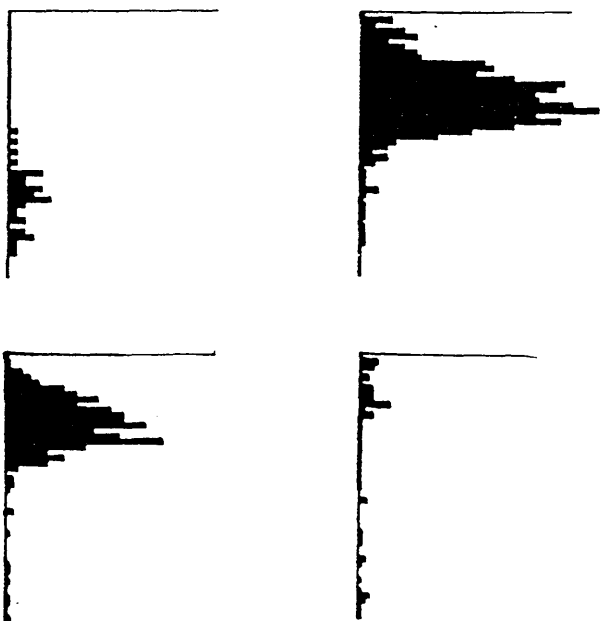
0.2Hz



SOR



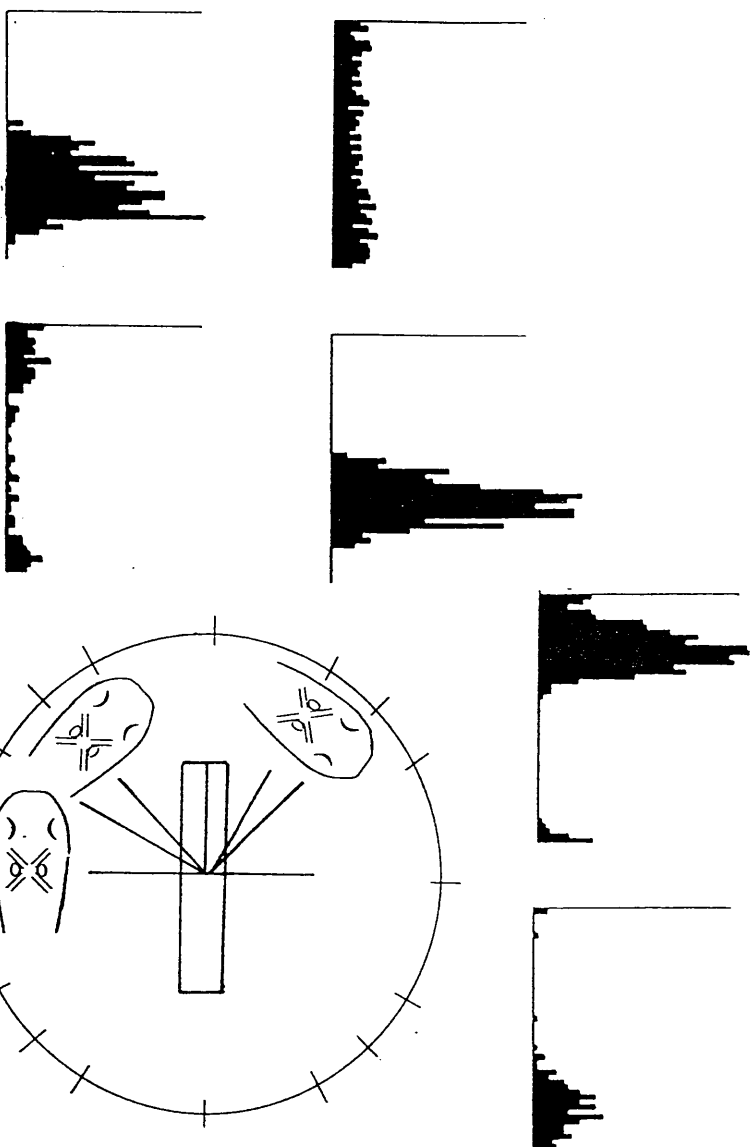
SOL



RIGHT SIDE DOWN

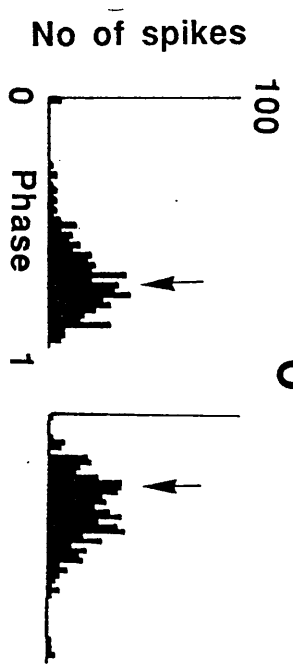
Fig 4.7 The SOR and SOL activity is presented as phase histograms at the planes of 0^0 , 30^0 , 120^0 , 180^0 , 210^0 , 300^0 for tilts at 0.8Hz.

0.8Hz



SOR

SOL

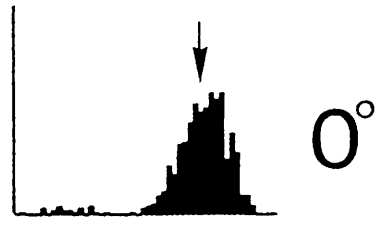
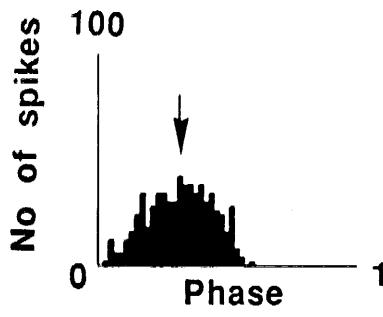


RIGHT SIDE DOWN

Fig 4.8 The phase histograms of the IOR and IOL activity are presented for tilts at 0.8Hz in the 0^0 , 45^0 , 90^0 , 135^0 , 180^0 planes.

IOR

IOL



RIGHT SIDE UP

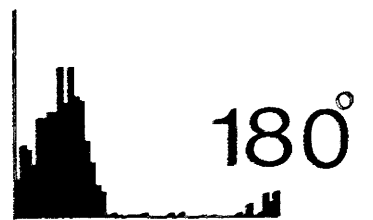
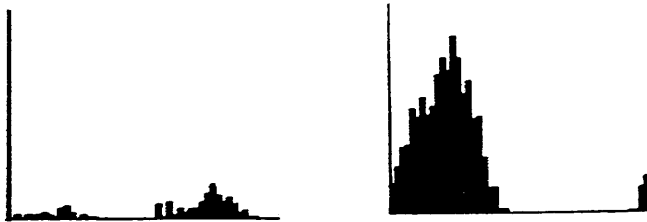
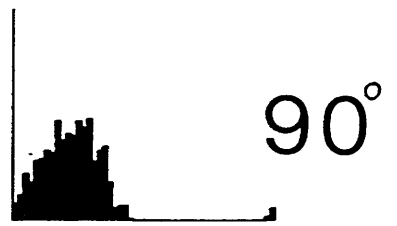
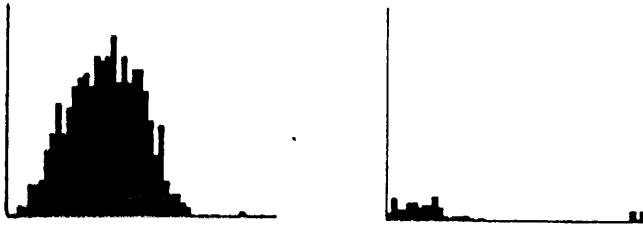
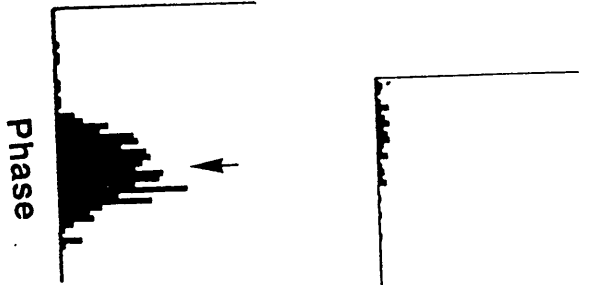
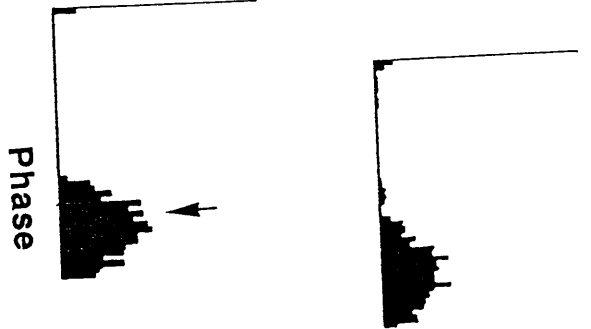


Fig 4.9 The phase histograms of the SRR and SRL activity are presented for tilts in the 0^0 , 45^0 , 90^0 , 135^0 , 180^0 planes at the frequency of 0.8Hz.

No of spikes



No of spikes

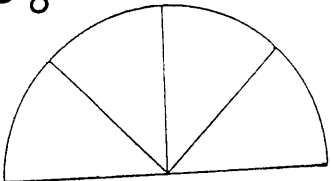


135°

90°

45°

0°



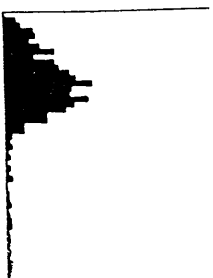
180°



SRR



SRL



RIGHT SIDE DOWN

Fig 4.10 The myographic activity of the IRL is shown for tilts at 0.2Hz and 0.8Hz in the 0^0 , 90^0 , 45^0 , 60^0 planes.

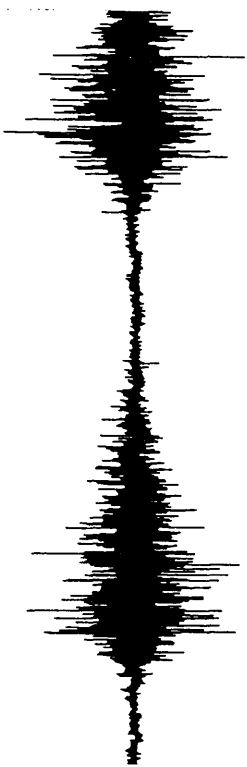
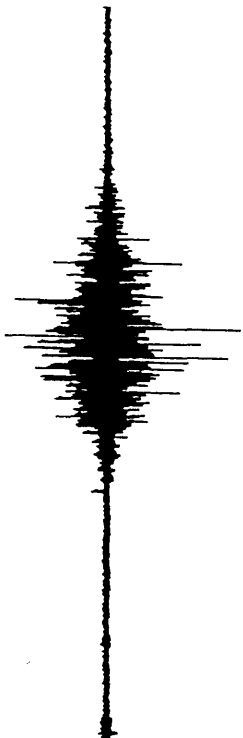


0°

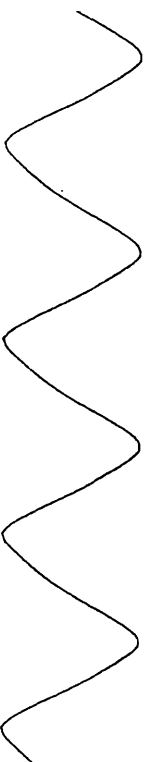
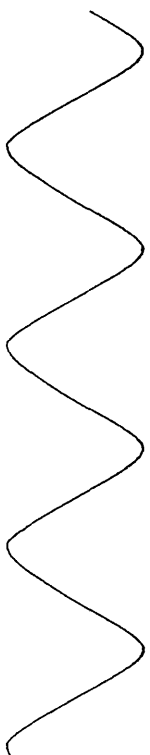
90°



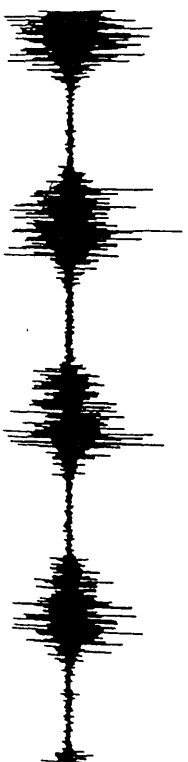
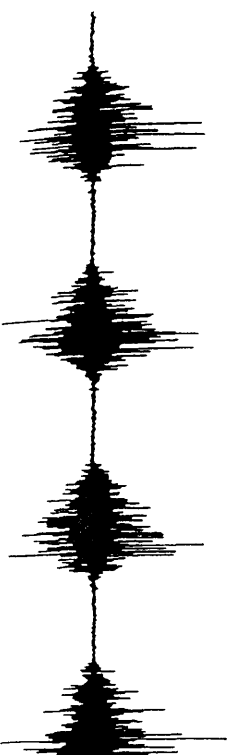
0.2Hz



IRL

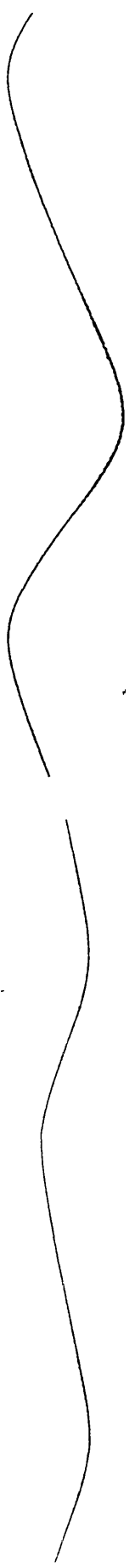


0.8Hz



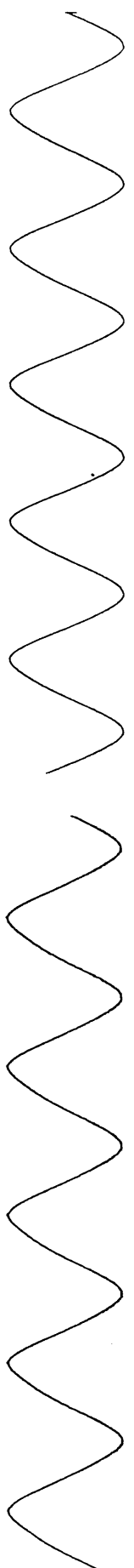
IRL

0.2HZ



IRL

0.8HZ



IRL

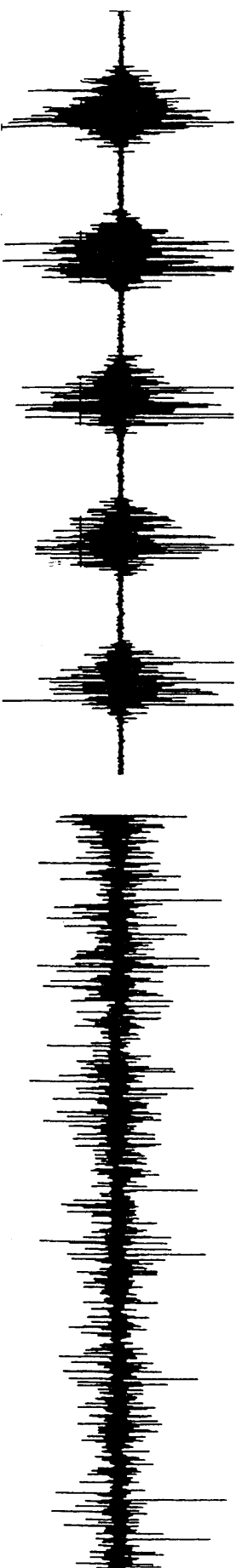
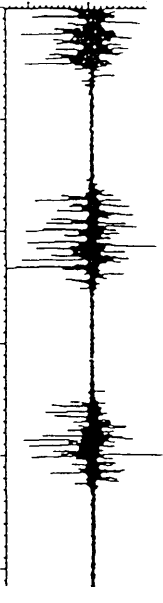
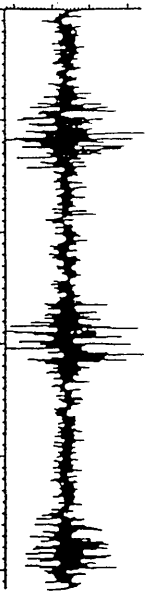
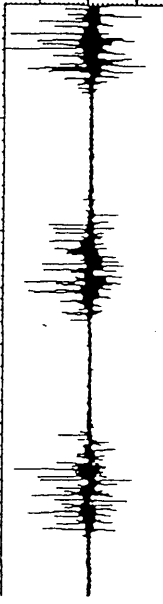
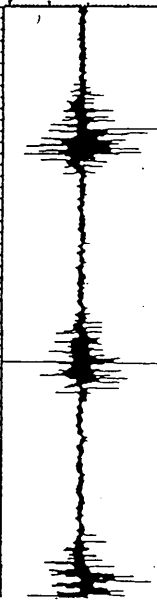
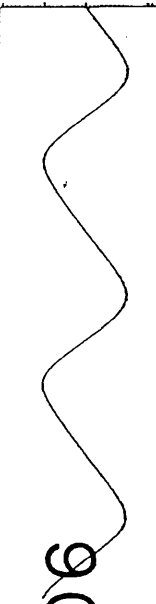


Fig. 4.11 The myographic activity of the EXT-R (R) and INT-R (R) is shown for frequency of 0.2Hz in the tilt planes of 0° , 45° , 90° , 120° , 180° .

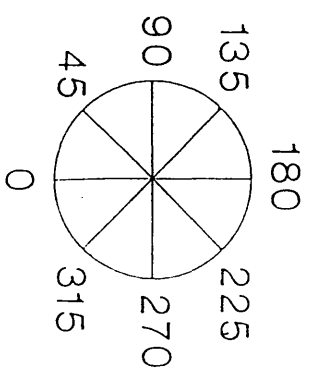
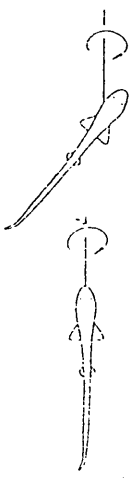
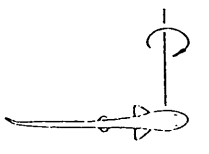
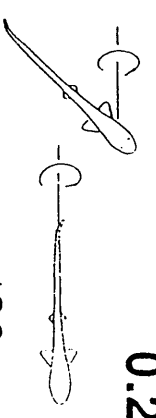
0°



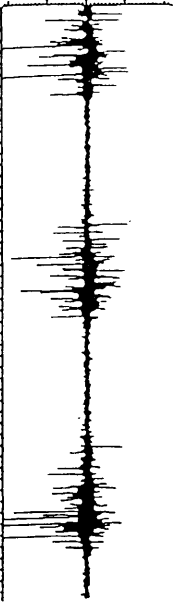
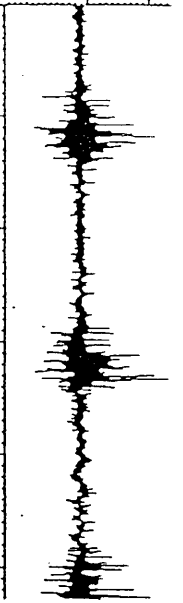
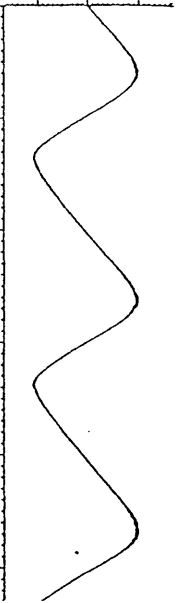
90°



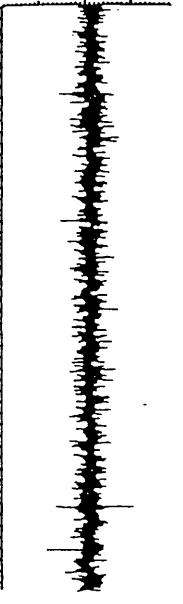
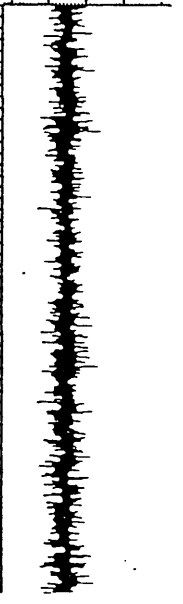
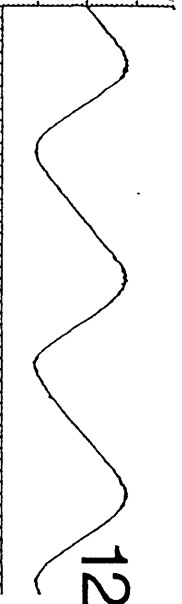
0.2Hz



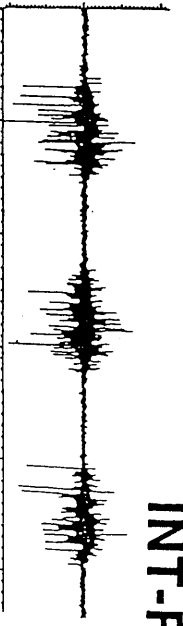
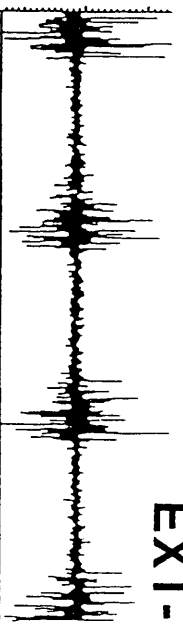
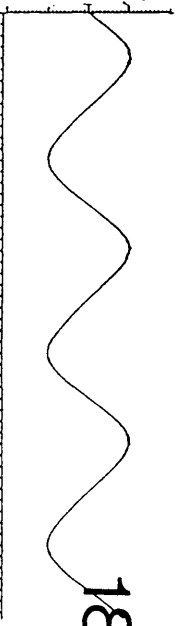
45°



120°



180°



EXT-R (R)

INT-R (R)

Fig 4.12 The activity of EXT-R and INT-R in the right and left eyes is illustrated by phase histograms for tilts at 0.8Hz in the 0^0 , 60^0 , 90^0 , 150^0 and 180^0 planes.

0.8Hz

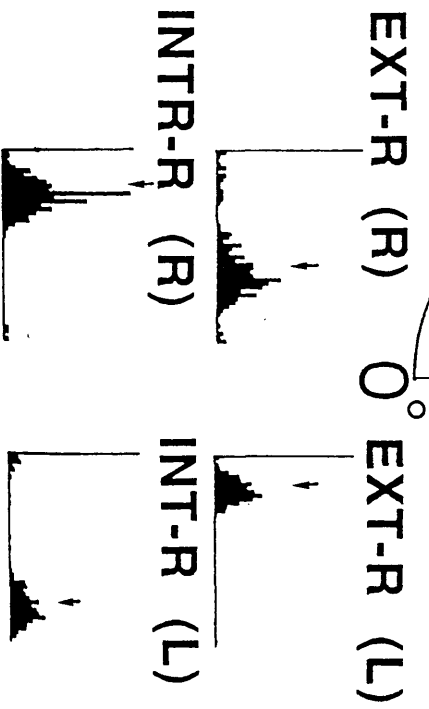
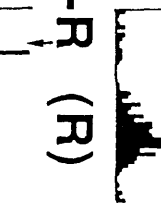
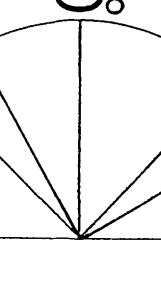
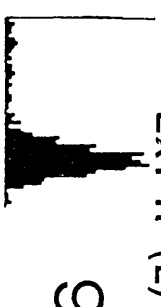
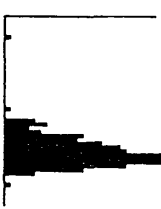
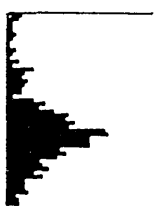
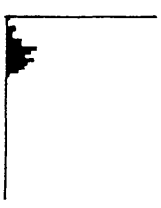
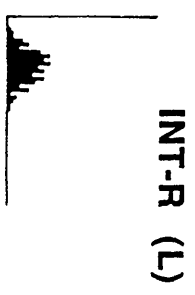
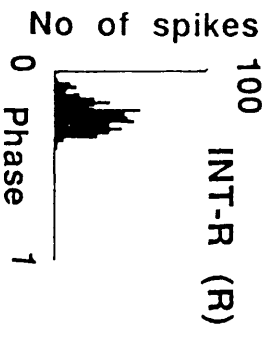
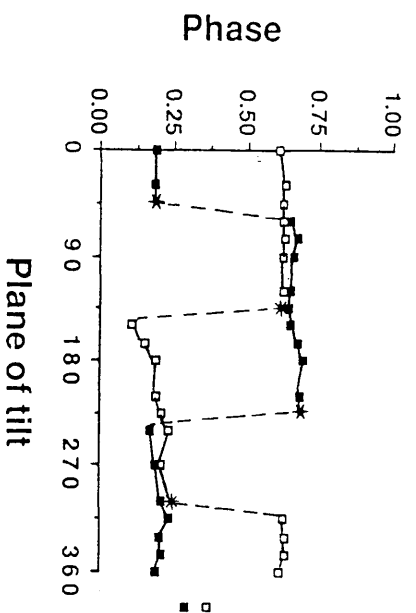


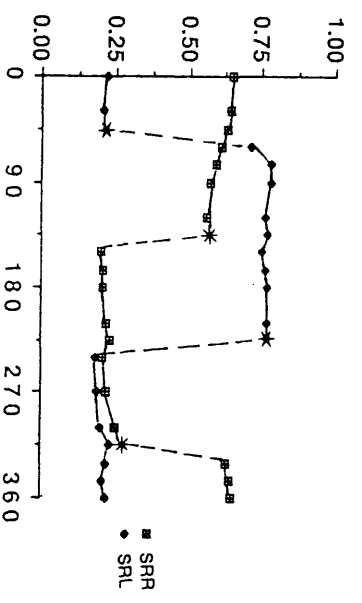
Fig 4.13 The circular mean values derived from the phase histograms of the EOM activity are plotted against the planes of tilt between 0^0 and 360^0 for tilts at 0.2Hz.

0.2Hz

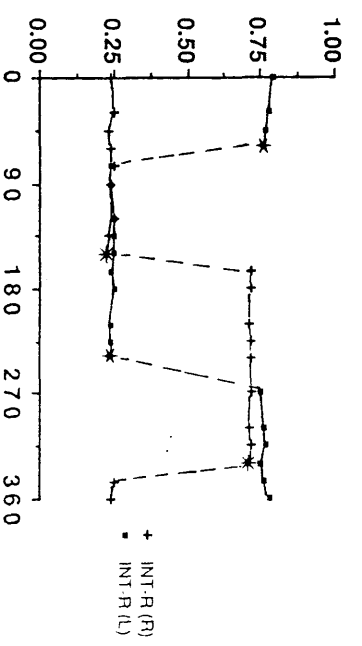
SO



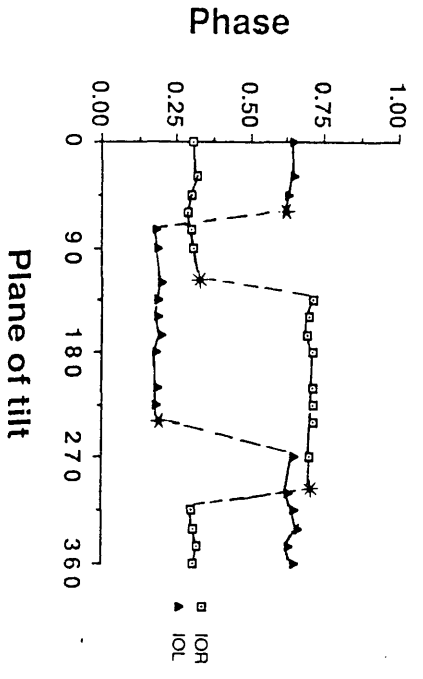
SR



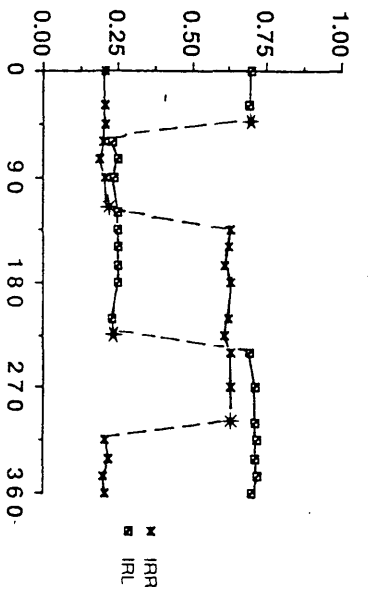
INT-R



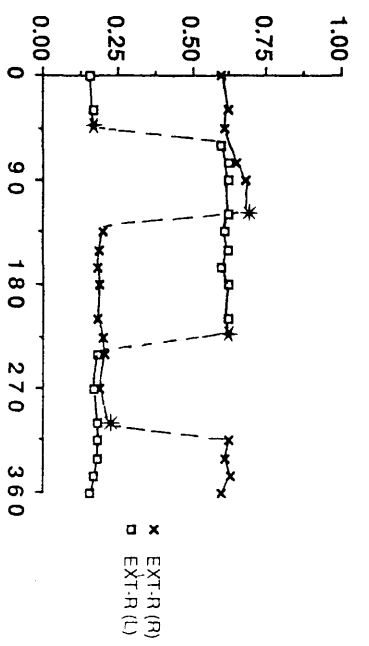
IO



IR

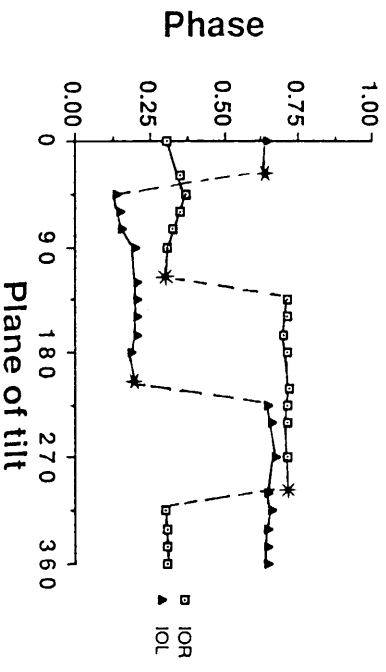
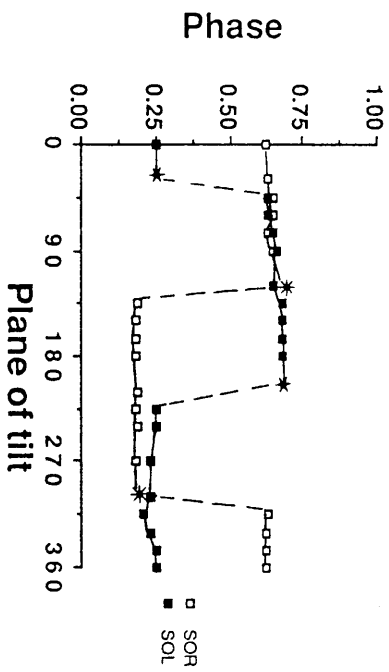


EXT-R

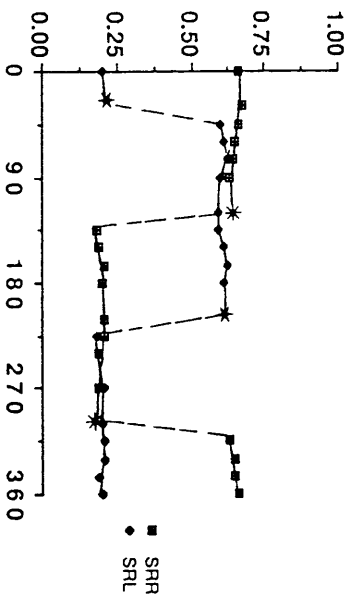


0.8Hz

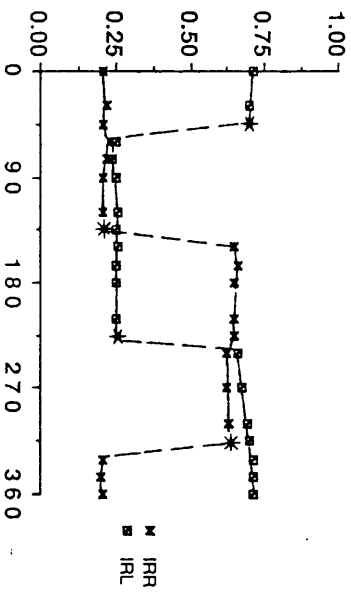
SO



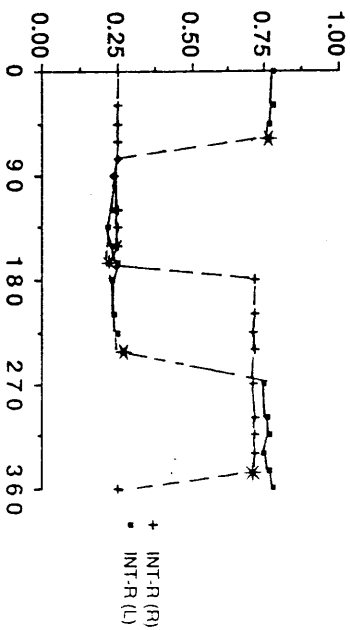
SR



IR



INT-R



EXT-R

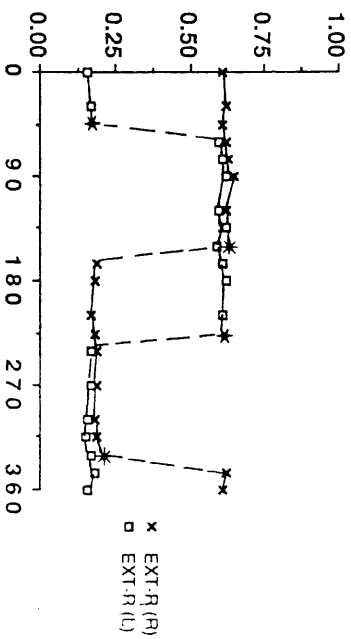


Fig 4.14 The circular mean values derived from the phase histograms of EOM activity are plotted against the planes of tilt between 0^0 and 360^0 for tilts at 0.8Hz.

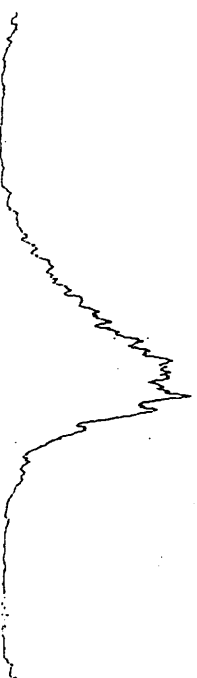
Fig 4.16 The integrated activity of the SOR, SOL and SOR, SRR is averaged over ten cycles for tilts at 0.2Hz and 0.8Hz in the 0^0 and 270^0 planes.

270°

SOR



SOL



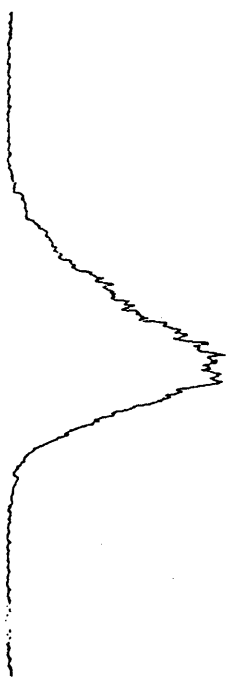
0.2Hz



SOR



SOL



0.8Hz



0°

SOR



SRR



0.2Hz



SOR

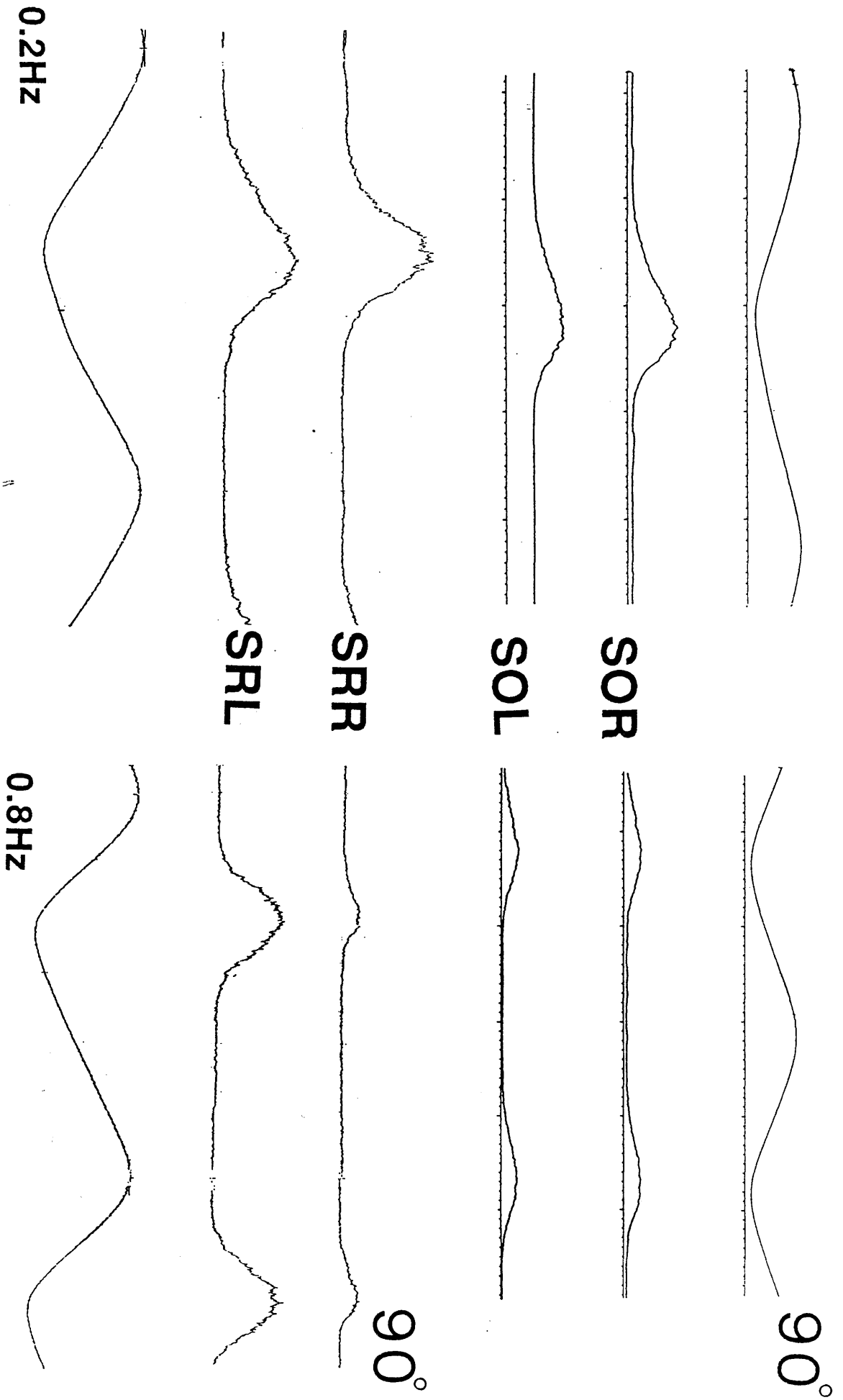


SRR



0.8Hz





90°

SOR

SOL

SRR

SRL

0.2Hz

0.8Hz

Fig 4.15 The integrated activity of the SOR, SOL and the SRR, SRL is shown for tilts in the pitch plane at frequency of 0.2Hz and 0.8Hz.

Fig 4.17 The myographic activity of SO in the right and the left eyes during right side down tilt at 0° , 15° , 30° , 45° , 60° and 75° .



0°



15°

30°

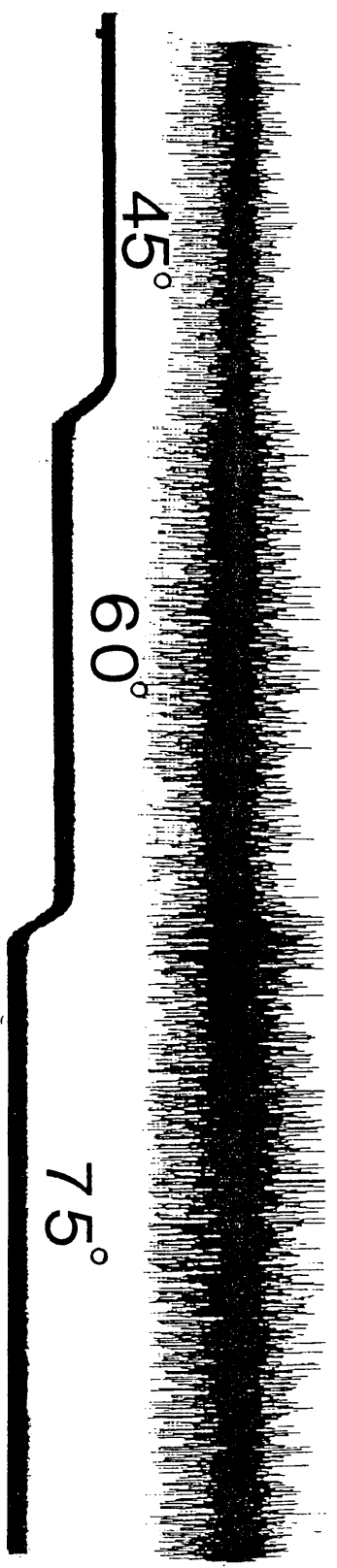


Fig 4.18 The tonic activity of SO in the left eye during a left side down tilt at 0° , 20° and 60° left side down and 40° left side up tilt.



0°



20°



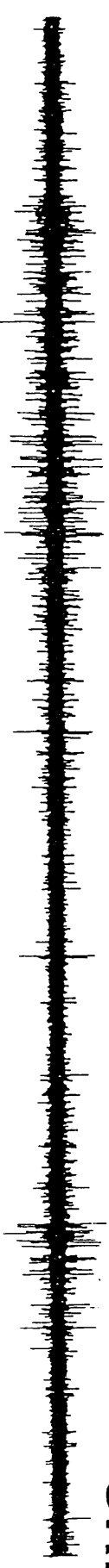
60°



40°

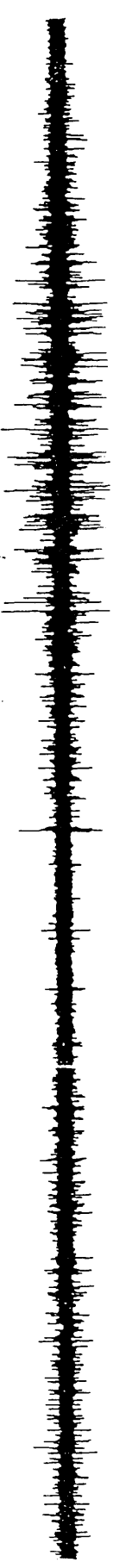


SRR



IRR

85



INT-R (R)

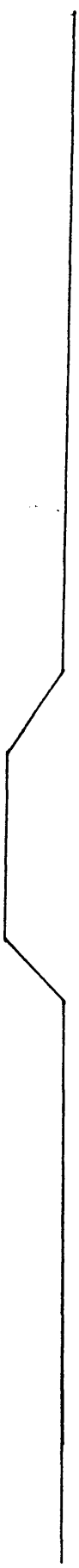
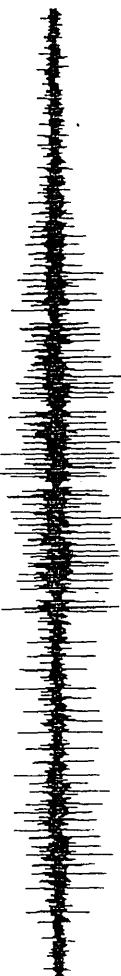


Fig 4.19 The myographic activity of INT-R, IR, SR, and SO in the right eye during an imposed horizontal body tilt at approximately 0.2Hz.

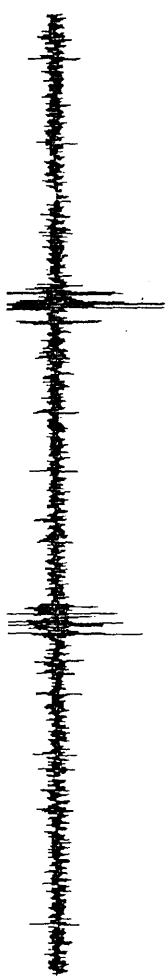
Fig 4.20 The myographic activity of INT-R and SR in the right eye during the slow phase of nystagmus response in a horizontal rotation.

19°

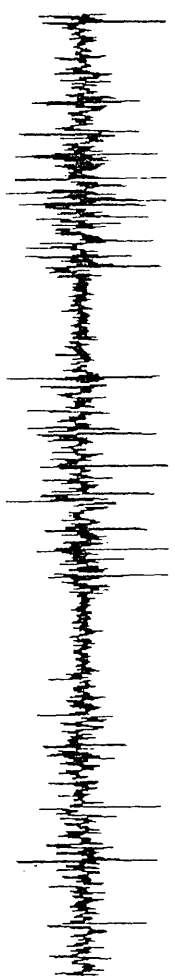
55



SR



INT_R



SR

Chapter 5. THE CONTROL OF EOM RESPONSE..

5.1 INTRODUCTION.

The compensatory vertical as well as horizontal eye movements are induced by the vestibular apparatus and the activity is carried by the VOR to the EOM.

In one of the earliest experiments Lee (1894, 1895) found that in fish mechanical stimulation of individual ampullae evoked two kinds of reflex response of the eyes depending on the intensity of stimulus. The two reflexes corresponded to responses to rotations in opposite directions in the plane of semicircular canal concerned. Maxwell (1920) observed only one kind of reflex response from each semicircular canal when the ampulla was directly stimulated or after unilateral ligaturing of an ampullae, and the fish being rotated in opposite directions in the appropriate plane. Also in amphibians McNally & Tait (1925, 1933) have established that the individual semicircular canal responds in one direction only. Lowenstein and Sand (1936) recorded the activity of the horizontal ampulla of fish and concluded that the the two opposite horizontal ampullae work antagonistically and that the reflex responses of normal fish must depend upon the balance of the afferent discharges from left and right vestibular apparatus. The results of these experiments provide an incomplete view of the reflexes of semicircular canals and nothing has been reported about the change in myographic activity of EOM during imposed head and body tilts of the intact animal and following the ligaturing of either all, or different combinations of semicircular canals.

The earlier experiments on the reflex responses of semicircular canals have also revealed the difference between the mode of function of the horizontal and vertical canals. In the horizontal canals

excitation occurs when the ampulla follows the canal during angular displacement, the stimulus being an ampullo-petal inertial movement of the endolymph. In the vertical canals excitation occurs by angular displacements in which the ampulla is leading, the stimulus being ampullo-fugal inertial movement of endolymph (Ross, 1936).

Some other aspects of the VOR which have been determined in fish include the investigation of the VOR in sea lamprey by Carl et al. (1976). Their experiments have demonstrated that mechanical stimulation of the vestibular system or electrical stimulation of the vestibular nerves produced stereotyped conjugate eye movements and appropriate electrical activities in individual EOM. They have also observed that no inhibition of discharges in the motor nerves was observed during stimulation of opposing reflexes. They concluded that these primitive reflexes of the lamprey probably correspond to the simple excitatory pathways from single ampulla to individual EOM of higher vertebrates.

The detailed analysis of the function of semicircular canals was made by Lowenstein & Sand (1940), and they have investigated the activity of individual semicircular canals in a preparation of the isolated labyrinth. The effects of tilts about vertical, longitudinal, and transverse axes were determined. They concluded that horizontal canals respond to rotation about the vertical primary axis, but are unaffected by rotations about the horizontal primary axes. In contrast to this they found that the anterior and posterior vertical canals respond to rotations about all three primary axes. Lowenstein & Sand (1940) have predicted the combined reflexes of all semicircular canals during rotation about the three primary axes: they suggested that for tilts in the vertical roll plane they are laterally synergic, whereas for tilts at the pitch plane they were transversely synergic.

Lowenstein & Sand (1940) also predicted the reflex effects onto the EOM evoked by the integrated action of the semicircular canals during induced body tilts in vertical and horizontal planes, suggesting a possible input to each EOM. Although their results are consistent with the pattern of semicircular canal activation and a possible control of EOM responses by each canal, these predictions have never been experimentally tested by recording myographically from EOM.

In mammals responses of oculomotor units to stimulation of single semicircular canals were studied in guinea pigs by Manni and Desole (1964). Their experiments have established that given units of the oculomotor nuclei were involved in three types of nystagmus brought about by separate stimulation of the three semicircular canals. These studies have established that there is a strict relationship between a given semicircular canal and a particular pair of EOM. Szentagothi (1964) has performed experiments on isolated semicircular canals of dog. He stimulated the cristae by inducing artificial endolymphatic currents and concluded that there was a localized projection between (i) the posterior ampulla and the ipsilateral SO and contralateral IR (ii) the anterior ampulla and the ipsilateral SR and contralateral IO (iii) the horizontal ampulla and the ipsilateral INT-R and contralateral EXT-R. These experiments have confirmed the results obtained by Flurr (1959) in cat after stimulating the ampullar nerves. Cohen, Suzuki, Shazner & Bender (1964) have stimulated the ampullar nerves in monkeys and obtained a similar pattern of EOM activation. Their results were different from the above experiments in the respect that they have also reported a weaker contraction of two other EOM. Stimulation of the left anterior canal was not only accompanied by a strong contraction of the left SR and right IO but also by a weaker contraction of left SO and right SR. In these experiments, although

myographic activation of different EOM as a result of mechanical stimulation of semicircular canals has been described, it still needs to be determined how these responses match with the myographic activity of EOM as a result of physiological stimulation of semicircular canals, and how this response alters following the elimination of one or both ipsilateral and contralateral canals.

The utricle is generally considered to be the receptor system monitoring position in space by having a discharge activity, the frequency of which is a function of the angle of deviation of head from its normal position. The static and dynamic behaviour of the utricle has been extensively studied in mammals, amphibians and fish (Lowenstein & Roberts, 1949, 1950; Vidal et al., 1971; Lowenstein & Saunders, 1975)

Lowenstein and Roberts (1949) have recorded the activity of the utricle in the ray. They have observed that the response of utricular units to a change of angular head position around a horizontal axis decayed within 30-60 seconds after the end of movement. Recording from the vestibular nerve of cat, Vidal et al (1971) found the utricle receptors to exhibit both static and dynamic characteristics, the relative proportion of which varied from cell to cell.

In dogfish the utricle input to EOM responses by physiological stimulation in the absence of semicircular canals still needs to be determined.

5.1.B Aims of the project.

Although semicircular canal reflexes in terms of their input to myographic activation of EOM have been predicted by Lowenstein and Sand (1940), these predictions were not experimentally tested and proved in the fish. In the present project the recordings of EOM in

intact fish have been compared with those determined after the ablation of different canals to investigate how the actual pattern of EOM firing corresponds to the model proposed by Lowenstein.

Very little is known about the utricle input to EOM, the nature of these reflexes or how they affect the myographic activity of EOM after eliminating the semicircular canals. In this project control experiments were performed at different frequencies of tilt to determine if canal and utricle input could be segregated by this factor. The EOM responses at these different frequencies were determined in the intact fish and following the elimination of either different combinations of vertical canals or all four canals. Also the change in responses of EOM was determined by unilateral and bilateral ablation of the utricle.

5.2 MATERIALS AND METHODS.

Experiments were performed on 12 dogfish. Under anaesthesia (MS222) each dogfish was decerebrated and pithed, and the body of the animal was then held in a specially designed frame assembly (see section 3.2). While operating, the gills of deeply anaesthetised fish were kept moist. In preparation for the surgical procedures, the semicircular canals were exposed by slicing through the cartilaginous roof of the auditory capsule. The electrodes were then inserted in the EOM to record its myographic response (section 3.2). After the operation the fish was left in a sea water tank for a few hours to recover completely. After recovery, the first recordings were made with the vestibular system exposed but intact. The animal was tilted in the roll (0°) and pitch (90°) planes and the transition in the response of EOM was determined by tilting the animal at each 45° in between roll and pitch (see section 4.2 for details of the especially designed frame assembly and for the description of tilt planes). In a series of pilot experiments the semicircular canals were either ligatured by tying a thread across the canals to block the fluid movements in the canals, or by ablating the canals by removing the exposed segment. Since no differences in the myographic responses of EOM was observed in the above two procedures, the latter was adapted as a standard procedure since it was more rapid and simple to execute. Different combinations of canals were ablated in each experiment. To identify the differences between the canal and utricle input all animals were tilted at both low (0.2Hz) and high frequency (0.8Hz) with an amplitude of $\pm 25^{\circ}$. In these experiments after eliminating the four vertical canals, unilateral and bilateral ablation of the utricle was performed to check the utricular responses.

5.3 RESULTS.

5.3.A S0 response in intact fish, canals exposed.

Before the ablation of semicircular canals and utriculi, recordings were made in the intact animal with exposed semicircular canals. The results of these experiments have established that the EOM response was not affected by this operation and the myographic activity of EOM was similar in its strength and phase position to that of the unoperated fish as described in the Chapter 4 (Fig 5.1.A, B).

The myographic activity of S0 in the right and left eyes in the roll and pitch planes have been discussed in section 4.3.A and 4.3.B. The transition in the response of the right and left S0 was determined by tilting the animal in intermediate planes (see section 4.3.C.1) (Fig 5.1.A.B).

A control experiment was designed to determine the relative contribution of utricular and semicircular canal inputs to the VOR of the EOM at different stimulus frequencies. This was achieved by a series of operations to ablate the canals on the left and right sides. In this experiment initially the animal was tilted in the roll plane (0^0) for a range of frequencies, 0.2Hz, 0.4Hz, 0.6Hz, 0.8Hz, while myographic recordings were made in the S0 of the right and left eyes (Fig 5.2).

In the first operation the two ipsilateral canals of left side were ablated. One hour after the operation recordings were made at a series of stimulus frequencies. The left S0 exhibited no change in its phase position and in the strength of myographic discharge for tilts at and below 0.2Hz, but at frequencies greater than 0.2Hz no burst was elicited in this muscle during a left side down tilt. The right S0 was unaffected by this operation and discharged strongly at all

frequencies during a right side down tilt (Fig 5.3).

In the second operation the two ipsilateral canals of the right side were ablated and as before the myographic activity of right and left SO was recorded 60 minutes after the operation. Both right and left SO were activated with a strong myographic discharge (as in the intact fish) for tilts at 0.2Hz, but at frequencies greater than 0.2Hz no myographic response was elicited by the right and left SO during right side down and left side down tilts (Fig 5.4).

The control experiment has established that at a frequency of 0.2Hz (and below), the myographic response of the EOM was not affected by ablation of the vertical semicircular canals, but at frequencies greater than 0.2Hz no EMG were elicited after the ablation, which suggests an activation of two different parts of the vestibular system at low and high frequency tilts. Based on the results of this experiment, recordings were made only at frequency of 0.2Hz and 0.8Hz in all other experiments.

5.3.B. Single canal ablation.

In a series of experiments only one semicircular canal was ablated leaving three vertical semicircular canals, the horizontal canals and the utriculi intact. In different experiments each of the four vertical canals was individually ablated.

5.3.B.a Anterior canal ablated.

After this operation, in which either the left anterior or right anterior canal was ablated, for tilts at 0.2Hz strong myographic discharges were elicited at each angle, whereas for tilts at 0.8Hz a comparatively weak response was elicited by the right and left SO at the roll plane (0^0 , 180^0) and the maximum number of spikes was

elicited only at the pitch plane (90^0 , 270^0) (Fig 5.5.A, 5.6.A). After ablation of the left anterior canal no response was elicited by the left S0 at the angles of 120^0 - 145^0 (transition in the contralateral S0) Fig 5.5.A.

Tilting at 0.8Hz after the ablation of right anterior canal, the left S0 discharged with a comparatively strong myographic activity in contrast to the weak myographic discharge at the transition angles (30^0 , 45^0) in the intact fish. The right S0 fired weakly at this angle of tilt and only a few spikes were elicited at 15^0 - 45^0 (before and after the transition). At the transition angle of the right S0 (120^0 - 145^0) the left S0 fired strongly, but weak myographic discharges were elicited by the ipsilateral S0 at these angles of the tilt (Fig 5.6.A).

For tilts at 0.2Hz and 0.8Hz there was no change in the phase of the firing of either S0 at the roll and pitch planes, and the transition in the S0 firing occurred at the same angles as in the intact fish (Fig 5.5.B, 5.6.B).

5.3.B.b Posterior canal ablation.

By ablation of a single posterior canal leaving two anterior canals and one posterior canal intact, strong myographic activity was elicited at each angle for the tilts at 0.2Hz. For the tilts at 0.8Hz (in contrast to the ablation of anterior canal, section 5.3.B.a) the maximum number of spikes was only elicited at the intermediate angles. A weaker myographic discharge was observed by the two EOM at the roll and pitch planes (Fig 5.7.A, 5.8.A).

After the ablation of the right posterior canal the ipsilateral S0 to the ablated side discharged strongly at 30^0 (transition in the contralateral S0). The myographic response of the contralateral S0 to

the ablated side at this angle was comprised of a strong discharge on both sides of the stimulus curve. At 120^0 (transition in the ipsilateral SO to the ablated side) the two EOM fired strongly (in contrast to the weak firing of the right SO at transition in the intact fish). Similar effects were recorded in the ipsilateral SO to the ablated side and contralateral SO to the ablated side after the ablation of left posterior canal (Fig 5.7.A, 5.8.A).

After the operation the phase of right and left SO firing in the roll and pitch planes, and the angles at which the transition occurred remained the same as in the intact fish (Fig 5.7.B, 5.8.B).

5.3.C Two vertical semicircular canals ablated.

In a series of experiments a pair of semicircular canals was ablated in different combinations leaving two vertical canals and the utriculi intact. The ablation was preceded by the myographic recordings of the EOM. The combinations of the canals ablated during these experiments were:

- A. Two anterior vertical canals ablated.
- B. Two posterior canals ablated.
- C. The diagonal pair of canals ablated.
- D. The ipsilateral canals ablated.

5.3.C.a Two anterior canals ablated, SO.

Results were obtained for the SO in the two eyes. After the ablation for tilts at 0.2Hz as in the intact fish strong myographic discharges were elicited at all the planes. For tilts at 0.8Hz an overall weaker myographic activity was elicited at each angle as compared to the intact condition. Strong activity was elicited by the two SO at the roll plane (0^0 , 180^0). In the right SO a double burst

was elicited at the roll plane and a strong second burst was also elicited around its transition angles. The two S0 fired strongly at the pitch plane (90^0 , 270^0). At the intermediate planes the left S0 discharged strongly around the transition angles of the right S0 (Fig 5.9.A.B)

5.3.C.b Two anterior canals ablated, IO.

Results were obtained for the right and left IO after the ablation of the two anterior canals. After the ablation for tilts at low and high frequencies the transition in the two IO occurred at the same planes as in the intact fish. For tilts at 0.8Hz weak myographic activity was elicited in the two IO at the roll and pitch planes. There was a total inhibition of the myographic activity at the null points of one IO, while the other discharged strongly at these planes of the tilt (Fig 5.10.A.B).

5.3.C.c Two posterior canals ablated, S0.

Results were obtained for the right and the left S0 after the ablation of the posterior vertical canals. For low frequency tilts the strength of the response and the planes of the tilts at which the transition occurred were the same as in the intact fish. For tilts at 0.8Hz the planes at which phase shifts occurred were not affected by the ablation, although an overall weaker activity was elicited in the S0. In the two S0 stronger discharges were only observed at the roll and the pitch planes. As in section 5.3.C.a after the ablation a total inhibition of the myographic discharges was recorded around the transition angles of one S0, while the other discharged strongly at these angles of the tilt (Fig 5.11.A.B).

5.3.C.d Diagonal pair ablated, S0.

Results were obtained for the left and the right S0 after the ablation of the left anterior and right posterior canals. For the tilts at 0.8Hz few spikes were elicited in the left S0 at the roll plane (0^0 , 180^0). For the tilts at the pitch plane strong myographic discharges were elicited in the left S0, its myographic activity being totally inhibited around the transition angles. At the transition angles of the right S0 weak activity was elicited in the left S0. For tilts at 0.8Hz a weaker response was elicited in the right S0 at the roll and pitch planes. There was no activity in the right S0 at its transition planes, while at the null points of the left S0 the maximum number spikes was elicited in the right S0 (Fig 5.12.A.B).

5.3.C.e Ipsilateral pair ablated, S0.

After the ablation of the vertical canals of the left side, for tilts at 0.2Hz strong myographic activity was elicited in the right and left S0 and the transition in the response of the two S0 occurred at the same planes as in the intact fish.

For tilts at 0.8Hz in the right S0 the planes at which transition occurred remained same as in the intact fish. Strong myographic discharges were recorded in the right S0 at all the tilt planes. At the intermediate planes the right S0 discharged strongly at its transition angles (Fig 5.13.A).

For tilts at 0.8Hz weak activity was elicited in the left S0 at all planes. A rather unusual pattern of myographic activity was recorded in the left S0 for tilts at the roll plane: instead of firing at the phase of 0.12 (as at low frequency tilts, and as in the intact fish) it now fired at the phase of 0.63 (in phase with the right S0). The two S0 stayed in phase at each plane of the tilt between 0^0 - 360^0

and the transition in the phase of left S0 now occurred at the same angle as that of the right S0 (Fig 5.13.B).

5.3.D. Single vertical canal intact.

After the ablation of the three vertical semicircular canals only one anterior or posterior canal was left intact and recordings were made in the S0 ipsilateral and S0 contralateral to the intact side.

5.3.D.a. Single anterior canal intact. S0.

With only one anterior canal intact for tilts at 0.2Hz which activate the utricular reflexes (section 5.3.A) strong myographic discharges were elicited at each angle and the phase of the two S0 firing at the roll and pitch planes remained the same as in the intact fish. However for tilts at 0.8Hz a generally weaker myographic response was elicited in the S0 of both sides.

Results for both intact right anterior and intact left anterior canals were very similar (Fig 5.14.A.B & 5.15.A.B). Very few spikes were elicited by either S0 at the roll plane. In the S0 ipsilateral to the intact side no response was elicited at the pitch planes (90^0 , 270^0) and at the angles in between 90^0 - 180^0 , while in the S0 contralateral to the intact side the maximum number of spikes was elicited at the pitch plane and strong activity was recorded for the tilts at 135^0 - 180^0 . At the null points of the S0 contralateral to the intact side strong activity was elicited by the S0 ipsilateral to the intact side (Fig 5.14.A.B & 5.15.A.B).

5.3.D.b. Single anterior canal intact, IO.

Results were obtained from the right IO with only the right anterior canal intact. For tilts at 0.8Hz very weak myographic

discharges were elicited at the roll plane in this ipsilateral IO and a comparatively stronger response was elicited at the pitch plane. A double burst and strong myographic discharges was elicited at the planes of 45° and 225° . Near the transition angle of the ipsilateral IO (135° - 180°) no response was recorded and it proved impossible to precisely determine the angle at which the transition occurred (Fig 5.16.A.B)

5.3.D.c. Single anterior canal intact, SR.

Results were obtained from the right SR with only the right anterior canal intact. For tilts at 0.8Hz weak myographic activity was elicited at the roll and pitch planes and no myographic discharges were recorded between the angles of 90° - 180° . A comparatively stronger response was elicited at the angles of 45° - 60° (Fig 5.17.A.B).

5.3.D.d. Posterior canal intact, S0.

Results were obtained in the S0 ipsilateral and contralateral to the single intact posterior semicircular canal. For tilts at 0.8Hz there was no change in the phase (compared with the intact fish) of either S0 at the roll and pitch planes. A weaker myographic activity was recorded in both S0 at the roll and pitch planes (Fig 5.18.A.B).

It was not possible to determine the transition angles precisely since near and at the null points of the two EOM no response was elicited. At the null points of the ipsilateral S0 a comparatively better response was elicited by the contralateral S0 (Fig 5.18.A.B).

5.3.D.e. Posterior canal intact, SR.

For tilts at 0.8Hz with right posterior canal intact weak myographic discharges were elicited in the right (ipsilateral S0) at

the roll and pitch planes and a comparatively strong response was elicited at the angles of 45° - 60° (Fig 5.19.A.B).

5.3.D.f. Single posterior canal intact, IO.

With a single intact posterior canal and for tilts at 0.8Hz, weak myographic discharges were elicited in the ipsilateral IO at the roll and pitch planes. In the contralateral IO a weak myographic activity was elicited for tilts at the roll plane, but a comparatively strong response was recorded at the pitch angles. Strong myographic discharges were elicited in the contralateral IO around the null points of the ipsilateral IO (Fig 5.20.A.B).

5.3.E. Four vertical canals ablated, utriculi intact, S0, IO, SR.

After the ablation of the four vertical canals, with the horizontal canal and the utriculi intact, recordings were made at 0.2Hz and 0.8Hz. At 0.2Hz myographic discharges were elicited at each angle and the transition in the firing of EOM was observed at the expected angles (section 3.3.C). For tilts at 0.8Hz either no response was elicited in the EOM recorded during these experiments or in some cases a very weak response was indicated at this frequency by the firing of a few units (Fig 5.21).

5.3.F. Single utricle intact, S0.

The myographic recordings in the S0 of the right and left eyes were made after ablating four vertical semicircular canals and the utricle of one side. In these experiments myographic response in the EOM was only observed for the tilts at 0.2Hz and only a few spikes were elicited in the S0 of both sides in the roll and pitch plane. In the pitch plane weak activity was elicited in the ipsilateral S0.

while in the contralateral SO a comparatively strong response was elicited. A strong response was elicited in the contralateral SO at the transition angles of the ipsilateral SO, while at the angles where transition in the contralateral SO was expected to occur its myographic activity was totally inhibited (Fig 5.22.A.B).

5.3.G. Unilateral ablation of the utriculus and vertical canals.

After the unilateral ablation of the left utriculus and vertical semicircular canals recordings were made in only the right and left SO. For tilts at 0.2Hz weak myographic discharges were elicited in the contralateral SO at the roll and pitch planes. In contrast to this, very strong myographic activity was recorded in the ipsilateral SO at this plane of the tilt. The myographic activity of the contralateral SO was totally inhibited around its transition angles while a maximum number of spikes was elicited in the ipsilateral SO at these planes of the tilt. At the null points of the ipsilateral SO a weak myographic response was elicited in the contralateral SO (Fig 5.23.A.B).

5.3.H Two utriculi ablated.

After ablating the four vertical canals and the two utriculi recordings were made for the tilts at 0.2Hz and 0.8Hz. There was a total absence of the myographic response at all angles of the tilts (Fig 5.24).

5.3.I Modelling of the semicircular canal system.

A model of the vestibular system was constructed by using the existing knowledge about the sensitivity of the hair cell receptors to fluid flow. The following assumptions were made in constructing the model.

1. All receptors in the macula of a canal respond to the same direction of fluid flow.
2. Due to their spontaneous activity, macula receptors are capable of signalling both directions of fluid flow by an increase or reduction in their firing level.
3. As demonstrated by the ablation experiments there is a drive from a canal to the contralateral EOM which incorporates a sign inversion. The strength of this drive is less than that to the ipsilateral EOM.
4. Considering tilts in different vertical planes, the hydromechanics of a closed canal dictate that the force acting on the cupula varies with the sine of the angle.

Based on these assumptions a computer model was constructed of the effects of the semicircular canal system on the firing of a particular muscle in one eye (the SO of right eye was selected). For one half cycle of the sinusoidal tilt (side down which causes ampullo-fugal inertial movement of the fluid flow in a canal, which in turn excites the macula receptors) the strength of an input from a canal and its anatomical plane were input variables. Arbitrary values of strength of 1 and 0.5 were assigned for the canals ipsilateral and contralateral to the selected EOM respectively, and a value of 0 was entered for each ablated canal. The planes of canals were designated 45° for right anterior canal, 135° , right posterior canal, 225° for left posterior canal and 315° for left anterior canal, using the long axis of the body as a reference.

The computer programme calculated the strength of input from each functional canal for all possible vertical planes of tilt (every 2° round the circle). In addition, the algebraic sum of these inputs was calculated. Data are presented as plots (Fig 5.25 & 5.26) in which positive values represent stimulatory drive from the semicircular

canal system to produce contraction of the selected EOM for one half cycle of the tilt. Negative values represent the same stimulatory drive for the other half cycle of tilt, and thus the point at which the curve crosses the origin is equivalent to the point of phase reversal of the EOM response with changing planes of tilt. Thus the curve produced by the model represents both the amplitude and phase of the VOR stimulus.

5.3.J Myographic activity to static tilts in the EOM after ablating four vertical canals and the right utriculus.

The myographic activity in the right SO to static tilts was recorded after ablating all four vertical canals and the right utriculus. After ablation no response was seen in the EOM until the 60° right side down and head down tilt was passed. For angular tilts greater than 60° strong myographic discharges were elicited. During a side down tilt only individual units of one size was fired and the maximum activity was elicited at 90° right side down (Fig 5.27). During tilts in the pitch plane a strong myographic response was elicited for 90° head down tilt. Firing in the pitch plane was different from that observed during roll tilts in respect that units of two sizes were seen and no single units were seen in this recording (Fig 5.28).

5.4 DISCUSSION.

Results obtained in Chapter 3 (section 3.4) have demonstrated differences in the operation of vestibular system at low (0.2Hz) and high (0.8Hz) frequency tilts. The same frequencies were selected to stimulate the animal after ablating different combinations of the vertical semicircular canals and the utricle. Further confirmation of the alternate dominant activation of the utricle and semicircular canals at 0.2Hz and 0.8Hz was provided by the control experiment in which myographic response of the right and left SO was first recorded in the intact fish followed by ablation of the left ipsilateral pair of vertical canals and all four vertical canals. The persistence of the myographic activity in the EOM of the intact side at all frequencies and an abolition of the EMG activity in SO of the ablated side at frequencies above 0.2Hz in first case, and a general absence of the myographic activity in the right and left SO at frequencies above 0.2Hz after ablating vertical semicircular canals leads to the suggestion that utricle input is dominantly shown in the myographic activity of EOM for tilts at 0.2Hz. Results of the control experiment have also suggested that EOM myographic patterns comprised of both small and large units is common to both the utricular and the semicircular canals reflexes. As the relative contribution of small and large units in the SO firing and the mean phase position of the right and left SO firing was unaffected even after the ablation of semicircular canals, it may be concluded that the main differences in the EOM myographic activity after ablation occur in the general strength of firing. Therefore to determine the control of EOM response in these experiments, changes in the strength of firing may be considered to be of primary significance, although the relative phase of the EOM firing in the roll and pitch planes and at intermediate

angles must also be considered.

When considering the responses of the semicircular canal receptors induced by the tilt, the canals lie in anatomical planes intermediate between the major axes of the body. Therefore tilt in a spatial plane which corresponds to the anatomical plane of a canal produces maximum fluid movement. Tilts in a plane orthogonal to the anatomical plane of the canal produces minimum fluid movement. Between these extremes the strength of this stimulus vector varies as a sine function. Movement in one direction in the plane of maximum sensitivity causes excitation of the receptors in the cristae. Movement in the opposite direction in this plane causes inhibition of firing by reversing the fluid movement across the canal and reduce below a level of spontaneous activity which occurs in the absence of stimulation. Based on this mechanism an algebraic model of the function of semicircular canal was prepared and results obtained during these experiments were compared with this model (model is described in section 5.3.I).

The phase plot and curve for the strength of right S0 response in the intact fish (Fig 5.1) follows the right anterior canal curve in the model (Fig 5.25, A), but compared with the combined effect of all four vertical canals (Fig 5.25.B) the S0 response in the actual recordings is different.

The series of ablation experiments ranged from the ablation of single vertical canal to ablation of all four vertical canals. The ablation of right anterior canal results in 50% reduction in the strength of EOM firing as compared with the intact animal. In the model the summed effects of contralateral intact canals and the intact ipsilateral canal response is different from the observed response in the EOM.

The myographic activity of the right and left SO is significantly reduced after ablating a posterior canal. This effect is unexpected and can not be explained by the model, since input from the intact anterior canal should be strong and as the model predicts there should be a little reduction in the strength of SO firing as a result of this ablation. After the ablation of posterior canal 4 peaks in the discharge of ipsilateral SO were seen at its own transition point and at the transition point of contralateral SO. A similar pattern of the EOM discharge was also seen in the contralateral SO. Results of this operation suggest that where input from the posterior canal is strong on to the contralateral eye response it reduces the size of peak, but even where input from the posterior canal is weak bursts in the ipsilateral SO are reduced which suggest that there may be an inhibitory cross-coupling to output pathways from other canals. Lack of modulation of firing of the canal during tilt may inhibit other outputs but they cause peaks of firing when their input are stronger. Contralateral inhibition within the vestibular neurons located in the lateral vestibular nucleus was first described by De vito et al., (1956). Moruzzi & Pompeiano (1957) and Batini, Moruzzi, Pompeiano (1957) have suggested that vestibular nuclei are subjected to inhibition arising from the contralateral labyrinth by studying postural changes after the interruption of the vestibular nerve.

After the ablation of two anterior canals, myographic activity in the right and left SO is stronger than observed after the ablation of a single anterior canal, while the model has predicted a comparatively weaker activity in the absence of these two canals.

For the ablation of diagonal pair (left anterior and right posterior canal), the model predicts 90° phase shift in the response of right SO which is not seen in the results and the phase of right SO is

the same as seen in the intact fish.

The ablation of an ipsilateral pair of canals has resulted in 90° phase shift in the myographic activity of the left SO which is contradictory to the predictions of model as it predicts a phase shift of 45° only.

In the experiments where only a single vertical canal was left intact, the effects from ipsilateral canals are generally weaker and comparatively stronger activity is elicited in the contralateral EOM. This contradicts the prediction made for the intact animal where ipsilateral effects are strongest.

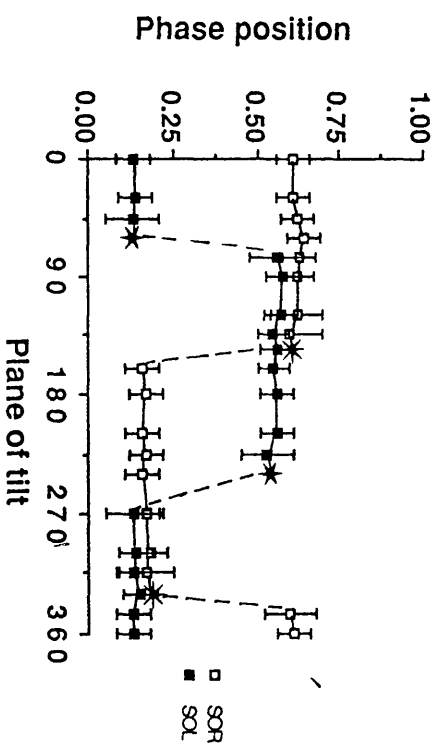
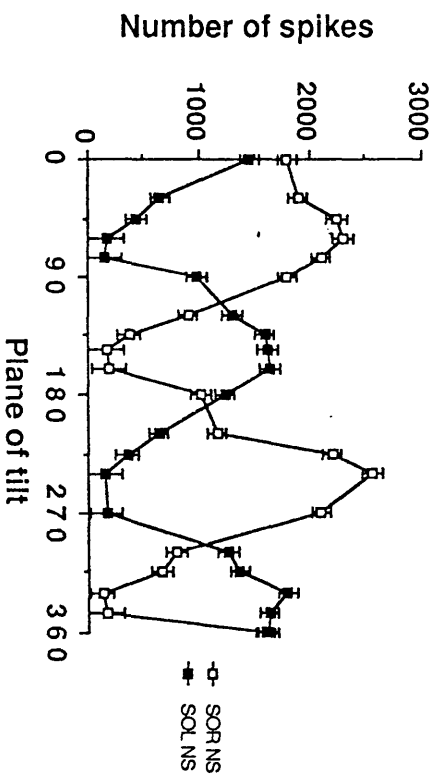
The unexpected pattern of EOM activity as a result of different ablation experiments suggests a complex wiring between different components of the vestibular system. The pattern of myographic activity obtained in the intact fish is indeed similar to that predicted by Lowenstein & Sand (1940) in as far as they made predictions only for the roll and pitch tilts. Experiments on the dogfish show that control to the EOM activity is much more complex and must be affected by central interaction.

In experiments where only one canal was left intact the presence of the myographic activity in the right and left EOM suggests both ipsilateral and contralateral control of this activity by a single intact canal. This control may be achieved by spontaneous activity of the vestibular sensory receptors.

The myographic recordings made in the absence of four vertical canals and unilateral ablation of the utricle also suggest a contralateral control of the EOM activity by the utricle input.

A

0.2HZ



B

0.8HZ

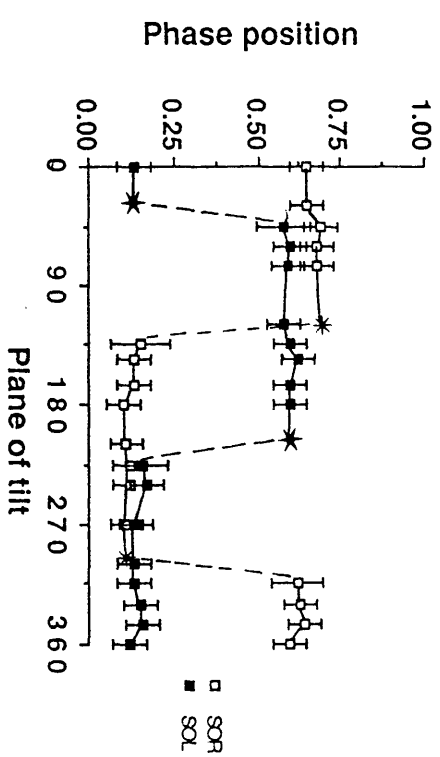
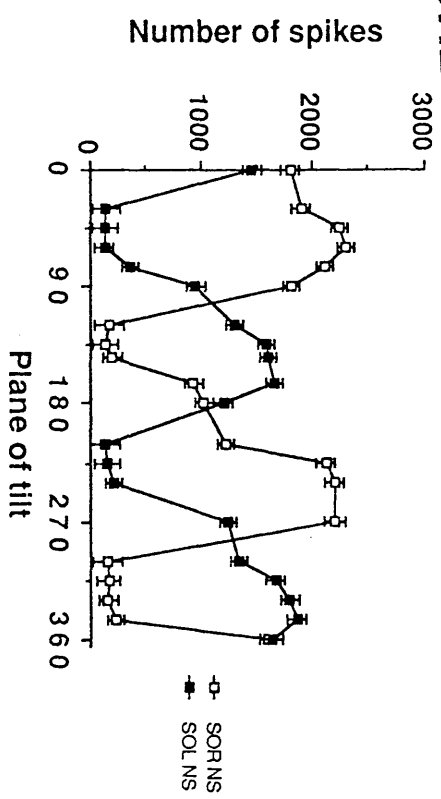


Fig 5.1.A The total number of spikes in the myographic response of the SOR and SOL, summed over ten cycle of sinusoidal tilt plotted against the plane of tilt.

5.1.A.a 0.2Hz

5.1.A.b 0.8Hz

Fig 5.1.B The circular mean values derived from the phase histogram of the SOR and SOL burst plotted against the plane of tilt.

5.1.B.a 0.2Hz

5.1.B.b 0.8Hz

Fig 5.2 The myographic recordings of SOR and SOL in the roll plane in the intact fish.

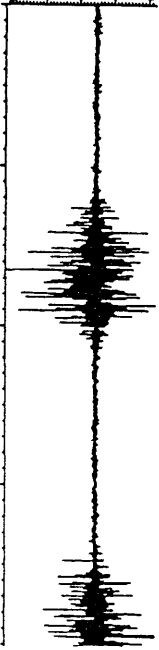
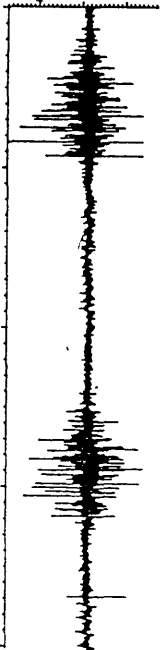
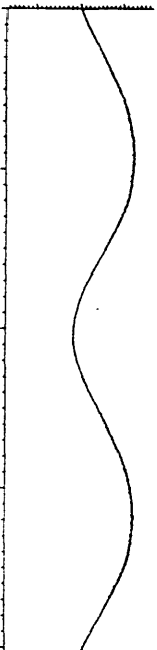
5.2.a 0.2Hz

5.2.b 0.4Hz

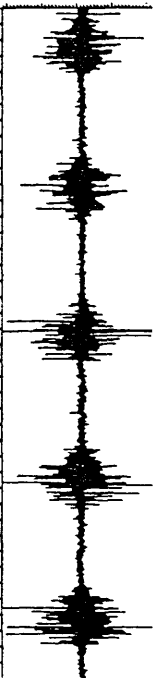
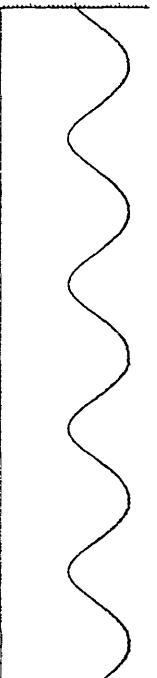
5.2.c 0.6Hz

5.2.d 0.8Hz

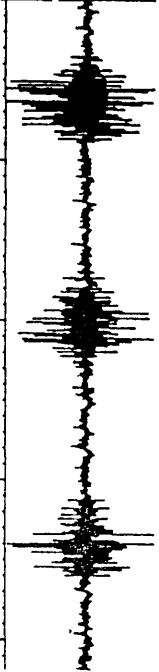
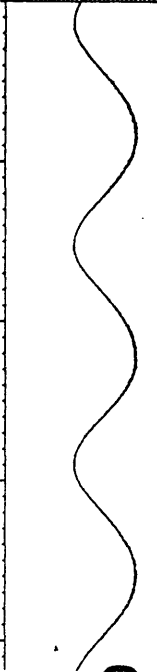
0.2Hz



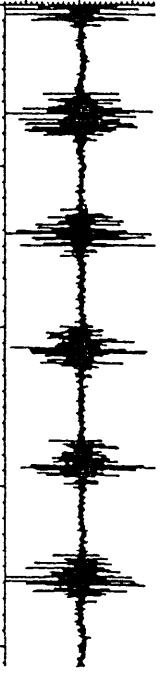
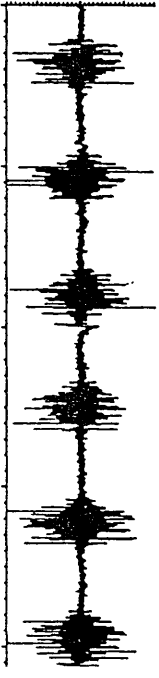
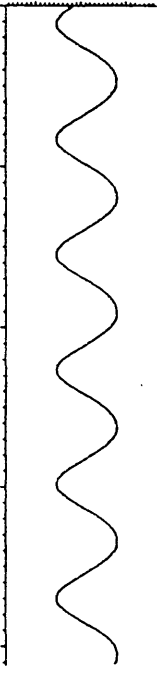
0.6Hz



0.4Hz



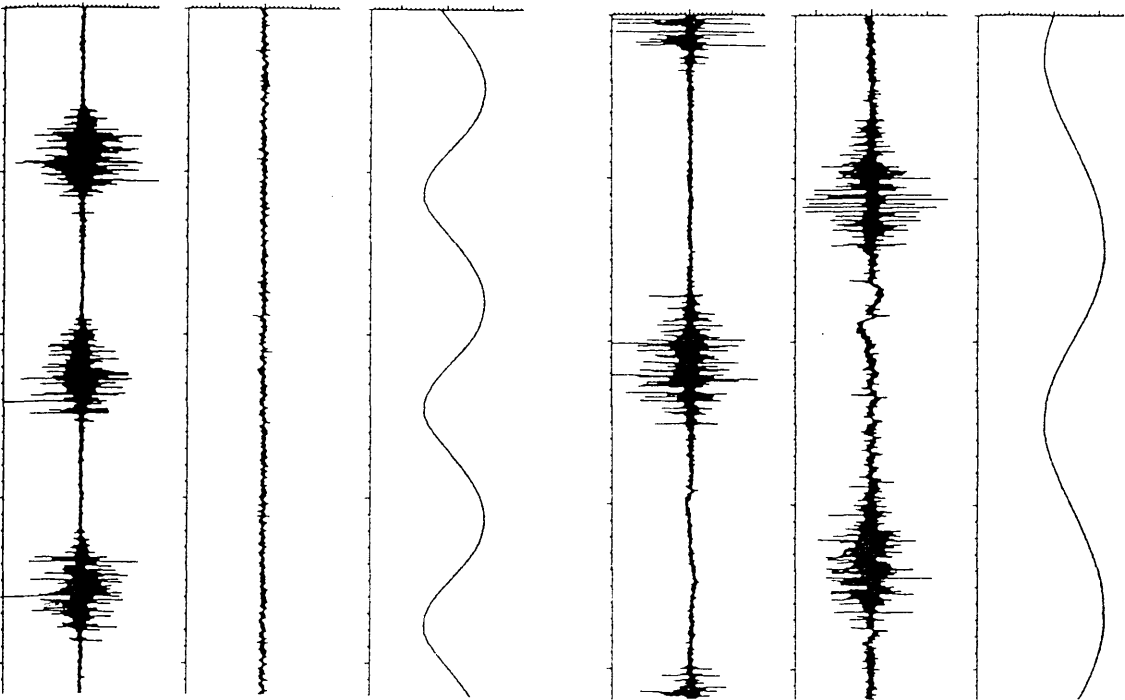
0.8Hz



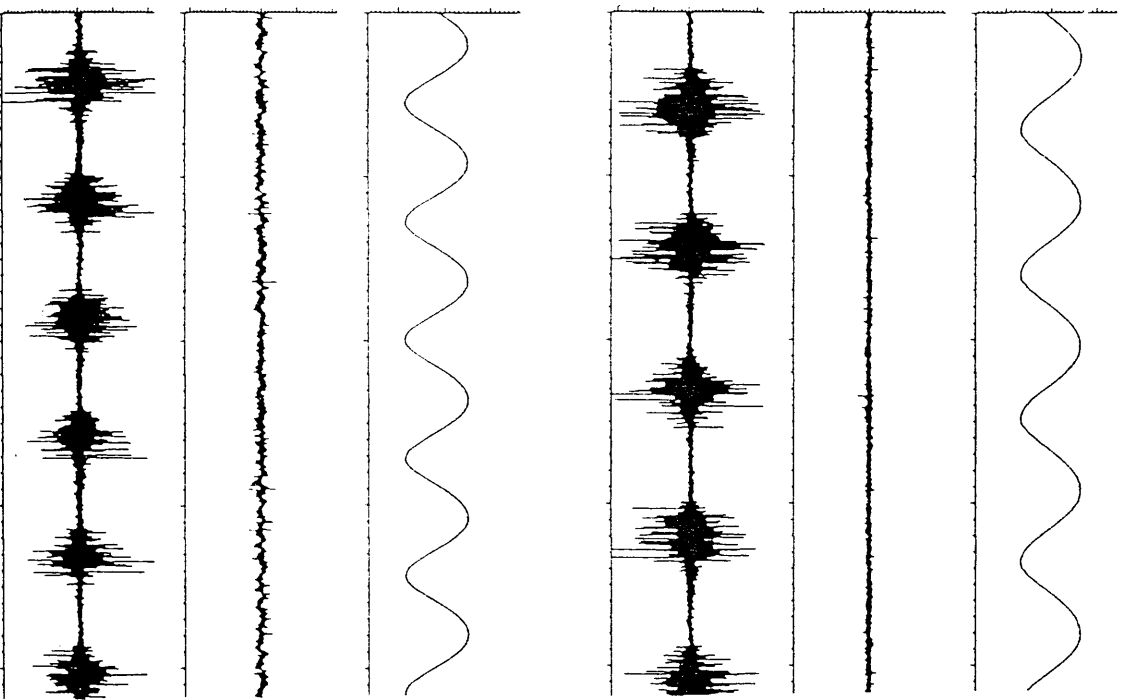
SOR

SOL

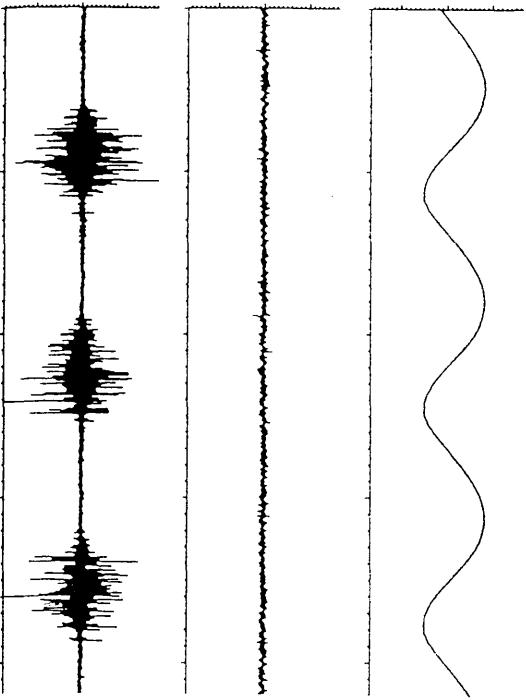
0.2Hz



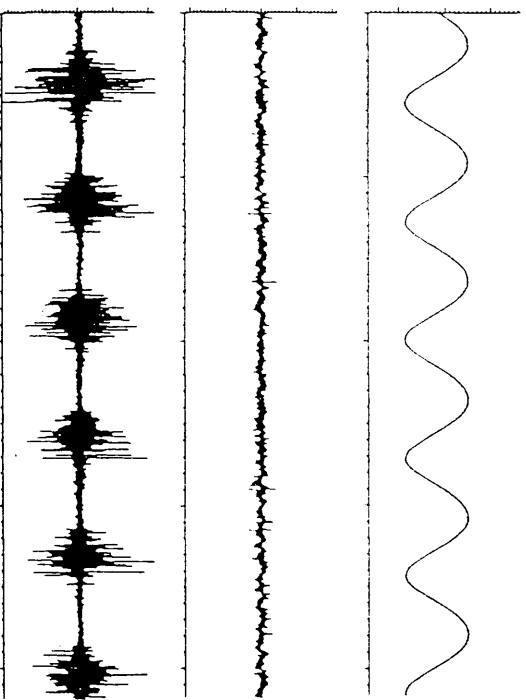
0.6Hz



0.4Hz



0.8Hz



SOL

SOR

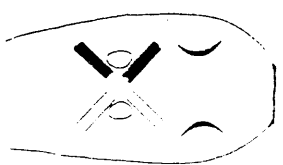


Fig 5.3 The myographic recordings in the SOR and SOL in the roll plane after ablating the left vertical semicircular canals.

5.3.a 0.2Hz

5.3.b 0.4Hz

5.3.c 0.6Hz

5.3.d 0.8Hz

Fig 5.4 The myographic recordings in the SOR and SOL in the roll plane after ablating the vertical semicircular canals of the left and right sides.

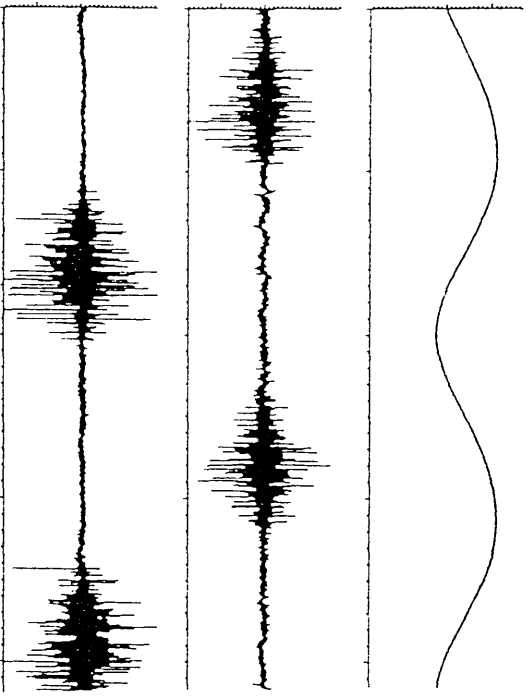
5.3.a 0.2Hz

5.3.b 0.4Hz

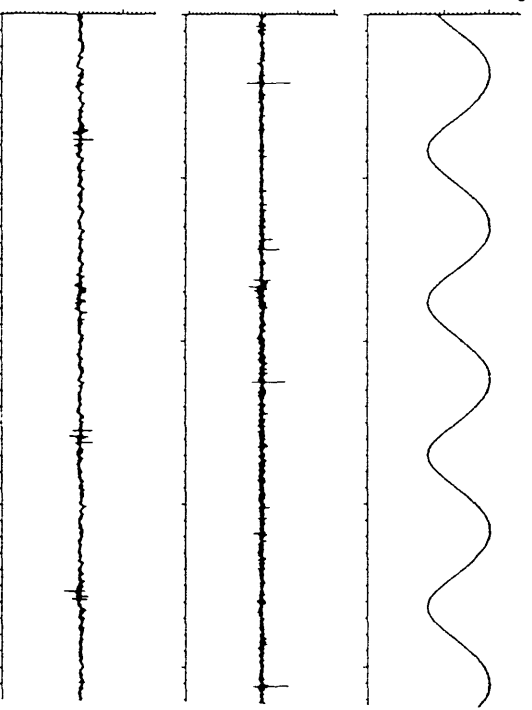
5.3.c 0.6Hz

5.3.d 0.8Hz

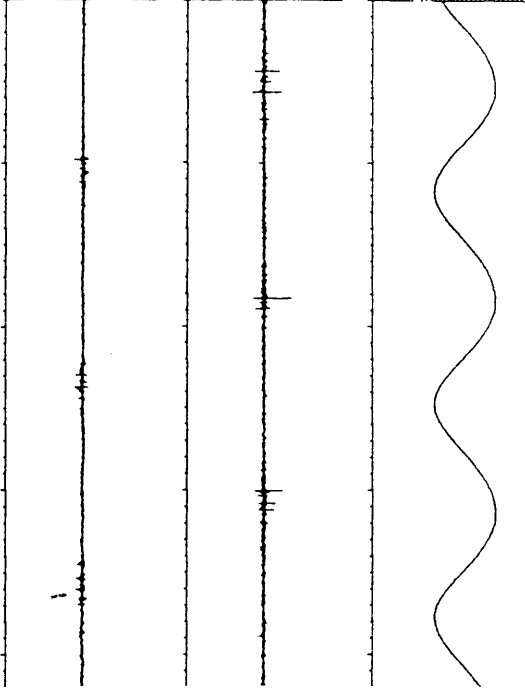
0.2Hz



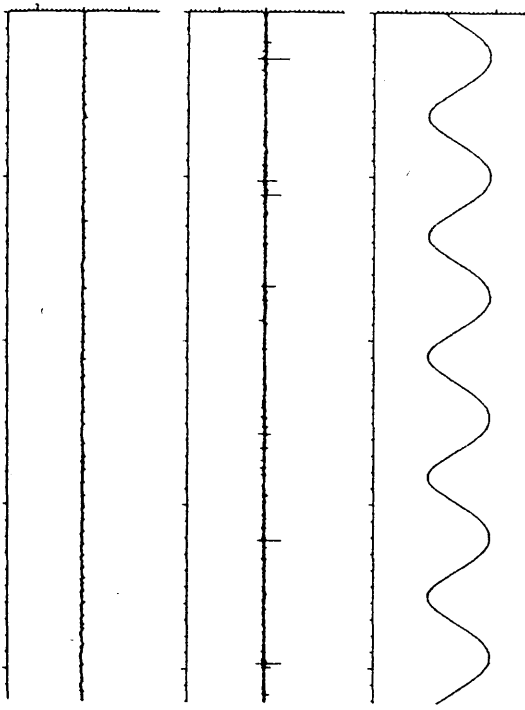
0.6Hz



0.4Hz

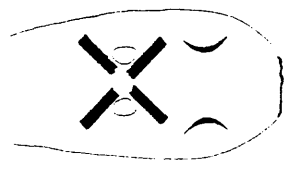


0.8Hz



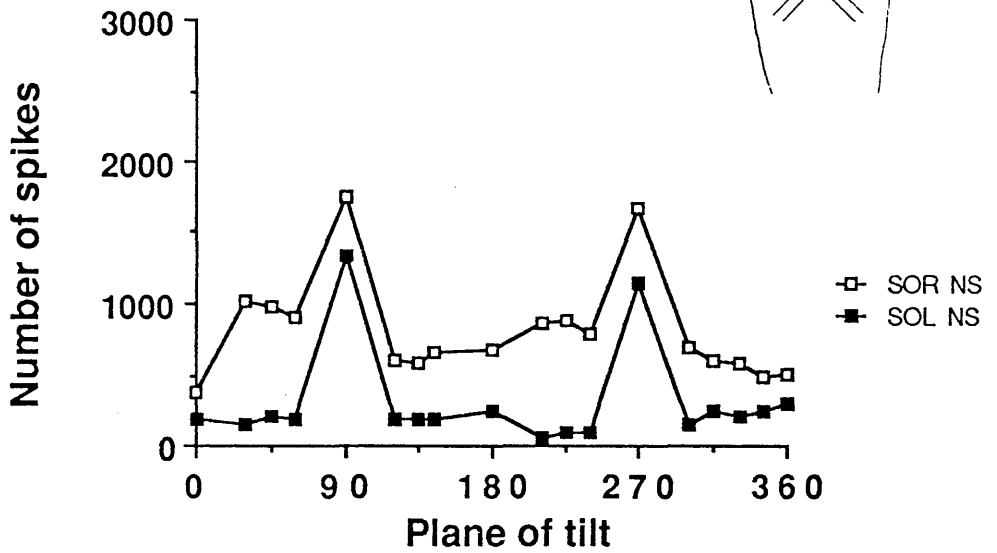
SOL

SOR



LEFT ANTERIOR CANAL ABLATED, SO

A



B

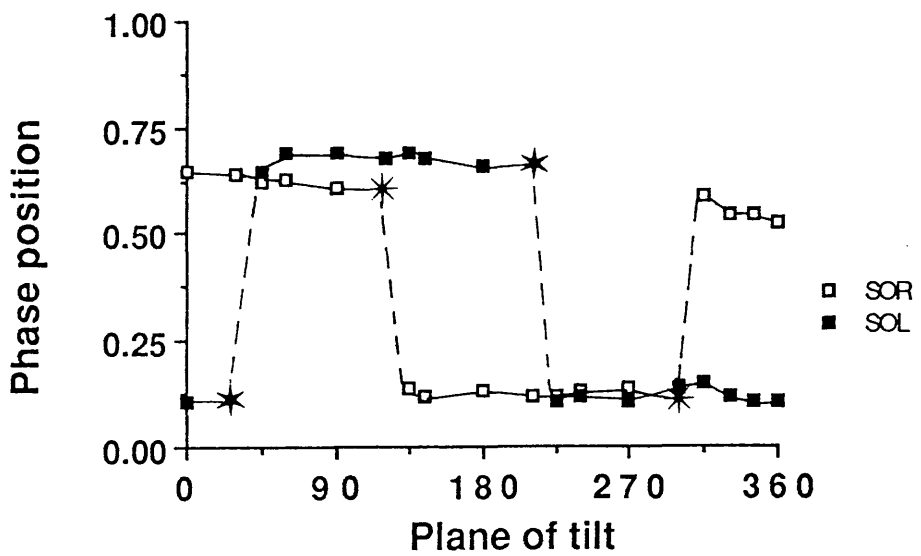


Fig 5.5.A The total number of spikes in the myographic response plotted against the plane of tilt between 0^0 - 360^0 after ablating left anterior vertical canal for tilts at 0.8Hz.

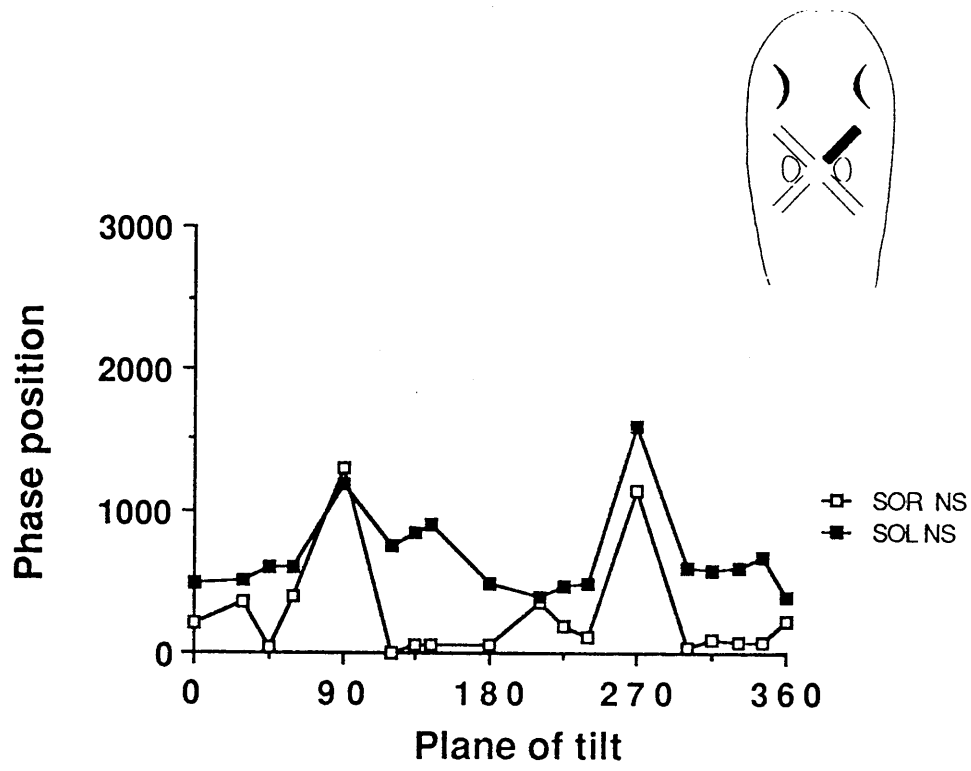
Fig 5.5.B The circular mean value in the phase of SOR and SOL plotted against the plane of tilt after ablating left anterior vertical canal for tilts at 0.8Hz.

Fig 5.6.A The total number of spikes as 5.1.A plotted against the plane of tilt after ablating right anterior vertical canal for tilts at 0.8Hz.

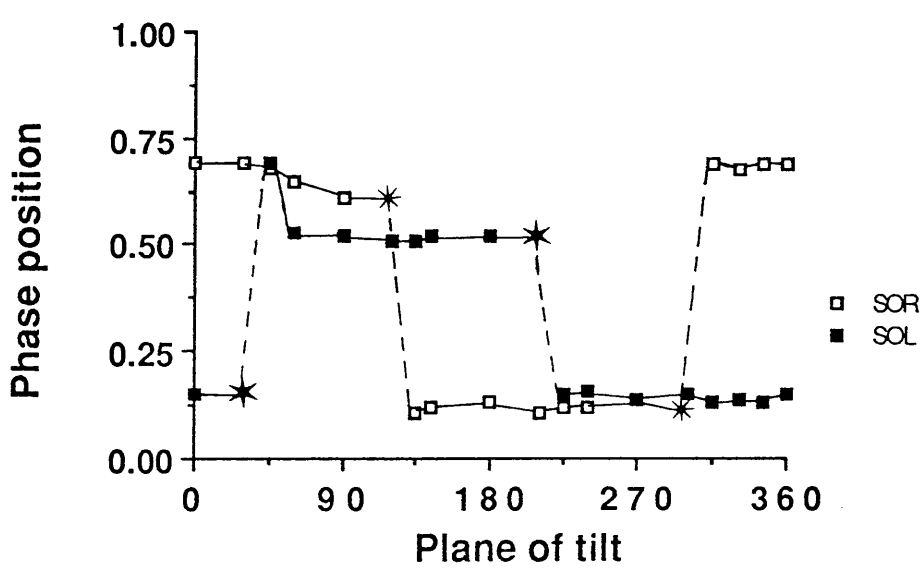
Fig 5.6.B The circular mean value plotted against the plane of tilt after ablating the right anterior vertical canal for tilts at 0.8Hz.

RIGHT ANTERIOR CANAL ABLATED, SO

A

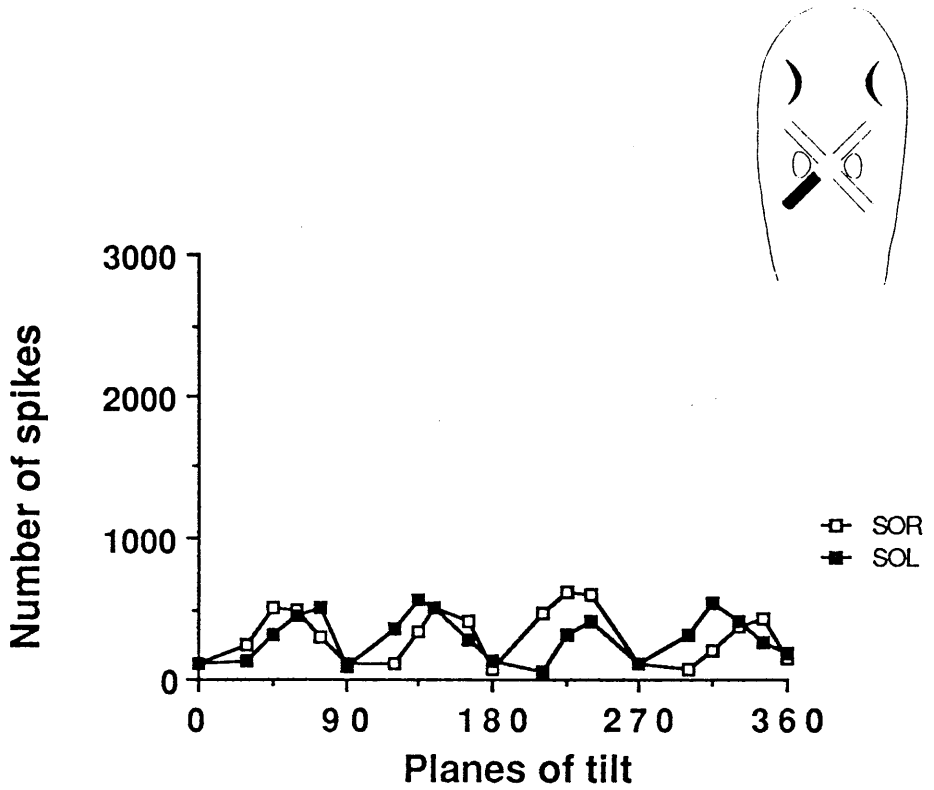


B



LEFT POSTERIOR CANAL ABLATED, SO

A



B

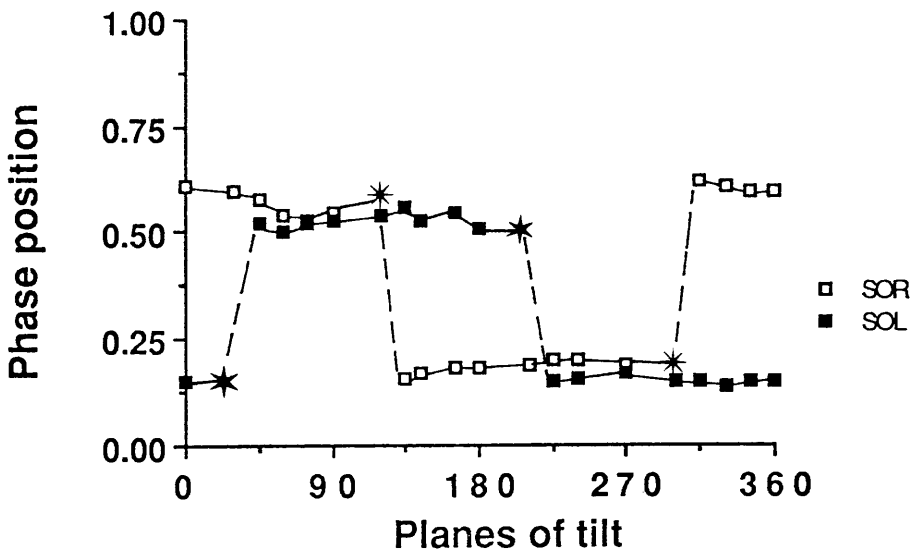


Fig 5.7.A The number of spikes is plotted against the plane of tilt after ablating left posterior vertical canal for tilts at 0.8Hz.

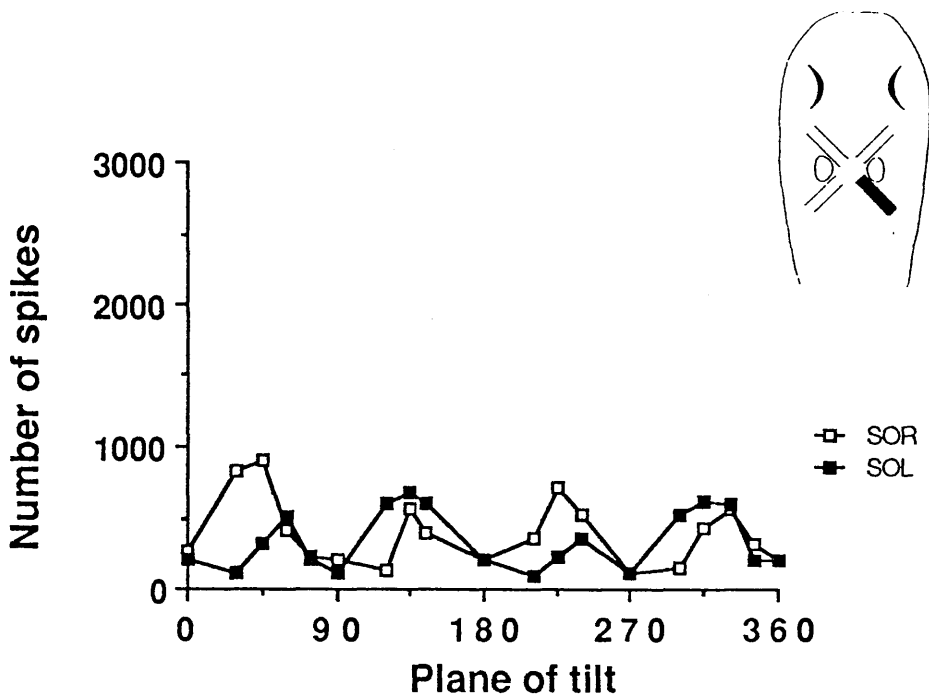
Fig 5.7.B The circular mean value plotted against the plane of tilt after ablating the left posterior vertical canal for tilts at 0.8Hz.

Fig 5.8.A The number of spikes plotted against the plane of tilt after ablating right posterior vertical canal for tilts at 0.8Hz.

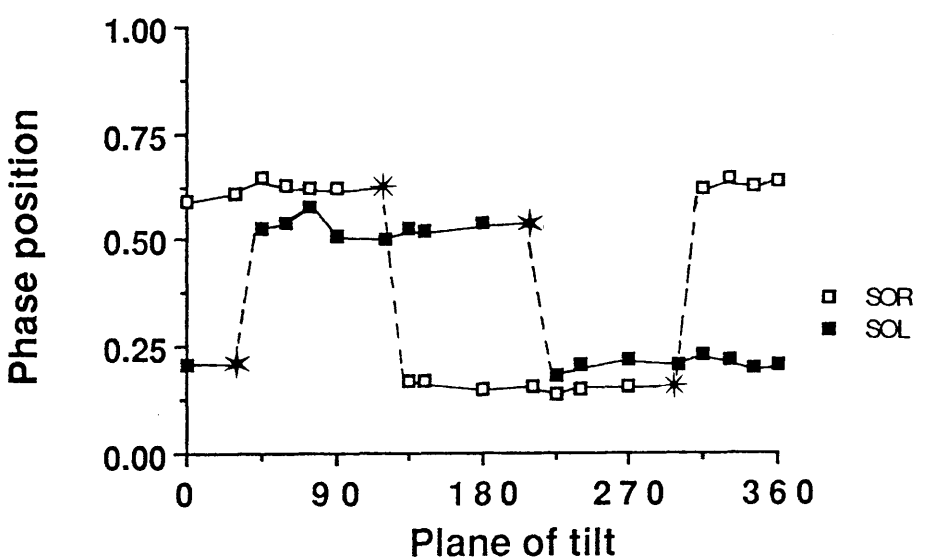
Fig 5.8.B The circular mean value is plotted against plane of tilt after ablating right posterior vertical canal for tilts at 0.8Hz.

RIGHT POSTERIOR CANAL ABLATED, SO

A

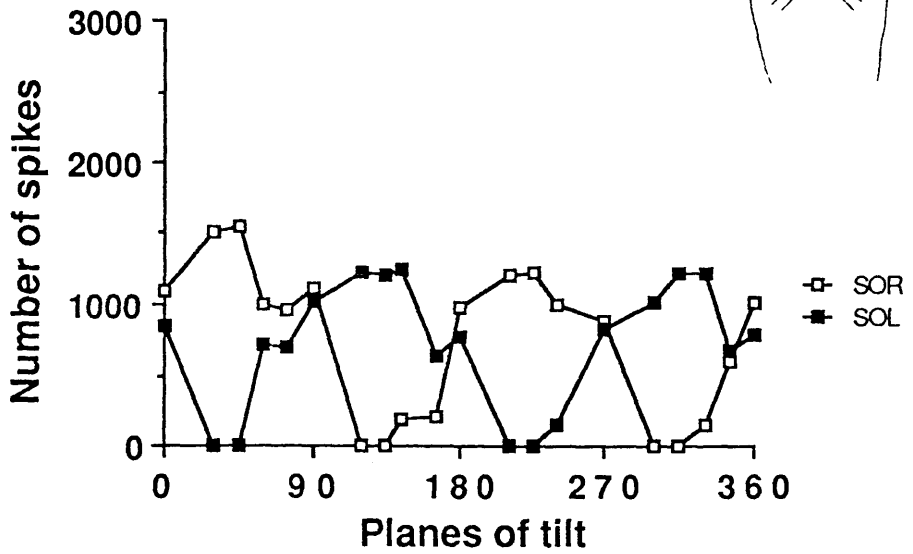


B



TWO ANTERIOR CANALS ABLATED, SO

A



B

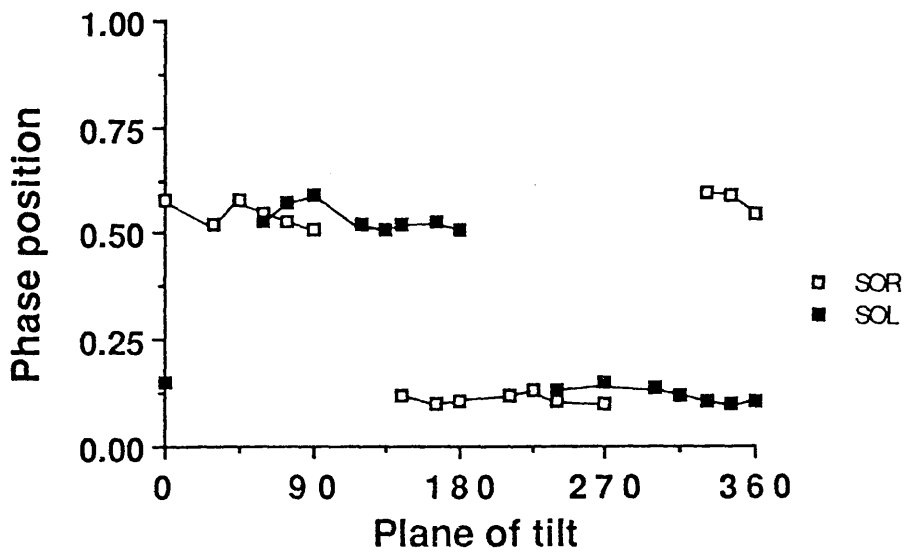


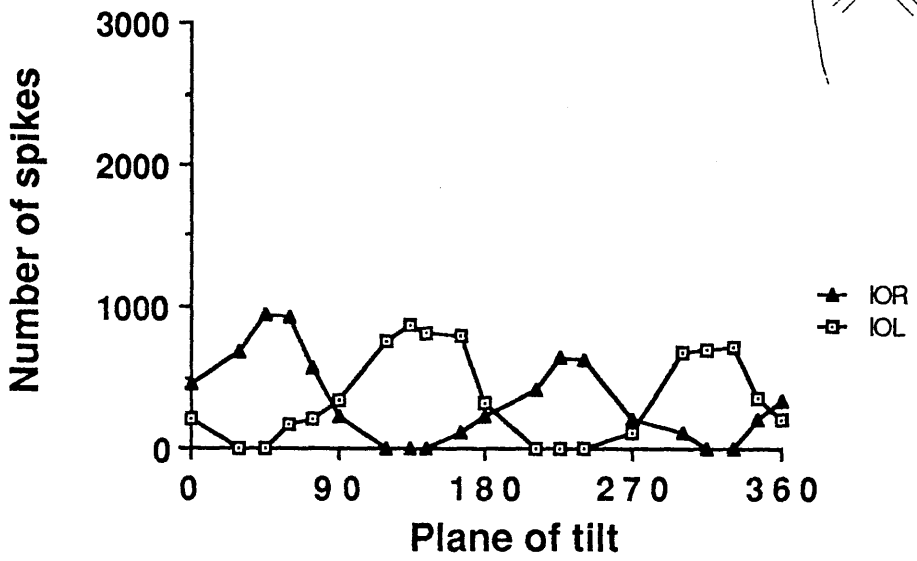
Fig 5.9.A The number of spikes plotted against plane of tilt after ablating two anterior vertical canals for tilts

Fig 5.10.A The number of spikes plotted against plane of tilt after ablating two anterior vertical canals for tilts at 0.8Hz.

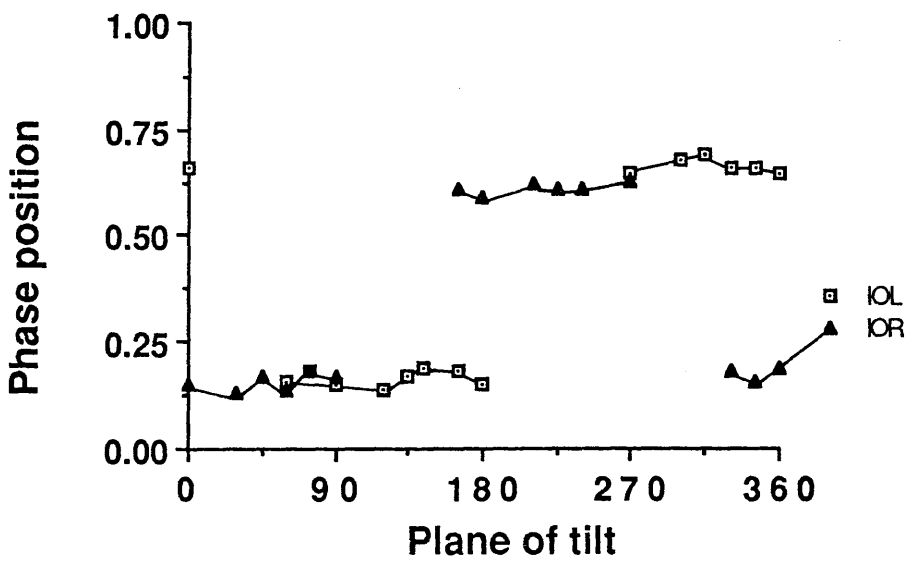
Fig 5.10.B The circular mean value is plotted against plane of tilt after ablating two anterior vertical canals for tilts at 0.8Hz.

TWO ANTERIOR CANALS ABLATED, IO

A

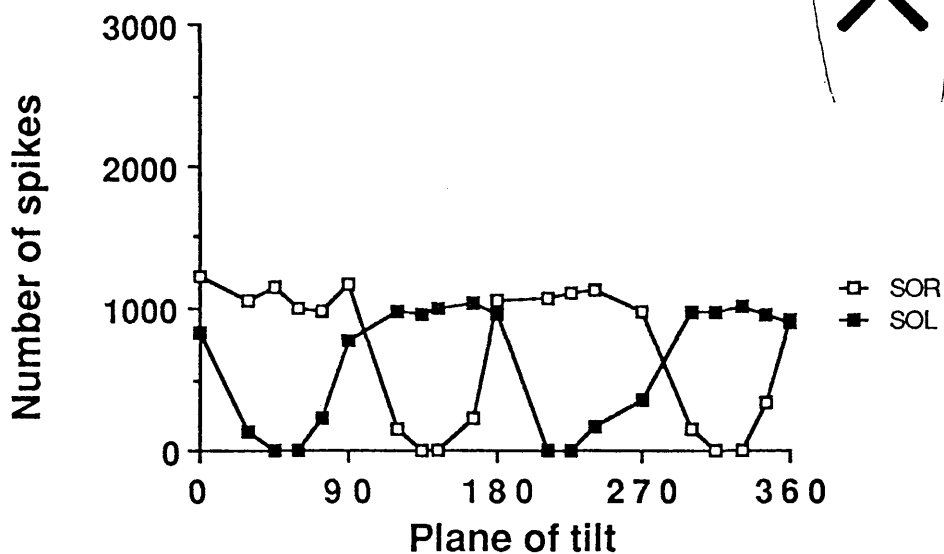


B



TWO POSTERIOR CANALS ABLATED, SO

A



B

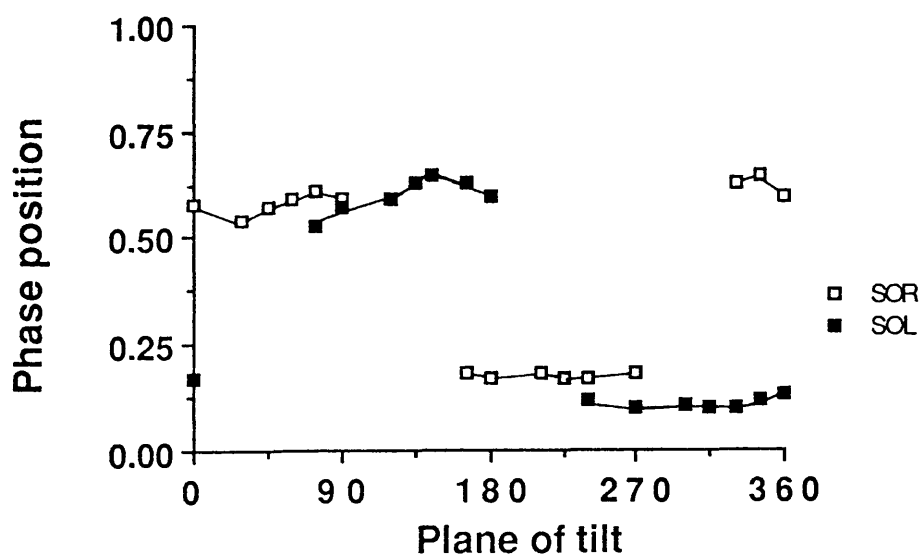


Fig 5.11.A The number of spikes is plotted against the plane of tilt after abalting two posterior vertical canals for tilts at 0.8Hz.

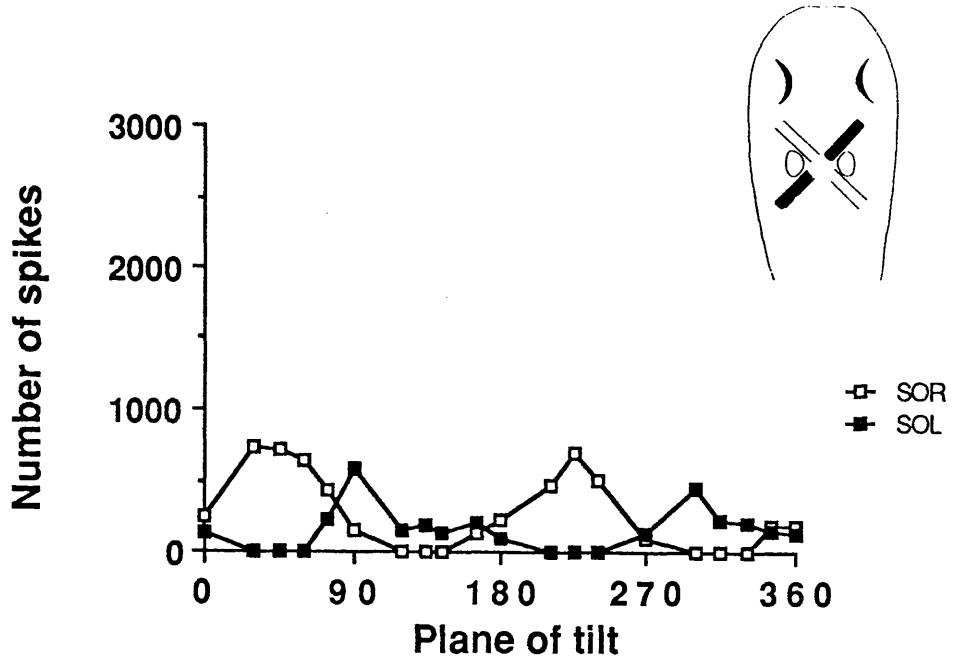
Fig 5.11.B The circular mean value is plotted against plane of tilt after ablating two posterior vertical canals for tilts at 0.8Hz.

Fig 5.12.A The number of spikes is plotted against plane of body tilts after ablating diagonal (left anterior and right posterior) pair of vertical canals for tilts at 0.8Hz.

Fig 5.12.B The circular mean value is plotted against plane of body tilt after ablating diagonal (left anterior and right posterior) pair of vertical canals for tilts at 0.8Hz.

DIAGONAL PAIR OF CANALS ABLATED, SO

A



B

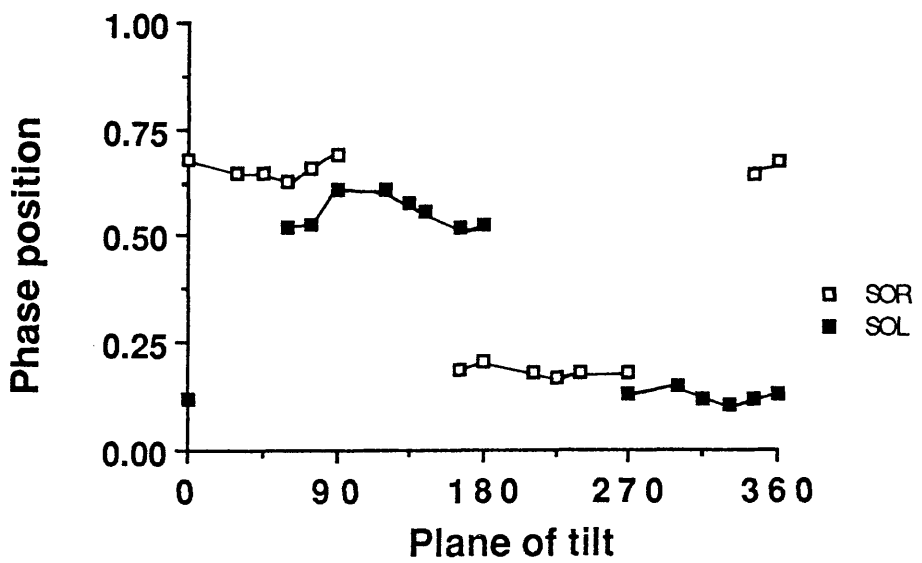
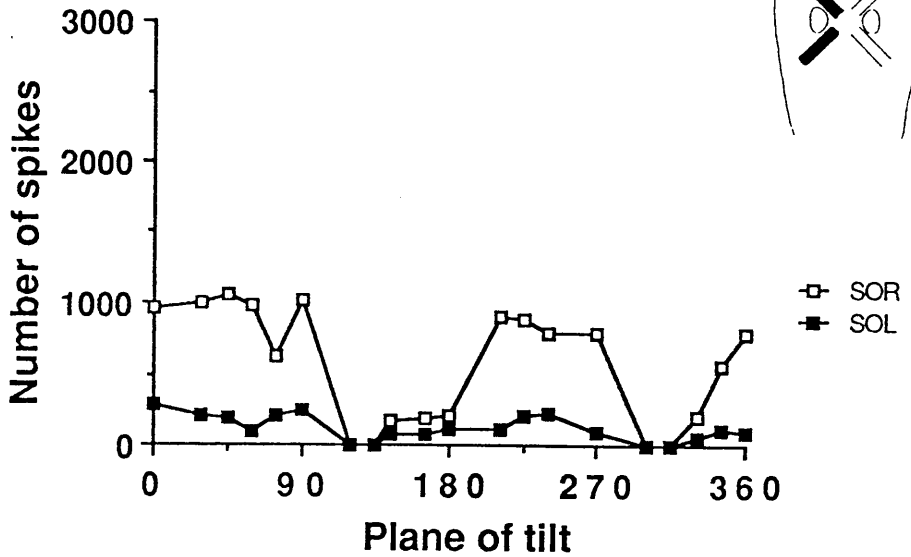


Fig 5.13.A The number of spikes is plotted against the plane of body tilt after abalting left ipsilateral pair of vertical canals for tilts at 0.8Hz.

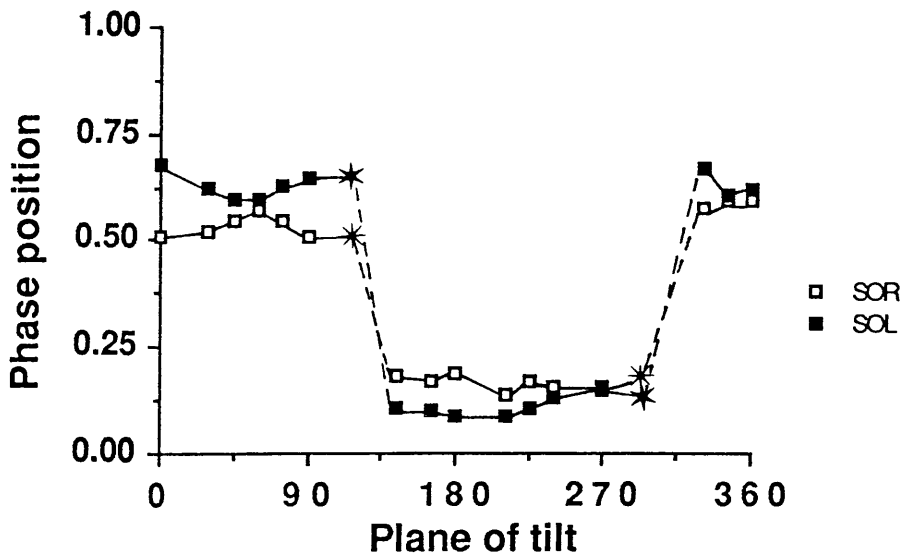
Fig 5.13.B The circular mean value is plotted against the plane of body tilt after abalting left ipsilateral pair of vertical semicircular canals for tilts at 0.8Hz.

LEFT IPSILATERAL PAIR OF CANALS ABLATED

A



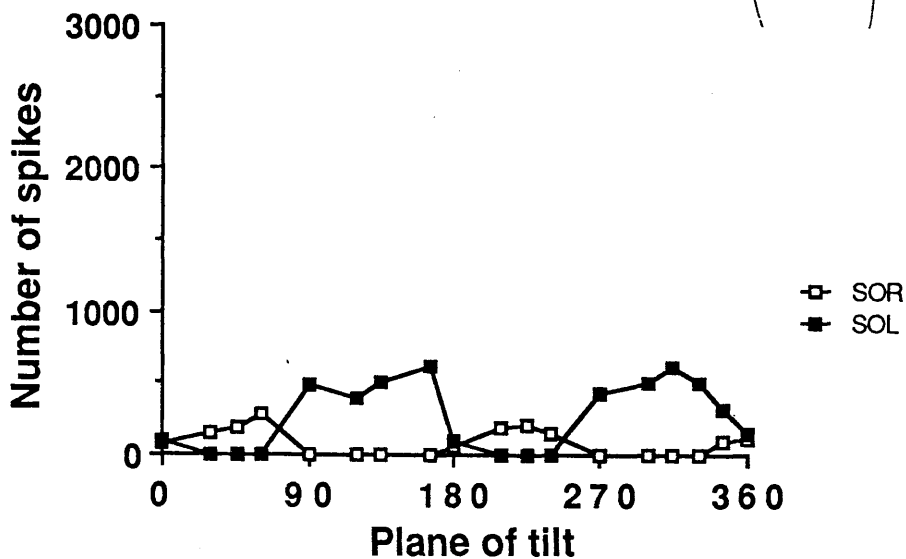
B



LEFT ANTERIOR AND TWO POSTERIOR CANALS ABLATED, SO



A



B

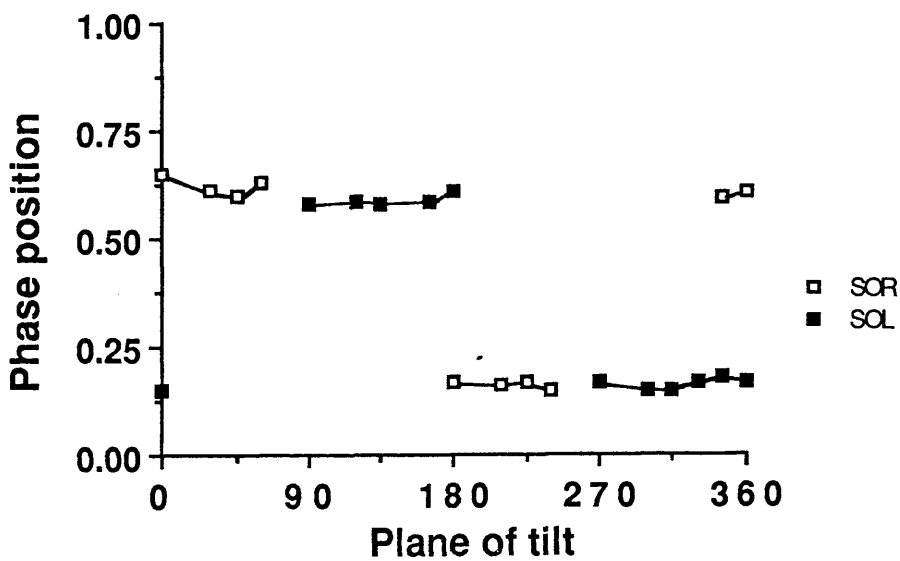


Fig 5.14.A The number of spikes is plotted against the plane of body tilt after ablating left anterior and two posterior vertical canals for tilts at 0.8Hz.

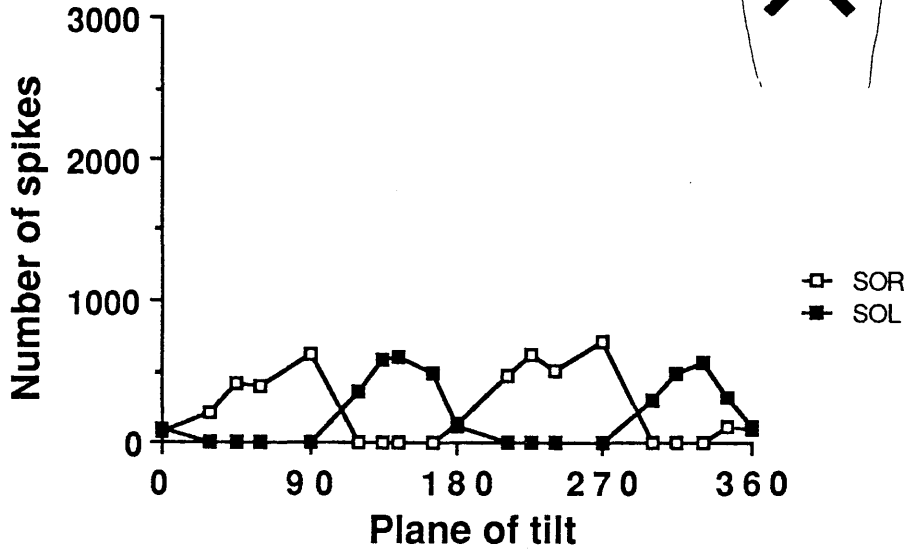
Fig 5.14.B The circular mean value is plotted against the body tilts after ablating left anterior and two posterior vertical canals for tilts at 0.8Hz.

Fig 5.15.A The number of spikes is plotted against the plane of body tilt after ablating right anterior and two posterior vertical semicircular canals for tilts at 0.8Hz.

Fig 5.15.B The circular mean value is plotted against the plane of body tilt after ablating right anterior and two posterior vertical canals for tilts at 0.8Hz.

RIGHT ANTERIOR AND TWO POSTERIOR CANALS ABLATED, SO

A



B

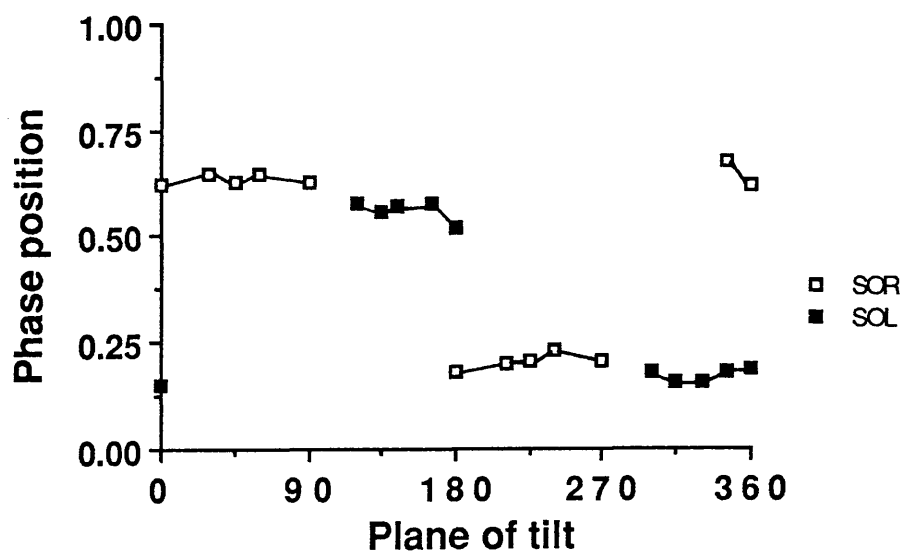


Fig 5.16.A The number of spikes plotted against the plane of body tilt after ablating left anterior and two posterior vertical canals for tilts at 0.8Hz.

Fig 5.16.B The circular mean value is plotted against the plane of body tilts after ablating left anterior and two posterior vertical canals for tilts at 0.8Hz.

LEFT ANTERIOR AND TWO POSTERIOR CANALS ABLATED, SO

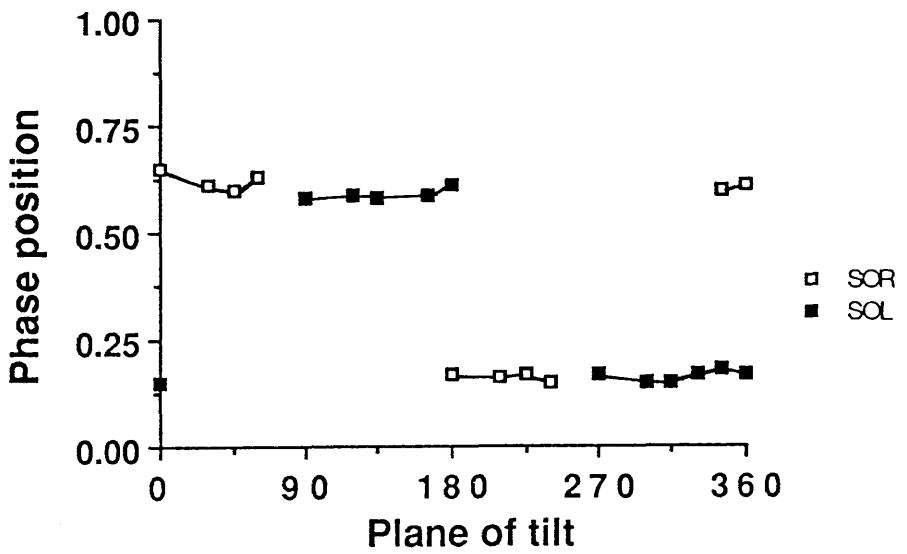
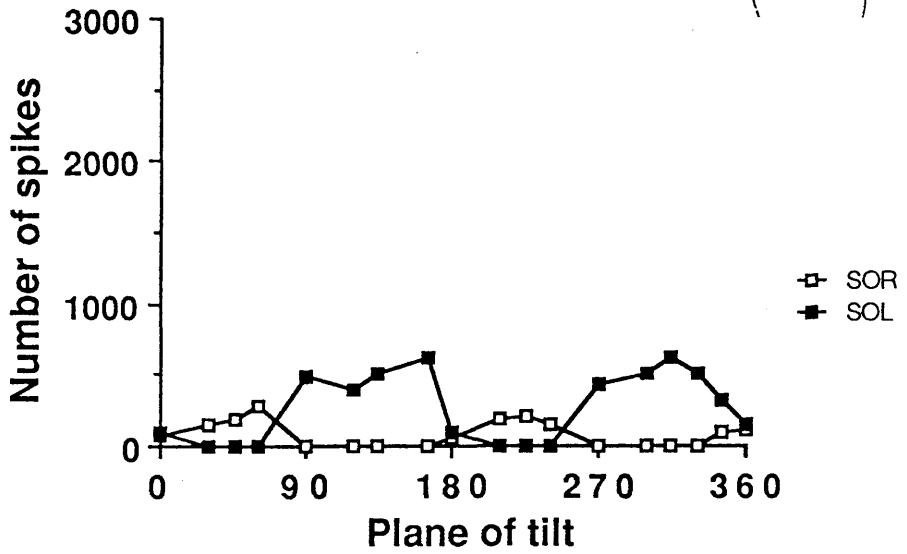
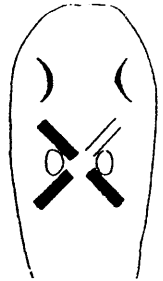
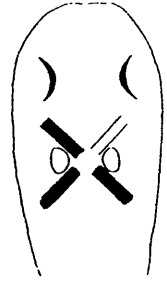


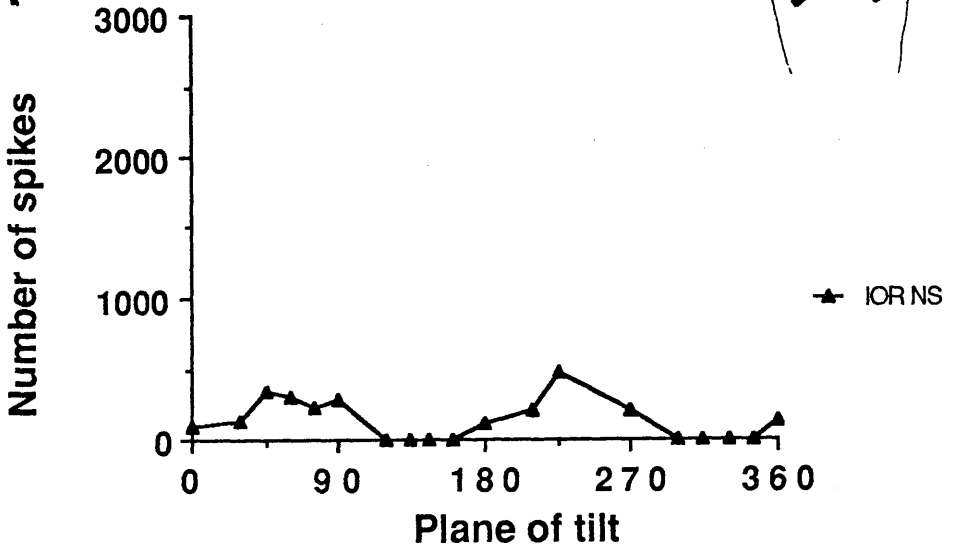
Fig 5.17.A The number of spikes is plotted against the plane of body tilts after ablating left anterior and two posterior vertical canals for tilts at 0.8Hz.

Fig 5.17.B The circular mean value is plotted against the plane of body tilt after abalting left anterior and two posterior vertical canals for tilts at 0.8Hz.

LEFT ANTERIOR AND TWO POSTERIOR CANALS ABLATED, IO



A



B

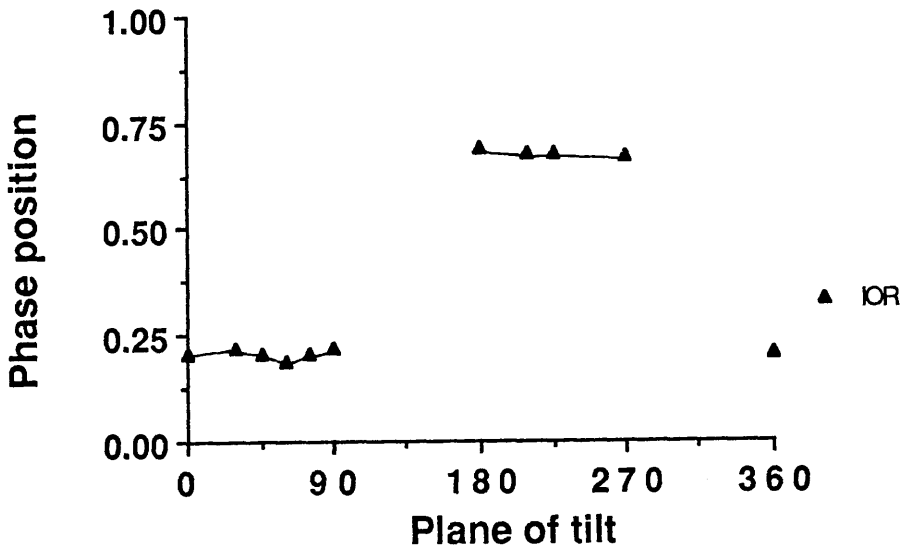
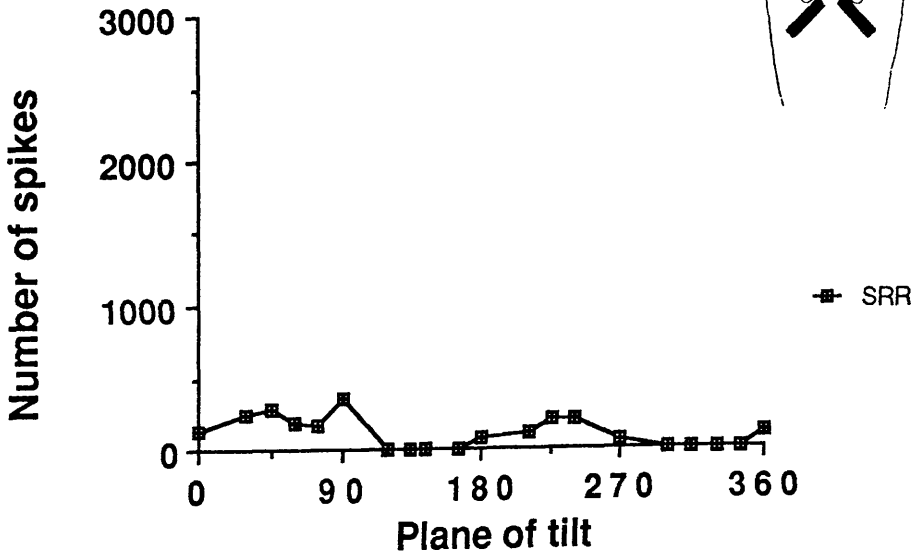


Fig 5.18.A The number of spikes is plotted against the plane of body tilt after ablating two anterior and left posterior canal for tilts at 0.8Hz.

Fig 5.18.B The circular mean value is plotted against the plane of body tilt after abalting two anterior and left posterior canals for tilts at 0.8Hz.

LEFT ANTERIOR AND TWO POSTERIOR CANALS ABLATED, SR

A



B

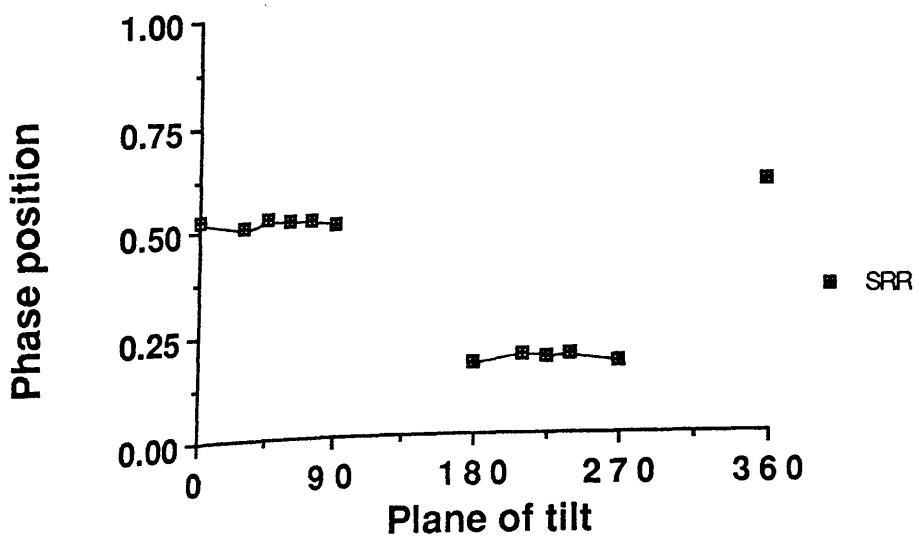
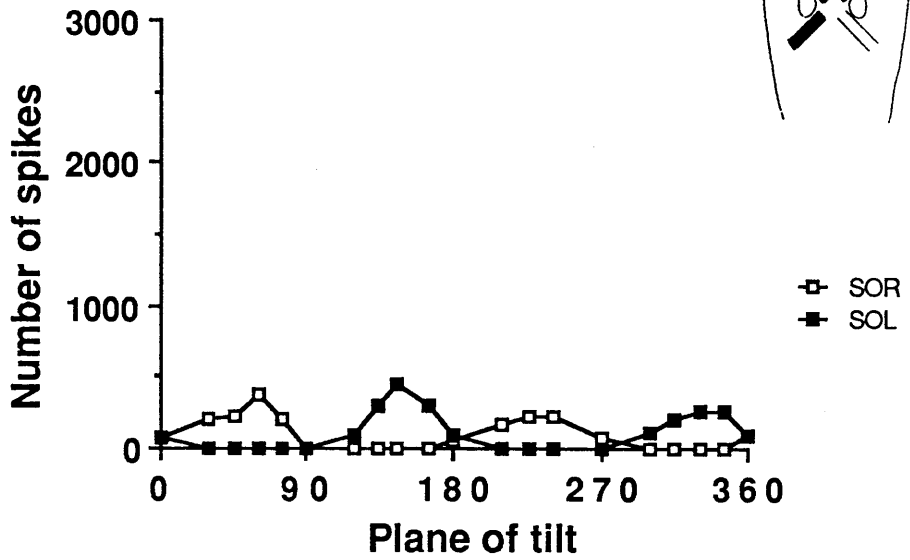


Fig 5.19.A The number of spikes is plotted against the plane of body tilt after abalting two anterior and right posterior vertical canals for tilts at 0.8Hz.

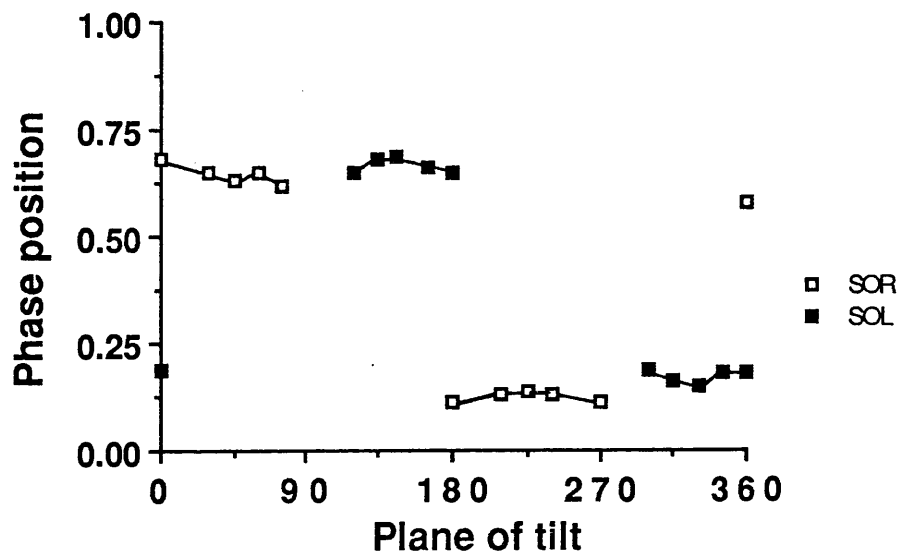
Fig 5.19.B The circular mean value is plotted against the plane of body tilt after ablating two anterior and right posterior canals.

LEFT POSTERIOR AND TWO ANTERIOR CANALS ABLATED, SO

A

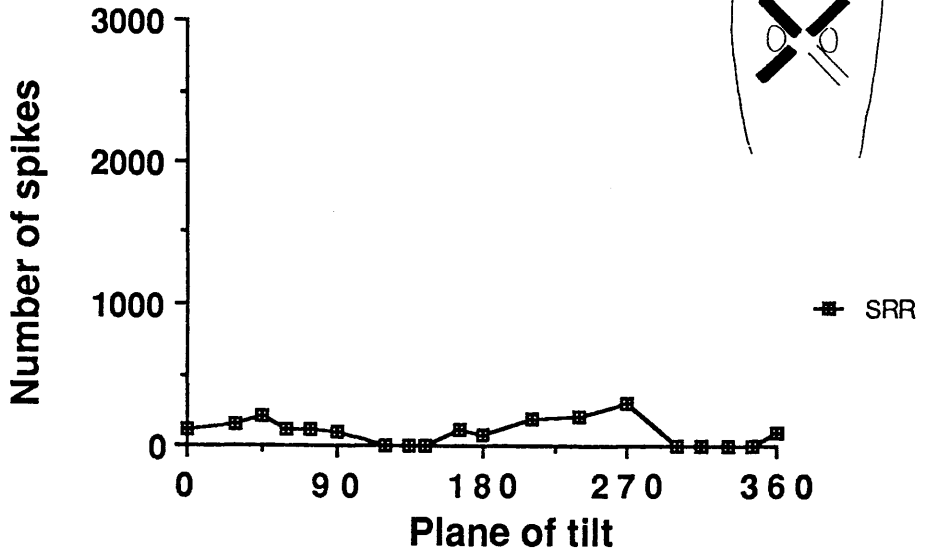


B



LEFT POSTERIOR AND TWO ANTERIOR CANALS ABLATED, SR

A



B

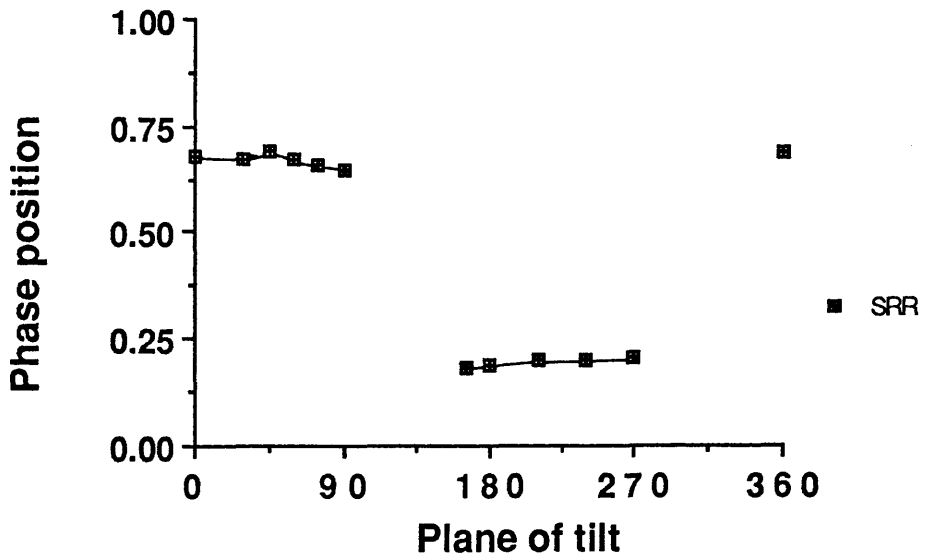


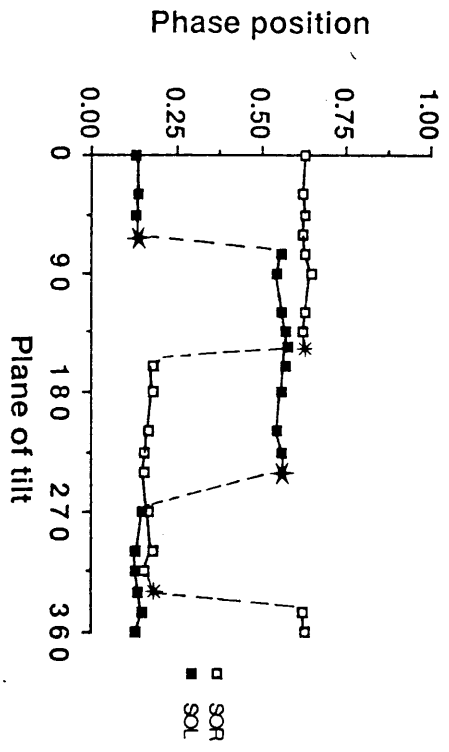
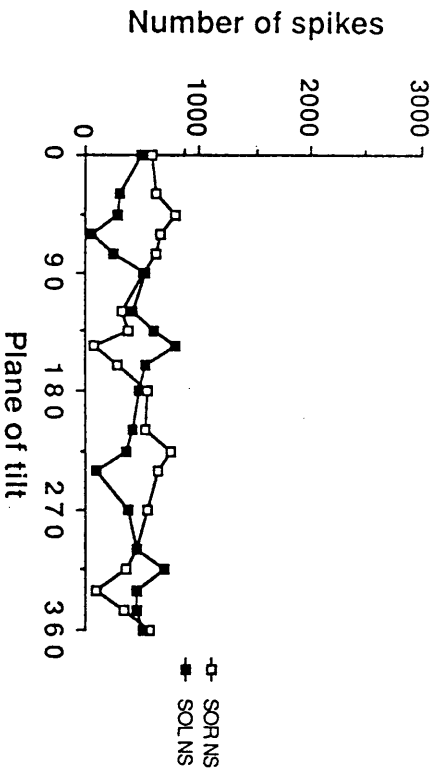
Fig 5.20.A The number of spikes is plotted against the plane of body tilt after ablating two anterior and left posterior vertical canals for tilts at 0.8Hz.

Fig 5.20.B The circular mean value is plotted against the plane of body tilt after abalting two anterior and left posterior vertical canals for tilts at 0.2Hz.

Fig 5.21.A The number of spikes is plotted against the plane of body tilt after ablating four vertical canals for tilts at 0.2Hz and 0.8Hz.

Fig 5.21.B The circular mean value is plotted against the plane of body tilt after abalting all four vertical canals for tilts at 0.2Hz and 0.8Hz.

0.2Hz



0.8Hz

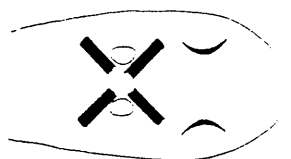
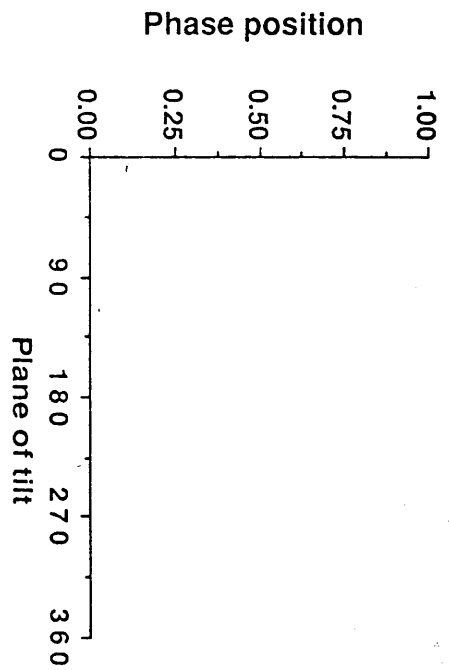
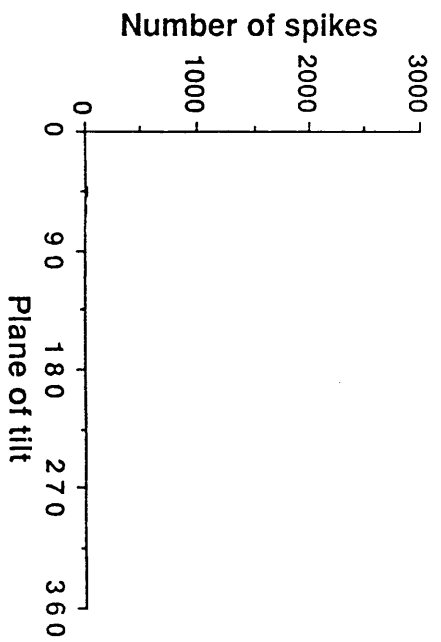
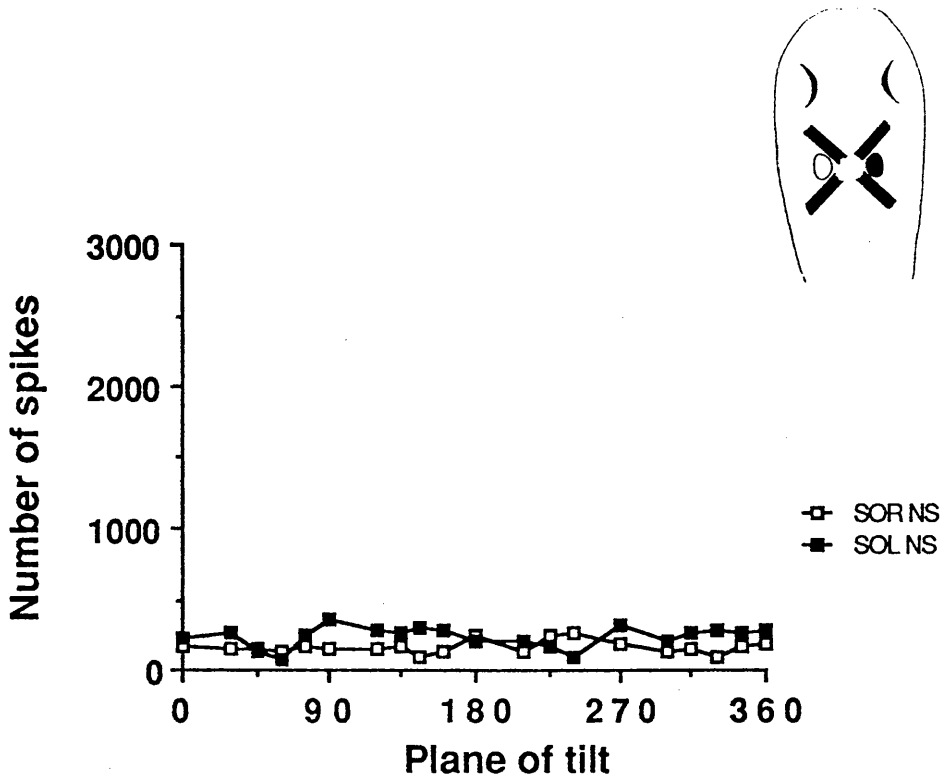


Fig 5.22.A The number of spikes is plotted against the plane of body tilt after abalting four vertical canals and the utriculus of right side for tilts at 0.2Hz.

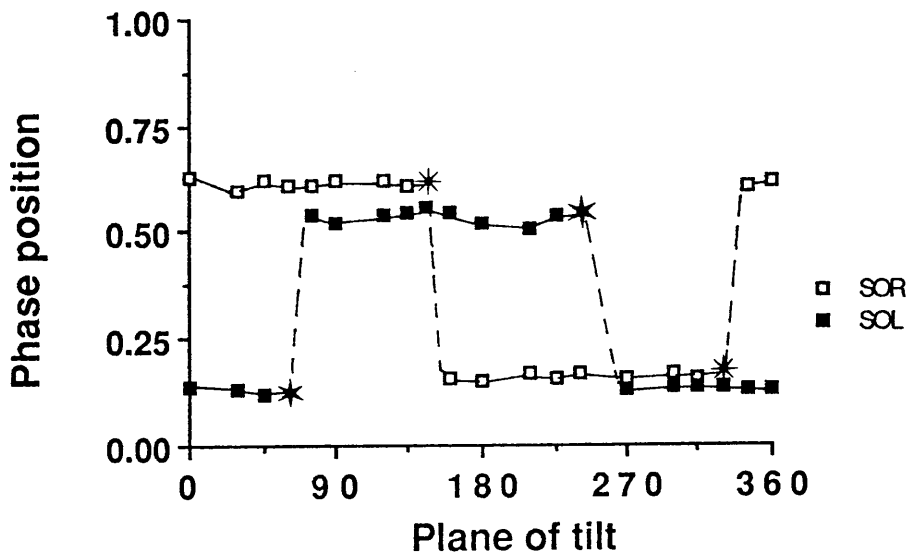
Fig 5.22.B The circular mean value is plotted against the plane of body tilt after ablating four vertical canals and the utriculus of right side for tilts at 0.8Hz.

VERTICAL SEMICIRCULAR CANALS AND RIGHT UTRICULUS ABLATED, SO

A

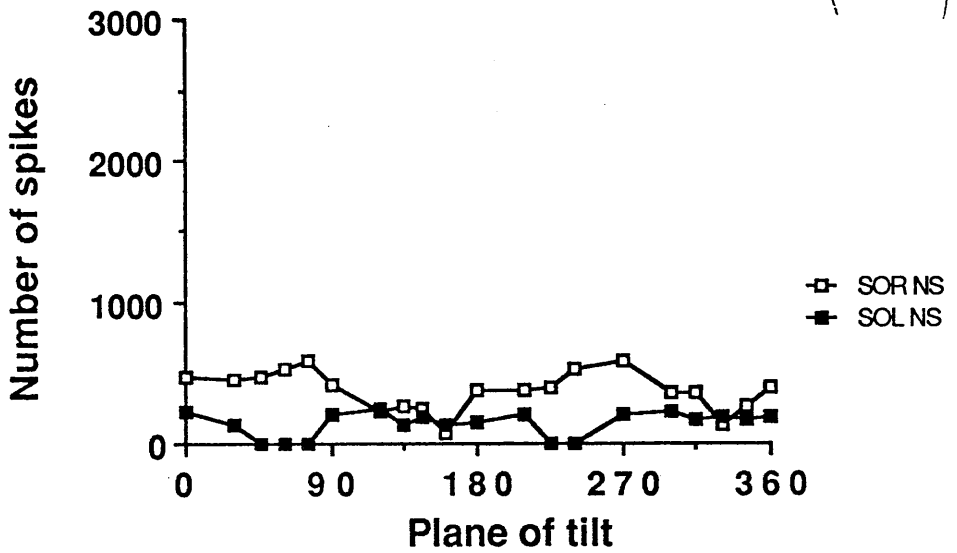
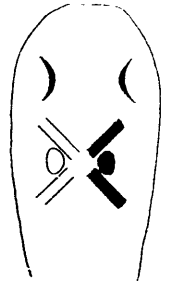


B



VERTICAL SEMICIRCULAR CANALS AND UTRICULUS OF RIGHT SIDE ABLATED, SO

A



B

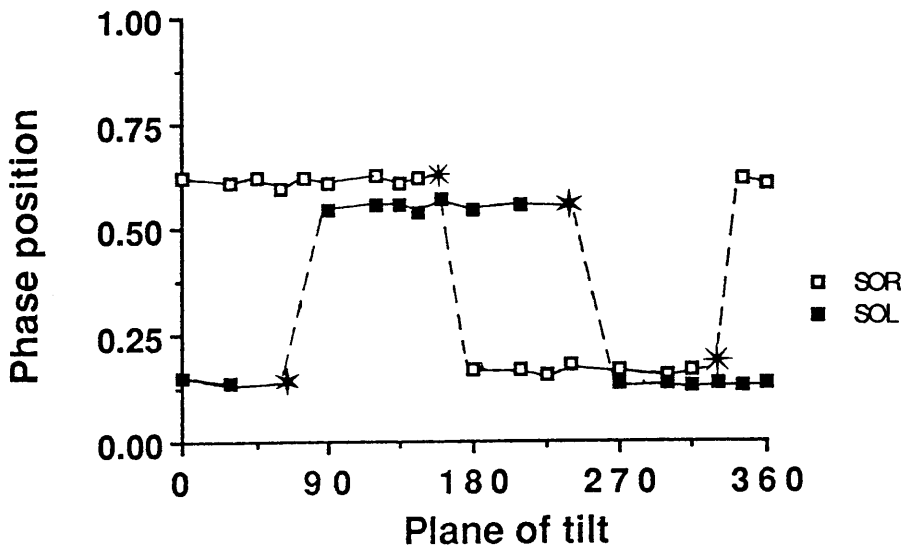


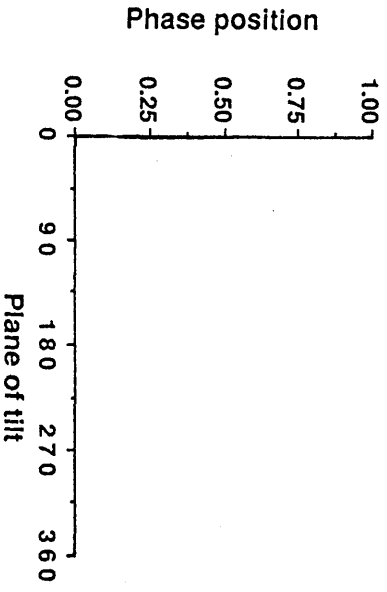
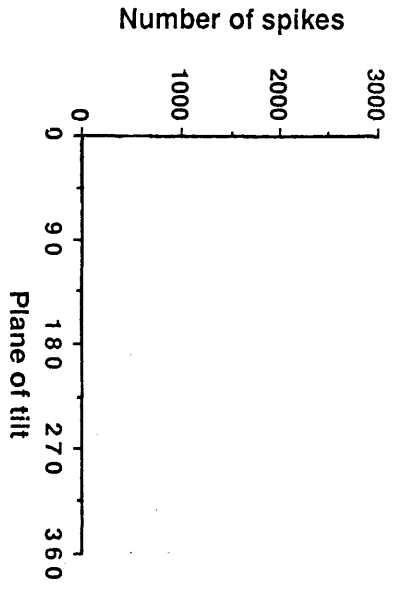
Fig 5.23.A The number of spikes is plotted against the plane of body tilt after abalting anteriorr and posterior vertical canals and the utriculus of right side for tilts at 0.8Hz.

5.23.B The circular mean value is plotted against the plane of body tilt after ablating anterior and posterior vertical canals and the utriculus of right side.

Fig 5.24.A The number of spikes plotted against the plane of body tilt after ablating all four vertical canals and the utriculi of both sides for tilts at 0.2Hz and 0.8Hz.

Fig 5.24.B The circular mean value plotted against the plane of body tilt after ablating four vertical canals and the utriculi of both sides for tilts at 0.2Hz and 0.8Hz.

0.2Hz



0.8Hz

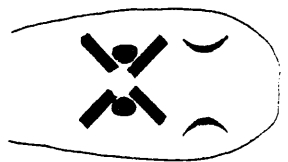
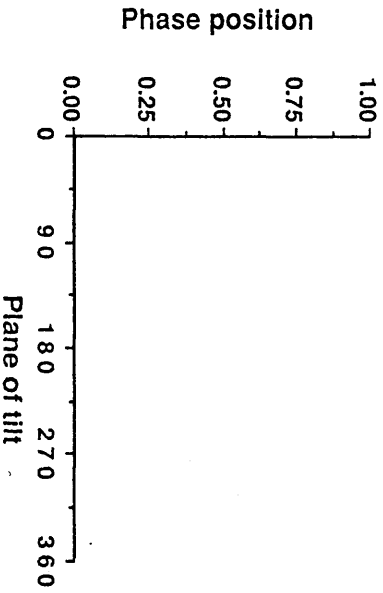
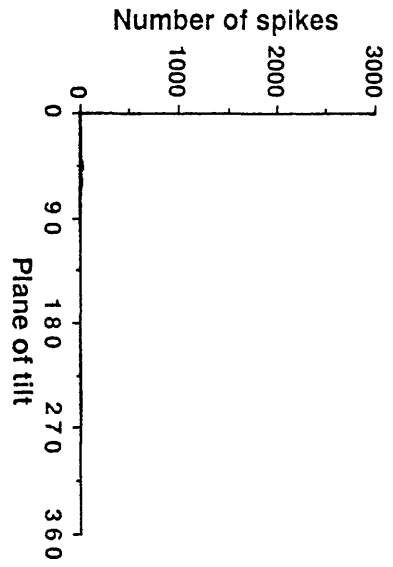


Fig 5.25

In the algebraic model of vertical semicircular canals the input strength of canals is plotted against the plane of tilt. Properties of the model are described in the text (section 5.3.I).

A. Input strength of four vertical canals in the intact fish.

B. Resultant curve of the combined input strength of each vertical canal in 5.25.A.

C. Curve obtained after ablating left anterior and right posterior vertical canals.

D. Resultant curve obtained after ablating right ipsilateral pair of canals.

E. Resultant curve after ablating left ipsilateral pair of canals.

F. Resultant curve after ablating two anterior vertical canals.

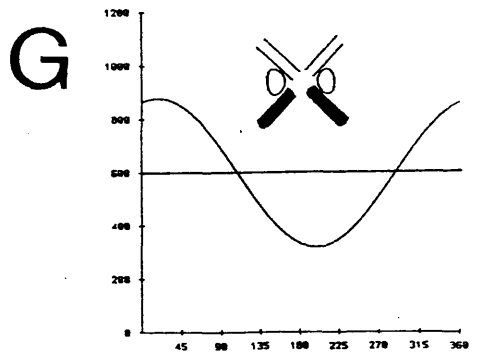
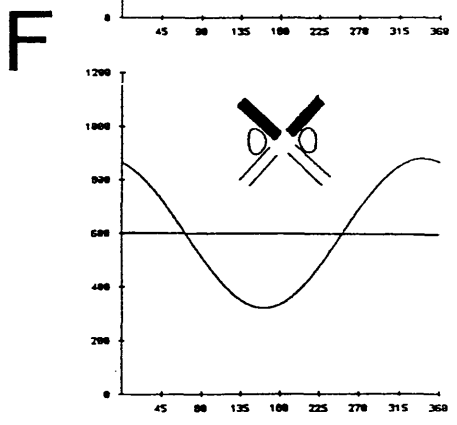
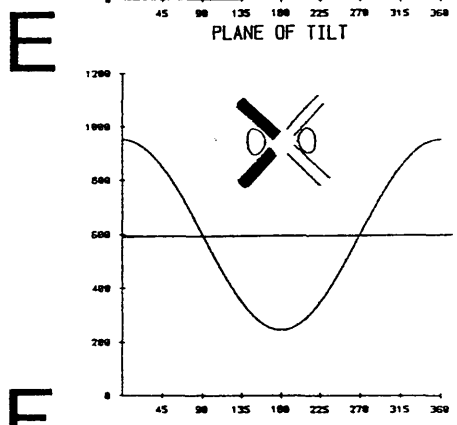
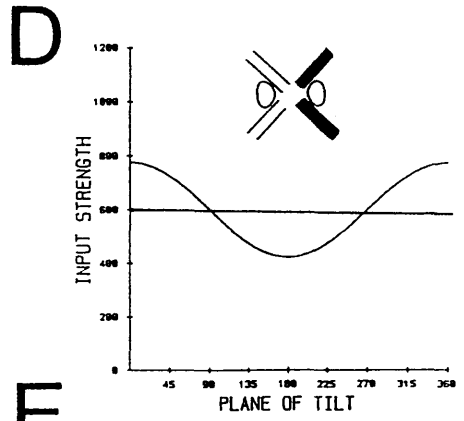
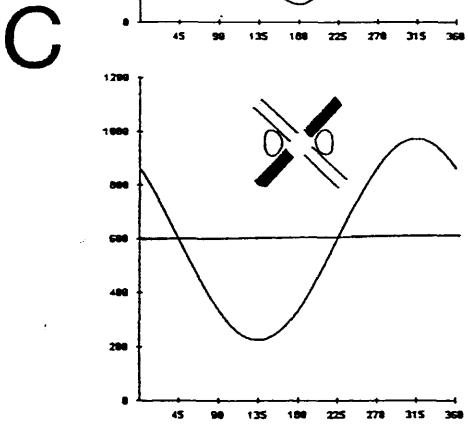
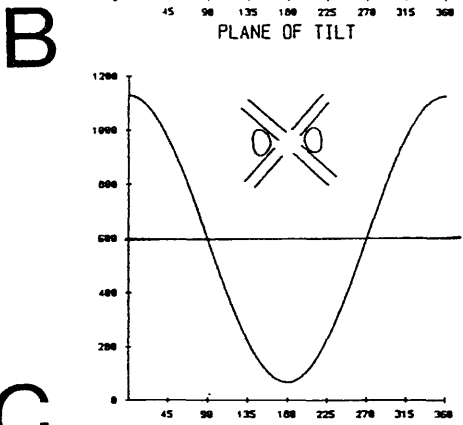
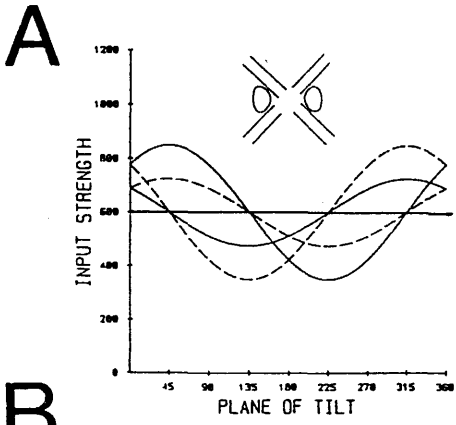
G. Resultant curve after ablating two posterior vertical canals.

RA = Right anterior

RP = Right posterior

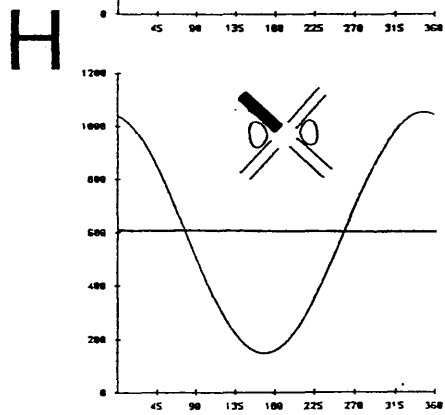
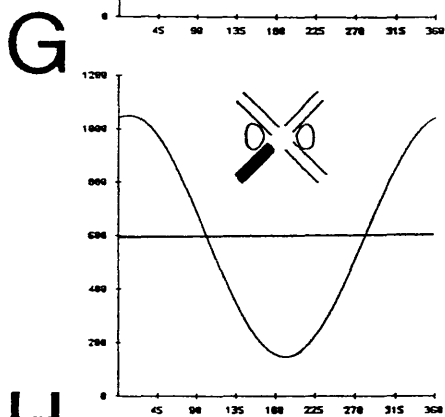
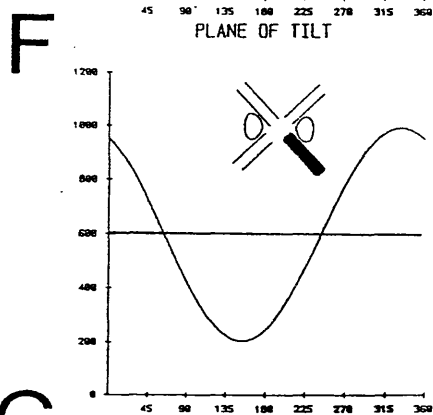
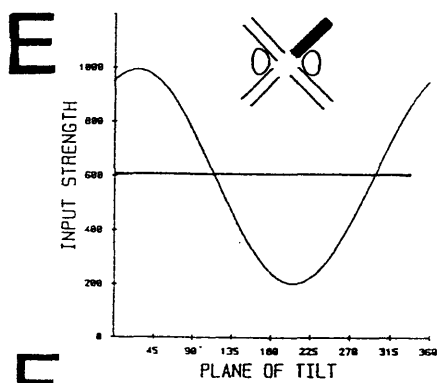
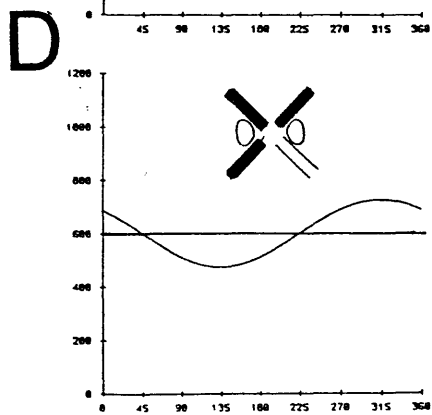
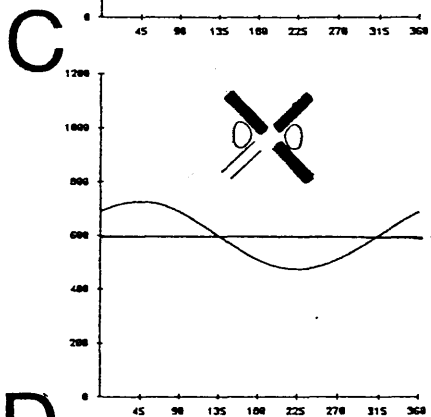
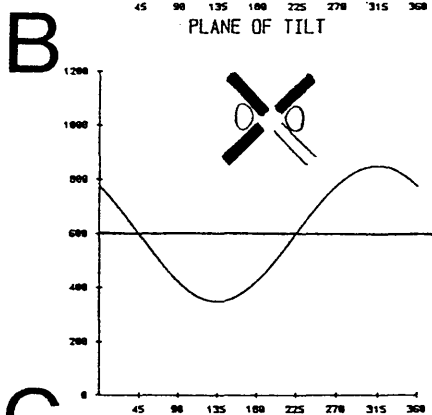
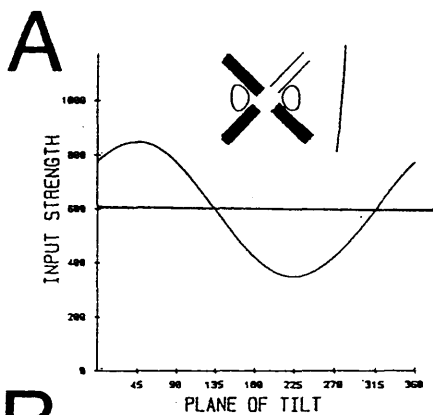
LA = Left anterior

LP = Left posterior



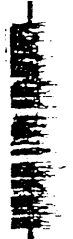
— RA

- - - RP



- Fig 5.26** In the algebraic model of semicircular canals the input strength is plotted against the plane of tilt.
- A. Resultant curve after ablating left anterior & two posterior vertical canals.
 - B. Resultant curve after ablating two anterior & left posterior vertical canals.
 - C. Resultant curve after ablating right anterior & two posterior vertical canals.
 - D. Resultant curve after ablating right posterior & two anterior vertical canals.
 - E. Resultant curve after ablating left anterior vertical canal.
 - F. Resultant curve after ablating left posterior vertical canal.
 - G. Resultant curve after ablating right anterior vertical canal.
 - H. Resultant curve after ablating right posterior vertical canal.

Fig 5.27 The recording of myographic activity in the SOR after ablating four vertical canals and the right utriculus recordings made at 0° , 15° , 30° , 45° , 60° , 80° , 90° right side down tilts at 0.2Hz, response in the SOR is only elicited after 60° tilt is passed.



0°



15°

RIGHT SIDE DOWN



30°



45°



60°



80°

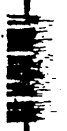


90°

SOR



90°



0.2HZ



0°

15°

30°



45°

60°



SOR



90°

0.2Hz

135°

Fig 5.28 The myographic activity of SOR, recorded at 0° , 15° , 30° , 45° , 60° , 90° , 135° head down tilts after the ablation of four vertical semicircular canals and the right utriculus for tilts at 0.2Hz. Myographic response in the SOR only appeared after fish was tilted 90° head down.

Chapter 6. GENERAL DISCUSSION.

GENERAL DISCUSSION.

Vertical and horizontal VOR are eye reflexes to an angular head acceleration which stabilize the vision against head movement. In dogfish the eye movements are produced by the coordinated activation of six EOM. The physiology, mechanical properties and innervation play a significant role in determining the kind of eye reflexes a particular animal can produce.

Physiological profile of the EOM.

As demonstrated by the implication of histological, histochemical, immunohistochemical and mechanical techniques, two fibre types are consistently present in all six EOM (Chapter 2). TYPE I fibres are small, lie mostly in the orbital region, stain negative with M-ATPase and are SDH positive. TYPE II fibres are large, lie mostly in the global region, give positive staining with M-ATPase and are SDH negative. In studies of the mechanical response of EOM, two levels of contractions were consistently observed which may have been elicited by the two different fibre types.

The majority of TYPE I fibres in all EOM stain positive with the two slow antibodies specific for tonic type myosin (α ALD & α SHC) which suggests that majority of these fibres are tonic in nature. TYPE II fibres give a negative reaction to this slow antibody.

Subgroups of TYPE I and TYPE II are consistently present in all EOM. TYPE I and TYPE II fibres in dogfish EOM have typical properties of **slow** and **fast or fast twitch** fibre types known to present in vertebrate EOM and skeletal muscle (Bone, 1966; Hess, 1967; Hidaka & Toida, 1969; Mayer, 1971; Alvaredo & Vanhorn, 1975; Ovalle, 1978; Gilly & Hui, 1980; Altringham & Johnston, 1982; reviewed by Morgan &

Proske, 1984; Sartore et al, 1987; Akster et al., 1988).

The majority of the TYPE I fibres are confined in the orbital region, while majority of TYPE II fibres are present in the global region. The morphology and physiological profile of the horizontal (EXT-R & INT-R) and vertical (SO, SR, IO, IR) muscles is consistent with the presence of TYPE I and TYPE II fibres in the orbital and global regions.

The size of motor units in the dogfish EOM is one motor axon per 9 fibres and one motor axon per 13 fibres in the SO and EXT-R. Compared with the large motor units present in vertebrate skeletal muscle, smaller motor units are a characteristic feature of the EOM (reviewed by Buchtchal & Schmalbruch, 1980) which shows an efficient motor control system which enables the eyes to perform precise and various kinds of movements ranging from compensatory eye reflexes to the nystagmus response.

The heterogenous structure of the EOM comprised of TYPE I slow and TYPE II fast fibre types (Chapter 2) is the same as reported in the amphibian and mammalian species (Bach-Y-Rita & Lennerstrand, 1975; Morgan & Proske, 1984). Two levels of response are also shown in the myographic activity of the individual EOM, where units of two size are consistently present in the burst of EOM firing (Chapter 4). Also during the hold of a tilt a strong level of tonic firing is seen. In the vertical plane the EOM response is mostly comprised of slow bursts, although in the horizontal plane there are separate slow and fast phases in the activity of the horizontal and the vertical EOM. Considering the heterogenous profile of the EOM it is entirely possible that the two levels of EOM activity shown in the vertical and horizontal VOR are contributed by the TYPE I and TYPE II fibres. However it is not confirmed that TYPE I, slow tonic fibres in the

orbital region are responsible for the tonic units firing in the vertical plane, or that the phasic firing in the horizontal plane during fast eye flicks results from the activation of TYPE II fibres in the global region. An experimental confirmation can only be obtained by recording intracellularly from the selected TYPE I and TYPE II fibres, and back filling these fibres with an intracellular dye. These labelled fibres can then be stained histochemically and immunohistochemically to determine their physiological profile.

Vertical eye reflexes.

In the present investigation of the vertical VOR, eye reflexes to an imposed vertical body tilt have been determined (Chapter 3). Eye reflexes in this plane are only compensatory and results suggest a strong vestibular input in to them.

Ablation of utriculus and the semicircular canals provide evidence for the strong vestibular influence, where after ablation of these two components the gain is significantly reduced and very small or no eye movements are seen under different ablation conditions. Relative gain values seen in the white light and in the dim red light show very small variations. Weak visual input is present in the vertical VOR, although these affects are generally suppressed by the strong vestibular influences and are only seen when the animal is provided with a strong visual stimulus. Some effect of visual input is suggested in the tests to establish the optokinetic nystagmus, where higher gain values were shown in the tests where the visual stimulus is reinforcing eye movements in the dim red light. As these fish often live in the deep sea environment under poor light conditions this shows an adaptation to that environment. In experiments where the fish is provided with a visual stimulus alone in

the absence of vestibular effects, small deviations of the eyes occur following the striped drum pattern, as reported in other vertebrates is seen (Hood & Leech, 1974; Baarsma & Collewijn, 1974; Gutman, Zeilg & Bergmann, 1964).

Coordinated activation of the EOM in vertical VOR.

The smaller gain values consistently observed in the pitch plane show that the amplitude of eye movements in the pitch plane is comparatively smaller than those observed during the roll tilts (Chapter 3). The myographic activity of the vertical EOM (Chapter 4) shows that their coordination in the pitch plane is unexpected and does not fit with the predictions made by Lowenstein & Sand (1940). The SO and SR in the two eyes are actually activated together, and therefore the torsional counter-rolling of the two eyes in the pitch plane is achieved by the difference in the relative strength of the SO and SR firing, rather than their antagonistic effects. The pattern of EOM activation in the roll plane is the same as predicted by Lowenstein & Sand (1940): the counter roll of an eye during the side down roll tilt is induced by the co-contraction of the SO and SR while IO and IR remain inactive. The myographic activities of the horizontal EOM stabilize the action of the vertical EOM in the roll and pitch planes.

Vestibular nystagmus in the vertical plane is known to occur in other vertebrates (Darlot, Barneo & Tracey, 1981; Correia, Perachio & Eden, 1985, Synder & King, 1988) but is totally absent in the dogfish vertical eye reflexes. In the myographic activity of the EOM during the vertical VOR nystagmus is not seen. However in the horizontal VOR vertical EOM are grouped with the horizontal EOM to produce a nystagmus response. The nystagmus in the vertical EOM may have a

stabilizing affect to the response of horizontal EOM.

The pattern of EOM activation at intermediate angles between the roll and pitch planes gives insight to the integration of the vertical canal outputs during the operation of vertical VOR. The EOM activity is coordinated to compensate the eye reflexes as they are affected by the tilts in the roll and pitch planes and at intermediate planes. The phase shift in the myographic activity of the EOM in the left eye occurs around 45° , while phase shift in the myographic response of the EOM in the right eye occurs around 135° .

Control of the vertical VOR.

The dogfish control of the vertical VOR has been determined by the selective ablation of the vertical semicircular canals and the utricle. Subtle differences in the semicircular canals and utricle input to the EOM are shown by the smaller phase differences in the beginning of a burst in the tilt planes where peaks of the myographic activity are in phase. These effects are best seen after the ablation of the vertical semicircular canals which results in a significant reduction of the gain of eye movements only for tilts at 0.8Hz, while after the ablation of utricle gain deficits are greater at 0.2Hz. The variations in the strength of EOM firing after the ablation of canals are strongly seen at 0.8Hz, while similar deficits in the EOM activity after the utricle ablation are best seen at 0.2Hz. Therefore these two frequencies represent the range in which different components of the vestibular system naturally operate.

Ipsilateral ablation of the vertical semicircular canals or the utricle results in a significant reduction of either in the gain of ipsilateral eye movement or in the strength of EOM firing. Therefore the ipsilateral ablation is most effectively seen in the vertical eye

reflexes and in the myographic activity of the EOM.

The algebraic model predicts the input strength of the vertical semicircular canals during tilts between the 0^0 - 360^0 . However it fails to explain the pattern of EOM activity obtained after the ablation of semicircular canals (Section 5.4) which is dis-proportionate to its predicted algebraic effect. 1. The ablation of a single vertical canal is most effective and results in significant reduction in the strength of EOM firing. 2. The ablation of the posterior vertical canal suggests an inhibitory cross-coupling to output pathways from the other canals. 3. In the experiments where only a single vertical canals is left intact a contralateral control which drives the response of both eyes is indicated. Thus the results obtained in different ablation experiments suggest a complex wiring between the different control components of the vestibular system. When a single canal is ablated either some functional abnormalities are introduced in the operation of the VOR, or a complex control is exerted centrally which affects the myographic activity of the EOM.

Prospects.

The experiments described in this thesis, particularly those on the reflex responses of the EOM to vestibular stimuli under a variety of operated conditions, demonstrate the many advantages offered by this decerebrated dogfish preparation for the study of the VOR. Firstly the preparation lasts several days and the eye reflexes remain consistent over this period. All the EOM are accessible and can be recorded myographically. The vestibular system is also easily accessible and allows the ablation to be simply performed. These factors have allowed a large body of the data to be obtained on the coordination of the EOM for an extensive range of the stimulus

conditions in the intact animal and under a large number of ablated conditions. Such a comprehensive set of data does not appear to have been obtained previously in any vertebrate species. For these reasons this preparation has great potential for use in the investigation of the central neuronal pathways which control the VOR.

REFERENCES.

REFERENCES.

- Akster, H.A. and Osse, J.W.M. (1978). Muscle fibre types in head muscles of the perch (Perca fluviatilis) Teleostei. a histochemical and electromyographical study. Neth.J.Zool. **28**, 94-110.
- Akster, H.A. (1981). Ultrastructure of muscle fibres in head and axial muscle of perch (Perca fluviatilis). A quantitative study. Cell.Tissue.Res. **219**, 111-131.
- Akster, H.a., Granzier, H.L.M. and keurs, H.E.D.J. (1984). A comparison of quantitative ultrastructural and contractile characteristics of muscle fibre types of the perch, Perca fluviatilis. J.Comp.Physiol. **155**, 685-691.
- Allum, J.H.J., Graf, W., Dichgans, J. and Schmidt, C.L. (1976). Visual vestibular interactions in the vestibular nuclei of the goldfish. Exp.Brain.Res. **26**, 263-485.
- Allum, J.H.J. and Graf, W. (1977). Time constants of the vestibular nuclei neurons in the goldfish: a model with ocular proprioception. Biol.Cybern. **28**, 95-99.
- Alvarado, J. and Vanhorn, C. (1975). Muscle types of the cat inferior oblique.In: basic mechanisms of ocular motility and their clinical implications. (Lennerstrand, G. and Bach-Y-Rita, P. eds). Pergamon press.New York. 15-44.
- Baarsma, E.A. and Collewijn, H. (1974). Vestibulo-ocular and optokinetic reactions to rotations and their interaction in the rabbit. J.Physiol. (London). **238**, 603-625.
- Bach-Y-Rita, P. and Ito, F. (1966). In vivo, studies on fast and slow muscle fibres in cat extraocular muscles. J.Gen.Physiol. **49**, 1177-1198.
- Bach-Y-Rita, P. (1971). Neurophysiology of eye movements. In: the

- control of eye movements. (Bach-Y-Rita, P. and Collins, C. eds). Academic. New York. 7-45.
- Bach-Y-Rita, P. and Lennerstrand, G. (1975). Absence of polyneuronal innervation in cat extra-ocular muscles. *J. Physiol. London.* **244**, 613-624.
- Barmack, N.H., Bell, C.C. and Rence, B.G. (1971). Tension and rate of tension development during isometric responses of extra-ocular muscles. *J. Neurophysiol.* **34**, 1072-1079.
- Barmack, N.H. (1981). A comparison of horizontal and vertical vestibuloocular reflexes of rabbit, *J. Physiol. (London).* **314**, 547-564.
- Barany, M. (1967). M. ATPase activity of myosin correlated with speed of muscle shortening. *J. Gen. Physiol.* **50**, 197-218.
- Batini, C. Morruzi, G., Pompeiano, O. (1957). Cerebellar release phenomenon. *Arch. Ital. Biol.* **95**, 71-95.
- Bergman, R.A. (1964). The structure of the dorsal fin musculature of the marine teleosts, Hippocampus hudsonius and Hippocampus zosterae. *Bull. Johns. Hopkins. Hosp.* **114**, 325-343.
- Bizzi, E., Khalil, R.E., Morasso, P. and Tagliasco, V. (1972). Central programming and peripheral feedback during eye-head coordination in monkeys. In: Cerebral control of eye movements and motion perception. (Dichgans, J. and Bizzi, E., eds) Basel Karger. 220-232.
- Bizzi, E. Khalil, R.E., and Tagliasco, V. (1971). Eye-head coordination in monkeys: evidence for centrally patterned organization. *Science.* **173**, 451-454.
- Blanks, R.H.I., Estes, M.S. and Markham, C.H. (1975). Physiological characteristics of vestibular first order canal neurons in the cat. II. response to constant angular acceleration.

- J.Neurophysiol. **38**, 1250-1267.
- Blanks, R.H.I. and Precht, W. (1976). Functional characterisation of primary vestibular afferents in the frog. *Exp.Brain.Res.* **25**, 369-390.
- Blanks, R.H.I., Precht, W. and Giretti, M.L. (1977). Response characteristics and vestibular receptor convergence of frog cerebellar purkinje cells: a natural stimulation study. *Exp.Brain.Res.* **27**, 181-201.
- Boeder, P. (1962). Cooperative action of extra-ocular muscles. *Br.J.Ophthalmol*, **46**, 397-403.
- Bone, Q. (1964). Patterns of muscular innervation in the lower chordates. *Int.Rev.Neurobiol.* **6**, 99-147.
- Bone, Q. (1966). On the function of the two types of myotomal muscle fibre in the elasmobranch fish. *J.Marine.Biol.Assoc.Uk.* **46**, 321-349
- Bone, Q. and Chubb, A.D. (1978). The histochemical demonstration of myofibrillar ATPase in elasmobranch muscle. *Histochem.J.* **10**, 489-494.
- Brooke, M.H. and Kaiser, K.K. (1970). Muscle fibre types: how many and what kind ?. *Arch.Neurol.* **23**, 369-379.
- Buchthal, F. and Schmalbruch, H. (1980). Motor units of mammalian muscle. *Physiol.Rev.* **60**, 91-142.
- Burke, R.E., Levine, D.M., Tsairis, P. and Zajac, F.E. Physiological Types and histochemical profiles in motor units of the cat gastrocnemius. *J.Physiol.(London)*. **234**, 723-748.
- Buettner, U.W., Buttner, U. and Henn, V. (1978). Transfer characteristics of neurons in vestibular nuclei of the alert monkey. *J.Neurophysiol.* **41**, 1614-1628.
- Buettner, U.W., Henn, V. and Young, L.R. (1981). Frequency response of the vestibulo ocular reflex (VOR) in monkey.

- Aviat.Space.Env.Med. 52, 73-77.
- Camis, M. and Creed, R.S. (1930). The physiology of the vestibular apparatus. London oxford university press. (Clarendon).
- Cheng, K. and Brenin, G.M. (1966). A comparison of the fine structure of extra-ocular and interosseous muscles in monkey. Invest.Opthal. 5, 535-549.
- Close, R. and Luff, A.R. (1974). Dynamic properties of inferior rectus muscle of the rat. J.Physiol.London. 236, 259-270.
- Cohen, B., Suzuki, J. and Bender, M.B. (1964). Eye movements from semicircular canal nerve stimulation in the cat. Ann.Otol.Rhinol.Lar. 73, 153-169.
- Cohen, B., Suzuki, J., Shanzer, S, and Bender, M.B. (1964). Semicircular canal control of eye movements. In: The oculomotor system. (Bender, M.B eds). Harper and Row. New York.
- Collewijn, H. (1977). Eye and head movements in freely swimming rabbits. J.Physiol. 266, 471-498.
- Darlot, C., Lopez-Barneo, J. and Tracey, D. (1981). Asymmetries of vertical vestibular nystagmus in the cat. Exp.Brain.Res. 41, 420-426.
- Davey, D.F., Mark, R.F., Marott, L.R. and Proske, U. (1975). Structure and innervation of extraocular muscles of the Carassius. J.Anat. 120, 131-147.
- Davies, P.R. (1978). Neural adaptation in humans and cats subjected to longterm optical reversal of vision: an experimental and analytical study of plasticity. PHD thesis.Mc Gill university. Montreal. Quebec, p120.
- Dieringer, N. and Precht, W. (1986). Functional organization of eye velocity and eye position signals in abducens motoneurons of the frog. J.Comp.Physiol A. 158, 179-194.

- Dietert, S.E. (1965). The demonstration of different types of muscle fibres in human extraocular muscle by electron microscopy and cholinestrerase staining. *Invest.Ophthalmol.* **4**, 51-63.
- Dubowitz, V. and Everson pearse, A.G. (1960). A comparative histochemical study of oxidative enzyme and phosphorylase activity in skeletal muscle. *Histochemie.* **2**, 105-117.
- Easter, S.S. (1972). Pursuit eye movements in goldfish Carassius auratus. *Vision.Res.* **12**, 673-688.
- Easter, S.S. and Johns, P.R. (1974). Horizontal compensatory eye movements in goldfish (Carassius auratus).II. A comparison of normal and deafferented animals. *J.Comp.physiol.* **92**, 37-57.
- Eddington, S. and Johnston, I.A. (1982). Morphometric analysis of regional differences in myotomal muscle ultrastructure in the juvenile eel Anguilla anguilla. *Cell.Tissue.res.* **222**, 579-596.
- Egmond, A.A.J.V., Groen, J.J. and Jongkeey, L.B.W. (1949). The mechanism of semicircular canal. *J.Physiol.* **110**, 1-17.
- Engel, W.K. and Irwin, A.L. (1967). a histochemical and physiological correlation of frog skeletal muscle fibres. *Am.J.Physiol.* **213 (2)**, 511-518.
- Fernandez, C. and Frederickson, J.M. (1963). Experimental cerebellar lesions and their effect on vestibular function. *Acta.Oto.Laryng.Suppl.* **192**, 52-62.
- Fernandez, C., Goldberg, J.M. and Abend, W.K. (1973). Response to static tilts of peripheral neurons innervating otolith organs of the squirrel monkey. *J.Neurophysiol.* **35**, 978-997.
- Flitney, F.W. and Johnston, I.A. (1979). Mechanical properties of isolated fish red and white fibres. *J.Physiol.* **295**, 49-50p.
- Fluur, E. (1959). Influences of semicircular ducts on extra-ocular muscles. *Acta.Oto.Lar.Suppl.* **149**.

- Focant, B. and Renzik, M. (1980). Comparison of the sarcoplasmic and myofibrillar proteins of twitch and tonic fibres of frog muscle. (Rana esculent). Eur.J.Cell.Biol. 21, 195-199.
- Fuchs, A.F. and Luschei, E.S. (1970). Firing patterns of abducens neurons of alert monkeys in relationship to horizontal eye movements. J.Neurophysiol. 33, 382-392.
- Fuchs, A. and Kimm, J. (1975). Unit activity in vestibular nucleus of the alert monkeys during horizontal angular acceleration and eye movement. J.Neurophysiol. 36, 1140-1161.
- Gestrin, P. and Sterling, P. (1977). Anatomy and physiology of goldfish oculomotor system.II. Firing patterns of neurons in abducens nucleus and surrounding medulla and their relation to eye movements. J.Neurophysiol. 40, 573-588.
- Gilly, W.F. and Hui, C.S. (1980). Mechanical activity in the slow and twitch skeletal muscle fibres of the frog. J.Physiol. 301, 137-156.
- Granzier, H.L.M., Wiersma, J., Akster, H.A. and Osse, J.W.M. (1983). Contractile properties of a white and a red fibre type of the m.hyohyoideus of the carp (Cyprinus carpio). J.Comp.Physiol. 149, 441-449.
- Gueritaud, J.P., Horcholle-Bossavit, G., Jami, L., Thiesson, D.A. and Tyc-Dumont, S. (1984). Histochemical analysis of cat extraocular muscle. Neurosci.Lett.Suppl. 18, S229.
- Guth, L. and Samaha, J.F. (1969). Qualitative differences between actomyosin ATPase of slow and fast mammalian muscle. Exp.Neurol. 25, 138-152.
- Harris, A.J. (1965). Eye movements of the dogfish Squalus acanthias. L.J.Exp.Biol. 43, 107-130.

- Hermann, H.T. and Constantine, M.M. (1971). Eye movements in the goldfish. *Vision.Res.* **11**, 313-331.
- Hermann, H.T. (1971). Eye movement correlated units in the mesencephalic oculomotor complex of goldfish. *Brain.Res.* **35**, 240-244.
- Hess, A. (1961). The structure of slow and fast extrafusal muscle fibres in the extraocular muscles and their nerve endings in guinea pigs. *J.Cell.Comp.Physiol.* **58**, 63-80.
- Hess, A. (1962). Further morphological observations of en plaque and engrappe endings on mammalian extrafusal muscle fibres with cholinesterase staining. *Rev.Canad.Biol.* **21**, 241-248.
- Hess, A. (1963). Two kinds of extrafusal muscle fibres and their nerve endings in the garter snake. *Am.J.Anat.* **113**, 347-367.
- Hess, A. and Pilar, G. (1963). Slow vertebrate muscle fibres in the extra-ocular muscle fibres of cat. *J.Physiol.Lond.* **169**, 780-798.
- Hess, A. (1970). Vertebrate slow muscle fibres. *Physiological.Reviews.* **50**, 40-62.
- Highstein, S.M. (1972). Electrophysiological investigation of the organization of the vestibulo-ocular pathways in the rabbit. In: cerebral control of eye movements and motion perception. (Dichgans, J. and Bizzi, E. eds). Basel.Karger, 89-98.
- Highstein, S.M. (1973). Synaptic linkage in the vestibulo-ocular and cerebello-vestibular pathway to the Vith nucleus in the rabbit, *Exp.Brain.Res.* **17**, 301-314.
- Hikada, T. and Toida, N. (1969). Biophysical and mechanical properties of red and white muscle fibres in fish. *J.Physiol.Lond.* **201**, 49-59.
- Hood, J.O. and Leech, J. (1974). The significance of peripheral vision in the perception of movement. *Acta.Oto.Laryngol.* **77**, 72-79.

- Housley, G.D. and Montgomery, J.C. (1984). The structure of the external rectus eye muscles of the carpet shark Cephaloscyllium isabella. J.Anat. 138, 643-655.
- Hudson, R.C.L. (1969). Polyneuronal innervation of the fast muscles of the marine teleost Cottus scorpius, J.Exp.Biol. 50, 47-67.
- Ito, M., Nishimaru, N. and Yamamoto, M. (1976). Inhibitory interaction between the vestibulo-ocular reflexes arising from semicircular canals of rabbits. Exp.Brain.Res. 26, 89-103.
- James, T. (1976). A rapid method for demonstrating skeletal muscle motor innervation in frozen sections. Stain.Tech. 51 No3, 1-8.
- Jansen, J.P., Andersen, P. and Jansen, J.K.S. (1963). On the structure and innervation of the parietal muscle of the hagfish, Myxine glutinosa. Acta.Morphol.Neerl.Scand. 5, 329-338.
- Johnston, I.A., Davison, W. and Goldspink, G. (1977). Energy metabolism of carp swimming muscles. J.Comp.Physiol. 114, 203-216.
- Johnston, I.A. and Moon, T.W. (1981). Fine structure and metabolism of multiply innervated fast muscle fibres in teleost fish. Cell.Tissue.Res. 219, 93-109.
- Johns, G.H. and Milsum, J.H. (1971). Frequency response analysis of central vestibular unit activity resulting from rotational stimulation of the semicircular canals. J.Physiol. 219, 191-215.
- Jongkees, L.B.W. (1950). On the function of the saccule. Acta.Oto.Laryngo. 38, 18-26.
- Kaczmarek, F. (1970). The fine structure of extra-ocular muscles of the bank vole Clethrionomys glareolus, Schr.Acta.Anat. 77, 570-580.
- Kaczmarek, F. (1974). Motor endplates in the extra-ocular muscles of small mammals. Acta.Anat. 89, 372-386.

- Kern, R.A. (1965). A comparative pharmacologic-histologic study of slow and twitch fibres in the superior rectus muscle of the rabbit. *Invest.Ophthalmol.* **4**, 901-910.
- Kilarski, W. and Bigaj, J. (1969). Organization and fine structure of extra-ocular muscles in the Carissus and Rana. *Z.Zellforsch.Mikrosk.Anat.* **94**, 194-204.
- Kordylewski, L. (1974). The anatomy and the fine structure of extraocular muscles of the gudgeon Gobio gobio. *Acta.Anat.* **87**, 597-614.
- Kyrvi, H. (1977). Ultrastructure of different fibre types in axial muscles of the sharks, Etmopterus spinax and Galeus melastomus. *Cell.Tissue.Res.* **184**, 287-303.
- Lannergren, J. and Smith, R.S. (1966). Type of muscle fibres in toad skeletal muscle. *Acta.Physiol.Scand.* **68**, 263-274.
- Lee, F.S. (1893). A study of sense of equilibrium in fishes.I. *J.Physiol.* **15**, 311-348.
- Lee, F.S. (1894). A study of the sense of equilibrium in fishes.II. *J.Physiol.* **17**, 192-210.
- Lennerstrand, G. (1972). Fast and slow units in the extrinsic eye muscles of cat. *Acta.Physiol.Scand.* **86**, 286-288.
- Llinas, R. and Precht, W. (1969). The inhibitory vestibular efferent system and its relation to the cerebellum in the frog. *Exp.Brain.Res.* **9**, 16-29.
- Lowenstein, O. and Sand, A. (1936). The activity of the horizontal semicircular canals of the dogfish Scyllium canicula. *J.Exp.Biol.* **13**, 416-429.
- Lowenstein, O. and Sand, A. (1940). The individual and integrated activity of the semicircular canals of the elasmobranch labyrinth. *J.Physiol.* **99**, 89-101.

- Lowenstein, O. and Roberts, T.D.M. (1950). The equilibrium function of the otolith organs of the thornback ray Raja calvata. J.Physiol.(London). **110**, 392-415.
- Lowenstein, O. (1956). Peripheral mechanism of the equilibrium. Br.Med.Bull. **12**, 114-118.
- Lowenstein, O. (1974). Comparative morphology and physiology. In: hand book of sensory physiology. (Kornhubers, H.H. eds) Berlin:Springer. **6**, 75-120.
- Lowenstein, O and Saunders, R.D. (1975). Otolith controlled responses from the first order neurons of the labyrinth of bullfrog Rana catesbeiana to changes in linear acceleration. Proc.Roy.Soc.London.B. **191**, 475-505.
- Loe, P.R. Tomko, D.L. and Werner, G. (1973). The neural signal of angular head position in primary vestibular nerve axons. J.Physiol.London. **239**, 29-50.
- Mabuchi, K. and Sreter, F.A. (1980). The actomyosin ATPase-II- fibre typing by histochemical ATPase reaction. Muscle and Nerve.**3**, 233-239
- Markham, C.H., Yagi, I. and Curthoys, I.S. (1977). The contribution of the contralateral labyrinth to second order vestibular neuronal activity in the cat. Brain.Res. **138**, 99-109.
- Manni, E. and Desole, C. (1966). Responses of oculomotor units to stimulation of single semicircular canal units. Exp.Neurol. **15**, 206-219.
- Matyushkin, D.P. (1961). Phasic and tonic neuromotor units in the oculomotor apparatus of the rabbit. J.Sechenov.Physiol.USSR, **47**, 960-965.
- Matyushkin, D.P. (1964). Motor systems in the oculomotor apparatus of higher animals. Federation.Proc. **23**. 1103-1106.

- Mayne, R. (1974). A system concept of the vestibular organs. In: hand book of sensory physiology. Vestibular system. (Kornhuber, H.H. eds). Berlin:Springer. 6, 493-580.
- Maxwell, S.S. (1923). Labyrinth and equilibrium. Saunders.Philadelphia.London.
- Mayer, R. (1971). Structure and distribution of fibre types in the external eye muscles of the rabbit. Tissue.Cell.Res. 3, 433-462.
- McNally, W.J. and Tait, J. (1925). Ablation experiments on the labyrinth of frog. Amer.J.Physiol. 75, 155-179.
- McNally. W.J. and Tait, J. (1933). Some results of section of particular nerve branches to the ampullae of the four vertical semicircular canals of frog. Quart.J.Exp.Physiol. 23, 147-196.
- Mayer, R. (1971). Structure and distribution of fibre types in the external eye muscles of the rat. Tissue.Cell.Res. 3, 433-462.
- Meyer, W. (1979). Oxidative enzymes and myosin-ATpase in the trunk musculature of the river lamprey Lampetra fluviatilis. Histochem.J. 11, 187-195.
- Miller, J.E. (1971). Recent histologic and electron microscopic findings in extraocular muscle. Trans.Am.Acad.Ophthalmol.Otolaryngol. 75, 1175-1185.
- Miles, F.A., Kawano, K. and Optican, L.M. (1986). Short latency ocular following responses of monkey.I. dependence on temporospatial properties of visual input. J.Neurophysiol. 56, 1321-1354.
- Money, K.E. and Scott, J.W. (1962). functions of seperate sensory receptors of non auditory labyrinth of the cat. Am.J.Physiol. 202, 1211-1220.
- Montgomery, J.C. (1980). Dogfish horizontal canal system: responses of primary afferents, vestibular and cerebellar neurons to rotational stimulation. Neurosci. 5, 1767-1769.

- Montgomery, J.C. (1983). Eye movement dynamics in the dogfish. *J.Exp.Biol.* **105**, 297-303.
- Morgan, D.L. and Proske, U. (1984). Vertebrate slow muscle: its structure, pattern of innervation and mechanical properties. *Physiol.Rev.* **64**, 103-170.
- Moruzzi, G. and Pompeiano, O. (1957). Inhibitory mechanisms underlying the collapse of decerebrate rigidity after unilateral fastigial lesions. *J.Comp.Neurol.* **107**, 1-26.
- Nag, A.C. and Peachey, L.D. (1972). Structural organization and distribution of fibre types in the extra-ocular muscles of cats. 30th Annu.Proc.Electron microscopy.Soc.America.Los Angeles.
- Nishihara, H. (1967). Studies on the fine structure of red and white fin muscles of the fish Carassius auratus. *Arch.Histol.Japan.* **28**, 425-447.
- Nowogrodzka-Zagorska, M. (1974). The organization of extraocular muscles in Anura. *Acta.Anat.* **87**, 22-44.
- O' Leary, D.P., Dunn, R.F. and Honrubia, V. (1976). Analysis of afferent responses from isolated semicircular canal of guitarfish using rotational acceleration white-noise inputs. I. correlation of response dynamics with receptor innervation. *J.Neurophysiol.* **39**, 631-644.
- O' Leary, D.P., Dunn, R.F. and Honrubia, V. (1974). Functional and anatomical correlation of afferent responses from the isolated semicircular canal. *Nature.* **251**, 225-227.
- Oman, C.M., Frishkop, L.S. and Goldstein, H.M. (1979). Cupula motion of the semicircular canal of the skate Raja erinacea. *Acta.Otolaryngol.* **87**, 528-538.
- Ovalle, W.K.J.R. (1982). Ultrastructural duality of extrafusil fibres in a slow (tonic) skeletal muscle. *Cell.Tissue.Res.* **222**, 261-267.

- Pachter, B.R., Davidowitz, J. and Breinin, M. (1976). Light and electron microscopic serial analysis of mouse extra-ocular muscle morphology, innervation and topographical organization of component fibre populations. *Tissue.Cell.Res.* **8**,547-560.
- Page, S.G. (1968). Fine structure of toroise skeletal muscle. *J.Physiol.London.* **197**, 709-715.
- Peachey, L.D. and Huxley, A.F. (1962). structural identification of twitch and slow striated muscle fibres of the frog. *J.Cell.Biol.* **13**, 177-180.
- Peachey, L.D. (1971). The structure of the extra-ocular muscle fibres of mammals.In: The control of eye movements. (Bach-Y-Rita, P. and Collins, C.C. eds). 45-66.
- Peachey, L.D., Takeichi, M. and Nag, C.A. (1974). Muscle fibre types and innervation in adult cat extra-ocular muscles. In:exploratory concepts in muscular dystrophy II. (Mill Hort, A.T. eds) Excerpta medicine Found.Amsterdam, 246-254.
- Pearse, A.G.E. (1972). Histochemistry, Theoretical and applied. Vol2. 3rd edition. Churchill livingstone.Edinburgh.London.
- Peters, A. and Mackay, B. (1961). The structure and innervation of the myotoms of the lamprey. *J.Anat.* **95**, 575-585.
- Peterson, B.W. (1970). Distribution of neural responses to tilting within vestibular nuclei of the cat. *J.Neurophysiol.* **33**, 750-767.
- Peter, J.B., Barnard, J.R., Edgerton, V.R., Gillespie, C.A. and Stemple, K.E. (1972). Metabolic profile of three fibre types of skeletal muscle in guinae pigs and rabbits. *Biochem.J.* **11**, 1227-1233.
- Pierobon-Bormioli, S., Sartore, S., Dalla Libera, S., Vitadello, M. and Schiaffin, O. (1981). Fast isomyosins and fibre types

- in mammalian skeletal muscle. *J.Histochem.Cytochem.* **29**, 1179-1188.
- Pilar, G. and Hess, A. (1966). Differences in internal structure and nerve terminals of slow and twitch muscle fibres in the cat superior oblique. *Anat.Rec.* **154**, 243-252.
- Pilar, G. (1967). Further studies of electrical and mechanical responses of slow fibres in cat extra-ocular muscles. *J.Gen.Physiol.* **50**, 2289-2300.
- Robinson, D.A. (1976). Adaptive gain control of vestibulo-ocular reflex by the cerebellum. *J.Neurophysiol.(London)*. **39**, 954-969.
- Robinson, D.A. (1981). The use of control system analysis in the neurophysiology of eye movements. *Ann.Rev.Neurosci.* **4**, 463-503.
- Ross, D.A. (1936). Electrical studies on the frog labyrinth. *J.Physiol.(London)*. **86**, 117-146.
- Rovainen, M.C. (1976). vestibulo-ocular reflexes in the adult sea lamprey. *J.Comp.Physiol.* **112**, 159-164.
- Rowett, H.G.Q. (1965). Guide to dissection. (Rowett, H.G.Q. eds). John Murray.London. p49
- Rowlerson, A., Pope, P., Murray, J., Whalen, R.B. and Weeds, A.G. (1981). A novel myosin present in cat jaw closing muscles. *J.Musc.Res.Cell.Motility.* **2**, 415-438.
- Sartore, S., Mascarello, F., Rowlerson, A., Gorza, L., Ausoni, S., Vianello, M. and Schiaffino, S. (1987). Fibre types in the extra-ocular muscles: a new myosin isoform in the fast fibres. *J.Musc.Res.Cell.Motility.* **8**, 161-172.
- Schmidt, R.S. (1963). Frog labyrinthine efferent impulses. *Acta.Oto.Laryng. (Stockh)*. **56**, 51-64.
- Schmidt, C.L., Wist, E.R. and Dichgans, J. (1971). Efferent frequency modulation in the vestibular nerve of goldfish correlated with saccadic eye movements. *Exp.Brain.Res.* **15**, 1-14.

- Schor, R.H. (1974). Responses of cat vestibular neurons to sinusoidal roll tilt. *Exp.Brain.Res.* **20**, 347-362.
- Shimazu, H. and Precht, W. (1965). Tonic and kinetic responses of cat vestibular to horizontal angular acceleration. *J.Neurophysiol.* **28**, 991-1013.
- Shimazu, H. and Smith, C.M. (1971). Cerebellar influence on the evoked potential of the oculomotor nucleus induced by stimulation of the oculomotor nerve branches in the cat. *Invest.Ophthalmol.* **9**, 236-244.
- Shinoda, Y. and Yoshida, K. (1974). Dynamic characteristics of responses to horizontal head acceleration in the vestibulo-ocular pathways in the act. *J.Neurophysiol.* **37**, 653-673.
- Skavenski, A.A. and Robinson, D.A. (1973). Role of abducens neurons in vestibulo-ocular reflex. *J.Neurophysiol.* **36**, 724-738.
- Smith, R.S. and Ovalle, K.W. (1973). Varieties of fast and slow extrafusal muscle fibres in amphibian hind limb muscles. *J.Anat.* **116**, 1-24.
- Snow, D.H., Billeter, R., Mascarello, F., Carpena, E., Rowlerson, A. and Jenny, E. (1982). No classical Type II.B fibres in dog skeletal muscle. *Histochem.* **75**, 53-65.
- Snyder, L.H. and King, W. (1988). Vertical vestibulo-ocular reflex in cat: asymmetry and adaptation. *J.Neurophysiol.* **59**, 279-298.
- Stanfield, P.R. (1972). Electrical properties of white and red muscle fibres of the elasmobranch fish Scyliorhinus canicula. *J.Physiol.London*, **222**, 161-186.
- Steinhaus, W. (1931). On the proof of the movement of the cupula in the complete ampulla of the labyrinth under rotatory and caloric stimulation. *Transl. P.Flügers.Arch.Ges.Physiol.* **228**, 322-328.
- Szentagothai, J. (1964). Pathways and synaptic articulation patterns

- connecting vestibular receptors and oculomotor nuclei. In: Bender, M.B., The oculomotor system. Harper and Row (Hoeber). New York
- Taglietti, V., Valli, P. and Casella, C. (1973). Discharge properties of the sensory units in the crista ampullaris, Arch.Sci.Biol. 57, 73-86.
- Teravainen, H. (1971). Anatomical and physiological studies of muscles of lamprey. J.Neurophysiol. 34, 954-973.
- Uhrig, B. and Schmidt, H. (1973). distribution of slow muscle fibres in the frog rectus abdominus muscle. Pfluegers.Arch. 340, 361-366.
- Vidal, J., Jeannerod, M., Lifschitz, W., Levitan, H., Rosenberg, J. and Segundo, J.P. (1971). Static and dynamic properties of gravity sensitive receptors in the cat vestibular system. kybernetic. 9, 205-215.
- Vita, G.F., Mastaglia, F.L. and Johnston, M.A. (1980). A histochemical study of fibre types in rat extraocular muscles. J.Neuropath.Appl.Neurobiol. 6, 449-463.
- Walls, G.L. (1962). The evolutionary history of eye movements. Vision.Res. 2, 69-80.
- Witalinski, W. and Loesch, A. (1975). Structure of muscle fibres and motor endplates in the intercostal muscles of the grass snake Matrix natrix. Z.Mikrosk.Anat.Forsch. 89, 1133-1146.
- Witalinski, W. and Labuda, H. (1982). Extra-ocular muscles in the lamprey, Lampetra fluviatilis. L.I. muscle fibres. Acta.Anat. 114, 165-176.
- Zenker, W. and Azenbacher, H. (1964). On the different forms of myoneural junction in two types of muscle fibres from the external ocular muscles of the rhesus monkey. J.Cellular.Comp.Physiol. 63, 273-285.